

**New insights into
nuclear/cytoplasmic partitioning
and posttranslational activation of
Arabidopsis PI4P 5-kinases**

Dissertation

Zur Erlangung des

Doktorgrades der Naturwissenschaften

„Doctor rerum naturalium“

der

Naturwissenschaftlichen Fakultät I

– Biowissenschaften –



MARTIN-LUTHER-UNIVERSITÄT
HALLE-WITTENBERG

vorgelegt von

Herrn Lennart Schwalgun

geb. am 14. November 1994

in Berlin

Gutachter:

Prof. Dr. Ingo Heilmann

Prof. Dr. Klaus Humbeck

Prof. Dr. Marcel Wiermer

Die vorliegende Dissertation wurde unter Anleitung von Dr. Mareike Heilmann in der Abteilung für Pflanzenbiochemie (Prof. Dr. Ingo Heilmann, Martin-Luther-Universität Halle-Wittenberg) angefertigt.

Eingereicht am: 26.09.2022

Tag der Verteidigung: 22.03.2023

Table of Contents

Abbreviations	V
Summary.....	VIII
1 Introduction.....	1
1.1 The Arabidopsis phosphoinositide system	1
1.1.1 Key enzymes of the PI-biosynthesis with a focus on PI4P 5-kinases.....	2
1.1.2 Subcellular localisation and the concept of PI4P 5-kinase/ PtdIns(4,5)P ₂ pools.....	5
1.1.3 Cytosolic functions of PI4P 5-kinases and PtdIns(4,5)P ₂	8
1.1.4 Nuclear functions of PtdIns(4,5)P ₂ and PI4P 5-kinases.....	11
1.2 Posttranslational modifications of plant PI4P 5-kinases	13
1.3 Protein phosphorylation as possible regulation of the PI4P 5-kinases PIP5K1 and PIP5K2.....	15
1.3.1 The protein kinase family CK2.....	17
1.3.2 AGC3 protein kinases	21
1.4 Research goals	25
2 Results	26
2.1 PIP5K1 and PIP5K2 dynamically localise to plant nuclei	26
2.2 AtPIP5K1 and AtPIP5K2 have a close homolog in <i>Papaver somniferum</i>: comparative biology to study nuclear cytoplasmic shuttling	30
2.2.1 Confirmation of the strong nuclear localisation of PsPIP5K1	32
2.2.2 PsPIP5K1 interacts with alpha-importins from Arabidopsis.....	35
2.2.3 The Lin-domain of PI4P 5-Kinases is key for the subcellular localisation.....	36
2.2.4 Tobacco pollen tube phenotypes and tip swelling upon overexpression of different PI4P 5-kinase variants.....	40
2.2.5 PsPIP5K1 rescues the <i>pip5k1 pip5k2</i> double mutant phenotype	42
2.3 Hints for a regulatory link between CK2 and PI4P 5-kinase functions	48
2.3.1 Subunits of CK2 interact with PIP5K1 and PIP5K2.....	48
2.3.2 CKA3 phosphorylates PIP5K1 <i>in vitro</i>	49
2.3.3 Coexpression of PIP5K1 with CKA3 seems to affect subcellular localisation of PIP5K1	53
2.3.4 CKA3 effects the catalytic activity of PIP5K1 upon phosphorylation	57
2.4 A new link between AGCVIII kinase PID and PI4P 5-kinase function	58
2.4.1 AGCVIII protein kinase PID interacts with PIP5K1 and PIP5K2.....	59
2.4.2 PID phosphorylates (PIP5K1 and) PIP5K2 in the NLS region within the Lin-domain.....	62
2.4.3 PIP5K2 does not show altered subcellular localisation upon phosphorylation by PID	65

2.4.4	Investigation of the nanodomain pattern of PIP5K2-EYFP and the A/ D variants at the plasma membrane.....	68
2.4.5	Influence of Phosphorylation by PID on the catalytic activity of PIP5K2.....	70
2.4.6	Effects of AGCVIII protein kinases on the functionality of PIP5K2 <i>in vivo</i>	73
3	Discussion	75
3.1	The nuclear localisation of PIP5K2 is dynamic and regulated.....	75
3.2	Comparative biology: a PIP5K1/ 2 ortholog from poppy displays almost exclusive nuclear localisation.	77
3.2.1	The Lin-domain is key for PI4P 5-kinase function and subcellular localisation.....	78
3.2.2	Functional studies with PsPIP5K1 in tobacco pollen tubes and the <i>pip5k1 pip5k2</i> double mutant	79
3.2.3	Observation of PsPIP5K1-EYFP in nuclear speckles.....	81
3.3	PIP5K1 and PIP5K2 are regulated by reversible protein phosphorylation ...	82
3.3.1	PIP5K1 interacts with the CK2 alpha-subunit CKA3	82
3.3.2	Phosphorylation of PIP5K1 by CKA3.....	83
3.3.3	Influence of CKA3 on the subcellular distribution of PIP5K1	84
3.3.4	Phosphorylation of PIP5K1 by CKA3 controls activity	85
3.3.5	PIP5K1 and PIP5K2 interact with the AGCVIII protein kinase PID.....	86
3.3.6	PID phosphorylates PIP5K2 in the NLS region of the Lin-domain	87
3.3.7	PIP5K2-EYFP apparently localises unaffected by PID	88
3.3.8	The AGCVIII protein kinases affect PI4P 5-kinase activity <i>in vitro</i> and <i>in vivo</i>	89
3.4	Regulators that need to be regulated	91
4	Material and Methods	94
4.1	Chemicals and consumables.....	94
4.2	Enzymes and size indicators.....	94
4.3	Microorganisms.....	94
4.4	Plants and plant cell cultures	95
4.5	Culture media.....	96
4.5.1	Yeast media	96
4.5.2	Plant media	97
4.5.3	Media additives	98
4.5.4	Growth conditions	98
4.6	Growing arabidopsis cell cultures.....	99
4.7	Vectors and plasmids.....	99
4.7.1	Vectors for protein expression in <i>E. coli</i>	99
4.7.2	Vectors for protein-protein interaction studies.....	99
4.7.3	Vectors for transient expression in plants and plant transformation.....	100
4.8	Buffers and stock solutions	101

4.9 Preparation of RNA, DNA and cDNA from plants	104
4.9.1 Isolation of RNA from Arabidopsis.....	104
4.9.2 Isolation of genomic DNA from Arabidopsis	104
4.9.3 Determining RNA and DNA Concentrations.....	105
4.9.4 cDNA synthesis.....	105
4.10 Separation of DNA and RNA in agarose gels.....	105
4.11 Molecular Biology Methods	106
4.11.1 Amplifying DNA fragments using polymerase-chain-reaction (PCR).....	106
4.11.2 Isolating plasmid DNA from <i>E. coli</i>	107
4.11.3 Isolating DNA from agarose gels.....	107
4.11.4 Restriction of DNA.....	107
4.11.5 DNA ligation.....	107
4.11.6 Gateway® cloning.....	107
4.11.7 Preparing chemo-competent <i>E. coli</i>	108
4.11.8 Transforming chemo-competent <i>E. coli</i>	108
4.11.9 Controlling DNA by sequencing	108
4.11.10 Preparing chemo-competent <i>A. tumefaciens</i>	109
4.11.11 Transforming chemo-competent <i>A. tumefaciens</i>	109
4.11.12 Transforming Arabidopsis with <i>A. tumefaciens</i>	109
4.11.13 Selection of transformed Arabidopsis.....	109
4.12 Cloning strategies	110
4.12.1 Constructs for the expression of recombinant proteins.....	110
4.12.2 Constructs for split-ubiquitin based yeast-two-hybrid assays.....	110
4.12.3 Constructs for bimolecular fluorescence complementation.....	111
4.12.4 Constructs for transient expression in plant cells and stable transformation of Arabidopsis.....	112
4.13 Recombinant protein expression and enrichment.....	113
4.13.1 Expression of MBP- and GST-fusion proteins.....	113
4.13.2 Expression of His-CK2 subunits.....	114
4.13.3 Cell disruption with a high-pressure-homogeniser.....	114
4.13.4 Cell disruption with ultrasonic	114
4.13.5 Enrichment of proteins by affinity chromatography.....	114
4.13.6 Determination of protein concentrations.....	115
4.13.7 Separation of proteins with sodium dodecyl sulfate polyacrylamid gel electrophoresis (SDS-PAGE).....	115
4.14 Immunodetection on nitrocellulose membranes (Westernblot)	116
4.15 Antibodies.....	116
4.16 <i>In vitro</i> protein phosphorylation assay	117
4.17 Mass spectrometry and phosphopeptide analysis	117
4.18 Determination of PI4P 5-Kinase activity <i>in vitro</i>.....	118
4.19 Determination of PtdIns(4,5)P₂ content in Arabidopsis.....	118

4.20	Testing protein-protein interactions using the split-ubiquitin-yeast-two-hybrid-assay (Y2H)	119
4.20.1	Preparing chemically competent <i>S. cerevisiae</i>	120
4.20.2	Transforming <i>S. cerevisiae</i>	120
4.20.3	Analysing protein-protein interactions by Y2H.....	121
4.21	Testing protein-protein interactions with <i>in vitro</i> pull-down	121
4.22	Testing protein-protein interactions using bimolecular fluorescence complementation assay	121
4.23	Preparing and transforming Protoplasts	122
4.23.1	NAA treatment of Arabidopsis leaf mesophyll protoplasts	123
4.24	Transforming tobacco pollen tubes	123
4.25	Microscopy and Image Analysis	124
4.25.1	Lasers scanning microscope 880 (LSM880).....	124
4.25.2	Spinning disc microscope	124
4.25.3	Elyra 7 with total internal reflection fluorescence (TIRF) module.....	125
4.26	Computer-based analyses and online tools	125
4.26.1	PIP5K1 and PIP5K2 phosphorylation sites prediction	125
4.26.2	Phylogenetic trees.....	125
4.26.3	Statistics and data management	126
5	Literature	127
6	Appendix	142
6.1	Additional Figures	142
6.2	Additional MS Data	144
6.2.1	His-CKA3/ MBP-PIP5K1 phosphorylation test	144
6.2.2	MBP-PID/ MBP-PIP5K2 phosphorylation test.....	144
6.3	Oligonucleotides	145
6.3.1	Primers used for cloning.....	145
6.3.2	Primers used for sequencing	149
6.3.3	Primers used for genotyping plants.....	150
Figures	X
Tables	XII
Danksagung	XIII
Curriculum Vitae	XV
Erklärung	XVI

Abbreviations

AGC	one of the protein kinase superfamilies
AGCVIII	plant specific AGC kinase family
AGC3	protein kinase subfamily of the AGCVIII family
AL	activation loop of PI4P 5-kinases in the cat. domain
Arabidopsis	<i>Arabidopsis thaliana</i>
AtPIP5K1	<i>Arabidopsis thaliana</i> phosphatidylinositol-4-phosphat 5-kinase isoform 1
AtPIP5K2	<i>Arabidopsis thaliana</i> phosphatidylinositol-4-phosphat 5-kinase isoform 2
AtPIP5K2_LinPs	chimeric protein: <i>Arabidopsis thaliana</i> phosphatidylinositol-4-phosphat 5-kinase isoform 2 with Lin-domain of PsPIP5K1
ATX1	arabidopsis homolog of trithorax 1
BRX	brevis radix transcription factors
BY-2	<i>Nicotiana tabacum</i> cell culture line from cultivar Bright Yellow
Cat	catalytic domain
CCA1	circadian clock associated 1
CFP	cyan fluorescent protein
CK2	casein kinase 2 family
CKA	casein kinase 2 alpha subunits
CKA1	casein kinase 2 alpha subunit isoform 1
CKA2	casein kinase 2 alpha subunit isoform 2
CKA3	casein kinase 2 alpha subunit isoform 3
CKA4	casein kinase 2 alpha subunit isoform 4
CKB	casein kinase 2 beta subunits
CKB1	casein kinase 2 beta subunit isoform 1
CKB2	casein kinase 2 beta subunit isoform 2
CKB3	casein kinase 2 beta subunit isoform 3
CKB4	casein kinase 2 beta subunit isoform 4
CKI	casein kinase 1 family
CME	clathrin-mediated endocytosis
CMGC	one of the protein kinase superfamilies
Cub	C-terminal half of ubiquitin (amino acid 34-76)
D6PK	D6 protein kinase from the AGC1 family
Dim	dimerization domain
DsRed	red fluorescent protein from <i>Discosoma</i>
EYFP	enhanced yellow fluorescent protein
FYVE domain	protein domain that binds PtdIns3P
GCN5	general control non-depressible 5
HFR1	long hypocotyl in far red 1
HY5	elongated hypocotyl 5

IMPA3	alpha-importin isoform 3
IMPA6	alpha-importin isoform 6
IMPA9	alpha-importin isoform 9
LHY	late elongated hypocotyl
Lin	linker domain
mCherry	red fluorescent protein derived from DsRed
MORN	membrane occupation and recognition nexus
MPK6	mitogen-activated protein kinase isoform 6
Mss4	<i>Saccharomyces cerevisiae</i> phosphatidylinositol-4-phosphat 5-kinase
NAA	1-Naphthaleneacetic acid
NLS	nuclear localisation signal
Nt	N-terminal domain
NtPIP5K6	<i>Nicotiana tabacum</i> phosphatidylinositol-4-phosphat 5-kinases isoform 6
Nub	N-terminal half of ubiquitin (amino acid 1-38)
NubG	N-terminal half of ubiquitin (amino acid 1-38) isoleucine at position twelve substituted by glycine
OE	overexpressor
OsPIP5K1	<i>Oryza sativa</i> phosphatidylinositol-4-phosphat 5-kinases isoform 1
OST4	oligosaccharyltransferase
PAX	protein kinase associated with BRX from the AGC1 family
PDK1	phosphoinositide-dependent protein kinase 1
PH domain of FAPP1	protein domain that binds PtdIns4P
PH domain of PLCδ1	protein domain that binds PtdIns(4,5)P ₂
PI	phosphoinositide
PI 4-kinase	phosphatidylinositol 4-kinase
PI3P 5-kinase	<i>Arabidopsis thaliana</i> phosphatidylinositol-3-phosphat 5-kinase
PI4P 5-kinase	<i>Arabidopsis thaliana</i> phosphatidylinositol-4-phosphat 5-kinase
PID	PINOID protein kinase
PIF	phytochrome-interacting factors
PIN	PIN-FORMED auxin efflux carrier
PIP5K1	<i>Arabidopsis thaliana</i> phosphatidylinositol-4-phosphat 5-kinase isoform 1
PIP5K2	<i>Arabidopsis thaliana</i> phosphatidylinositol-4-phosphat 5-kinase isoform 2
PIP5K2_NLS _{AAA}	<i>Arabidopsis thaliana</i> phosphatidylinositol-4-phosphat 5-kinase isoform 2 R271A K272A R273A variant that shows reduced nuclear localisation
PIP5K2 S274A S275A	<i>Arabidopsis thaliana</i> phosphatidylinositol-4-phosphat 5-kinase isoform 2 S274D S275D phosphoablation variant
PIP5K2 S274D S275D	<i>Arabidopsis thaliana</i> phosphatidylinositol-4-phosphat 5-kinase isoform 2 S274A S275A phosphomimikri variant
PIP5K3	<i>Arabidopsis thaliana</i> phosphatidylinositol-4-phosphat 5-kinase isoform 2

PIP5K4	<i>Arabidopsis thaliana</i> phosphatidylinositol-4-phosphat 5-kinase isoform 3
PIP5K5	<i>Arabidopsis thaliana</i> phosphatidylinositol-4-phosphat 5-kinase isoform 4
PIP5K6	<i>Arabidopsis thaliana</i> phosphatidylinositol-4-phosphat 5-kinase isoform 5
PIP5K7	<i>Arabidopsis thaliana</i> phosphatidylinositol-4-phosphat 5-kinase isoform 6
PIP5K8	<i>Arabidopsis thaliana</i> phosphatidylinositol-4-phosphat 5-kinase isoform 7
PIP5K9	<i>Arabidopsis thaliana</i> phosphatidylinositol-4-phosphat 5-kinase isoform 8
PIP5K10	<i>Arabidopsis thaliana</i> phosphatidylinositol-4-phosphat 5-kinase isoform 10
PIP5K11	<i>Arabidopsis thaliana</i> phosphatidylinositol-4-phosphat 5-kinase isoform 11
PKA	cyclic-AMP dependent protein kinase A
PKC	diacylglycerol/ phospholipid dependent protein kinase C
PKG	cyclic-GMP dependent protein kinase G
Poppy	<i>Papaver somniferum</i>
PP2A	protein phosphatase 2
PP6	protein phosphatase 6
PsPIP5K1	<i>Papaver somniferum</i> phosphatidylinositol-4-phosphat 5-kinase isoform 1
PsPIP5K1_LinAt	chimeric protein: <i>Papaver somniferum</i> phosphatidylinositol-4-phosphat 5-kinase isoform 1 with Lin-domain of AtPIP5K2
PtdIns	phosphatidylinositol
PtdIns3P	phosphatidylinositol-3-phosphate
PtdIns4P	phosphatidylinositol-4-phosphate
PtdIns5P	phosphatidylinositol-5-phosphate
PtdIns(3,4)P ₂	phosphatidylinositol-3,4-bisphosphate
PtdIns(3,5)P ₂	phosphatidylinositol-3,5-bisphosphate
PtdIns(4,5)P ₂	phosphatidylinositol-4,5-bisphosphate
PtdIns(3,4,5)P ₃	phosphatidylinositol-3,4,5-trisphosphate
RuBisCO	ribulose-1,5-bisphosphat-carboxylase-oxygenase
SDS-PAGE	sodium dodecyl sulfate polyacrylamide gel electrophoresis
TF	transcription factor
TLC	thin-layer chromatography
Tobacco	<i>Nicotiana tabacum</i>
VI	variable insert in the catalytic domain of PI4P 5-kinases
VPS34	vascular protein sorting 34
WAG1	Protein kinase WAG1 of the AGC3 family
WAG2	protein kinase WAG2 of the AGC3 family
WOX	WUSCHEL homeobox-containing protein family
YTH	yeast-two-hybrid

Summary

The signalling lipid PtdIns(4,5)P₂ is a minor component of eukaryotic membranes and affects a broad range of physiological processes and signalling pathways by acting as a lipid ligand for effector proteins. PI4P 5-kinases are responsible for the production of PtdIns(4,5)P₂, which is present in a variety of subcellular locations, including the plasma membrane and the nucleus. The presence of an NLS in PIP5K2 from *Arabidopsis* and the localisation of PIP5K1 and PIP5K2 in plant nuclei has previously been reported. Nuclear localisation of PI4P 5-kinases appears to be dynamic and is not observed in cells of all plant tissues. The dynamic subcellular targeting of PI4P 5-kinases allows specific and temporary production of PtdIns(4,5)P₂ in certain cellular locations to initiate local effects. The activity and localisation of PI4P 5-kinases of different eukaryotic organisms can be modulated by phosphorylation. The aims of this thesis were to better understand which sequences or domains of PI4P 5-kinases are responsible for their spatial distribution within the cell. And whether *Arabidopsis* PI4P 5-kinases are regulated in their localisation and activity by phosphorylation. We had to identify upstream protein kinases and to characterise biochemical and physiological effects of phosphorylation *in vitro* and *in vivo*. Comparative biology with PIP5K1 from poppy and PIP5K2 from *Arabidopsis* revealed that the linker (Lin)-domain is important for PI4P 5-kinase recruitment and is responsible for both nuclear and plasma membrane localisation. The Lin-domain, as a disordered protein domain, may serve as a platform for various protein interactions and posttranslational modifications that subsequently affect the spatial distribution and temporal activity of the enzymes. Two very different protein kinases were identified, CK2 and AGCVIII protein kinase PID, for which there was evidence that they phosphorylate PIP5K1 and/ or PIP5K2. Y2H studies showed that the catalytic alpha-subunit CKA3 of CK2 interacts with PIP5K1 but not with PIP5K2, and that PID interacts with both, PIP5K1 and PIP5K2. These protein interaction studies could be substantiated by pull down and BiFC tests. The interaction of PIP5K2 with PID in BiFC *in vivo* studies occurs at the plasma membrane of protoplasts, suggesting functional relevance for the interaction. Purified recombinant PIP5K1 was phosphorylated by CKA3 at position S2 in the N-terminus, PIP5K2 was not phosphorylated, consistent with the observation of protein interactions, and CKA3 apparently discriminates between PIP5K1 and PIP5K2. PID phosphorylated both PIP5K1 and PIP5K2, and for PIP5K2, phosphorylation sites S274, S275, and S282 were identified to be located directly in or adjacent to the identified NLS in the Lin-domain of PIP5K2. Phosphorylation of PIP5K1 and PIP5K2 did not result in any detectable change in subcellular localisation, even at the level of nanodomain structure in TIRF studies. Although the identified phosphorylation sites

in PIP5K1 and PIP5K2 were localised in the N-terminal domains rather than in the catalytic domain, the *in vitro* activity of PIP5K1 and PIP5K2 was significantly enhanced by the phosphorylation, presumably by conformational change due to the introduction of the negative charge and thus abolition of the autoinhibitory effect of the N-terminal domains on catalytic activity. The *in vitro* results were partially confirmed by *in vivo* experiments, which showed that reduced PtdIns(4,5)P₂ levels could be measured in *pid*-mutated seedlings, suggesting that the absence of PID activity affects intrinsic PIP5K1 / PIP5K2 activity. Thus, the Lin-domain and phosphorylation appear to be important for controlling the subcellular distribution and activation of Arabidopsis PI4P 5-kinases.

1 Introduction

Living cells cope with the coordination of complex cellular processes, such as the establishment and maintenance of cellular integrity and cellular polarity, complex metabolic reactions and growth. In eukaryotes, distinct cellular compartmentalisation adds the possibility of independent functionality of simultaneous but opposing reactions, for example in anabolic and catabolic processes. This cellular compartmentalisation in organelles is enabled by various membranes and the composition of the membranes often defines their functionality. Moreover, phospholipids as structural components of all membranes can not only physically influence membrane properties and thus affect their functionality, but some phospholipids, such as phosphoinositides (PIs) are also signalling molecules and serve as messengers.

PIs have been identified in plants in all cytosol-facing membranes, and their functions at the plasma membrane have been best studied. Recent studies show that both PIs and the corresponding PI biosynthetic enzymes, phosphatidylinositol-4-phosphate 5-kinases (PI4P 5-kinases) can be detected in the nucleus and most likely have distinct functions there. One of the open questions is how both the dual localisation of PI4P 5-kinases to the plasma membrane/ cytosol and the nucleus and the respective distinct exerted regulatory functions of PI4P 5-kinases are regulated. One way of regulating key enzymes such as PI4P 5-kinases are posttranslational modifications including protein phosphorylation. This study attempts to further elucidate how the dual localisation of PI4P 5-kinases is regulated and how their functionality is affected by comparative biology and the study of phosphorylation of PI4P 5-kinases by protein kinases.

1.1 The Arabidopsis phosphoinositide system

PIs are regulatory glycerophospholipids found in all eukaryotic membranes, but account for only a small fraction of max. 1 % of total phospholipids (Heilmann, 2016a; Heilmann, 2016b). PIs are not uniformly distributed but locally enriched in so-called micro- or nanodomain structures. Thus, local enrichment of PIs recruits PI-binding proteins to the membrane and therefore alters membrane properties (Eyster, 2007; Ischebeck et al., 2008; Lundbæk et al., 2010; Ischebeck et al., 2011; Heilmann, 2016a; Gerth et al., 2017a; Jaillais and Ott, 2020; Fratini et al., 2021). This recruitment of proteins and/ or the change in membrane properties can have various cellular effects, depending on the present PI species. PI species can be classified according to the phosphorylation status of their inositol headgroup (Fig. 1A). In plants and thus also in the model organism *Arabidopsis thaliana* (Arabidopsis), the

PI monophosphates phosphatidylinositol 3-phosphate (PtdIns3P), phosphatidylinositol 4-phosphate (PtdIns4P) and phosphatidylinositol 5-phosphate (PtdIns5P) and the PI-bisphosphates phosphatidylinositol 4,5-bisphosphate (PtdIns(4,5)P₂) and phosphatidylinositol 3,5-bisphosphate (PtdIns(3,5)P₂) occur (Mueller-Roeber and Pical, 2002; Heilmann, 2016a; Heilmann, 2016b; Gerth et al., 2017a; Colin and Jaillais, 2020)). In contrast to mammals no phosphatidylinositol 3,4-bisphosphate (PtdIns(3,4)P₂) and phosphatidylinositol 3,4,5-trisphosphate (PtdIns(3,4,5)P₃) could be detected in plants (Mueller-Roeber and Pical, 2002; Heilmann, 2016a). The phosphorylation and antagonised dephosphorylation of the inositol headgroup is modulated by specific PI-kinases and PI-phosphatases resulting in a dynamic and highly regulated PI network in plant cells (Fig. 1B, (Heilmann, 2016b; Gerth et al., 2017a)).

1.1.1 Key enzymes of the PI-biosynthesis with a focus on PI4P 5-kinases

The precursor of all PIs is the structural phospholipid phosphatidylinositol (PtdIns) displayed in figure 1A. PtdIns is generated in the cytosolic leaflet of the endoplasmic reticulum membrane by PHOSPHATIDYLINOSITOL SYNTHASES (PIS) which catalyse the condensation of cytidine-diphosphodiacylglycerol (CDP-DAG) with *D*-myo-inositol (Justin et al., 1995; Ohlogge and Browse, 1995; Jackson et al., 2000). In this reaction the D1-position of the *D*-myo-inositol is esterified with the phosphate group of the activated 1,2-diacylglycerine. Sterically, only the hydroxyl groups in D3, D4 and D5 position of the *D*-myo-inositol headgroup are possible targets for further phosphorylation (Fig. 1A). PtdIns3P is produced by the phosphorylation in position D3 by a single copy gene coding for a class III phosphatidylinositol 3-kinase (PI 3-kinase) called VASCULAR PROTEIN SORTING 34 (VPS34) and only accepts PtdIns as a substrate (Fig. 1B, (Welters et al., 1994)). In Arabidopsis, there are four active PI 4-kinases which can be subcategorised in an alpha-subfamily, PI4K α 1 and PI4K α 2 and a beta-subfamily, PI4K β 1 and PI4K β 2 (Fig. 1B). PI 4-kinases phosphorylate the position D4 of the inositol at the PtdIns whereby PtdIns4P is formed (Fig. 1B, (Stevenson et al., 1998; Xue et al., 1999)). PtdIns5P is probably not produced by phosphorylation, but rather by dephosphorylation of the PtdIns-bisphosphates (Meijer et al., 2001; Zhong et al., 2005; Williams et al., 2005; Ndamukong et al., 2010; Pribat et al., 2011; Nováková et al., 2014).

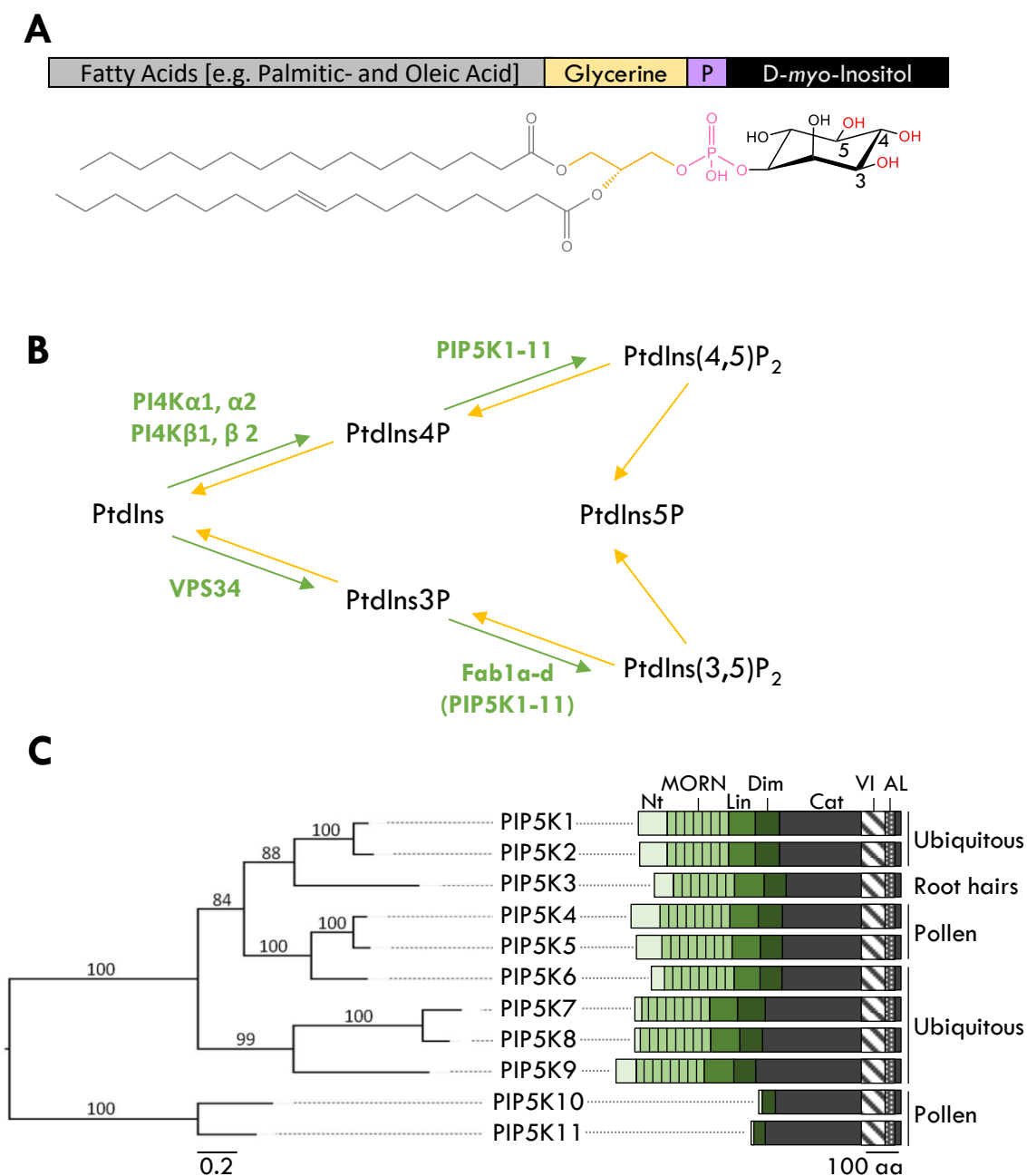


Figure 1 PI network and domain structure of PI4P 5-kinases. **A** Chemical structure of Phosphatidylinositol. Exemplary 16:0 (Palmitic acid) in *sn*-1 and 18:1 Δ 9 (Oleic acid) in *sn*-2 are esterified to the glycerine backbone in yellow. The phosphor ester in purple connects the name giving D-*myo*-inositol headgroup with the glycerine. In the inositol ring the hydroxy groups in position D3, D4, and D5 are numbered and sterically available for phosphorylation. **B** The PI network with phosphate adding PI-kinases in green and phosphate removing PI-phosphatases in yellow. **C** Phylogenetic comparison of the Arabidopsis PI4P 5-kinases PIP5K1-PIP5K11. PIP5K10 and PIP5K11 were manually separated into one clade. Branch length indicates amino acid changes per position (see scale bar). The domain structure of PIP5K1-PIP5K11 is depicted and the main expression location is written down according to Heilmann 2016. Nt, N-terminus; MORN, Membrane Occupation and Recognition Nexus; Lin, Linker domain; Dim, Dimerization domain, Cat, Catalytic domain, VI, variable Insert; AL, Activation Loop. B and C are modified from Gerth PhD 2018.

PtdIns-monophosphates can be further phosphorylated to PtdIns-bisphosphates (Fig. 1B). PtdIns3P is phosphorylated by phosphatidylinositol-3-phosphat 5-kinases (PI3P 5-kinases) to PtdIns(3,5)P₂. The Arabidopsis genome encodes four PI3P 5-kinase isoforms named Fab1 a-d (Fig. 1B, (Mueller-Roeber and Pical, 2002; Heilmann and Heilmann, 2015; Heilmann, 2016a)). PtdIns4P is phosphorylated by phosphatidylinositol-4-phosphate 5-kinases (PI4P 5-kinases) resulting in PtdIns(4,5)P₂ (Fig. 1B). *In vitro* studies showed, that PI4P 5-kinases also accept PtdIns3P as a substrate (Mueller-Roeber and Pical, 2002; Stenzel et al., 2008; Camacho et al., 2009; Bak et al., 2013). Arabidopsis has eleven isoforms of PI4P 5-kinases (PIP5K1-11), separated into the two subfamilies type A and type B. The type A subfamily includes the isoforms PIP5K10 and PIPK11, which consist of a catalytical domain (Cat) with an activation loop (AL), a variable insert (VI), and a dimerization domain (Dim) (Fig. 1C). The PI4P 5-kinase type B subfamily, with the isoforms PIP5K1 to PIP5K9, has additional plant specific N-terminal protein domains termed linker (Lin)-domain, membrane occupation and recognition nexus (MORN) and N-terminal domain (Nt) (Fig. 1C (Mueller-Roeber and Pical, 2002; Stenzel et al., 2012; Heilmann and Heilmann, 2015; Gerth et al., 2017a)). The MORN-, dimerization- and catalytic domain are conserved between those isoforms, while the Nt- and Lin-domain are highly variable and intrinsically disordered that display great differences between the isoforms (Stenzel et al 2012). It is suggested that regulation, including subcellular localisation and protein-protein interaction may occur through the Lin-domain (Stenzel et al., 2012; Gerth et al., 2017a; Fratini et al., 2021).

Phylogenetically, PIP5K1-11 can be divided into four clades (Mueller-Roeber and Pical, 2002). The type A family of PIP5K10 and PIP5K11 forms its own separate clade within the phylogenetic tree, the type B PI4P 5-kinases are grouped into three additional clades with PIP5K1-PIP5K3, PIP5K4-PIP5K6, and PIP5K7-PIP5K9 (Fig. 1C, (Mueller-Roeber and Pical, 2002; Stenzel et al., 2012; Heilmann and Heilmann, 2015)). The eleven PI4P 5-kinases show distinct expression patterns and thus functional differences (Fig. 1C). PIP5K1, PIP5K2 and PIP5K6-PIP5K9 are ubiquitously expressed (Ischebeck et al., 2013; Heilmann, 2016a; Kuroda et al., 2021) while the isoforms PIP5K4, PIP5K5, PIP5K10 and PIP5K11 are expressed in pollen and pollen tubes (Fig. 1C). The isoform PIP5K3 is expressed in root hairs and cortical and epidermal root cells (Fig. 1C, (Kusano et al., 2008; Sousa et al., 2008; Ischebeck et al., 2008; Ischebeck et al., 2008; Heilmann, 2016a; Heilmann, 2016a)). Beside the tissue-specific expression, developmental stages also influence PI4P 5-kinase expression (Elge et al., 2001; Kusano et al., 2008; Ischebeck et al., 2008; Stenzel et al., 2012; Ischebeck et al., 2013; Tejos et al., 2014; Gerth et al., 2017a;

Kuroda et al., 2021) and expression levels of PIP5K1 and PIP5K2 are in addition directly enhanced by auxin treatments (Mei et al., 2012; Tejos et al., 2014).

1.1.2 Subcellular localisation and the concept of PI4P 5-kinase/ PtdIns(4,5)P₂ pools

Regarding their subcellular distribution, PI4P 5-kinases are described as soluble proteins mostly in the cytosol and at the plasma membrane (Rao et al., 1998; Lee et al., 2007; Stenzel et al., 2008; Kusano et al., 2008; Ischebeck et al., 2008; Stenzel et al., 2012; Ischebeck et al., 2013; Gerth et al., 2017b; Hempel et al., 2017; Menzel et al., 2019; Fratini et al., 2021). PI4P 5-kinases and PtdIns(4,5)P₂ were found in and on various cellular membranes using specific fluorescent PI-binding markers or fluorescence protein tagged PI4P 5-kinases (Fig. 2). Examples of such PI specific biosensors is the PtdIns3P-specific FYVE domain (Fab 1 (yeast orthologue of PIKfyve), YOTB/ ZK632.12, Vac 1 (vesicle transport protein), and EEA1 (early endosome antigen 1) (Gaulhier et al., 1998; Jensen et al., 2001). In human there is the PH domain of PHOSPHATIDYLINOSITOL-4-PHOSPHATE ADAPTOR PROTEIN-1 (FAPP1), which only binds to PtdIns4P (Dowler et al., 2000) and the PtdIns(4,5)P₂ specific PH domain of the PHOSPHOLIPASE C DELTA 1 (PLC δ 1) (Garcia et al., 1995).

Using the fluorescence-labelled PLC δ 1PH-domain, PtdIns(4,5)P₂ was shown to be polar distributed in many cell types (Fig. 2A, (Stenzel et al., 2012; Ischebeck et al., 2013; Tejos et al., 2014; Hempel et al., 2017; Fratini et al., 2021)). The fluorescently labelled PI4P 5-kinases, such as PIP5K1 and PIP5K2, can also be detected polarly in sub-domains at the plasma membrane in many cell types such as pollen tubes, root hairs and root cortical cells (Fig. 2B, (Stenzel et al., 2008; Ischebeck et al., 2011; Stenzel et al., 2012; Ischebeck et al., 2013; Tejos et al., 2014; Fratini et al., 2021)). Within a membrane, PIs and especially PtdIns(4,5)P₂ can be distributed asymmetrically and accumulate in so-called microdomains (membrane areas below 1 μ m) or nanodomains (below 200 nm) (Fig. 2A, (Furt et al., 2010; Fratini et al., 2021; Heilmann and Heilmann, 2022)). Probably this distribution pattern of lipids and proteins/ enzymes serves to ensure that certain physiological functions only take place in certain membrane areas (Fratini et al., 2021; Heilmann and Heilmann, 2022).

In addition to the polar distribution of PIs in the plasma membrane in asymmetric (nano)domains, it has been shown that PI4P 5-kinases and PI4P 5-kinase activity can also be found in subcellular fractions other than membranes, e.g. in the actin cytoskeleton of yeast and plants (Desrivières et al., 1998; Doughman et al., 2003;

Ischebeck et al., 2011) and in endomembranes of animal and plant cells (Heilmann et al., 1999; Heilmann et al., 2001; Im et al., 2007). PI4P 5-kinases and the PIs, PtdIns4P and PtdIns(4,5)P₂, were found in the cell nuclei of Arabidopsis (Fig. 2C and D, (Lou et al., 2007; Dieck et al., 2012b; Ischebeck et al., 2013; Tejos et al., 2014; Gerth et al., 2017b)), mammals and yeast (Ciruela et al., 2000; Audhya and Emr, 2003; Santarius et al., 2006). It has been shown that the Arabidopsis isoform PIP5K2 contains a nuclear localisation sequence (NLS) in the Lin-domain, through which it interacts with alpha-importins and thus PIP5K2 is likely to be actively transported into the nucleus (Fig. 3A, (Gerth et al., 2017b)).

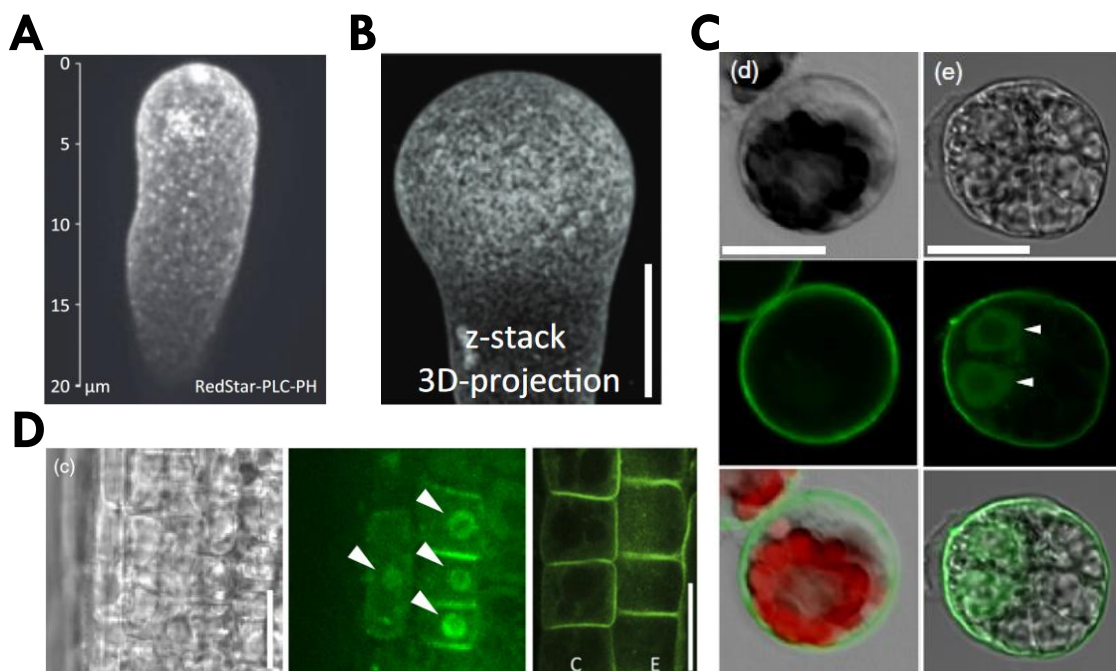


Figure 2 PIP5K2 localises in microdomains at the plasma membrane and to the nucleus in developmental young root cells. **A** 3D projection from a z-stack image acquisition (0.3 μm slices) of a representative pollen tube expressing the PtdIns(4,5)P₂ biosensor RedStar-PLC-PH. Scale as indicated. **B** 3D projection from a z-stack image acquisition (0.3 μm slices) of a representative pollen tube expressing PIP5K2-EYFP. Scale bar 10 μm. Figure A and B from Fratini et al. 2021. **C** Tobacco leaf (left) and BY-2 root cell culture (right) protoplasts expressing PIP5K2-EYFP (green). Chlorophyll A fluorescence is depicted in red. White arrows highlight nuclear PIP5K2-EYFP. Scale bars, 20 μm. Protoplasts were taken from Gerth et al. 2017. **D** PIP5K2-EYFP localisation in Arabidopsis seedlings under the control of its intrinsic promoter in the meristematic root zone (left/ middle panel) and in β-estradiol induced overexpression in the elongation zone (right panel). White arrows indicate nuclear PIP5K2-EYFP. C, cortex; E, epidermis; Scale bars, 50 μm (left panel) and 10 μm (right panel). Left/ middle panel from Gerth et al. 2017. Right panel from Ischebeck et al. 2013.

The mutation of the basic RKR cluster in the NLS of PIP5K2 to alanine (PIP5K2_NLS_{AAA}) led to an inefficient nuclear import and a reduced nuclear localisation of PIP5K2_NLS_{AAA} in plant cells (Fig. 3B, (Gerth et al., 2017b)). Since PIP5K1 and PIP5K2 are very similar with up to 82.3 % amino acid sequence identity, the

NLS appears to be conserved in PIP5K1 and PIP5K2 isoforms. It is assumed that nuclear localisation of PIP5K1 is also enabled by this NLS.

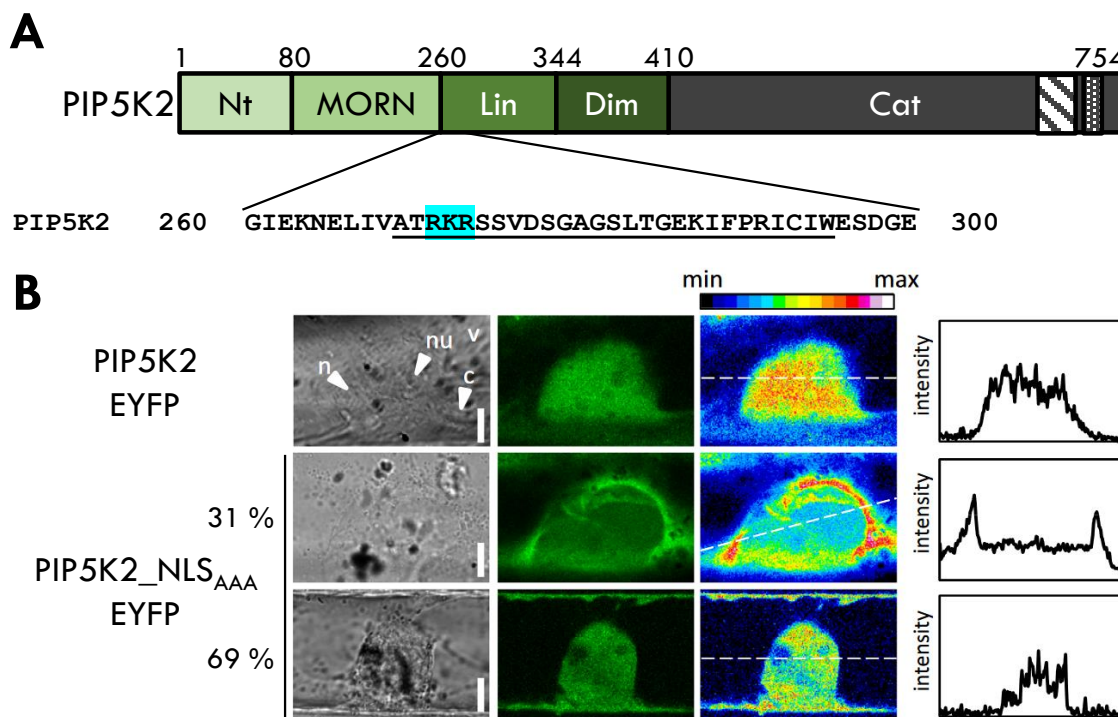


Figure 3 PIP5K2 contains a functional NLS. **A** Schematic representation of the protein domains of PIP5K2. Numbers indicate the position in the amino acid primary structure at domain transitions. Sequence shows section of amino acid sequence in the Lin-domain containing the NLS. NLS is underlined. The amino acids highlighted in blue mark the basic amino acid cluster. Nt, N-terminus; MORN, Membrane Occupation and Recognition Nexus; Lin, Linker domain; Dim, Dimerization domain; Cat, Catalytic domain; Hatched, Variable Insert; Dotted, Activation Loop. **B** Substitution of the basic amino acids RKR in the NLS of PIP5K2 with three alanines (PIP5K2-NLS_{AAA}) leads to a decrease in nuclear localisation in onion epidermal cells. N, nucleus; nu, nucleolus; v, vacuole. Scale bars, 10 μ m. Images from B are taken from Gerth et al. 2017.

Interestingly, it was consistently observed that there are cell types in which the nuclear localisation of PIP5K1 or PIP5K2 is only weakly detectable, as it is often the case in differentiated leaf cells (Fig. 2C, left panel). On the other hand, there are also cell types, as in meristematic root and tobacco cell culture cells, in which a very pronounced nuclear localisation is detectable in addition to the localisation at the plasma membrane (Fig. 2 C and D). Whether this dual localisation of PIP5K1 and PIP5K2 at the plasma membrane and in the nucleus is regulated or whether there are always two PI4P5-kinase pools in/ at both compartments is still unclear. As it will be described in the next sections, there are multiple functions for PI4P 5-kinases and PtdIns(4,5)P₂. This can take place in an orderly fashion when PI4P 5-kinases and PtdIns(4,5)P₂ are delineated in pools in the corresponding membranes of the

different organelles or within a membrane in membrane microdomains. However, the formation of sub-compartmental PI4P 5-kinase pools, e. g. plasma membrane and nucleus, or microdomains within a membrane suggests that there must be some sort of regulatory mechanisms, that guide PI4P 5-kinases to their target membranes or compartments in a cell, but these are not yet known.

1.1.3 Cytosolic functions of PI4P 5-kinases and PtdIns(4,5)P₂

Cellular processes regulated by PI4P 5-kinases and their lipid product PtdIns(4,5)P₂ in the cytoplasm and at the plasma membrane have been particularly well studied in both animals and plants. Research revealed that PI4P 5-kinases and PtdIns(4,5)P₂ are important regulators of ion channels in the plasma membrane, regulating the actin cytoskeleton, as well as endocytosis and exocytosis, and thus also regulating the distribution and abundance of proteins in and at the plasma membrane, thereby also affecting cell polarity (Fig. 4, (DeWald et al., 2001; König et al., 2008; Sousa et al., 2008; Ischebeck et al., 2008; Camacho et al., 2009; Zhao et al., 2010; Ischebeck et al., 2011; Mei et al., 2012; Ischebeck et al., 2013; Fratini et al., 2021)). PI4P 5-kinases and PtdIns(4,5)P₂ are also involved in signal transduction including plant immunity, drought and salt stress (DeWald et al., 2001; König et al., 2008; Mei, 2014; Menzel et al., 2019; Carella, 2020; Qin et al., 2020).

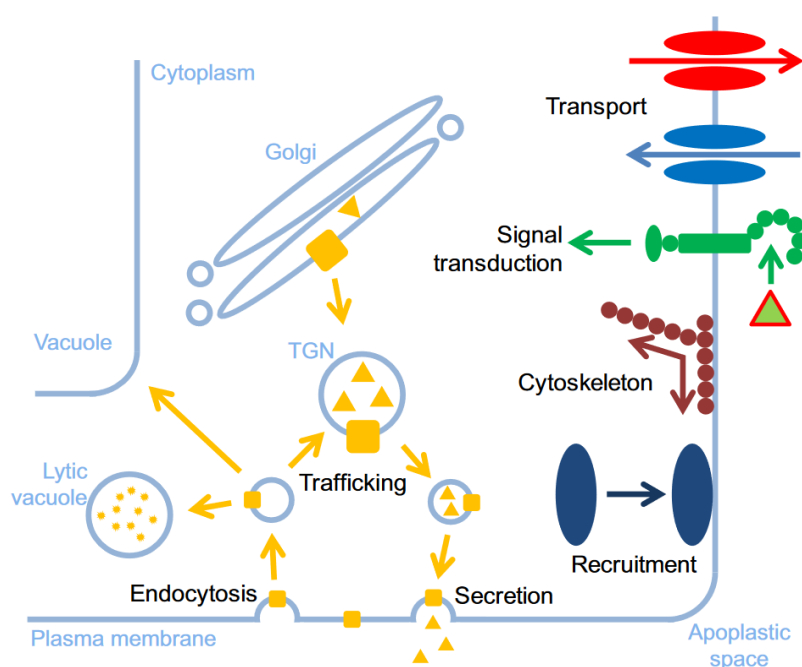


Figure 4 PIs are involved in several plasma membrane associated processes. PI regulate the clathrin mediated endocytosis and exocytosis (secretion), the recruitment of proteins with PI binding properties to the plasma membrane, cytoskeleton attachment and dynamics, signal transduction and regulation of membrane localised receptors and transport proteins in the membrane. Figure taken from Heilmann 2016.

Overall, the influence of PIs, especially PI4P 5-kinases and PtdIns(4,5)P₂, on polar distribution and orientation of cells is pronounced and diverse. Therefore, extremely polar growing cells such as root hairs and pollen tubes are a suitable system to

investigate the influence of PIs on polarity. It was found that the synthesis of $\text{PtdIns}(4,5)\text{P}_2$ by the Arabidopsis PI4P 5-kinase AtPIP5K3 is essential for the growth and polarity of root hairs (Stenzel et al., 2008; Kusano et al., 2008; Watari et al., 2022). Overexpression of the pollen-specific PI4P 5-kinases AtPIP5K5 and the more ubiquitously expressed isoform NtPIP5K6 in *Nicotiana tabacum* (tobacco) pollen tubes leads to an increased deposition of pectin at the apical plasma membrane, which led to a branching pollen tube phenotype (Fig. 5, (Stenzel et al., 2008; Ischebeck et al., 2008; Ischebeck et al., 2010b; Zhao et al., 2010; Stenzel et al., 2012)). Whereas the overexpression of the Arabidopsis PI4P 5-kinase AtPIP5K2 (and AtPIP5K10 and AtPIP5K11) in pollen tubes leads to the misregulation of the cytoskeleton and thus to a swelling of the pollen tube tip (Fig. 5, (Stenzel et al., 2012; Fratini et al., 2021)). During pollen tube growth all tested PI4P 5-kinases localise at the apical plasma membrane. The observed pollen tube phenotypes are triggered by the increased availability of the PI lipid, $\text{PtdIns}(4,5)\text{P}_2$ and not by the increasing amount of the respective overexpressed PI4P 5-kinase (Ischebeck et al., 2008; Ischebeck et al., 2010b).

This implies that PI4P 5-kinases have different functions, whereas PI4P 5-kinases, lipid substrate, and lipid product share the same localisation at subcellular level. Reciprocal exchange of the Lin-domains between NtPIP5K6 and AtPIP5K2 showed that this leads to a shift in the corresponding pollen tube phenotypes after expression in pollen tubes (Fig. 5, (Stenzel et al., 2012; Fratini et al., 2021)). As mentioned above, it is proposed that the Lin-domain of PI4P 5-kinases is likely responsible for the specificity of the respective PI4P 5-kinase (Stenzel et al. 2012; Fratini et al. 2021).

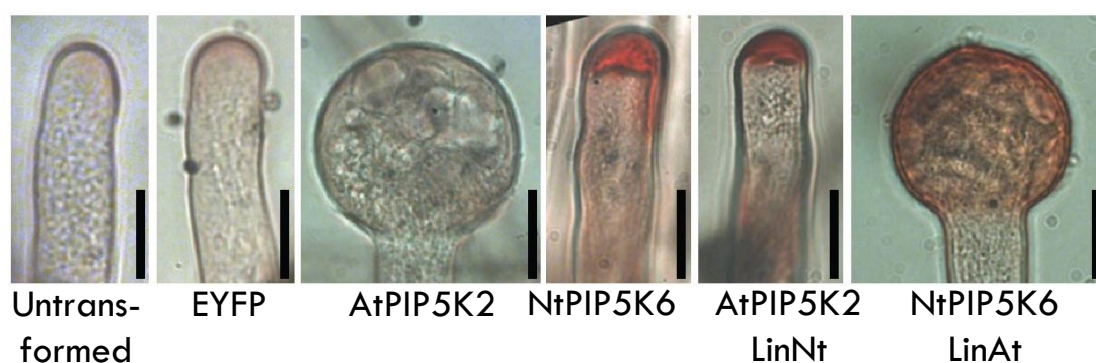


Figure 5 Overexpression of PI4P 5-kinases from different clades in pollen tubes cause different phenotypes. Untransformed and EYFP transformed pollen tubes grow normally. Overexpression of AtPIP5K2 leads to a tip swelling “cytoskeleton” phenotype. Overexpression of NtPIP5K6 causes a “secretion” phenotype visible as pollen tube tip branching and pectin accumulation. Exchanging the Lin-Domains of AtPIP5K2 and NtPIP5K6 resulted in reciprocal phenotypes as depicted. The figure was originally made by Fratini et al. 2022 and has been adapted here. Scale bars, 10 μm .

Another example in which PI4P 5-kinases influence polar cell identity and thus also strongly interfere with plant development and growth is the polar distribution of PIN-FORMED (PIN) auxin efflux carrier proteins by the two sister isoforms PIP5K1 and PIP5K2 (82.3 % sequence identity). In *pip5k1 pip5k2* double mutant plants clathrin-mediated-endocytosis (CME) is perturbed leading to false localisation of the transmembrane PIN proteins (Ischebeck et al., 2013). By polarising the PIN proteins, PIP5K1 and PIP5K2 indirectly regulate the polar auxin distribution (Mei et al., 2012; Ischebeck et al., 2013; Tejos et al., 2014; Marhava et al., 2020) and this is also reflected in the strong phenotype of *pip5k1 pip5k2* double mutants. They show strong dwarfism, shortened roots and less root hairs, no flower formation and infertility, as well as anthocyanin accumulation and increased cell wall deposition (Fig. 6, (Ischebeck et al., 2013; Ugalde et al., 2016; Watari et al., 2022)). Complementation studies in which the *pip5k1 pip5k2* double mutant was supplemented with *PIP5K1-EYFP* or *PIP5K2-EYFP* under control of the intrinsic *pPIP5K1* or *pPIP5K2* promoter almost completely rescued the *pip5k1 pip5k2* double mutant phenotype (Fig. 6, (Ischebeck et al., 2013)).

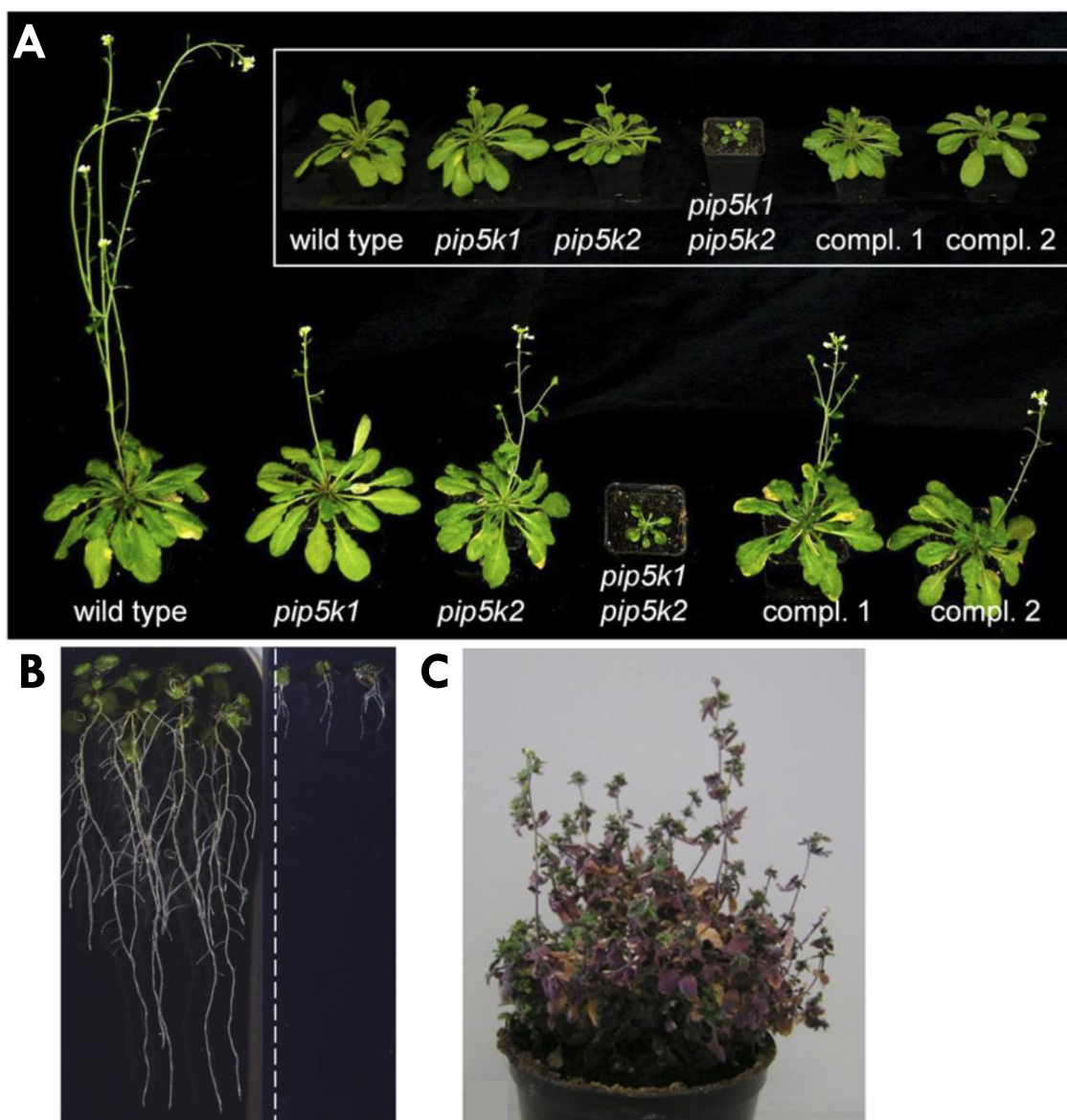


Figure 6 The *pip5k1 pip5k2* double mutant shows a severe phenotype. **A** Documented phenotypes of five-week-old wildtype plants, single mutants, double mutant, and double mutant plants expressing ectopically PIP5K1-EYFP (compl. 1) or PIP5K2-EYFP (compl. 2) under the control of the native *pPIP5K1* or *pPIP5K2* promoter fragments. Plants were grown in soil under long-day conditions in the greenhouse for five weeks. The inset shows the identical four-week-old plants after 4 weeks. Genotypes are as indicated. **B** Seedlings grown for ten days on MS medium under 24 h of light on a vertical plate. Left, wild-type Col-0 controls; right, *pip5k1 pip5k2* double mutants **C** The *pip5k1 pip5k2* double mutant with delayed senescence after ten months under long-day conditions. Figures from Ischebeck et al. 2013.

1.1.4 Nuclear functions of PtdIns(4,5)P₂ and PI4P 5-kinases

The existence of a nuclear PI system, in addition to the PI system in the cytosol and at the membranes facing the cytosol, was described for animal cells as early as 1983 (Smith and Wells, 1983). Since then, a wide variety of processes have been assigned to nuclear PIs in animal cells, yeast and plant cells.

Nuclear PI4P 5-kinases from yeast and mammals have been reported to be partially localised in nuclear speckles and have regulatory effects on cell cycle regulation, meiosis and gene expression control including DNA silencing (Clarke et al., 2001; Divecha et al., 2002; Strahl and Thorner, 2007; Fiume et al., 2019). Studies with plant cells and different plant species provide evidence for functional roles of PI4P 5-kinases and PIs in plant nuclei. For example, overexpression of the human PI4P 5-kinase HsPIP5K1 α in tobacco cell cultures led to changes in histone modification and a reduction in phosphorylation status of the cell cycle regulator retinoblastoma (Dieck et al., 2012b). This suggests that the human PI4P 5-kinase may also influence plant functions. Another study showed that a histone methyltransferase, the ARABIDOPSIS HOMOLOG OF TRITHORAX 1 (ATX1), selectively binds to PtdIns5P via its plant homeodomain finger (Alvarez-Venegas et al., 2006a; Alvarez-Venegas et al., 2006b). This leads to translocation of ATX1 from the nucleus to the cytoplasm, thereby reducing histone modifications by ATX1 and consequently altering transcriptional activity of the corresponding genes (Alvarez-Venegas et al., 2006a; Ndamukong et al., 2010). The nuclear localised OsPIP5K1, a member of the rice PI4P 5-kinase family, interacts with the WUSCHEL-related rice homeobox transcription factor DWARF TILLER 1 DWT1 (Fang et al., 2020). OsPIP5K1, together with the DWT1 / WUSCHEL RELATED HOMEBOX (WOX) appears to regulate the coordination of uniform growth of rice shoots, probably through nuclear phosphoinositide signalling (Fang et al., 2020).

As mentioned previously, Arabidopsis PIP5K2 contains a monopartite NLS within the highly variable Lin-domain (Fig. 3A underlined sequence, (Gerth et al., 2017b)). Ectopic expression of the nuclear-excluded variant PIP5K2_NLS_{AAA} in the *pip5k1 pip5k2* double mutant resulted in a not fully rescued/ complemented phenotype with partial recovery of the overall habitus, root growth and meristem size (Gerth PhD 2018, unpublished). In some cases plants showed severe polarity problems that led to the formation of abnormal flowers and thus to a reduction of seed set in the siliques (Fig. 7, (Gerth PhD 2018, unpublished)). It was shown that PI4P 5-kinases, PtdIns4P and PtdIns(4,5)P₂ have physiological functions in plant nuclei (Alvarez-Venegas et al., 2006b; Ndamukong et al., 2010; Dieck et al., 2012a; Dieck et al., 2012b; Fang et al., 2020), but that their molecular mode of action is currently not well understood. A general role for PIs in the nucleus in the control of transcription, possibly related to the recruitment of transcription factors and thus possibly affecting histone modification. Furthermore, these data suggest that the functions of PI4P 5-kinases and PtdIns(4,5)P₂ in the nucleus are distinct and independent from those at the plasma membrane and in the cytosol, suggesting an independent nuclear localised PI network. How the cell coordinates this without accepting limitations

in the respective compartments is yet unclear. It can be assumed that there are different PIs as well as PI4P 5-kinase pools, which are differently regulated and/ or posttranslationally labelled, so that cellular processes, regulated by PIs or PI4P 5-kinases, can take place in a targeted and coordinated manner (Gerth et al., 2017a; Heilmann and Heilmann, 2022).

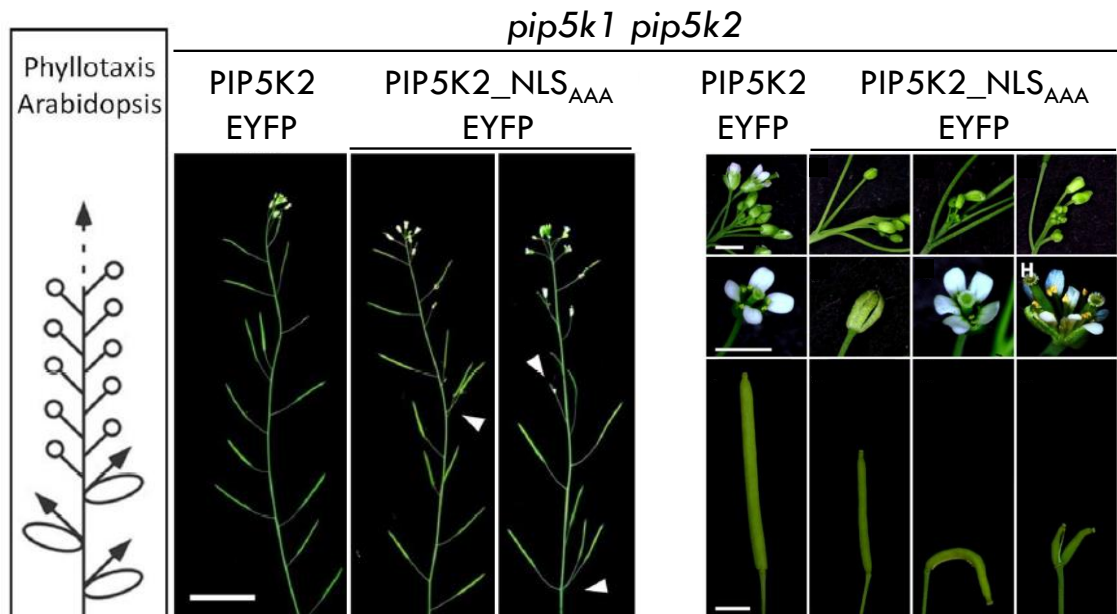


Figure 7 PIP5K2-NLS_{AAA} can partially rescue the *pip5k1 pip5k2* double mutant phenotype. The *pip5k1 pip5k2* double mutant was transformed with PIP5K2 or PIP5K2-NLS_{AAA} under the control of the endogenous *pPIP5K2* promoter. The PIP5K2 control complemented the double mutant phenotype as described in Ischebeck et al 2013. PIP5K2-NLS_{AAA} displayed abnormal phyllotaxis, floral and silique growth. Scale bars, 2 cm (left) and 2 mm (right). White arrows highlight abnormal and asymmetric growth. Figures were taken from Gerth PhD 2018, unpublished.

1.2 Posttranslational modifications of plant PI4P 5-kinases

The regulation of an assumed dynamic PI4P 5-kinase localisation and the regulation of local PI levels is not well understood. However, it is assumed that PI4P 5-kinases are not regulated at the transcriptional level but are subject to posttranslational modification control (Heilmann, 2016a; Hempel et al., 2017; Menzel et al., 2019). Posttranslational modifications (PTMs) of PI modifying enzymes is also supported by the fact that this would be a very fast way to quickly adapt PI4P 5-kinases and thus PI levels to the corresponding cellular needs. The best-known posttranslational modification is reversible protein phosphorylation. Recently published Arabidopsis phospho-proteome studies show that almost half of the Arabidopsis proteome has at least one protein phosphorylation (Mergner et al., 2020). This finding underlines the importance of reversible protein phosphorylation as a posttranslational modification. In conclusion, phosphorylation of a protein can lead to transient changes in

its conformation, which in turn affects catalytic activity, protein stability, interactions with other biomolecules or the subcellular localisation (Burnett and Kennedy, 1954; Jans and Hubner, 1996; Humphrey et al., 2015; Humphrey et al., 2015). In plants, protein phosphorylation occurs mainly at serine and threonine residues, with about 80-85 % of all phosphorylation sites in *Arabidopsis* occurring at serine residues, about 10-15 % at threonine residues and only up to 5 % at tyrosine residues (van Wijk et al., 2014).

In yeast, animal cells and plants, PI4P 5-kinases are targets for protein phosphorylation (Fernandis and Subrahmanyam, 1998; Vancurova et al., 1999; Fernandis and Subrahmanyam, 2000; Park et al., 2001; Audhya and Emr, 2003; Hempel et al., 2017; Menzel et al., 2019). Thus, phosphorylation of human type I PI4P 5-kinase (HsPIP1K1) by CYCLIC AMP-DEPENDENT PROTEIN KINASE A (PKA) resulted in reduced catalytic activity (Park et al., 2001). Similarly, for the PI4P 5-kinase from the yeast *Schizosaccharomyces pombe*, phosphorylation by a casein kinase I (CKI) resulted in reduced *in vitro* activity of the phosphorylated PI4P 5-kinase. (Vancurova et al., 1999; Park et al., 2001; Audhya and Emr, 2003). Also, CKI phosphorylates the only PI4P 5-kinase, *Mss4*, from baker's yeast (*Saccharomyces cerevisiae*). Interestingly, *Mss4* contains a NLS and shows a dynamic dual localisation at both the plasma membrane and the nucleus of yeasts (Audhya and Emr, 2003), like what has been described for PIP5K1 and PIP5K2 from *Arabidopsis* (Ischebeck et al., 2013; Tejos et al., 2014; Gerth et al., 2017b). The phosphorylation of *Mss4* has been reported to be crucial for its correct localisation at the plasma membrane (Audhya and Emr 2003).

For PI4P 5-kinases from *Arabidopsis*, the phosphorylation of PIP5K6 by MITOGEN-ACTIVATED PROTEIN KINASE 6 (MPK6) could be shown. PIP5K6 phosphorylation by MPK6 reduced the catalytic activity of PIP5K6 *in vitro* and *in vivo* and influenced PtdIns(4,5)P₂-dependent pollen tube growth (Hempel et al., 2017) and endocytosis as a response of pathogen-associated molecular patterns (PAMP) treatment (Menzel et al., 2019). The subcellular localisation of PIP5K6 was not affected by MPK6 treatment and PIP5K6 was always localising to the plasma membrane when coexpressed with MPK6. Thus, the effect of MPK6 phosphorylation appears to be regulation of PIP5K6 catalytical activity in response to a stimulus at the plasma membrane (Hempel et al., 2017; Menzel et al., 2019; Heilmann and Heilmann, 2022).

Other protein kinases and phosphorylations in PI4P 5-kinases have not yet been identified. However, studies searching the *Arabidopsis* proteome for protein kinase targets suggest that PI-kinases in general and PI4P 5-kinases in particular are distinct targets for protein phosphorylations (Wang et al., 2020b).

1.3 Protein phosphorylation as possible regulation of the PI4P 5-kinases PIP5K1 and PIP5K2

The dual localisation of Arabidopsis PIP5K1 and PIP5K2 to the plasma membrane and the nucleus is indicative for a separate PI system in the nucleus of plant cells besides the already well-studied cytosolic/ plasma membrane PI system. While there is evidence for the function of such a nuclear PI system, it is still largely unclear how active transport of PI4P 5-kinases from plasma membrane to nucleus is induced. Although a nuclear localisation signal has been detected in the Lin-domain of PIP5K1 and PIP5K2, the nuclear localisation of PIP5K1 and PIP5K2 is not observed to be equally pronounced in all plant organ and cell types (Fig. 2). Hence, nuclear transport is likely to be subject to dynamic regulation (Dieck et al., 2012a; Gerth et al., 2017a).

In different yeast species, casein kinases have been shown to be a family of protein kinases that have regulatory effects on PI4P 5-kinases and can influence PI-kinases both by changing their activity and by altering or enhancing the corresponding subcellular localisation, thus presumably affecting the formation of local PI contents (Vancurova et al., 1999; Park et al., 2001; Audhya and Emr, 2003). Casein kinases are serine/ threonine protein kinases that tend to prefer acidic substrate motifs for phosphorylation, in contrast to most other protein kinases that favour basic amino acid residues upstream of or around the serine or threonine residues to be phosphorylated (Pinna, 1990; Meggio and Pinna, 2003). The recognition sequences of casein kinases are motifs such as S/TxxD/E/S, SxxE/D, S/TDxE, SE, ESE, SxE, ESxE, SxxxE, ESxxxE (Salvi et al., 2009). A peculiarity of the amino acid sequences of PIP5K1 and PIP5K2 is that they have a conspicuous number of glutamate and aspartate residues interrupted with serine or threonine residues at their respective N-termini (Fig. 8A). Such an amino acid composition, at least theoretically, serves casein kinases as substrates. Furthermore, *in silico* studies using online analysis programs (GPS5.0 and NetPhos-3.1, see 4.25.1) predicted serine residues in typical casein kinase phosphorylation motifs in both the N-termini and the Lin-domain, more specifically, in the NLS of PIP5K1 and PIP5K2 (Fig. 8A). And, interestingly, the predicted typical casein kinase phosphorylation motifs appear to be conserved in PIP5K1 and PIP5K2 (Fig. 8). That makes casein kinases good protein kinase candidates to test whether PIP5K1 and PIP5K2 may be regulated by phosphorylation either in function and/ or in their localisation.

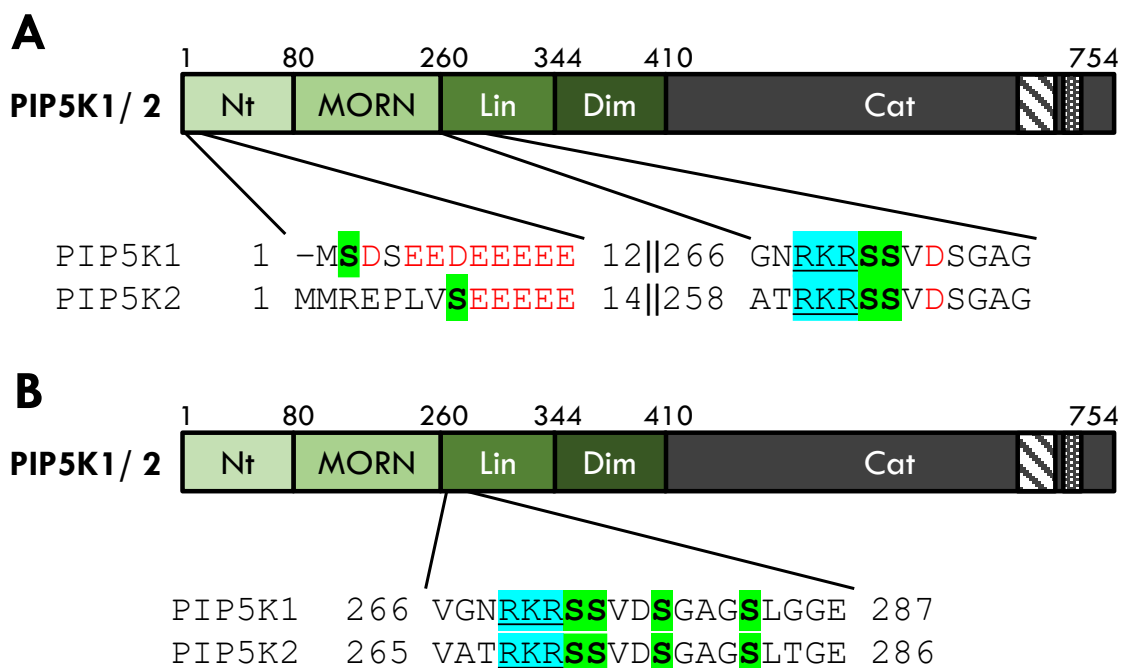


Figure 8 PIP5K1 and PIP5K2 have multiple putative phosphorylation sites. A Putative phosphorylation sites for protein kinase CK2 in the N-terminus and linker domain of PIP5K1 and PIP5K2. **B** *In silico* predicted phosphorylation sites for AGC3 kinase PINOID in the NLS region within the linker domain. Schematic representation of the protein domains of PIP5K1 and PIP5K2. Numbers indicate the position in the amino acid primary structure at domain transitions. Putative phosphorylation sites are marked green. Basic cluster RKR in the NLS region is marked blue. Red letters in A highlight acidic amino acid residues typical for CK2 phosphorylation motifs.

A second candidate protein kinase to phosphorylate PIP5K1 and PIP5K2 in this context is the AGC family serine/ threonine protein kinase, PINOID (PID). PID has an important role in controlling the polarisation of members of the PIN protein family, which mediate polar auxin distribution (Christensen et al., 2000; Benjamins et al., 2001b; Zegzouti et al., 2006; Michniewicz et al., 2007; Kleine-Vehn et al., 2009). Crucial is that PIP5K1, PIP5K2 and PtdIns(4,5)P₂ are also important regulators of PIN trafficking and cell polarity (Mei et al., 2012; Ischebeck et al., 2013; Tejos et al., 2014). Preliminary results from our group showed that PID interacts with PIP5K2 and phosphorylates PIP5K2 *in vitro*. A further indication of a physiological regulatory relationship between PIP5K1 / PIP5K2 and PID protein kinase comes from the comparison of Arabidopsis mutants and overexpression plants (Fig. 9). PID overexpression (OE) and *pip5k1 pip5k2* double mutants both showed strongly shortened root growth and dwarfism (Fig. 9A). Vice versa, plants in which PIP5K1 or PIP5K2 is overexpressed (Ischebeck et al., 2013) and AGC3 protein kinase mutants (PID *pid wag1 wag2*; Dhonukshe et al., 2015) show the same agravitropic phenotype in which the root displays a wavy growth (Fig. 9B). These corresponding and reciprocal exchangeable Arabidopsis phenotypes could also indicate a possible

regulatory link between the interaction partners PIP5K1, PIP5K2 and AGC3 kinases, such as PID. But until now the sites and the function of the PID mediated PI4P 5-kinase phosphorylation remains unclear.

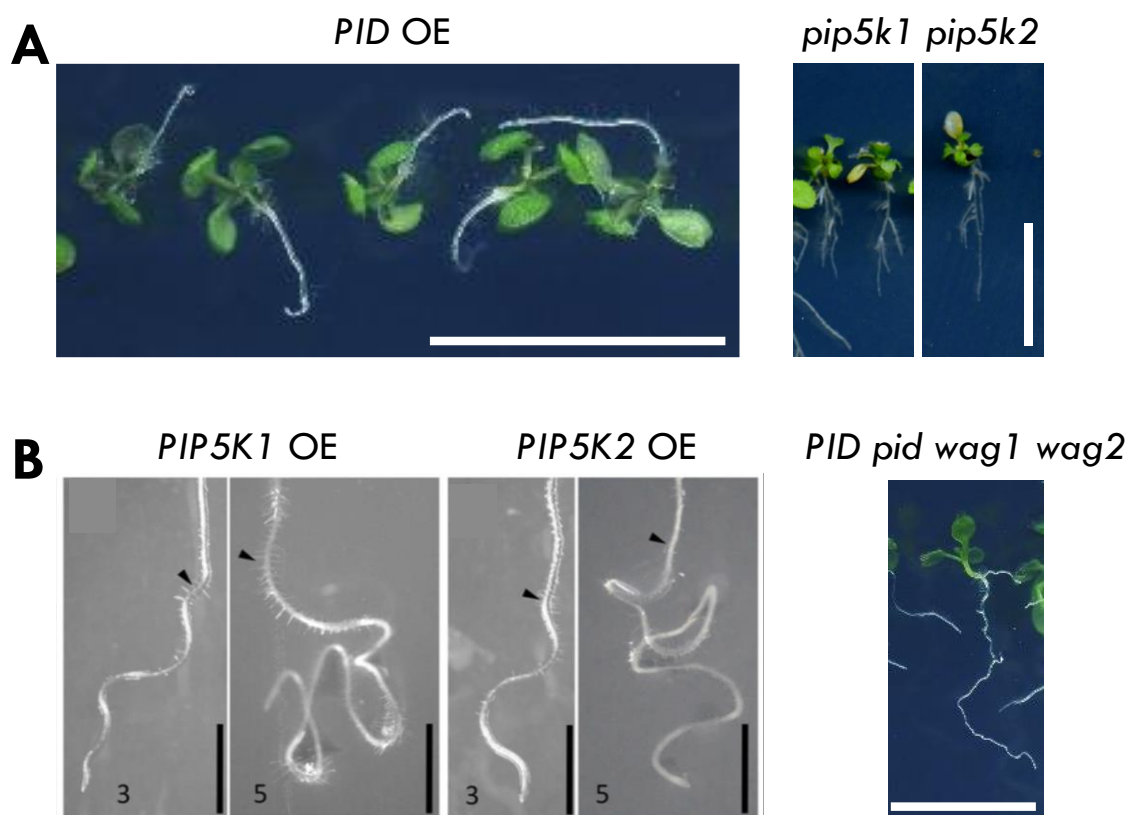


Figure 9 Arabidopsis with altered PI4P 5-kinase and AGC3 protein kinase expression share reciprocal phenotypes. A *PID* overexpressor (OE) lines and *pip5k1 pip5k2* double mutant share dwarfism, shortened roots, polarity issues and anthocyanin incorporation. Scale bars, 1 cm **B** β -estradiol induced overexpression of *PIP5K1* or *PIP5K2* display dose dependent wavy root growth. Similar phenotypes are depicted in the triple mutants of *PID pid wag1 wag2*. Scale bar in PI4P 5-kinase overexpressors is 1 mm, Scale in *PID pid wag1 wag2* is 1 cm. Black arrows indicate root tip location before treatment with β -estradiol. PI4P 5-kinase overexpressors are taken from Ischebeck et al. 2013.

The known functions of the protein kinases of the casein kinase family, as well as the AGC3 kinase family are discussed in the following sections:

1.3.1 The protein kinase family CK2

Casein kinases were named after casein from milk because it was used as an *in vitro* test substrate for the protein kinases originally extracted from rat liver mitochondria (Burnett and Kennedy, 1954), although it was always clear that casein was not the natural substrate of casein kinases (Allende and Allende, 1995). Casein kinases are ubiquitously expressed, constitutive active serine/ threonine protein kinases present in all eukaryotic organisms (Allende and Allende, 1995; Litchfield, 2003). Casein kinases are divided into two unrelated independent protein kinase

groups, representatives of the casein kinase 1 (CK1) family forming a separate protein kinase group, whereas representatives of the casein kinase 2 (CK2) family are assigned to the superfamily of CMGC protein kinases (Allende and Allende, 1995; Hanks and Hunter, 1995). The CMGC super family also includes, for example, cyclin-dependent kinases and mitogen-activated protein kinases including the already mentioned MPK6 (see 131.2).

In contrast to CK2, which can phosphorylate unphosphorylated substrates with the above-mentioned "acidic" recognition sequences, it is assumed that CK1 enzymes are not able to phosphorylate "unphosphorylated" substrates. This means that CK1 enzymes require an already existing phosphor-serine residue within the recognition motif of the substrate, which is equivalent to a "hierarchical phosphorylation" (Flotow and Roach, 1991; Ferrarese et al., 2007; Venerando et al., 2014). Also, the importance of the acidic environment around the amino acid residue (mostly serine) to be phosphorylated is more typical for CK2 than for CK1 (Venerando et al., 2014). For this reason, this study focused on the family of CK2 protein kinases.

Native CK2, isolated from animal tissues, is a heterotetrametric holoenzyme consisting of two catalytic alpha- and two regulatory beta-subunits (Fig. 11, (Hathaway and Traugh, 1979; Niefind et al., 2001; Filhol et al., 2004)). The Arabidopsis genome contains four genes each encoding the alpha-subunits (CKA1, CKA2, CKA3 and CKA4) and beta-subunits (CKB1, CKB2, CKB3 and CKB4). In literature, it is discussed that plant alpha-subunits are likely able to be individually catalytically active even outside the holoenzyme formation (Yan and Tao, 1982; Niefind et al., 2001; Mulekar and Huq, 2014). A crystal structure analysis of CK2 showed that the beta-subunit mediates the formation of inactive polymer structures (Lolli et al., 2012; Lolli et al., 2014; Venerando et al., 2014). It is not clear whether this also happens within living cells, but if this is the case it would mean an unexpected mechanism for the regulation of the otherwise constitutively active CK2 protein kinases (Lolli et al., 2012; Lolli et al., 2014; Venerando et al., 2014).

Most of the Arabidopsis CK2 alpha- and beta-subunits showed clear nuclear localisation in subcellular localisation studies (Fig. 10). While the alpha-subunits were almost exclusively detected in the nucleus, most beta-isoforms also showed cytosolic localisation (Fig. 10, (Salinas et al., 2006)). Exceptions were the subunits CKA4, which clearly localised in plastids, and CKB4, which showed exclusively cytoplasmic localisation (Fig. 10, (Salinas et al., 2006; Schönberg et al., 2014; Mulekar and Huq, 2015)).

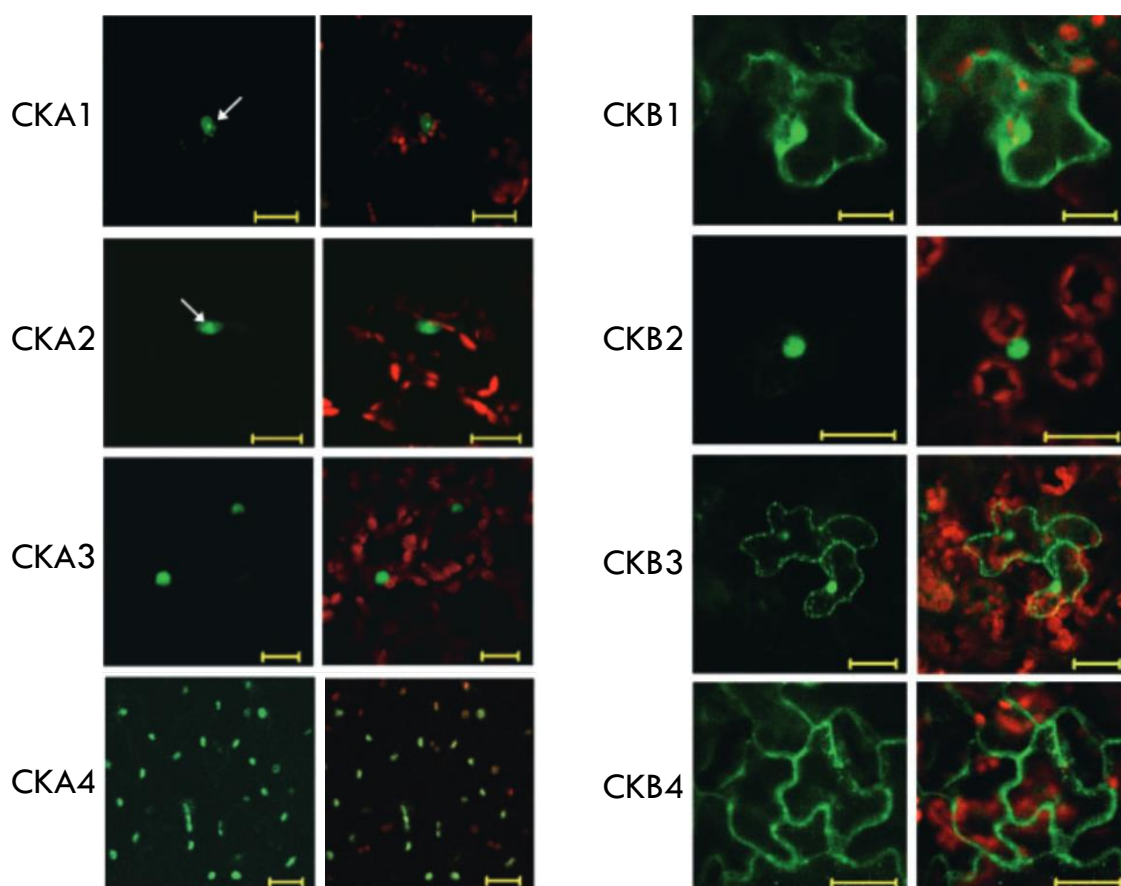


Figure 10 CK2 subunits localise mainly to the nucleus. Summary of subcellular localisation studies with CK2 subunits in Arabidopsis and tobacco. CKA2 and CKA3 were expressed as GFP-fusions in Arabidopsis under the control of a β -estradiol inducible promoter. All other subunits were transfected into *Nicotiana benthamiana* leaves using *Agrobacterium tumefaciens* and expressed under the control of the pCaMV35S promoter. Green, GFP fluorescence. Red, Chlorophyll A. White arrows highlight discrete structure within the nucleus, presumably the nucleolus. Scale bars, 20 μ m. Images from Salinas et al. 2006.

Overall, the protein kinases CK2 from Arabidopsis, or plants in general, have not been studied very intensively. However, studies on CK2 protein kinases in a wide variety of plant species is also increasing the number of CK2 substrates in plants (Riera et al., 2004; Salinas et al., 2006; Mulekar and Huq, 2014; Vilela et al., 2015; Chen et al., 2018; Rödiger et al., 2020; Wang et al., 2022). CK2 substrates include proteins that function as transcription factors and are involved in translation and the cell cycle (Mulekar et al., 2012; D'Alessandro et al., 2019). For example, CK2 protein kinases in plants regulate the circadian clock (Sugano et al., 1998; Sugano et al., 1999; Lu et al., 2011) and other light-regulated processes (Krohn et al., 2003; Zhang et al., 2020a), as has been well described for CK2 in animals (Tamaru et al., 2009), which suggests that many functions of this CK2 protein kinase occurring in all eukaryotes seem to be conserved.

The regulation of the circadian clock by CK2 in Arabidopsis is based on the phosphorylation of the transcription factors CIRCADIAN CLOCK ASSOCIATED 1 (CCA1) and

the myb-like transcription factor LATE ELONGATED HYPOCOTYL (LHY), and subsequently affects the binding affinity of CCA1 to DNA and the gene expression of CCA1-controlled genes as well (Fig. 11 A, B and C, (Sugano et al., 1999; Daniel et al., 2004)).

First evidence of CK2 involvement in light signalling was published in 1999, when knockdown of CK2 affected the transcript levels of CHALCONE SYNTHASE, chlorophyll A/ B-binding proteins and the small subunit of RIBULOSE-1,5-BISPHOSPHATE CARBOXYLASE-OXYGENASE (RuBisCO) (Lee et al., 1999). The ELONGATED HYPOCOTYL 5 (HY5) bZIP transcription factor is phosphorylated by CK2 in light, inhibiting the interaction with the E3 ligase COAT PROTEIN COMPLEX 1 (COP1) and stabilising HY5 (Fig 11 D and E, (Hardtke et al., 2000; Lau and Deng, 2012)). The CK2 dependent phosphorylation simultaneously decreases DNA binding affinity of HY5. Phosphorylated and dephosphorylated variants of HY5 are detectable in plant cells, indicating further fine tuning due to CK2 phosphorylation in light signalling with HY5 (Hardtke et al., 2000). The same was observed for other positive regulators of photomorphogenesis, such as the Helix-Loop-Helix transcription factor LONG HYPOCOTYL IN FAR RED (HFR1) (Fig 11 D and E, (Park et al., 2008)).

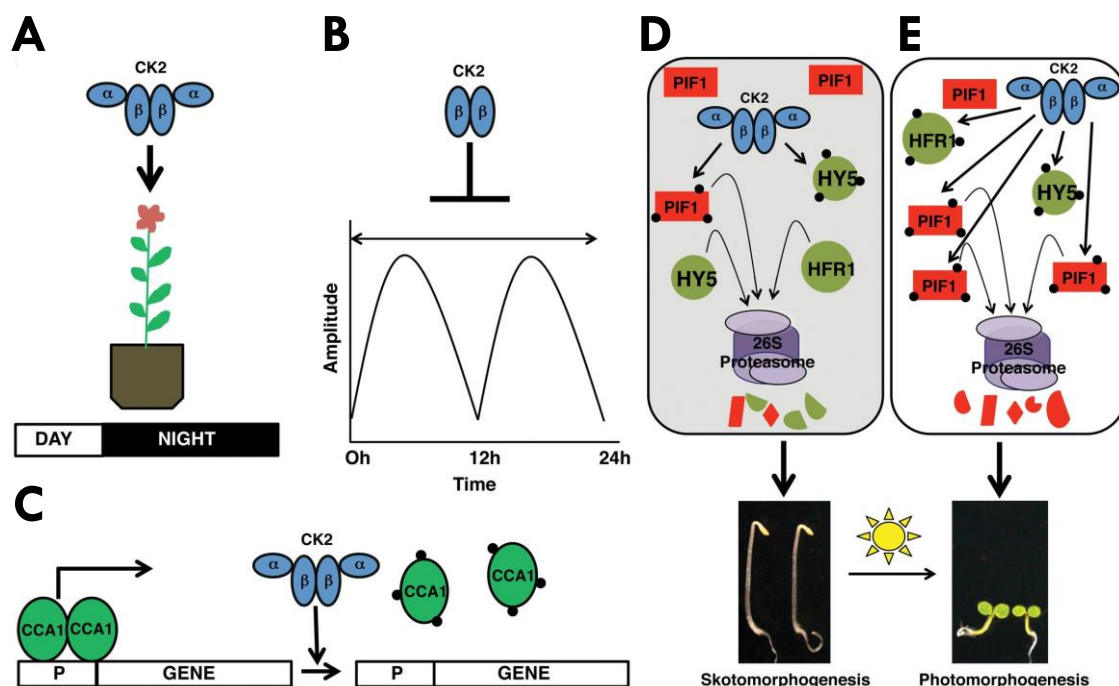


Figure 11 Plant CK2 regulates circadian clock and photomorphogenesis. **A** CK2 regulates flowering time under short-day and long-day conditions. **B** CKB subunits deregulate period length when overexpressed. **C** CK2 phosphorylates CCA1 and the phosphorylation reduces dimerization of CCA1 resulting in reduced DNA binding and CCA1 dependent gene expression. **D** In the dark, the positively acting transcription factors (HY5 and HFR1) are degraded through the 26S proteasome. The negatively acting transcription factor PIF1A is highly abundant in the dark, repressing photomorphogenesis resulting in etiolated seedling growth. **E** In response to light, HY5 and HFR1 are stabilised by CK2 phosphorylation and light promotes rapid degradation of PIF1 and other PIFs to promote

photomorphogenesis resulting in de-etiolated seedlings. CK2 phosphorylates both the positive and negatively acting components presumably under both dark and light conditions. CCA1, Circadian clock associated 1; PIF, Phytochrome interacting factor; HY5, Elongated hypocotyl 5; HFR1, Long hypocotyl in far red. Figures from Mulekar and Huq 2014.

Antagonistic to the positive regulators of photomorphogenesis HY5 and HFR1 the negative regulators of photomorphogenesis with phytochrome-interacting factors (PIFs) are also regulated through phosphorylation by CK2 (Fig. 11 D and E, (Bu et al., 2011)). CK2 phosphorylation of PIF results in degradation of PIF in red light conditions, meaning that CK2 promotes plant growth under such light conditions by stabilising positive regulators of photomorphogenesis and promoting the degradation of negative regulators such as PIF (Bu et al., 2011). Interestingly, PIF itself regulates the transcript of PIP5K1 (Calderon et al., 2022). The mechanism of HY5, HFR1 and PIF1 in light signalling has been identified but other substrate specificities and molecular mechanism in plant CK2s still remain unknown (Mulekar and Huq, 2014).

Further studies with CK2 mutants also indicate that CK2 can phosphorylate transcription factors (TFs) that regulate hormone signalling pathways in plants and that these are also subject to regulation. Regulated TFs of phytohormone signalling pathways include, for example, the TF TGA2 of salicylic acid signalling (Kang and Klessig, 2005; Mulekar et al., 2012) and the bZIP TFs EmBP-2 and EmBZ-1 in the abscisic acid signalling pathway (Riera et al., 2004; Nieva et al., 2005). Preliminary studies also indicate a link to the auxin signalling pathway (Moreno-Romero and Martínez, 2008; Moreno-Romero et al., 2011). Overexpression of a dominant-negative alpha-subunit of CK2 resulted in reduced auxin transport and misexpression of some PIN proteins, leading to reduced lateral root growth in both dominant-negative and the *cka1 cka2 cka3* triple mutant (Moreno-Romero and Martínez, 2008). Thus, there is also evidence here for another level of regulation of PIN proteins and thus auxin transport, which also involves the PI4P 5-kinases PIP5K1 and PIP5K2 (section 1.1.3).

1.3.2 AGC3 protein kinases

AGC kinases are the best studied protein kinase family in eukaryotes and are commonly acting as effector from second messengers including the name giving CYCLIC AMP-DEPENDENT PROTEIN KINASE A (PKA), CYCLIC GMP-DEPENDENT PROTEIN KINASE G (PKG) and DIACYLGLYCEROL ACTIVATED/ PHOSPHOLIPID-DEPENDENT KINASE C (PKC) (Bögge et al., 2003; Rademacher and Offringa, 2012). AGC kinases have been shown to play important roles in the regulation of growth, metabolism, proliferation, cell division, and apoptosis.

In *Arabidopsis* 39 members of the AGC kinases are known, of which 23 are classified as plant specific forming the family of AGCVIII kinases (Fig. 12, (Bögge et al., 2003; Galván-Ampudia and Offringa, 2007; Rademacher and Offringa, 2012)). The AGCVIII kinases show high similarities to PKAs, which are otherwise not found in plants as direct homologous enzymes. AGCVIII kinases probably perform similar functions in the regulation of growth and cell polarity as PKAs do in animals. The family of AGCVIII kinases is further divided into four subfamilies named AGC1-AGC4 (Fig. 12, (Hanks and Hunter, 1995; Galván-Ampudia and Offringa, 2007; Rademacher and Offringa, 2012)). The AGC3 subgroup of AGCVIII has four members: PINOID (PID) WAG1, WAG2 and AGC3-4 (Fig. 12). The kinases PID, WAG1 and WAG2 can phosphorylate the large central hydrophilic loop of PIN proteins (Christensen et al., 2000; Benjamins et al., 2001b; Kleine-Vehn et al., 2009; Dhonukshe et al., 2015). As mentioned before, PIN proteins are integral membrane transporters that mediate the directed auxin transport in plant tissues and thus enable the establishment and maintenance of an auxin gradient (Fig. 13, (Friml et al., 2004; Dhonukshe et al., 2007; Adamowski and Friml, 2015)). This auxin gradient is crucial for plant growth and development (Mockaitis and Estelle, 2008). PROTEIN PHOSPHATASE-2 (PP2A) and PROTEIN PHOSPHATASE-6 (PP6), which influence the polarity of PIN proteins in the cell, have been identified as antagonists of PIN-phosphorylating kinases (Fig. 13, (Michniewicz et al. 2007; Dai et al. 2012)). Phosphorylation by AGC3 kinases or dephosphorylation of PIN proteins, exemplified by the isoform PIN1, contributes to recycling from the basal plasma membrane and sorting to the apical side of the cell (Fig. 13) and/ or influences the activity of PIN proteins (Friml et al., 2004; Zourelidou et al., 2014).

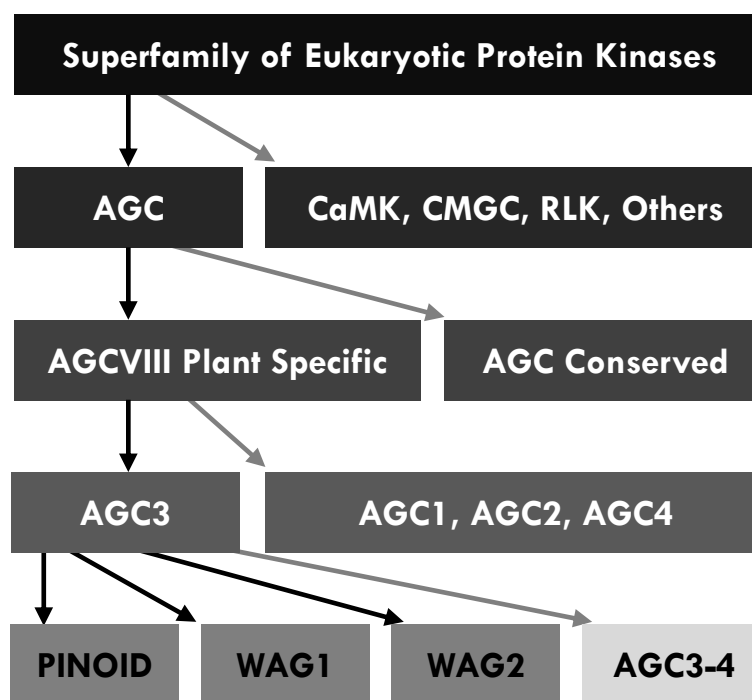


Figure 12 Origin of AGC3 protein kinases PINOID, WAG1 and WAG2. The superfamily of eukaryotic protein kinases is grouped into different families. AGC kinase family is divided into conserved kinase families that exist in all species while plant specific AGC kinases are grouped into the AGCVIII protein kinase family. Further classification leads to the four subgroups AGC1-AGC4. The AGC3 group has four members, of which PINOID, WAG1 and WAG2 are important protein kinases for cell polarity regulation. CaMK, Calcium and calmodulin dependent kinases; CMGC, Cyclin dependent-, cyclin dependent like- and mitogen-activated-protein-kinases; RLK, receptor-like kinases.

This asymmetric distribution of PIN proteins is mediated by directed exocytosis and clathrin-mediated endocytic recycling (Fig. 13). As previously described in section 1.1.3, PIP5K1, PIP5K2 and PtdIns(4,5)P₂ regulate CME and thus have a direct influence on PIN polarisation (Mei et al., 2012; Ischebeck et al., 2013; Tejos et al., 2014). Furthermore, PI4P 5-kinases and PtdIns(4,5)P₂ also show apico-basal polar localisation in root cells (Fig. 2D and 13 (Ischebeck et al., 2013; Tejos et al., 2014; Gerth et al., 2017b)). In the *pip5k1 pip5k2* Arabidopsis double mutant the polar apico-basal distribution of PIN proteins is disturbed, and these mutants show clear auxin distribution defects (Ischebeck et al., 2013; Tejos et al., 2014). This non-polar PIN distribution in the *pip5k1 pip5k2* double mutant can at least partially be explained by an impaired endocytic recycling of the PIN proteins from the plasma membranes (Ischebeck et al., 2013; Tejos et al., 2014; Marhava et al., 2020). The described reciprocal phenotypes of Arabidopsis with altered PI4P 5-kinase and AGC3 kinase expression also give a hint that PIP5K1 and PIP5K2 might be targets of the AGC3 protein kinase family (Fig. 9, (Benjamins et al., 2001b; Ischebeck et al., 2013; Dhonukshe et al., 2015)).

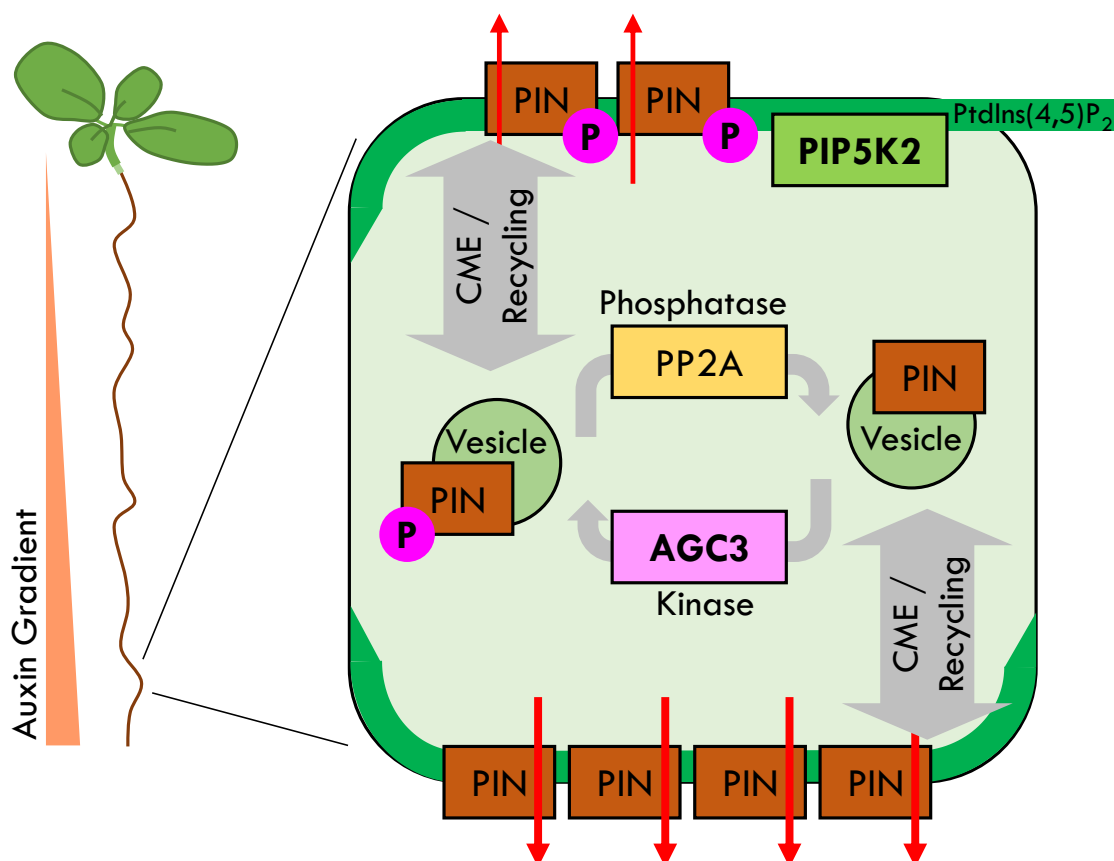


Figure 13 The direction of auxin flow is determined by the polar PIN localisation. Polar distribution of the auxin transporters PIN is affected by phosphorylation or dephosphorylation of PIN-transporters. Thereby, the protein kinases of the AGC3 family PID, WAG1 and WAG2 as well as phosphatases such as PP2A play a role. The PIN proteins are removed from the membranes by CME and reinstalled into corresponding target membranes via distribution of the endo-membrane system. The PI4P 5-kinases PI5PK1, PIP5K2 and PtdIns(4,5)P₂, which are also polar distributed in the cell, play an important role in the regulation of the CME and thus also in PIN distribution. Green lines indicate polar distribution of PtdIns(4,5)P₂. Red arrows indicate auxin transport. CME, Clathrin-mediated endocytosis.

The control of PI metabolism by protein phosphorylation most likely is an important regulator of the temporal and local formation of PIs and the associated control of subsequent physiological and cellular responses. However, it has also been shown that PIs can act as upstream effectors for protein kinases, as some protein kinases have been shown to bind to PIs. These include the prominent example of the master regulator of AGCVIII kinases, PHOSPHOINOSITIDE-DEPENDENT PROTEIN KINASE 1 (PK1) (Anthony et al., 2004; Mora et al., 2004; Zegzouti et al., 2006), but also the protein kinases of the AGCVIII family, which includes PID, WAG 1, and WAG2 (Barbosa et al 2016). These protein kinases bind to PIs and/ or other anionic lipids and are thus recruited to the plasma membrane (Zegzouti et al. 2006; Barbosa et al 2016; Wang et al. 2019). This suggests that regulatory feedback effects may occur (Marhava et al., 2020; Heilmann and Heilmann, 2022).

1.4 Research goals

The regulatory network that controls PI4P 5-kinases and PI abundance is very complex and little research has been done on it. The broad goal of this work was to develop a better understanding of the posttranslational mechanisms by which the signal transducers themselves, the PI4P 5-kinases, are regulated. One hypothesis was that nuclear-cytoplasmic shuttling of PIP5K1 and PIP5K2 depends on cellular requirements and that subcellular localisation, especially nuclear localisation of PI4P 5-kinases, is regulated by NLSs that may be masked or active, depending on posttranslational modifications. Recent studies indicate that posttranslational regulation of PI4P 5-kinases has an important role in both subcellular distribution within the cell and influencing their function and/ or PI-kinase activity. To date, not much is known about regulators of PI-kinase and little has been studied. However, two protein kinases have been identified, protein kinase CK2 and the AGCVIII kinase PID, for which there is evidence that they appear to influence regulation of PI signals. The following research aims were defined:

- Investigate in which tissue, cell types and developmental stages the well-studied PIP5K2 localises in the nucleus.
- Perform comparative studies between PIP5K2 from Arabidopsis and a very distinct nuclear localised PIP5K1 from poppy.
- Determine whether there are specific protein-protein interactions between PIP5K1 and/ or PIP5K2 with protein kinase CK2 subunits and the AGCVIII family members, PID, WAG1, and WAG2.
- Determine whether PIP5K1 and/ or PIP5K2 are phosphorylated by either the catalytic active protein kinase alpha subunits of CK2 or by the AGCVIII protein kinase PID.
- Investigate initial steps to determine the specific phosphorylation sites in PIP5K1 or PIP5K2 and establish a link between phosphorylation and PI4P 5-kinase function.

2 Results

2.1 PIP5K1 and PIP5K2 dynamically localise to plant nuclei

PIs including PtdIns(4,5)P₂ are involved in fundamental cellular processes such as cytoskeleton dynamics, endo- and exocytosis, vesicle transport and are acting in biotic and abiotic stress responses (König et al., 2008; Ischebeck et al., 2008; Stenzel et al., 2012; Ischebeck et al., 2013; Heilmann and Heilmann, 2015; Heilmann, 2016a). While most of these functions are studied at the plasma membrane, the PtdIns(4,5)P₂ producing enzymes PI4P 5-kinases were repeatedly discovered in plant nuclei (Lou et al., 2007; Dieck et al., 2012b; Ischebeck et al., 2013; Tejos et al., 2014). For PIP5K2 from Arabidopsis at least one functional NLS was discovered and characterised (Gerth et al., 2017b). While having one functional NLS, the subcellular localisation of fluorescent protein tagged PIP5K2-EYFP in plant nuclei appears very dynamic and limited to certain developmental stages and cell types. In general, the EYFP signal of PIP5K2-EYFP in the nucleus could be observed more frequently in root and meristematic cells than in leaf cells (Tejos et al., 2014; Gerth et al., 2017b).

Since little to no fluorescent signal can be detected in Arabidopsis plants stably transformed with fluorescently labelled PI4P-5 kinases (Ischebeck et al., 2013; Tejos et al., 2014), protoplasts were used for the localisation studies. Protoplasts were isolated from either Arabidopsis wild type leaves, Arabidopsis leaf cell culture, Arabidopsis roots or tobacco BY-2 cell culture (see 4.22) and transformed with a *pCaMV35S:PIP5K2-EYFP* construct (see 4.12.4), and the subcellular fluorescence distribution was analysed by laser-scanning-microscopy (LSM880; see 4.24.1).

The images shown in figure 14 are maximum intensity z-projections of z-stacks covering the entire protoplasts or confocal planes highlighting the nuclear area. In Arabidopsis leaf mesophyll protoplasts, the fluorescence of PIP5K2-EYFP showed in all cells a cytosolic and plasma membrane pattern (Fig. 14A). In 60 % of the observed cells PIP5K2-EYFP showed exclusively plasma membrane localisation (Fig. 14A). In 40 % of the cells, a nuclear localisation pattern was detectable (Fig. 14B). A clear presence or absence of PIP5K2-EYFP in the nucleus was shown by cotransformation with a nuclear NLS-DsRed marker but was mostly avoided to eliminate crosstalk of different fluorescent proteins and outshining as NLS-DsRed depicted extensive fluorescence intensities compared to PI4P 5-kinase-EYFP constructs (Fig. 14B, lower panel). In contrast, after expression of PIP5K2-EYFP in BY-2 tobacco root cell culture protoplasts, 80% of protoplasts displayed PIP5K2-EYFP

signal in both, the plasma membrane, and in the nucleus (Fig. 15A, lower panel). Only 20% of BY-2 protoplasts showed exclusive plasma membrane localisation (Fig. 15A, upper panel). The results suggest that PIP5K2-EYFP may localise more frequently to the nucleus in root cells than in leaf cells.

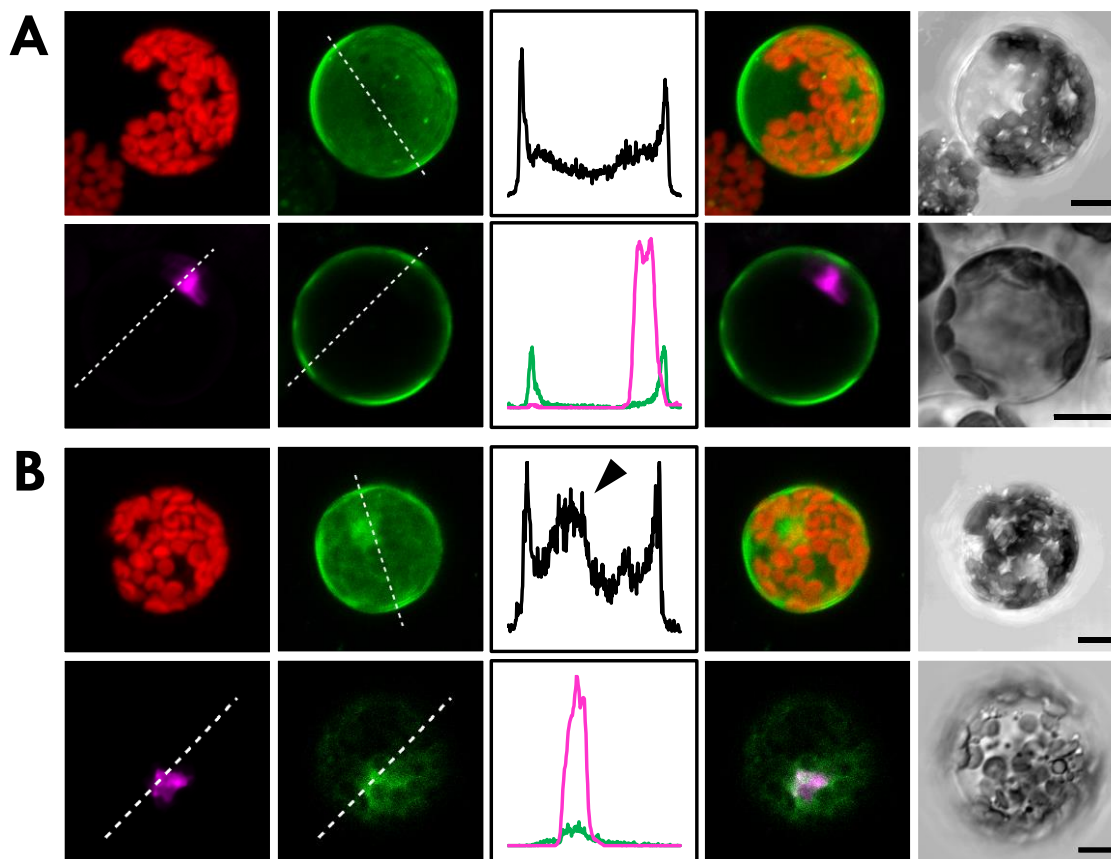


Figure 14 PIP5K2 localises dynamically to plant nuclei in Arabidopsis mesophyll protoplasts. Arabidopsis mesophyll protoplasts were transiently transformed with *pEntryA-pCaMV35S::PIP5K2-EYFP* or *pEntryA-pCaMV35S::PIP5K2-EYFP* and *pEntryA-pCaMV35S::NLS-DsRed*. Subcellular localisation of fluorescent protein fusions was analysed with the LSM880. **A** and **B** Arabidopsis mesophyll protoplasts expressing PIP5K2-EYFP (upper panels) and PIP5K2-EYFP and NLS-DsRed (lower panels). Shown are projections of z-stacks covering the entire protoplast with 1 μm intervals between sections (upper panels) or confocal planes highlighting the nuclear area (lower panels). Autofluorescence of chlorophyll A is depicted in red, NLS-DsRed in magenta and PIP5K2-EYFP in green. Black arrow highlights nuclear PIP5K2-EYFP signal. Scale bars, 10 μm . Images from A are representative for four independent experiments with 31 (upper panel) and eleven (lower panel) protoplasts. Images from B are representative for three independent experiments counting 21 (upper panel) and seven (lower panel) cells in total.

A previous study reported that PIP5K2-EYFP localised to the nucleus particularly in meristematic root cells (Gerth et al. 2017). Since cell culture cells are also stimulated to divide by the presence of phytohormones, it was suggested that phytohormones such as auxin and cytokinin might influence the subcellular distribution of PIP5K2-EYFP in the cells. Studies connecting the alteration of PIP5K1 and PIP5K2 transcript levels upon auxin treatments (Mei et al. 2012; Tejos et al. 2014) and findings on

PIs that modulate auxin-dependent transcription by altering the activity of the histone acetyltransferase GENERAL CONTROL NON-DEPRESSIBLE 5 (GCN5) support this theory (Daamen PhD, 2022).

To investigate a possible link between auxin signalling, cell cultures, and root cells with more prominent nuclear PIP5K2, a new cell culture line from Arabidopsis leaves was established (see 4.6) and Arabidopsis roots used as basis for protoplast isolations (see 4.22) and PIP5K2-EYFP localisation studies as described above. Leaf cell cultures displayed huge, often multiple, nuclei when nuclear marker NLS-DsRed was transformed (Fig. 15B upper panel). In leaf cell culture protoplasts PIP5K2-EYFP was prominently localising to the plasma membrane (Fig. 15B lower panel). Arabidopsis root cell protoplasts displayed PIP5K2-EYFP mainly at the plasma membrane but, as described for Arabidopsis leaf mesophyll protoplasts, other protoplast species in low percentages showing an additional nuclear localisation of PIP5K2-EYFP were detectable (Fig. 15C). Arabidopsis leaf mesophyll protoplasts were also hormone treated directly with 1 μ M 1 naphthaleneacetic acid (NAA) prior imaging (Fig. 15D). The NAA treatment did not alter the subcellular localisation of PIP5K2-EYFP in our experiments.

In essence, the localisation studies of PIP5K2-EYFP showed that PIP5K2 localises mainly to the plasma membrane, except for BY-2 root cells of tobacco, which reliably showed additional localisation to the nucleus.

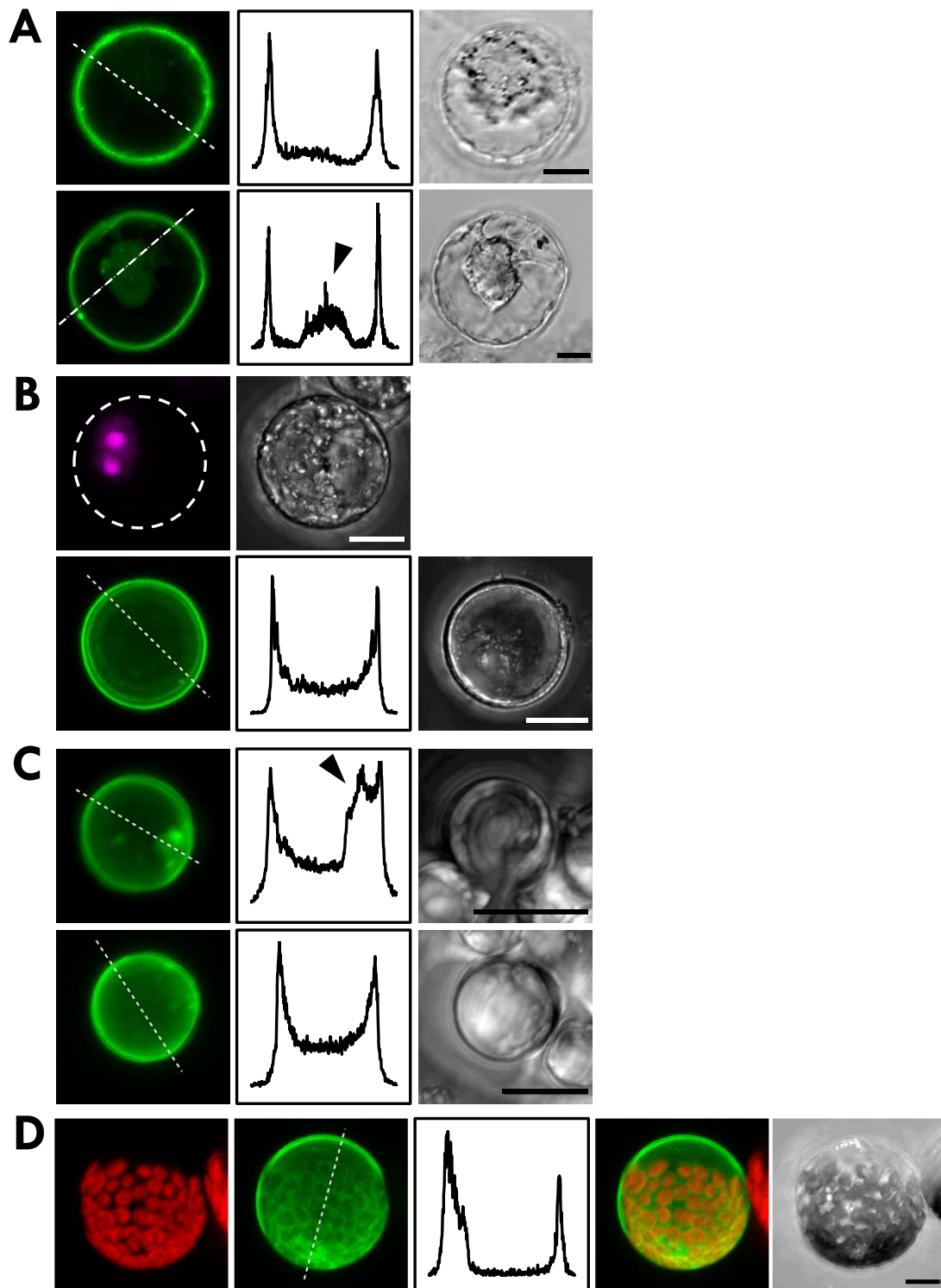


Figure 15 PIP5K2-EYFP displays enhanced nuclear localisation in BY-2 protoplasts. Tobacco BY-2 cell culture, Arabidopsis leaf cell culture and Arabidopsis root and mesophyll protoplasts were transiently transformed *pEntryA-pCaMV35S::PIP5K2-EYFP* or *pEntryA-pCaMV35S::NLS-DsRed*. Subcellular localisation of fluorescent protein fusions was analysed with the LSM880. **A** BY-2 cell culture protoplasts expressing PIP5K2-EYFP. **B** Arabidopsis leaf cell culture protoplasts expressing NLS-DsRed (upper panel) or PIP5K2-EYFP (lower panel). **C** Arabidopsis root protoplasts expressing PIP5K2-EYFP. **D** Arabidopsis leaf mesophyll protoplasts expressing PIP5K2-EYFP after treatment with 1 μm NAA. Shown are projections of a z-stack covering the entire protoplast with 1 μm intervals between sections (B, C and D) or confocal planes highlighting the nuclear or plasma

membrane area (A). Autofluorescence of chlorophyll A is depicted in red, NLS-DsRed in magenta and PIP5K2-EYFP in green. Black arrow highlights nuclear PIP5K2-EYFP signal in intensity profiles. Scale bars measure 10 μm . Images from A are representative of four independent experiments using a total of 25 cells. Images from B are representative for one independent experiment with five cells in total (upper panel) and for three independent experiments using a total of 27 cells (lower panel). Images from C are representative of three independent experiments counting 18 cells and were done in cooperation with bachelor student Thea Stephan. In D, image represents protoplasts of three experiments with a total of 35 cells.

2.2 AtPIP5K1 and AtPIP5K2 have a close homolog in *Papaver somniferum*: comparative biology to study nuclear cytoplasmic shuttling

The importance of PtdIns(4,5)P₂ and PI4P-5 kinases is underlined by the constant presence of several PI4P-5 kinase isoforms in higher eukaryotes, including plants. The number of PI4P 5-kinase isoforms also indicates the multitude of distinct functions of the individual isoforms. However, phylogenetic studies showed that the number of PI4P 5-kinases differs between different species (Zhang et al., 2020b). *Arabidopsis* and rice each have eleven genes, *Phaseolus vulgaris* only six genes coding for PI4P 5-kinase isoforms (Zhang et al., 2020b). Today, many genomes of various plant species have now been sequenced, including the genome of the opium poppy (*Papaver somniferum*; (Guo et al., 2018)). In opium poppy, five PI4P 5-kinase isoforms were identified, which were annotated as PsPIP5K1, PsPIP5K6, PsPIP5K7/8 and PsPIP5K10/11. The coding sequence of PsPIP5K1 (LOC113283286, XM_026532494.1) was cloned (see 4.1.2.4, Barbora Hans, Comenius University Bratislava/ MLU Halle) and started to be characterised. PsPIP5K1 was classified as Type B PI4P 5-Kinase and shows high sequence homology to *Arabidopsis* PIP5K1 (AtPIP5K1) and PIP5K2 (AtPIP5K2)(see 4.25.2) with 70.4 % and 69.4 % amino acid identity, respectively (Fig. 16A).

In AtPIP5K2, a functional NLS in the Lin-domain was identified and characterised as functional (Gerth et al., 2017b). This sequence region is highly conserved in PsPIP5k1 although the Lin-domain is described as a highly variable and disordered region (Stenzel et al., 2012). One difference from AtPIP5K2 is that PsPIP5K1 has an additional amino acid stretch N-terminal to the NLS (Fig. 16B). Thus, the Lin-domain of PsPIP5K1 is slightly longer than in AtPIP5K. In this extended Lin-domain sequence of PsPIP5K1, two additional basic arginine are present twelve amino acids upstream the amino acid cluster of the putative NLS sequence in PsPIP5K1 (Fig. 16B, amino acids highlighted in blue).

Initial studies on the subcellular localisation (see 4.22) of *pEntryA-pCaMV35S::PsPIP5K1-EYFP* (see 4.1 2.4) showed that PsPIP5K1-EYFP located in the nucleus of Arabidopsis mesophyll protoplasts and faint cytosolic or plasma membrane localised PsPIP5K1-EYFP fluorescence signal was detectable (Fig. 16C). By the reciprocal localisation of PsPIP5K1 (especially in the cell nucleus) to AtPIP5K2 (especially at the plasma membrane), PsPIP5K1 thus appeared to be well suited for using comparative biology to find out the sequence determinants for nuclear-cytoplasmic shuttling of AtPIP5K2.

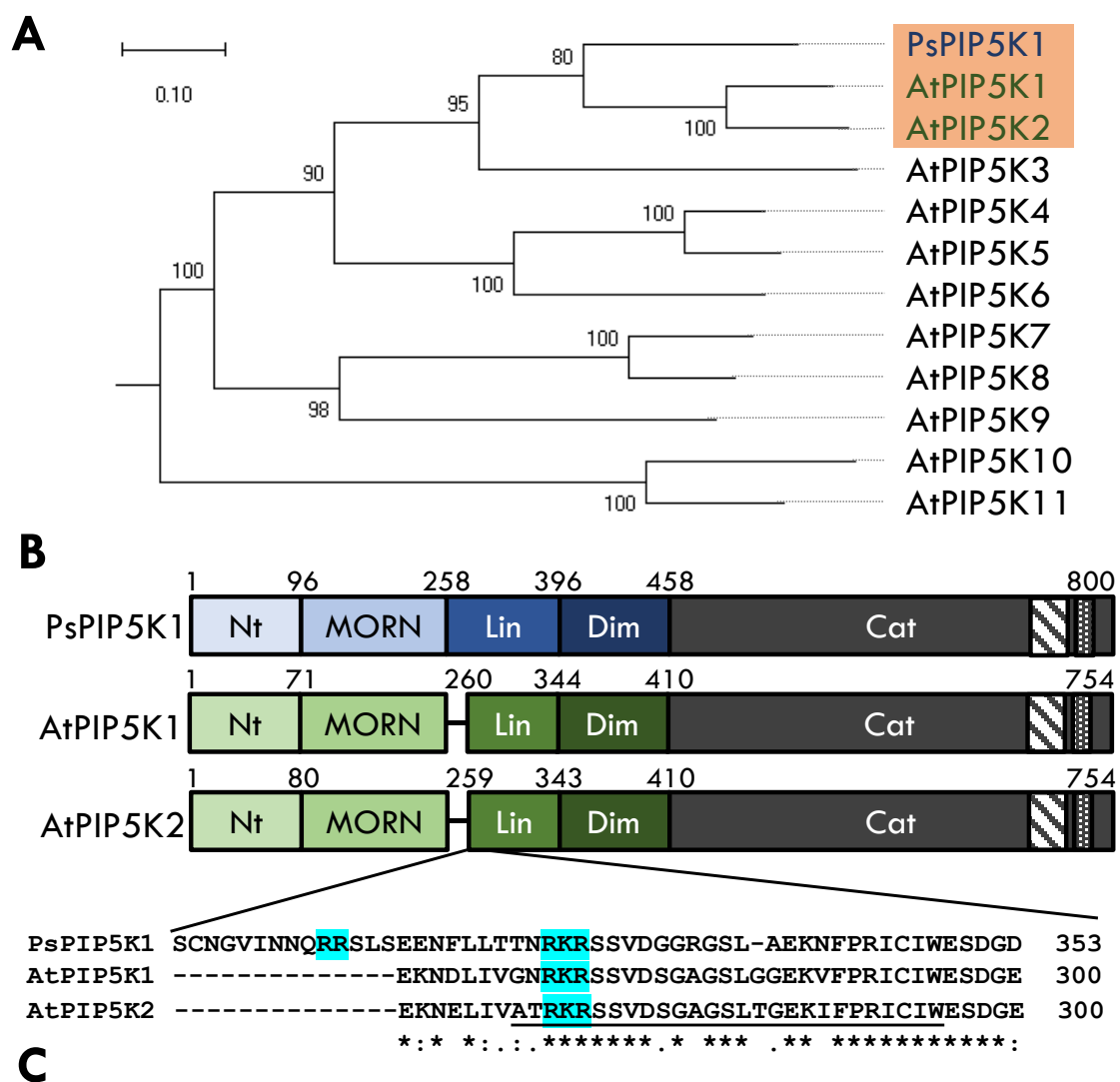


Figure 16 AtPIP5K1 and AtPIP5K2 have a close homologue in opium poppy. A Maximum likelihood phylogenetic tree with the full-length amino acid sequence of Arabidopsis AtPIP5K1-AtPIP5K11 and the poppy homologue *Papaver somniferum* PsPIP5K1. Numbers at nodes represent percentage of ML bootstrap support. Scale indicates a difference of

10 %. **B** The PI4P 5-kinases AtPIP5K1, AtPIP5K2 and PsPIP5K1 belong to the type B PI4P 5-kinase family and share the same domain structure. Numbers indicate the amino acid position at the beginning and at the end of a protein domain. A short sequence alignment (Multalin; Corpet 1988) of the NLS area within the Lin-domains is shown in detail. Blue marked are basic amino acid residues Lysin (K) and Arginine (R). Characterized NLS from AtPIP5K2 is underlined. Asterisk (*) indicate full conserved-, colon (:) indicates conservation of strongly similar properties and period (.) indicates conservation of weakly similar properties. Nt, N-terminus; MORN, Membrane Occupation and Recognition Nexus; Lin, Linker; Dim, Dimerization; Cat, Catalytical; hatched, Variable insert; dotted, Activation loop. **C** Arabidopsis mesophyll protoplasts were transiently transformed with *pEntryA-pCaMV35S::PsPIP5K1-EYFP*. Subcellular localisation of fluorescent protein fusions was analysed with the LSM880. Displayed is a z-projection of a z-stack covering the entire protoplast with 1 μm intervals between sections. Autofluorescence of chlorophyll A is depicted in red and PsPIP5K1-EYFP in green. Protoplast from C were documented in cooperation with Barbora Hans, Comenius University Bratislava/ MLU Halle and represents two independent experiments with a total of seven cells.

2.2.1 Confirmation of the strong nuclear localisation of PsPIP5K1

In initial experiments, PsPIP5K1-EYFP showed a strong and almost exclusively nuclear localisation and only a weak plasma membrane localisation. Nevertheless, it must be considered that the previous localisation studies with PsPIP5K1 in Arabidopsis leaf protoplasts have been carried out in a heterologous system, the results of the strong nuclear localisation could therefore also be artifacts. To exclude this, the subcellular localisation of PsPIP5K1-EYFP was performed in poppy mesophyll protoplasts. To this end, the existing protocol for isolation of leaf mesophyll protoplasts from Arabidopsis (Yoo et al. 2007) was adapted to the isolation of poppy protoplasts as described in section 4.22. Surprisingly, some poppy protoplasts lacked chloroplasts, which may have been the epidermal cells (Fig. 17C).

For comparison Arabidopsis and poppy protoplasts were then transformed with *pCaMV35S::PsPIP5K1-EYFP* or with *pCaMV35S::AtPIP5K2-EYFP* and the EYFP fluorescence distribution was analysed with the confocal LSM880 (see 4.24.1).

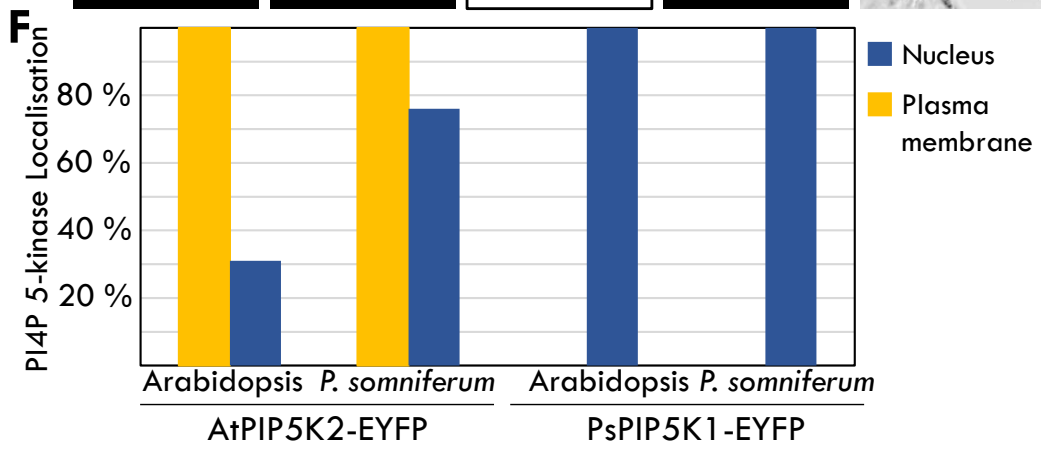
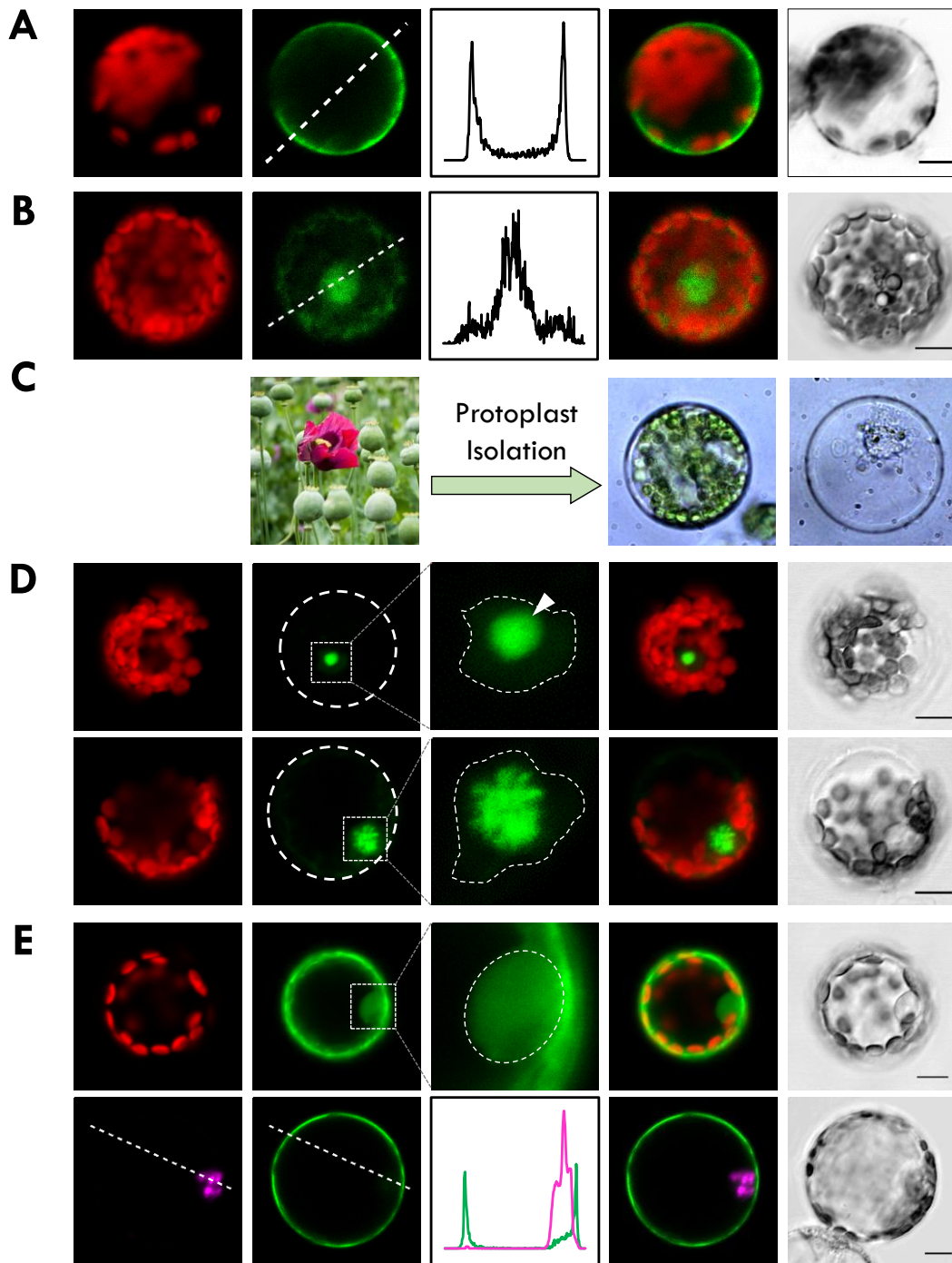


Figure 17 AtPIP5K2 displays enhanced nuclear localisation in poppy protoplasts. Arabidopsis and poppy mesophyll protoplasts were transiently transformed with *pEntryA-pCaMV35S::AtPIP5K2-EYFP* or *pEntryA-pCaMV35S::PsPIP5K1-EYFP*. Subcellular localisation of fluorescent protein fusions was analysed with the LSM880. **A** and **B**, Arabidopsis mesophyll protoplasts expressing AtPIP5K2-EYFP (A) or PsPIP5K1-EYFP (B). **C** Protoplast isolation of *Papaver somniferum* leaves originates chloroplast containing and chloroplast free protoplasts. **D** and **E** Poppy mesophyll protoplasts expressing PsPIP5K1-EYFP (D) and AtPIP5K2-EYFP (E). Shown are confocal planes highlighting either the plasma membrane or nuclear area. Autofluorescence of chlorophyll A is depicted in red, NLS-DsRed in magenta and PsPIP5K1-EYFP and AtPIP5K2-EYFP in green. Dotted lines in nuclear enlargement indicate nuclear envelope. White arrow highlights nucleolus. Scale bars measure 10 μm . **F** Subcellular distribution patterns of AtPIP5K2-EYFP and PsPIP5K1-EYFP cells were counted and categorised into two groups, showing fluorescence in the nucleus or in nucleus and plasma membrane. Protoplast from A represents 13 cells in total from one independent experiment. Image from B is representative for one individual experiment with seven cells. Protoplasts in C were imaged in one independent experiment with 51 protoplasts of which 25 were without chloroplasts. Protoplasts from D are representative for 25 protoplasts from five individual experiments. Images from E represent six individual experiments with 34 cells in total. Microscopic imaging was performed in collaboration with the bachelor student Marie Lebescond.

As previously described and observed, AtPIP5K2-EYFP localised distinctly at the plasma membrane and PsPIP5K1-EYFP showed localisation in the nucleus of Arabidopsis protoplasts (Fig. 17A and B). Localisation in poppy protoplasts showed a similar fluorescence distribution in the homologous system. PsPIP5K1-EYFP localised to the nucleus and showed almost no cytosolic or plasma membrane localisation (Fig. 17B and D). In some poppy protoplasts, PsPIP5K1 also showed distinct nucleoli localisation (Fig. 17D, upper panel, white arrow highlights nucleoli) or localised in nuclear speckles (Fig. 17D, lower panel). Thus, the nuclear localisation of poppy PsPIP5K1 is also detectable in poppy protoplasts and the observations in Arabidopsis cells do not represent an artifact. AtPIP5K2-EYFP showed similar localisation in the plasma membrane in poppy protoplasts as in Arabidopsis protoplasts but was detected more frequently in the nucleus in addition to plasma membrane localisation in poppy protoplasts than in localisation studies with Arabidopsis cells (Fig 17E). In studies with Arabidopsis protoplasts, nuclear localisation was detected in 31 % of the cells examined in addition to localisation to the plasma membrane. In poppy protoplasts, however, PIP5K2-EYFP was additionally localised to the nucleus in 76 % of the cells examined (Fig 17F). Nuclear localisation of AtPIP5K2-EYFP always showed uniform fluorescence in the nucleus in the studies here, speckles or localisation in the nucleolus could not be observed for AtPIP5K2-EYFP. In some experiments, NLS-DsRed was co-expressed as a nuclear marker to visualize the nucleus and served here as a control. (Fig. 17E, lower panel). In all cases, no differences were found in localisation studies between mesophyll (with chloroplasts) and epidermal protoplasts (without chloroplasts).

These experiments support PsPIP5K1 as a (nearly) exclusively nuclear PI4P 5-kinase. PsPIP5K1-EYFP localises to the nucleus in heterologous and homolog systems. AtPIP5K2 displayed enhanced nuclear subcellular signals when transformed into poppy protoplasts.

2.2.2 PsPIP5K1 interacts with alpha-importins from Arabidopsis

Since PsPIP5K1 strongly localises in the nucleus of leaf protoplasts and, like AtPIP5K1 and AtPIP5K2, shows the NLS in the Lin-domain, PsPIP5K1 was tested for interaction with alpha-importins. The classic nuclear import is mediated by NLS and the interaction with alpha -importins (Kalderon et al., 1984; Zhou et al., 1991; Kosugi et al., 2009). Since the classical yeast-two-hybrid (YTH) system artificially introduce an NLS into the bait and prey proteins, which would disturb the assay, the split-ubiquitin-based two-hybrid system was used for the analysis of possible interaction between PsPIP5K1 and alpha-importins (see 4.19 and 4.12.2). For AtPIP5K2 it could be shown that it interacted with the ubiquitously expressed alpha-importin isoforms IMPA3, IMPA6 and IMPA9 in Arabidopsis (Gerth et al., 2017b), therefore PsPIP5K1 was also investigated for interaction with these alpha-Importin isoforms. For control, AtPIP5K1 and AtPIP5K2 were tested again for the interaction with the corresponding alpha-Importins The results of the representative Y2H-assays are imaged in figure 18.

As it was already shown, interactions between AtPIP5K1 and AtPIP5K2 with IMPA3, IMPA6 and IMPA9 were observed as indicated by growth on SD-LWH selection medium (Fig. 18). In addition, interaction of PsPIP5K1 with IMPA3, IMPA6 and IMPA9 was detected (Fig. 18). For an unexplained reason, these tests showed only weak yeast growth indicating protein-protein interaction between AtPIP5K2 with the selected alpha-Importins, in contrast to the data already published (Gerth et al., 2017b) and presented in other theses of our group (Gerth PhD, 2018). Nevertheless, PsPIP5K1 could be identified to be targeted by the Arabidopsis nuclear import machinery.

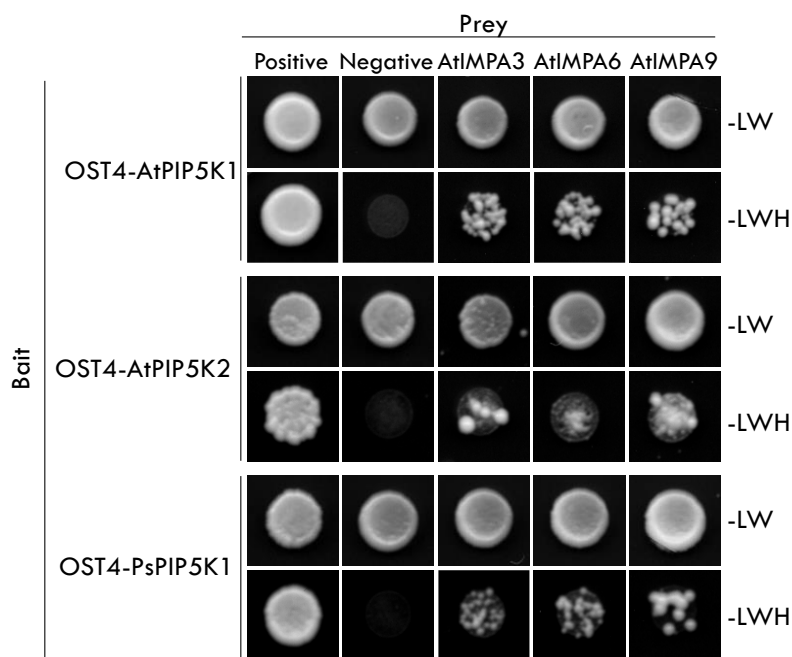


Figure 18 PsPIP5K1 interacts with Arabidopsis alpha-importins. Interaction of AtPIP5K1, AtPIP5K2 and PsPIP5K1 with Arabidopsis alpha-importins IMPA3, IMPA6 and IMPA9 was tested in a split-ubiquitin based Y2H-assay. Baits were fused to oligosaccharyltransferase OST4. pAl-Alg5 and pDL2-Alg5 vectors were used as positive and negative controls, respectively. Uniformly growing yeast on SD-

LW (excluding leucine and tryptophane) indicated similar cell density and the presence of both, bait- and prey constructs. Protein-protein interaction is indicated by yeast growth on SD-LWH (excluding leucine, tryptophane and histidine). Yeast colonies were grown at 30 °C for six days. Results are representative for four independent experiments with five colonies of each combination; exception: for AtPIP5K1 three independent experiments with five colonies each combination were performed. Three of four experiments were performed in cooperation with bachelor student Julia Urbanski.

2.2.3 The Lin-domain of PI4P 5-Kinases is key for the subcellular localisation

The distinct strong nuclear localisation of PsPIP5K1 compared to AtPIP5K2 raised the question of which protein regions and/ or specific amino acids lead to this differently pronounced localisation. Because the amino acid sequence of PsPIP5K1 and AtPIP5K2 matches up to 68%, PsPIP5K1 is well suited for identifying determinants responsible for the differential localisation. An interesting difference between AtPIP5K2 and PsPIP5K1 can be found in the Lin-domain, as already mentioned in section 2.2. Although the Lin-domain of PsPIP5K1 in the NLS area is very similar to that in AtPIP5K2, an N-terminal extension of this NLS sequence has been found in PsPIP5K1 with additional basic amino acids (Fig. 16 in section 2.2). These additional basic amino acids close to the amino acids of the known NLS, suggested that PsPIP5K1 may contain a bipartite NLS. To address this, the Lin-domains of AtPIP5K2 and PsPIP5K1 were reciprocally exchanged (see 4.11.1.1 and 4.12.4) resulting in chimeric PI4P 5-kinases named as AtPIP5K2_LinPsPIP5K1 (AtPIP5K2_LinPs) and PsPIP5K1_LinAtPIP5K2 (PsPIP5K1_LinAt) (Fig. 19A). The chimeric proteins were expressed under the control of the pCaMV35S promoter as EYFP- fusions (see 4.12.4) in Arabidopsis leaf mesophyll protoplasts for localisation studies (see 4.22). For control, wild type PIP5K2-EYFP and PsPIP5K1-EYFP fusions were also documented.

Wild type AtPIP5K2-EYFP and PsPIP5K1-EYFP showed the described and prominent localisations at the plasma membrane and in the nucleus: PIP5K2-EYFP localised mainly to the plasma membrane (Fig. 19B); PsPIP5K1-EYFP showed the described nuclear localisation (Fig. 19B). Expression of the chimeric AtPIP5K2_LinPs-EYFP showed an increased nuclear localisation (Fig. 19B), whereas the expression of the chimeric PsPIP5K1_LinAt-EYFP lead to an increased proportion of fluorescence signal at the plasma membrane (Fig. 19B). Additionally, in some cases nuclear speckles were observed when AtPIP5K2_LinPs-EYFP chimera was expressed (Fig. 19B, black arrows indicate nuclear speckles). These nuclear speckles could previously only be detected after expression of PsPIP5K1-EYFP (see Fig. 17 section 2.2.1).

The subcellular distribution of wild type AtPIP5K2-EYFP, PsPIP5K1-EYFP and the chimeric Lin-domain PI4P 5-kinases were statistically evaluated (Fig. 19F). For this purpose, the transformed cells were divided into plasma membrane (two peaks in line intensity profile), plasma membrane and nucleus (three peaks in line intensity profile) and exclusively nuclear localisation (one peak in line intensity profile).

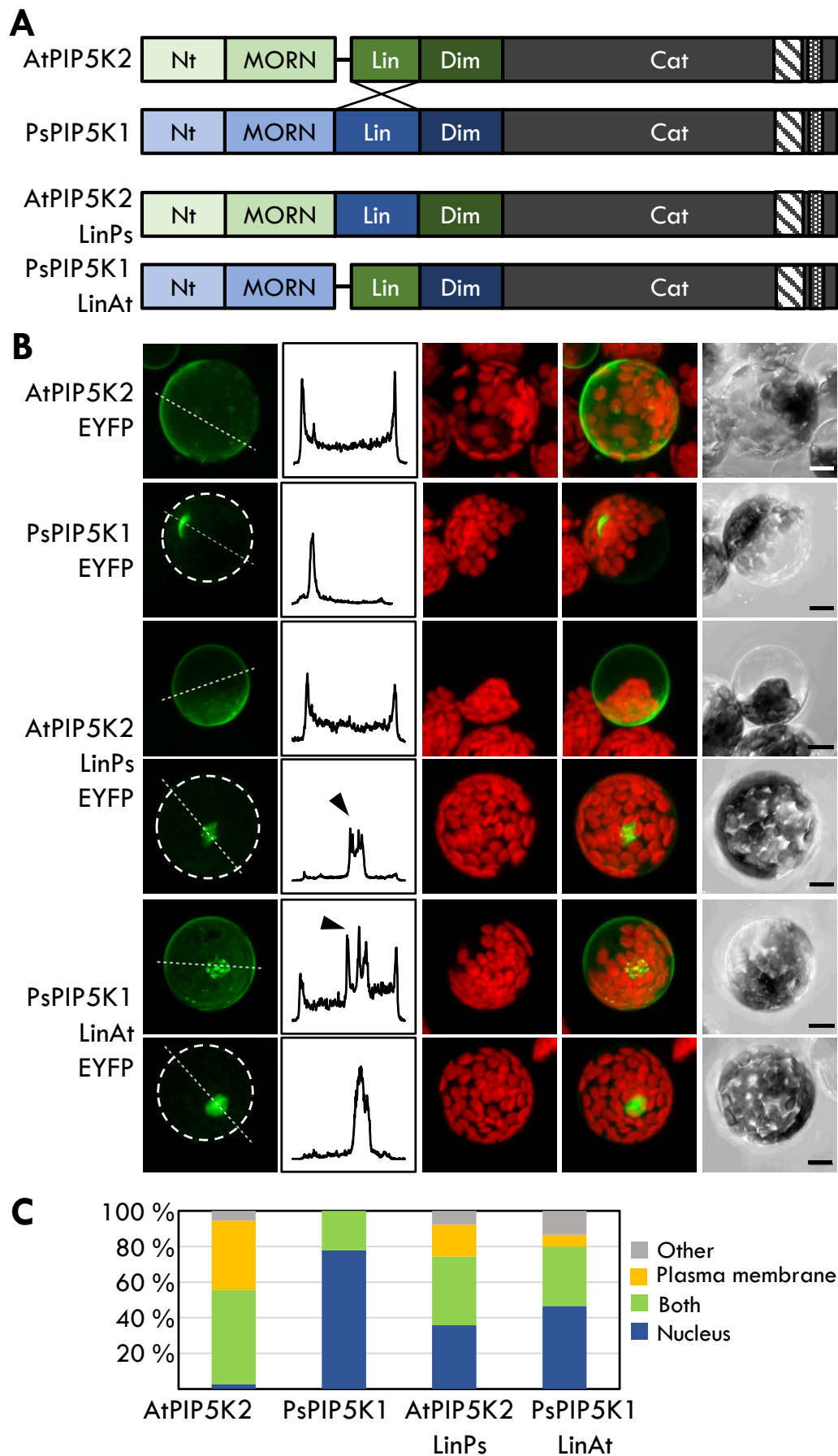


Figure 19 The Lin-domain of PI4P 5-kinases greatly modulates the subcellular localization. **A** The Lin-domains of AtPIP5K2 and PsPIP5K1 were reciprocally exchanged,

resulting the chimeric proteins PsPIP5K1_LinAt and AtPIP5K2_LinPs. The chimeric enzymes were overexpressed in Arabidopsis protoplasts as EYFP fusion proteins and the subcellular distribution was monitored using the LSM880. Nt, N-terminus; MORN, Membrane Occupation and Recognition Nexus; Lin, Linker; Dim, Dimerization; Cat, Catalytical domain; Hatched, Variable insert; Dotted, Activation loop. **B** Arabidopsis mesophyll protoplasts expressing AtPIP5K2-EYFP, PsPIP5K1-EYFP or chimeric AtPIP5K2_LinPs-EYFP or PsPIP5K1_LinAt-EYFP. Shown are projections of z-stacks covering the entire protoplast with 1 μm intervals between sections. Autofluorescence of chlorophyll A is depicted in red and PI4P 5-kinase-EYFP constructs in green. Black arrows indicate nuclear speckles. Scale bars, 10 μm . Images represent AtPIP5K2-EYFP n= 22, PsPIP5K1-EYFP n=9, AtPIP5K2_LinPs-EYFP n=32 and PsPIP5K1_LinAt n=12. **C** Quantification of fluorescence distribution after expression of AtPIP5K2-EYFP, PsPIP5K1-EYFP, AtPIP5K2_LinPs-EYFP, and PsPIP5K1_LinAt-EYFP in Arabidopsis protoplasts. The cells examined were counted and differentiated into fluorescence in the nucleus, in the nucleus and at the plasma membrane, at the plasma membrane, or neither (other) localisation.

By introducing the Lin-domain of PsPIP5K1 into AtPIP5K2 the subcellular distribution of AtPIP5K2_LinPs-EYFP shifted more to the nucleus, increasing exclusive nuclear localisation from 5 % in wild-type PIP5K2-EYFP to 44 % in PIP5K2_LinAt-EYFP (Fig. 19F). Plasma membrane localisation dropped from 63 % to 22 % (Fig. 19F). Conversely, the introduction of the Arabidopsis AtPIP5K2 Lin-domain into the PsPIP5K1 protein led to a reduced nuclear localisation and more pronounced plasma membrane localisation which is not observed after expression of the wild type PsPIP5K1-EYFP (Fig. 19F). While in 78 % of the examined cells PsPIP5K1-EYFP localised almost exclusively in the cell nucleus, this clear nuclear localisation was observed in expression of PsPIP5K1_LinAt EYFP only in about 54% of the examined cells (Fig. 19F). Wild-type PsPIP5K1-EYFP displayed dual localisation in 22 % of observed protoplasts whereas PsPIP5K1_LinAt-EYFP showed dual localisation in 38 % (Fig. 19F). The chimeric protein PsPIP5K1_LinAt could even be localised in 8 % of the examined protoplasts exclusively on the plasma membrane and showed no nuclear localisation at all in these cells. This could not be observed for the wildtype form PsPIP5K1 (Fig. 19F).

In summary, this experiment showed that the mutual exchange of the Lin-domains in AtPIP5K2 and PsPIP5K1 also led to an exchange of the respective subcellular localisation. This indicates that the Lin-domain is responsible for both the plasma membrane and nuclear localisation. Possibly in the interaction of further sequence determinates, which may lie in the N-terminus or in the variable linker. These experiments support the regulatory importance of the Lin-domain of PI4P 5-kinases.

2.2.4 Tobacco pollen tube phenotypes and tip swelling upon overexpression of different PI4P 5-kinase variants

It was shown that plasma membrane localised AtPIP5K2-EYFP controls the dynamic actin cytoskeleton in tobacco pollen tube tip (Stenzel et al., 2012; Fratini et al., 2021). The strong overexpression of AtPIP5K2-EYFP in tobacco pollen tubes led to significantly increased actin stabilisation in the pollen tube tip and to pollen tube tip swelling (Stenzel et al., 2012; Fratini et al., 2021). This actin phenotype is explained as a response to too much PtdIns(4,5)P₂ at the plasma membrane.

Experiments were conducted, to determine whether PsPIP5K1 and the chimeric PsPIP5K1-LinAt and AtPIP5K2_LinPs will behave like AtPIP5K2. The localisation of PsPIP5K1-EYFP, PsPIP5K1_LinAt-EYFP and AtPIP5K2_LinPs-EYFP as well as the phenotypes of pollen tubes after overexpression of these enzymes were studied. The fluorescence tagged PI4P 5-kinases were expressed in tobacco pollen tubes under the control of the pollen tube specific *pLAT52* promoter from *Solanum lycopersicum* (see 4.1.2.4, (Muschiatti et al., 1994)). Pollen tube morphology and PI4P 5-kinase-EYFP localisation was analysed by LSM or spinning disk (SD) microscopy (see 4.24.1 and 4.24.2). Representative pollen grains, tubes and tips are displayed in figures 20 and 21.

Pollen tubes transformed with AtPIP5K2-EYFP showed strong fluorescence signal at the plasma membrane that was restricted to the pollen tube tip and the typical tip swelling phenotype (Fig.20A). Pollen tubes transformed with PsPIP5K1-EYFP displayed a strong nuclear localisation and only weak fluorescence signal at the plasma membrane (Fig. 20B). If fluorescence signal could be detected at the membrane, it was mainly limited to the pollen tube tip (Fig. 20B, upper panel).

Surprisingly, PsPIP5K1-EYFP, that was mostly localising in the nucleus, also caused a phenotype of swelling pollen tube tips after overexpression (Fig. 20B, upper and middle panel). There were also pollen tubes that showed little or no tip-swelling phenotype after expression of PsPIP5K1-EYFP, but this has also been described for overexpression of PIP5K2 (Stenzel et al., 2012). In some cases, the swelling phenotype appeared to be even stronger after expression of PsPIP5K1-EYFP than after expression of AtPIP5K2-EYFP (Fig. 20). Such pollen grains seemingly swell directly or produced stunted pollen tubes and formed a pear like appearing structure (Fig. 20B middle and lower panel). As described for *Arabidopsis* leaf mesophyll protoplasts (section 2.2.1, Fig. 17) PsPIP5K1-EYFP often localised in nuclear speckles (Fig. 20B middle and lower panel).

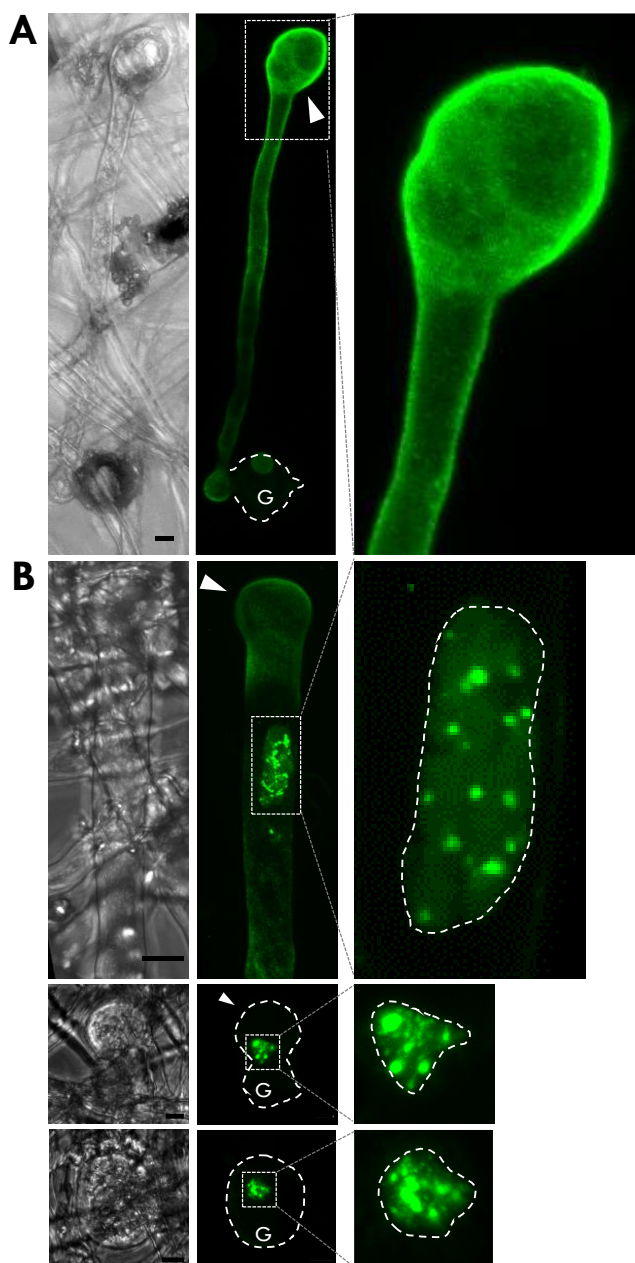


Figure 20 Effects of PsPIP5K1 over-expression on tobacco pollen tube phenotype. Tobacco pollen were transiently transformed with *pEntryA-plat52::AtPIP5K2-EYFP* or *pEntryA-plat52::PsPIP5K1-EYFP*. Subcellular localisation of fluorescent protein fusions and pollen tube morphogenesis was analysed with the LSM880 or SD-microscopy. **A** Tobacco pollen tube expressing PIP5K2-EYFP. **B** Tobacco pollen grain and pollen tubes expressing PsPIP5K1-EYFP. Shown are projections of z-stacks covering the entire pollen tube with 1 μ m intervals between sections or confocal planes highlighting the nuclear area (B, upper panel, nuclear focus). PI4P 5-kinase-EYFP fluorescence is displayed in green. Dashed lines indicate non-fluorescent plasma membrane of the pollen tubes or the nuclear envelope in enlarged nuclear sections. White arrows highlight swollen pollen tube tips. G, Grain. Scale bars measure 10 μ m. Images from A are representative for four independent experiments using a total of 18 cells. Pollen tubes from B are representative for four independent experiments counting 33 cells. 14 cells from A and 17 from B were images in cooperation with bachelor student Julia Urbainski.

The chimera protein *AtPIP5K2_LinPs-EYFP* localised both to the plasma membrane, there mainly at the apical tip, and distinctly to the nucleus of pollen tubes (Fig. 21). The pollen tubes transformed with *AtPIP5K2_LinPs-EYFP* showed a phenotype intermediate between that of *AtPIP5K2-EYFP* and *PsPIP5K1-EYFP*. *AtPIP5K2_LinPs-EYFP* overexpression conveys tip swelling and stunted and swollen pollen tubes (Fig. 21). In contrast to *AtPIP5K2_LinAt-EYFP*, *PsPIP5K1_LinAt-EYFP* was not successfully transformed into pollen tubes.

The localisation and morphology experiments with poppy PI4P 5-kinases in pollen tubes showed that *PsPIP5K1* also mediates pollen tube tip swelling despite only weakly detectable plasma membrane localisation to the pollen tube tip. *PsPIP5K1*

thus has similar functions to AtPIP5K2, although the two enzymes differ in the intensity of their localisation. The chimeric AtPIP5K2-LinPs enzyme revealed that the localisation of AtPIP5K2 is changed to a more nuclear localisation, but it does not need a large proportion of PI4P 5-kinase at the plasma membrane to convey the tip swelling phenotype.

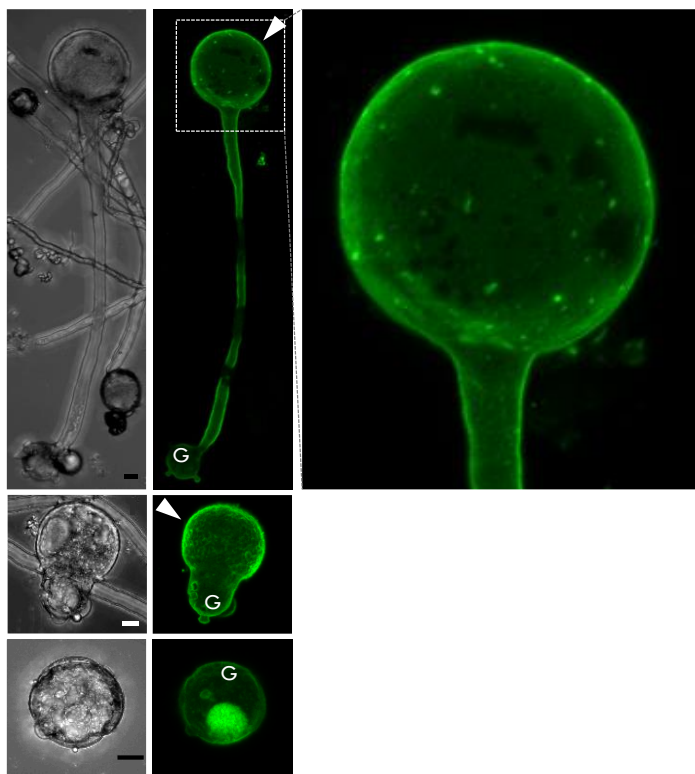


Figure 21 Effects of chimeric AtPIP5K2_LinPs overexpression on tobacco pollen tube phenotype. Tobacco pollen were transiently transformed with *pEntryA-pLat52::AtPIP5K2_LinPs-EYFP*. Subcellular localisation of fluorescent protein fusions and pollen tube morphogenesis was analysed with the LSM880. Shown are projections of z-stacks covering the entire pollen tube with 1 μm intervals between sections. AtPIP5K2_LinPs-EYFP fluorescence is displayed in green. White arrow highlights swollen pollen tube tip. G, Grain. Scale bars, 10 μm . Images are representative for three independent experiments with a total of 31 pollen tubes. Experiment was performed in collaboration with bachelor student Julia Urbainski.

2.2.5 PsPIP5K1 rescues the *pip5k1 pip5k2* double mutant phenotype

PsPIP5K1 showed strong nuclear localisation and only weak plasma membrane signal in tobacco pollen tubes, as it did in mesophyll protoplasts. Nevertheless, overexpression of PsPIP5K1-EYFP produced pollen tube tip swelling phenotypes, as previously described for AtPIP5K2-EYFP. To test *in planta*, to what extent the functionalities of PsPIP5K1 and AtPIP5K2 are similar and/ or whether there are differences in function, *pip5k1 pip5k2* double mutant complementation studies were initiated with PsPIP5K1-EYFP and the chimeric constructs PsPIP5K1_LinAt-EYFP and AtPIP5K2_LinPs-EYFP under the control of the *PIP5K1* and *PIP5K2*-intrinsic promoters *pPIP5K1* and *pPIP5K2* (see 4.11.12 and 4.12.4).

This experiment may allow to draw conclusions about the importance of the balance between nuclear and plasma membrane-localised PI4P5-kinases. It is likely that these PsPIP5K1 variants do not complement the strong phenotype of the *pip5k1 pip5k2* double mutant to the same extent as a wildtype AtPIP5K2 can.

The *pip5k1 pip5k2* double mutant shows a severe phenotype including dwarfism, shortened roots, strong anthocyanin accumulation, no senescence, reduced apical dominance which leads to the formation of excessive inflorescences, but the flower development aborts at the silique stage and results in flower sterility (Introduction 1.1.3 Fig. 6, (Ischebeck et al., 2013)). Complementations of *pip5k1 pip5k2* with AtPIP5K1 or AtPIP5K2 could almost fully balance the phenotype, and the complemented plants then showed only slightly delayed flowering, as the single mutants *pip5k1* or *pip5k2* (Introduction 1.1.3 Fig. 6 (Ischebeck et al., 2013)). When the *pip5k1 pip5k2* double mutant was complemented with the nuclear excluded AtPIP5K2_NLS_{AAA}, the phenotype of the *pip5k1 pip5k2* double mutant was only partially complemented, but not to the same extent as when PIP5K2-EYFP was expressed (Introduction 1.1.4 Fig. 7). The most pronounced phenotypes still included delayed growth of above- and below-ground organs, still severely delayed flowering time, asymmetric flower formation, and fewer embryos in the siliques (Gerth PhD, 2018).

pip5k1 pip5k2 double mutant plants transformed (see 4.11.12) with *pAtPIP5K1::PsPIP5K1-EYFP*, *pAtPIP5K1::PsPIP5K1_LinAt-EYFP* or *pAtPIP5K2::PsPIP5K1_LinAt-EYFP* were selected using glufosinate (see 4.11.13) and were genotyped. In this process, plants were tested for both, the presence of the transgene, as well as for the double mutant background. The genotyping of the selected plants was performed using specific primer combinations (see 4.11.13). Other promotor/ construct combinations including *pPIP5K2::PsPIP5K1-EYFP* and the chimeric *PsPIP5K1_LinAt-EYFP* constructs were not successfully cloned or transformed.

The roots of the *pip5k1 pip5k2* double mutant showed strongly reduced growth (Ischebeck et al., 2013; Tejos et al., 2014; Gerth et al., 2017b) and therefore the complemented lines were examined for their root growth. For this purpose, *pip5k1 pip5k2* double mutants transformed with either PIP5K2-EYFP, PsPIP5K1-EYFP, AtPIP5K2_LinPs-EYFP were grown on 1/2 MS medium under long day conditions and 14-day-old seedlings were then analysed for their respective root length using “root detection” plugin from ImageJ (Fig. 22A and B). All lines analysed showed comparable root growth (Fig. 22). The poppy PsPIP5K1-EYFP and the linker exchange variant AtPIP5K2_LinPs were able to compensate for the strong *pip5k1 pip5k2* root phenotype (Fig. 22A and B).

The transformed plants with the correct genetic background of *pip5k1 pip5k2* double mutant were examined for the subcellular localisation of PsPIP5K1-EYFP, or AtPIP5K2_LinPs-EYFP (Fig. 22C). All complementation constructs were EYFP tagged,

thus microscopic studies were performed to localisation experiments with the EYFP-tagged PI4P5-kinases. Unfortunately, the low expression strength of the PI4P-5 kinase promoters led to hardly detectable fluorescence signals as described previously (Ischebeck et al., 2013; Tejos et al., 2014; Gerth et al., 2017b). For *pip5k1 pip5k2* double mutants transformed with pPIP5K1::PsPIP5K1-EYFP (L23) and pPIP5K2::PsPIP5K1_LinAt_EYFP (L41), weak but detectable signals could be detected in one line respectively (Fig. 22C). The roots of these lines were documented as Z-stacks on LSM880 and are shown as Z-projections in figure 22C. Near the root tip, in the meristematic region of the root, fluorescence signals of PsPIP5K1_LinAt-EYFP expression could be detected in the nucleus (Fig. 22C upper panel). Root epidermal cells with expanding root hairs exhibited fluorescence signals showing PsPIP5K1-EYFP in the nucleus and at the plasma membrane (Fig. 22C lower panel).

Figure 23 shows representative plant individuals of each complementation experiment, as well as Col-0 wild type and the previously mentioned and published complementation line *pip5k1 pip5k2* transformed with *pPIP5K2::PIP5K2-EYFP*. The complementation studies revealed that both, the wildtype variant from poppy PsPIP5K1-EYFP, and the chimeric protein AtPIP5K2_LinPs-EYFP can complement the *pip5k1 pip5k2* phenotype (Fig. 23A). As already described the complementation line with PIP5K2-EYFP nearly fully complemented the *pip5k1 pip5k2* phenotype (Fig. 23A and B). Complementation with PsPIP5K1-EYFP and AtPIP5K2_LinPs-EYFP showed similar results. In few cases, leaves of the complemented lines showed a curled phenotype (Fig. 23A lower panel). The inflorescences of *pip5k1 pip5k2* double mutants expressing either PsPIP5K1-EYFP or AtPIP5K2_LinPs-EYFP showed partial asymmetries. The siliques did not develop in a strictly alternate arrangement, but asymmetrically and unevenly (Fig. 23A lower panel). This was also observed for the *pip5k1 pip5k2* PIP5K2-EYFP control (Fig. 23 (Ischebeck et al., 2013; Gerth PhD, 2018)).

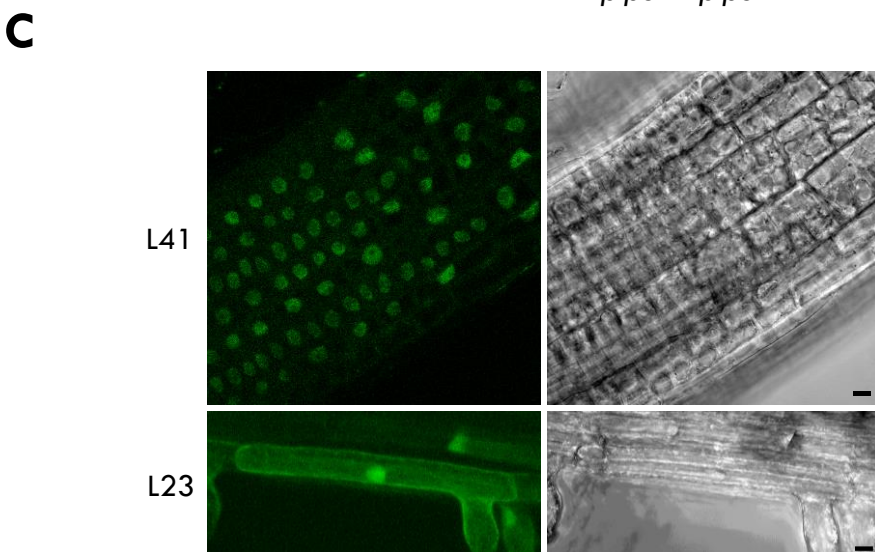
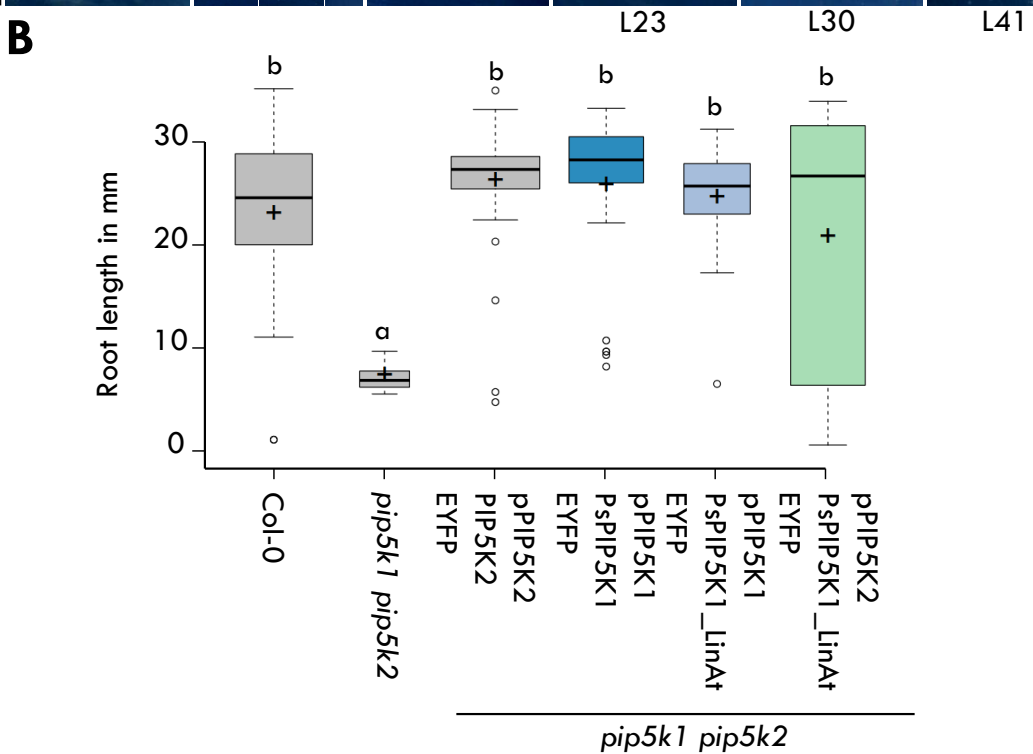
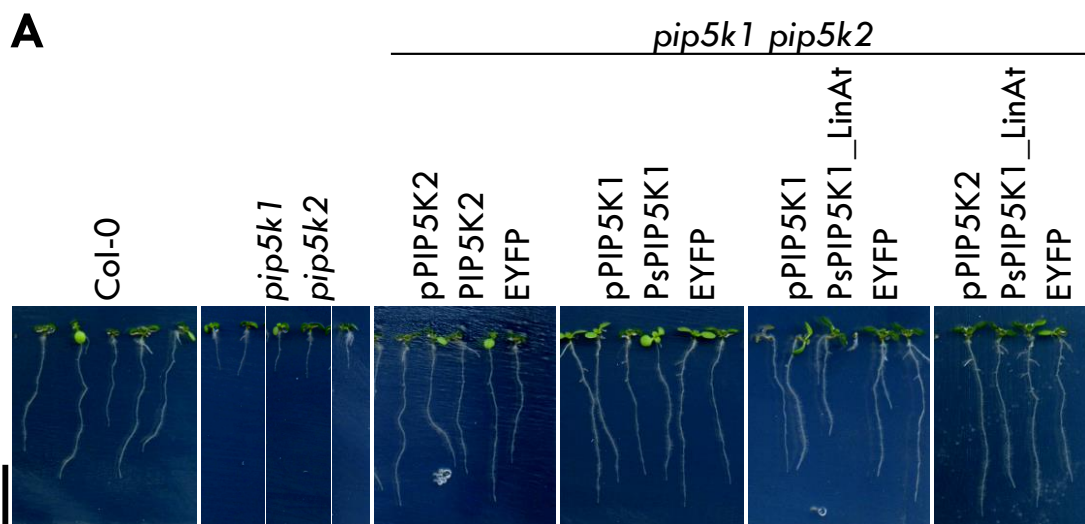


Figure 22 PsPIP5K1 and PsPIP5K1_LinAt complement the *pip5k1 pip5k2* double mutant shortened root phenotype. PsPIP5K1-EYFP or AtPIP5K2_LinPs-EYFP were expressed under control of the *PIP5K1* or *PIP5K2* promoter in the *pip5k1 pip5k2* double mutant background. Selected plants were grown vertical on 1/2 MS agar plates under long day conditions for seven days. **A** Documentation of the root length of seven days old seedlings. Scale bar 1 cm. **B** Graphical representation of the root lengths as box blot. With the help of the program Fiji the root length of 31 PIP5K2-EYFP, 13 non-transformed *pip5k1 pip5k2* double mutants, and 23-29 PIP5K1-EYFP or AtPIP5K2_LinPs-EYFP expressing seedlings were evaluated. Significant differences were determined using one-way ANOVA with a Tukey's post-hoc test ($p \leq 0.05$) and are indicated by letters a-b. **C** Arabidopsis seedlings expressing PsPIP5K1-EYFP (Line L23) and AtPIP5K2_LinPs-EYFP (Line L41) were analysed for -EYFP fluorescence (green) using the LSM880. Scale bar, 10 μm .

Since the double mutant does not start flowering, it was tested whether this phenotypic aspect could be completely rescued by expression of PsPIP5K1 and AtPIP5K2_LinPs. For the determination of the flowering time, the day on which the primary inflorescence opened its first flower was determined. The control plants *pip5k1 pip5k2* transformed with PIP5K2-EYFP flowered on average after 82.3 days (Fig. 23B) and that was comparable with the flowering onset of the wildtype Col-0 plants (Fig. 23B). Comparison of the onset of flowering of the PsPIP5K1-EYFP or AtPIP5K2_LinPs-EYFP variant with that of the PIP5K2-EYFP control showed that they have comparable flowering times to the control and can compensate for the very delayed flowering time of the *pip5k1 pip5k2* double mutant (Fig. 23 B).

The comparisons and investigations of PsPIP5K1 with AtPIP5K2 have shown that phylogenetically very similar enzymes with high sequence similarity can show clearly different subcellular localisations. Nevertheless, PsPIP5K1 and AtPIP5K2 seem to perform the same functions within the plant. Overexpression of PsPIP5K1 in pollen tubes leads, as described for AtPIP5K2, to a pollen tube tip swelling and the *pip5k1 pip5k2* double mutant is rescued by the expression of PsPIP5K1. The amount of the corresponding PI4P 5-kinase at the plasma membrane or nucleus visible in the fluorescence microscope may not necessarily seem to be the percentages of the active enzymes it needs to induce a function. The Lin-domain is clearly involved in the regulation of the subcellular distribution of PsPIP5K1 and AtPIP5K2. The NLS is in the Lin-domain of both PsPIP5K1 and AtPIP5K2. Here, accessibility, i.e., the possible masking of NLS for alpha-importins, may be a reason for the different subcellular distribution. However, it remains unclear to what extent other protein domains of the PI4P 5-kinases, such as the N-terminus or the variable insert, contribute to regulation. Masking or accessibility of the NLS itself could occur via further protein-protein interactions with yet unknown protein partners and/ or post-translational modifications such as protein phosphorylation.

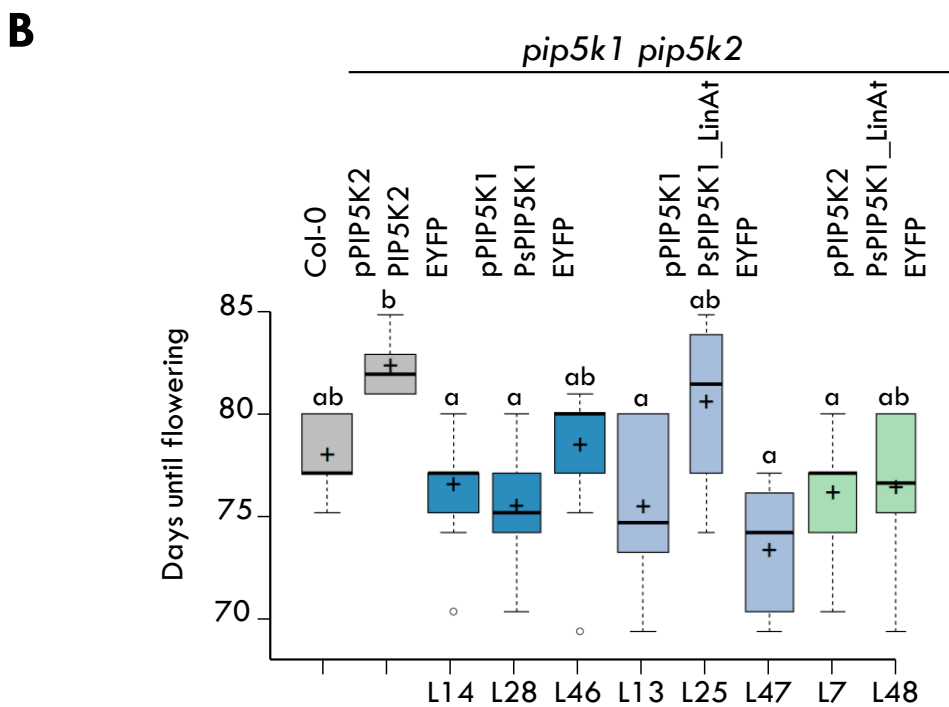
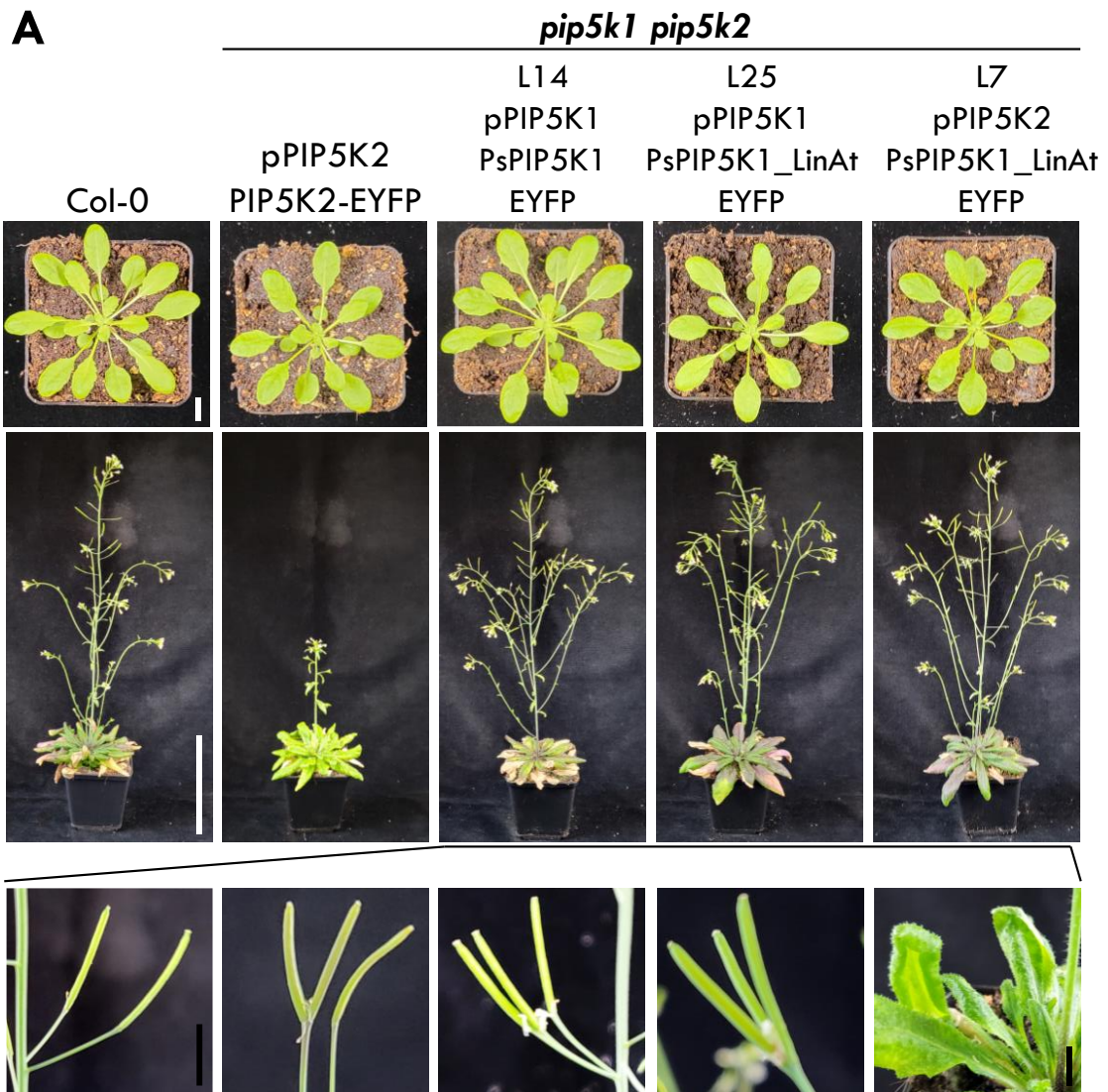


Figure 23 PsPIP5K1 and PsPIP5K1_LinPs complement the *pip5k1 pip5k2* double mutant. PsPIP5K1-EYFP or AtPIP5K2_LinPs-EYFP were expressed under control of the

endogenous *PIP5K1* or *PIP5K2* promoter in the *pip5k1 pip5k2* double mutant background. **A** One representative plant of wildtype control and each transformed construct is imaged. Upper panel shows seven-week-old plants grown under short day conditions. The panel in the middle displays twelve-week-old plants grown under short day conditions for seven-weeks followed by growth under long day conditions. Lower panel highlights occasional morphological abnormalities in PsPIP5K1-EYFP or AtPIP5K2-LinPs-EYFP expression in the *pip5k1 pip5k2* double mutant background. **B** Plants from A were used to document and plot the starting point of flowering. Width of the boxes is proportional to the square root of the sample size. Sample sizes were $n \geq 9$, except for pPIP5K1::PsPIP5K1_LinAt-EYFP L25 ($n=4$) and pPIP5K2::PsPIP5K1_LinAt-EYFP L48 ($n=6$). Significant differences were determined using one-way ANOVA with a Tukey's post-hoc test ($p < 0.05$) and are indicated by letters a-b.

2.3 Hints for a regulatory link between CK2 and PI4P 5-kinase functions

Several proteins undergo a nuclear cytoplasm shuttling, e.g. Arabidopsis transcription factor BZR1 (Wang et al., 2021) and immune regulator EDS1 (Garcia et al., 1995) and many others (Goldstein, 1958; Ryu et al., 2007). A well-studied regulatory mechanism for NLS sequences is by masking or exposing NLS by protein phosphorylation (Jans and Hubner, 1996; Schwab and Dreyer, 1997; Jensen et al., 1998; Harreman et al., 2004; Liku et al., 2005; Youn and Shin, 2006). The nuclear localisation of PIP5K2 from Arabidopsis is not equally distributed and not clearly detectable in all cell types. Thus, it is hypothesised that the NLS of PIP5K2 is dynamically regulated and is either masked or activated by posttranslational modifications, such as protein phosphorylation. Yeast studies show that nuclear-cytoplasmic shuttling of the only yeast PI4P 5-kinase Mss4 is regulated via phosphorylation by casein kinase (Introduction 1.3, (Audhya and Emr, 2003)). CK2 from Arabidopsis has special recognition motifs, the phosphorylation of serine or threonine residues occurs mainly when acidic amino acid residues such as aspartate or glutamate are present (Introduction 1.3). Analyses of the primary amino acid sequence of PIP5K1 and PIP5K2 show classical CK2 phosphorylation motifs in the N-terminus and the characterised NLS of PIP5K2, leading to the hypothesis that also the nuclear localisation of AtPIP5K2 is regulated via phosphorylation by CK2 (Introduction 1.3 Fig. 8).

2.3.1 Subunits of CK2 interact with PIP5K1 and PIP5K2

The protein kinase CK2 is a serine-threonine kinase and is described as a heterotetrameric enzyme of two separate catalytic active alpha (CKA1-CKA4) and two regulatory beta (CKB1-CKB4) subunits (Salinas et al., 2006). In plants, the monomeric CKA subunits also appear to have protein kinase functions (Boldyreff and

Issinger, 1997; Filhol et al., 2004; Bibby and Litchfield, 2005). To test whether CK2 subunits interact with PIP5K1 and PIP5K2 from Arabidopsis, a split ubiquitin-based Y2H-assay was performed (see 4.19). PIP5K1 and PIP5K2 were tested for interaction with the CK2 subunits CKA1-CKA3 and CKB1-CKB3 in split-ubiquitin-based YTH studies where the PI4P 5-kinase-bait proteins were attached to the endoplasmic reticulum (ER) by fusion to an oligosaccharyltransferase 4 (OST4) anchor (see 4.7.2 and 4.12.2). Positive protein interaction was found for CKB1 and CKB3 for both PI4P 5-kinases, PIP5K1 and PIP5K2 (Fig. 24). PIP5K1 also interacted with the CK2 subunit CKA3 but PIP5K2 did not interact with any of the CKA subunits (Fig. 24).

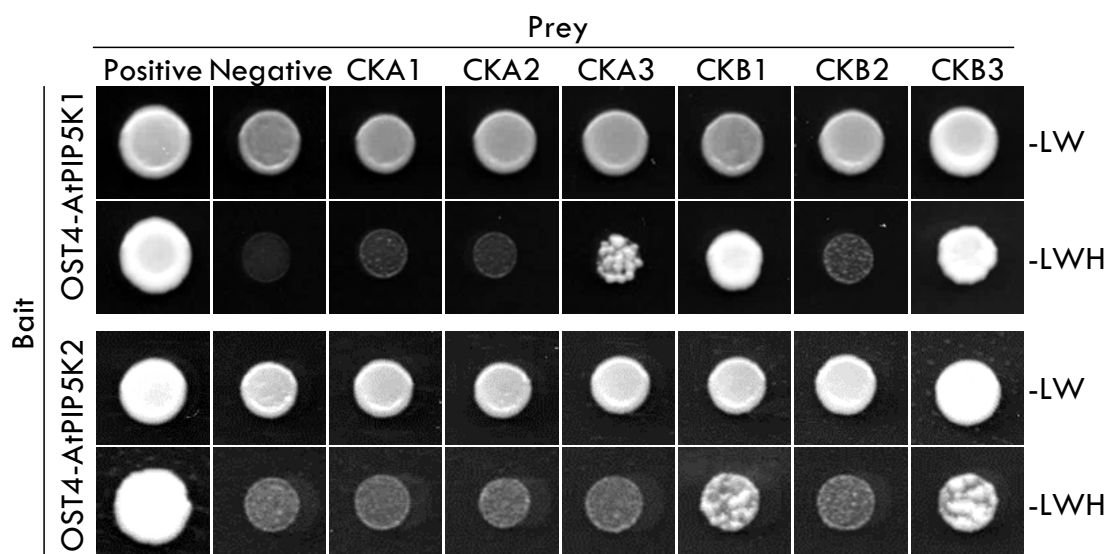


Figure 24 PIP5K1 and PIP5K2 interact with CK2 isoforms. Interaction of PIP5K1 and PIP5K2 with Arabidopsis alpha- and beta-CK2 isoforms CKA1-CKA3 and CKB1-CKB3 was tested in a split-ubiquitin based Y2H-assay. Baits were fused to OST4. *pAI-Alg5* and *pDL2-Alg5* vectors were used as positive and negative controls, respectively. Uniformly growing yeast on SD-LW (excluding leucine and tryptophane) indicated similar cell density and the presence of both, bait- and prey constructs. Protein-protein interaction is indicated by yeast growth on SD-LWH (excluding leucine, tryptophane and histidine). Yeast colonies were grown at 30 °C for six days. Results are representative for three independent experiments using $n \geq 3$ colonies of each combination, exception: CKA2 and CKB3 were tested two times using five colonies of each combination.

2.3.2 CKA3 phosphorylates PIP5K1 *in vitro*

From the experiments performed so far, CKA3 was found to be a candidate protein kinase possibly responsible for phosphorylation of PIP5K1 and possibly also PIP5K2. It was tested whether recombinant CKA3 would phosphorylate PIP5K1 or PIP5K2 *in vitro*. To test this, MBP fusions of PIP5K1 and PIP5K2 were expressed in *E. coli* Rosetta2 cells (see 4.13.1) and enriched by affinity chromatography (see 4.13.5 and appendix Fig 40A and B). The protein kinase subunit CKA3 was expressed as His-tagged fusion protein in *E. coli* BL21(DE3) (see 4.13.2 and

appendix Fig. 40C) and the cell lysate was used directly in the *in vitro* tests. Non-radioactive and radioactive *in vitro* phosphorylation assays were performed, using γ -S-ATP or radioactive labelled γ -[³²P]-ATP (see 4.15). Results of representative non-radioactive and radioactive *in vitro* phosphorylation test using MBP-PIP5K1, MBP-PIP5K2 and His-CKA3 are shown in figure 25A.

Non-radioactive and radioactive phosphorylation tests showed almost equal results (Fig. 25A and B). Full-length MBP-PIP5K1 protein with a size of 128 kDa as well as a protein fragment of ~50 kDa were phosphorylated by His-CKA3 (Fig. 25A and B). In the mock treated control, no phosphorylation was detected for MBP-PIP5K1 (Fig. 25A and B). In contrast, MBP-PIP5K2 was not phosphorylated by His-CKA3 (Fig. 25A and B). These data are supported by the protein-protein interaction studies in the YTH system described above, where PIP5K1 showed interaction with CKA3, whereas PIP5K2 did not (previous section 2.3.1). This observation implied a putative phosphorylation site in MBP-PIP5K1. Since CKA1 and CKA2 were not/ very weakly expressed in *E. coli*, only CKA3 was tested for its ability to phosphorylate PIP5K1 or PIP5K2 (see appendix Fig. 40). The CKB subunits do not have protein kinase activity, but rather modulate the activity of CKAs (Moreno-Romero et al., 2011; Mulekar and Huq, 2014). Nevertheless, CKB subunits were expressed as His-fusions as described for CKA3 (see 4.13.2) and purified (see 4.13.5 and appendix Fig. 40D) and tested for potential phosphorylation. MBP-PIP5K1 was not phosphorylated by any of the His-CKB isoforms in the phosphorylation assays (Fig. 25C). The individual combinations of CKA3 with the respective CKB1-CKB3 subunits reduced the intensity of MBP-PIP5K1 phosphorylation (Fig. 25C).

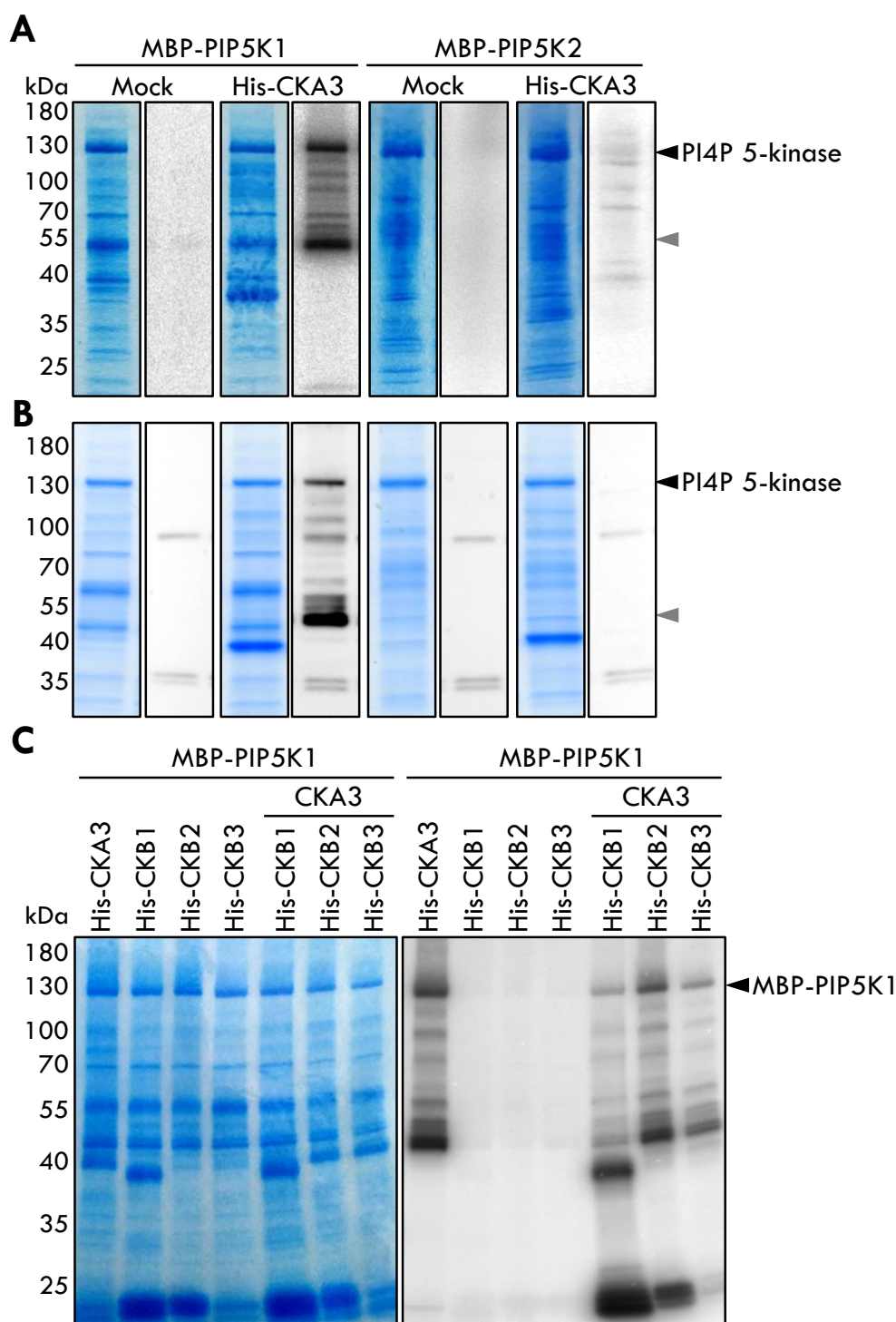


Figure 25 CKA3 phosphorylates PIP5K1 *in vitro*. Enriched recombinant MBP-PIP5K1 and MBP-PIP5K2 were tested for CK2 mediated phosphorylation. **A** γ -[32 P]-ATP radioactive and **B** γ -[S]-ATP non-radioactive phosphorylation test. PI4P 5-kinase were incubated either with *E. coli* cell extract after expression of His-CKA3 or with control cell lysate (Mock) expressing an empty vector control. The samples were incubated for 90 min at RT and separated by SDS-PAGE. Phosphorylated proteins were visualised by phosphorimager screens (A) or immunodetection (B). Radioactive CKA3 phosphorylation experiments were performed with MBP-PIP5K1 four times with duplicates; with MBP-PIP5K2 once with triplicates. Non-radioactive phosphorylation tests were performed with MBP-PIP5K1 two times with duplicates and MBP-PIP5K2 once with duplicates by master's student Juliane Zwöck. **C** Radioactive MBP-PIP5K1 phosphorylation test like described in (A) using different CK2

subunit combinations. Phosphorylated proteins were visualised by phosphorimager screens. Experiment was performed once using single sample sizes.

To analyse the phosphorylation sites by phosphoproteomics, recombinantly expressed MBP-PIP5K1 protein was incubated with His-CKA3 *E. coli* cell extract in the presence of unlabelled ATP (see 4.15) to conduct *in vitro* phosphorylation. The reaction mixtures were tryptically digested, and the resulting peptides were analysed by LC-MS-MS (see 4.16, Dr. Dirk Dobritzsch and Dr. Matt Fuzard, Core Facility Proteomic Mass Spectrometry MLU). The coverage for MBP-PIP5K1 was 68 % (see Appendix 6.2.1) and two phosphorylation sites, S2 and S408, were identified (Fig. 26). Phosphorylation site S2 is positioned in the N-terminus and was found phosphorylated in ten out of 24 peptides. Phosphorylation site S408 is located within the Dim-domain of PIP5K1 (Fig. 26) and was detectable in only one peptide out of three in total. However, due to the specific amino acid motif specification of CK2 (SD/SxD/SxxD; Introduction 1.3), it can be assumed that the two amino acid positions S2 and S408 can be considered as targets for CKA3.

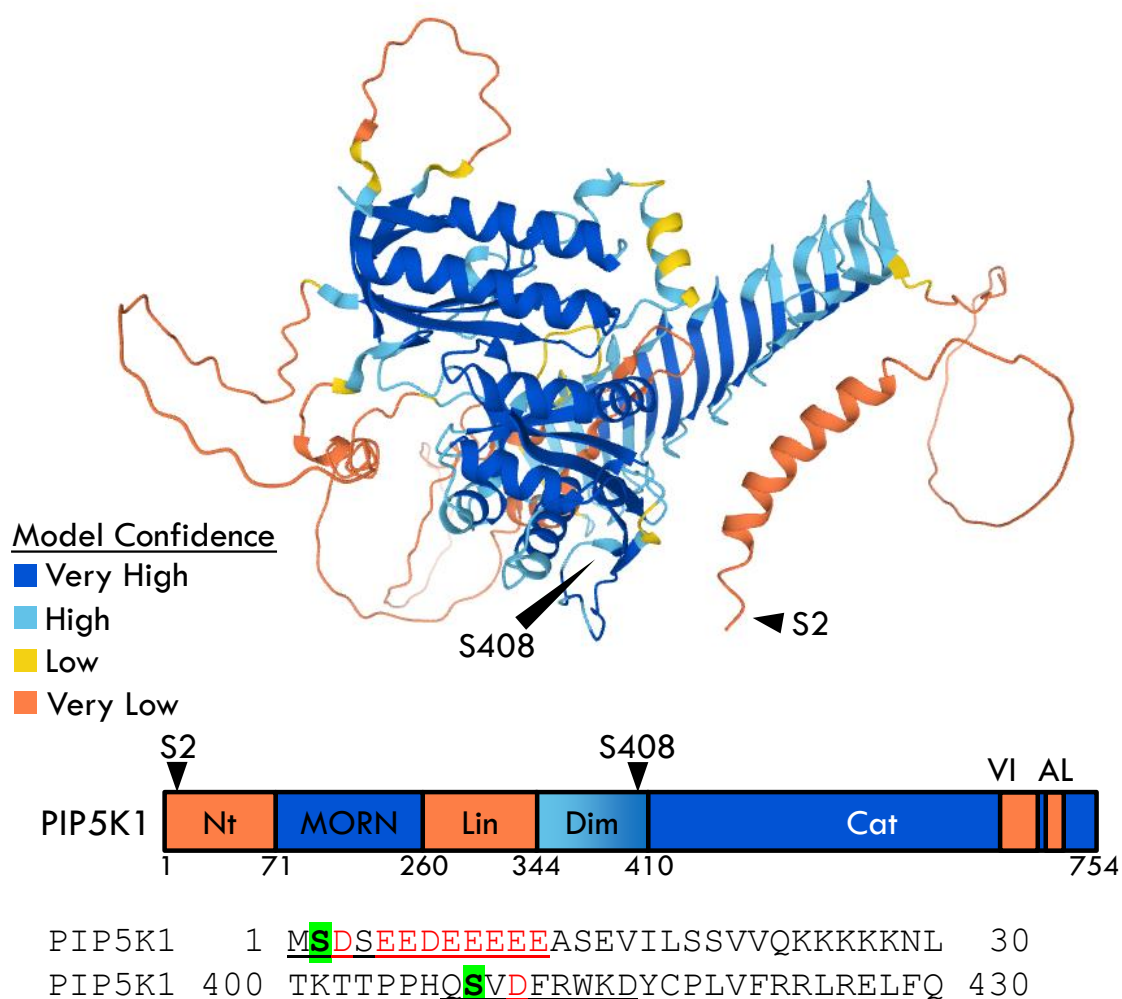


Figure 26 CKA3 phosphorylates PIP5K1 in position S2 and S408. Shown is an alpha fold model (Jumper et al., 2021; Varadi et al., 2022) and a domain scheme of PIP5K1,

in which the phosphorylation sites S2 and S408 discovered by MS have been highlighted with arrows. Amino acid sequence of phosphorylated PIP5K1 regions is displayed in detail. Underlines sequence is the detected peptide in MS analysis. Green marked serines are the discovered phosphorylation sites. Red letters indicate CK2 typical acidic amino acids in the recognition sites. Nt, N-terminus; MORN, Membrane Occupation and Recognition Nexus; Lin, Linker; Dim, Dimerization; Cat, Catalytical; VI, Variable insert; AL, Activation loop. The MS measurement was supported by Dr. Dirk Dobritzsch and the ZMG Core Facility Proteomic Mass Spectrometry of the MLU. MS measurement was performed once.

2.3.3 Coexpression of PIP5K1 with CKA3 seems to affect subcellular localisation of PIP5K1

Previous data show that CKA3 phosphorylates MBP-PIP5K1 at CK2 typical sequence motifs. Phosphorylation of proteins usually leads to regulation of the phosphorylated protein. This includes changes in protein conformation, binding properties but also activity changes and changes in subcellular localisation. It has been described for the PI4P 5-kinase *Mss4* from yeast that phosphorylation of *Mss4* by casein kinase can affect its subcellular localisation (Audhya and Emr, 2003). Although no phosphorylation site has yet been identified within the NLS of MBP-PIP5K1, the potential effects of phosphorylation on nuclear cytoplasmic shuttling of PIP5K1 should be investigated. To test whether phosphorylation of PIP5K1 by CKA3 also affects the subcellular distribution of PIP5K1 in plant cells, CKA3-mCherry and PIP5K1-EYFP (constructs, see 4.12.4) were coexpressed under the control of the *pCaMV35S* promoter in Arabidopsis leaf mesophyll and BY-2 protoplasts (see 4.22). As a control, both constructs were individually transformed into the cells and the distribution of the fluorescence was analysed (Fig. 27A and B).

Protoplasts based localisation studies with CKA3 revealed that CKA3-mCherry localised to the nucleus of Arabidopsis mesophyll and BY-2 protoplasts as described in the literature (Fig. 27B and D, (Salinas et al., 2006)). Coexpression of an NLS-CFP confirmed nuclear CKA3 signal (Fig. 27D) PIP5K1-EYFP fluorescence could be observed at the plasma membrane as well as in the cytosol and in Arabidopsis leaf protoplasts up to 45% and in BY2 cells up to 72% additionally in the nucleus (Fig. 27A and C, Fig. 28C). Like for PIP5K2-EYFP in section 2.1, NLS-DsRed marker was used to validate the absence of PIP5K1-EYFP in the nucleus in confocal plane images (Fig. 27C, upper panel).

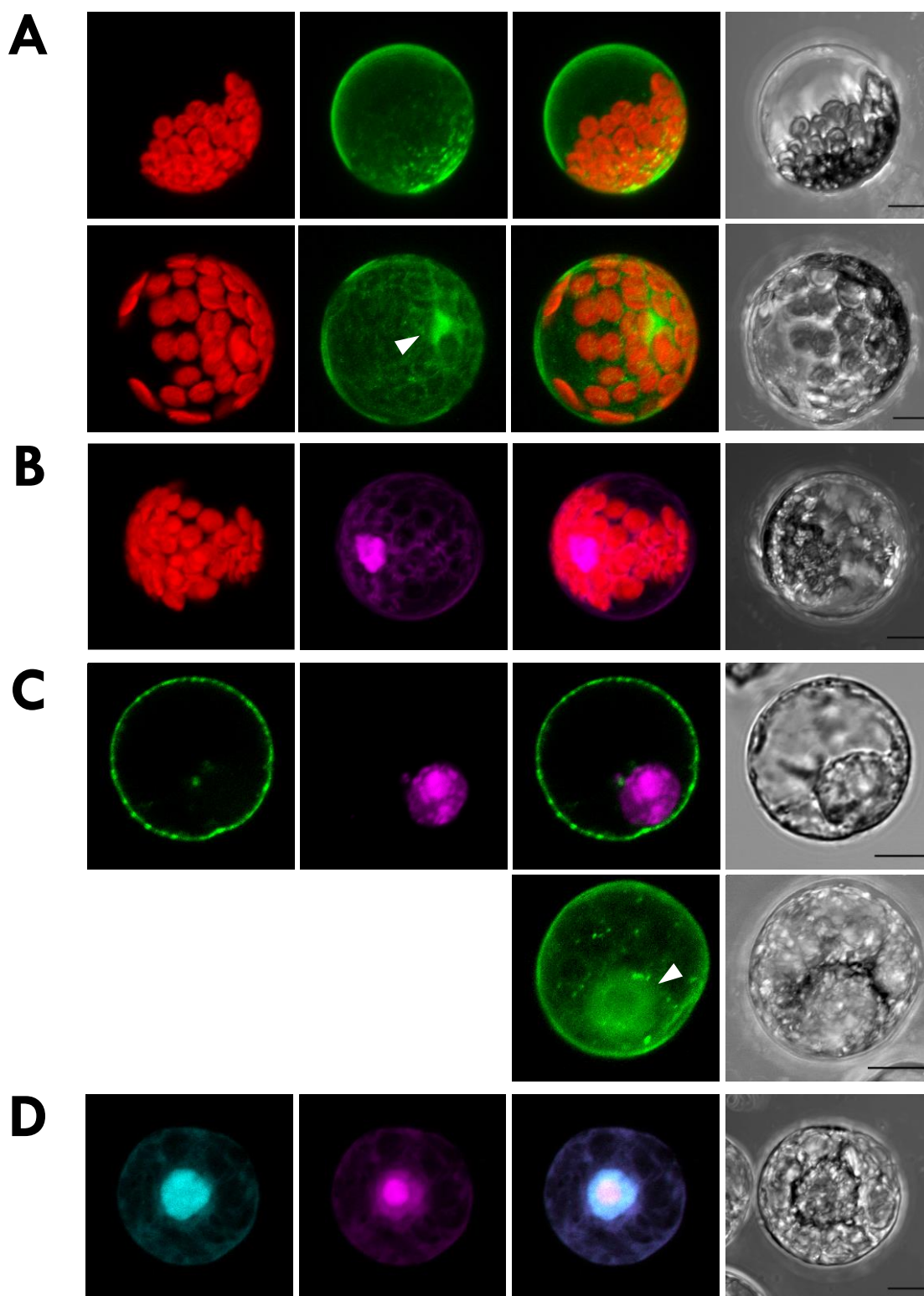


Figure 27 CKA3 localises to plant nuclei in Arabidopsis mesophyll and tobacco BY-2 protoplasts. Arabidopsis mesophyll and/ or tobacco BY-2 protoplasts were transiently transformed with *pEntryA-pCaMV35S::PIP5K1-EYFP* or *pEntryA-pCaMV35S::PIP5K1-EYFP* and *pEntryA-pCaMV35S::NLS-DsRed* or *pEntryA-pCaMV35S::CKA3-mCherry* or *pEntryA-pCaMV35S::CKA3-mCherry* and *pEntryA-pCaMV35S::NLS-CFP*. Subcellular localisation of fluorescent protein fusions was analysed with the LSM880. **A** and **B** Arabidopsis mesophyll protoplasts expressing PIP5K1-EYFP (A) or CKA3-mCherry (B). **C** and **D** BY-2 protoplasts expressing PIP5K1-EYFP or PIP5K1-EYFP and NLS-DsRed. **D** BY-2 protoplasts expressing CKA3-mCherry and NLS-CFP. Shown are projections of a z-stack covering the entire

protoplast with 1 μm intervals between sections (A, B, C lower panel and D) or confocal plane highlighting the nuclear area (C). Autofluorescence of chlorophyll A is depicted in red, NLS-CFP in blue, CKA3-mCherry in magenta and PIP5K1-EYFP in green. White arrows highlight nucleus. Scale bars, 10 μm . Images from A are representative for four independent experiments counting eleven (upper panel) and nine (lower panel) cells in total. Protoplast from B represents four cells in total from two sessions. Protoplasts in C represent 19 cells from two independent experiments. Protoplast from D represents five protoplasts from two independent experiments. Experiments were done in cooperation with master's student Juliane Zwoch.

Coexpression of PIP5K1-EYFP with CKA3-mCherry resulted in slightly increased nuclear localisation of PIP5K1-EYFP in both Arabidopsis leaf protoplasts and tobacco BY2 cells (Fig. 28A-C). Differences in nuclear PIP5K1-EYFP upon coexpression of CKA3 in leaf mesophyll protoplasts were not statistically significant (students t-test $p \leq 0.15$). Nevertheless, the data suggests that PIP5K1-EYFP shows increased nuclear signal upon coexpression and hypothetical phosphorylation of CKA3.

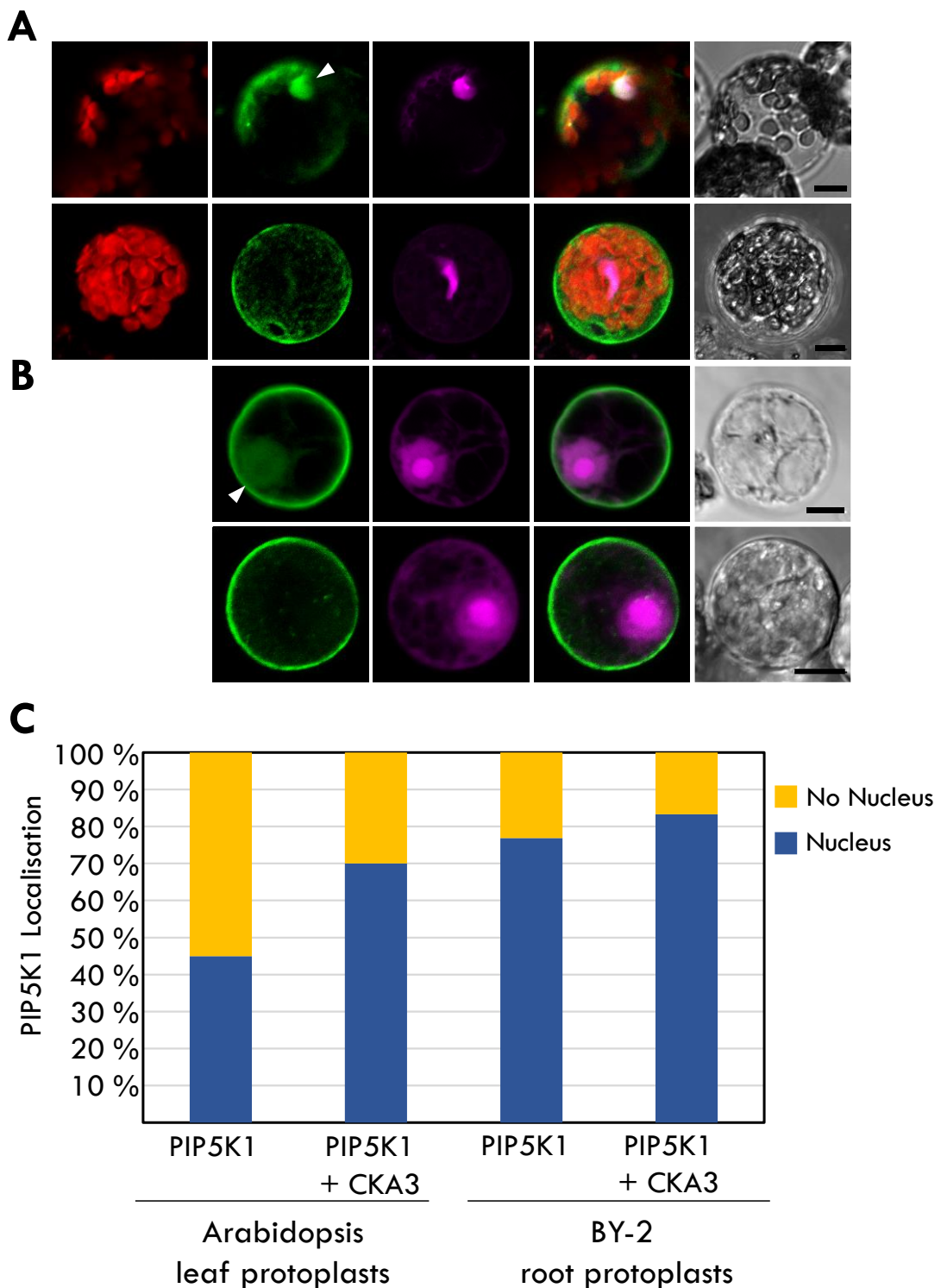


Figure 28 CKA3 coexpression increases PIP5K1 localisation to the nucleus in protoplasts. Arabidopsis mesophyll and/ or tobacco BY-2 protoplasts were transiently transformed with *pEntryA-pCaMV35S::PIP5K1-EYFP* or *pEntryA-pCaMV35S::PIP5K1-EYFP* and *pEntryA-pCaMV35S::CKA3-mCherry*. Subcellular localisation of fluorescent protein fusions was analysed with the LSM880. **A** and **B** Arabidopsis mesophyll (A) and BY-2 (B) protoplasts expressing PIP5K1-EYFP and CKA3-mCherry. Shown are projections of a z-stack covering the entire protoplast with 1 μm intervals between sections (upper panels) or confocal planes highlighting the nuclear area (lower panels). Autofluorescence of chlorophyll A is depicted in red, CKA3-mCherry in magenta and PIP5K1-EYFP in green. White arrow highlights nucleus. Scale bars, 10 μm . Images from A are representative for three

independent experiments counting ten cells in total. Images from B represent three independent experiments with twelve cells in total. C Subcellular distribution patterns of AtPIP5K2-EYFP and PsPIP5K1-EYFP cells were counted and categorised into two groups, showing fluorescence in the nucleus or at the plasma membrane. Experiments were performed in cooperation with master's student Juliane Zwoch.

2.3.4 CKA3 effects the catalytic activity of PIP5K1 upon phosphorylation

Previous studies have already shown that phosphorylation of PI4P 5-kinases by various protein kinases can lead to a change in the catalytic activity of PI4P 5-kinases (Hempel et al., 2017; Menzel et al., 2019). Therefore, we aimed to test here whether phosphorylation of PIP5K1 by CKA3 not only leads to a subcellular change but also whether it affects the catalytic activity of PIP5K1 *in vitro*.

To test this, both recombinantly expressed enzymes were preincubated in a protein phosphorylation assay so that the PI4P-5 kinase could be phosphorylated by CKA3 (see 4.15). Subsequently, the PI4P-5 kinase activity of the phosphorylated MBP-PIP5K1 was analysed by measurement of formed PtdIns(4,5)P₂, which resulted from phosphorylation of the lipid substrate PtdIns4P in the presence of γ -[³²P]-ATP (see 4.15). To ensure phosphorylation of MBP-PIP5K1, the identical experimental setup as described in the previous section (see 2.3.2) was used for the kinase assay and phosphorylated MBP-PIP5K1 was strongly detectable (Fig. 29A). The results of the activity assay were compared with a sample containing identical amounts of the same MBP-PIP5K1 preparation without treatment and an MBP-PIP5K1 sample incubated with control cell lysate from *E. coli*. (Fig. 29A). As a negative control MBP was used alone in the reaction.

MBP displayed no activity for the tested reaction (Fig. 29B). Untreated MBP-PIP5K1 converts PtdIns4P to PtdIns(4,5)P₂ as previously reported (Fig. 29B). However, it should also be noted that the addition of *E. coli* cell lysate in general drastically reduced the activity of MBP-PIP5K1 (Fig. 29B). In comparison, MBP-PIP5K1 samples that were preincubated with CKA3 showed a twofold increased PtdIns(4,5)P₂ formation ($p \leq 0.09$ in students t-test) compared to the MBP-PIP5K1 samples incubated with the control lysate (Fig. 29B, lower panel). These experimental data suggest an increase of catalytical activity of PIP5K1 upon phosphorylation of CKA3 *in vitro*.

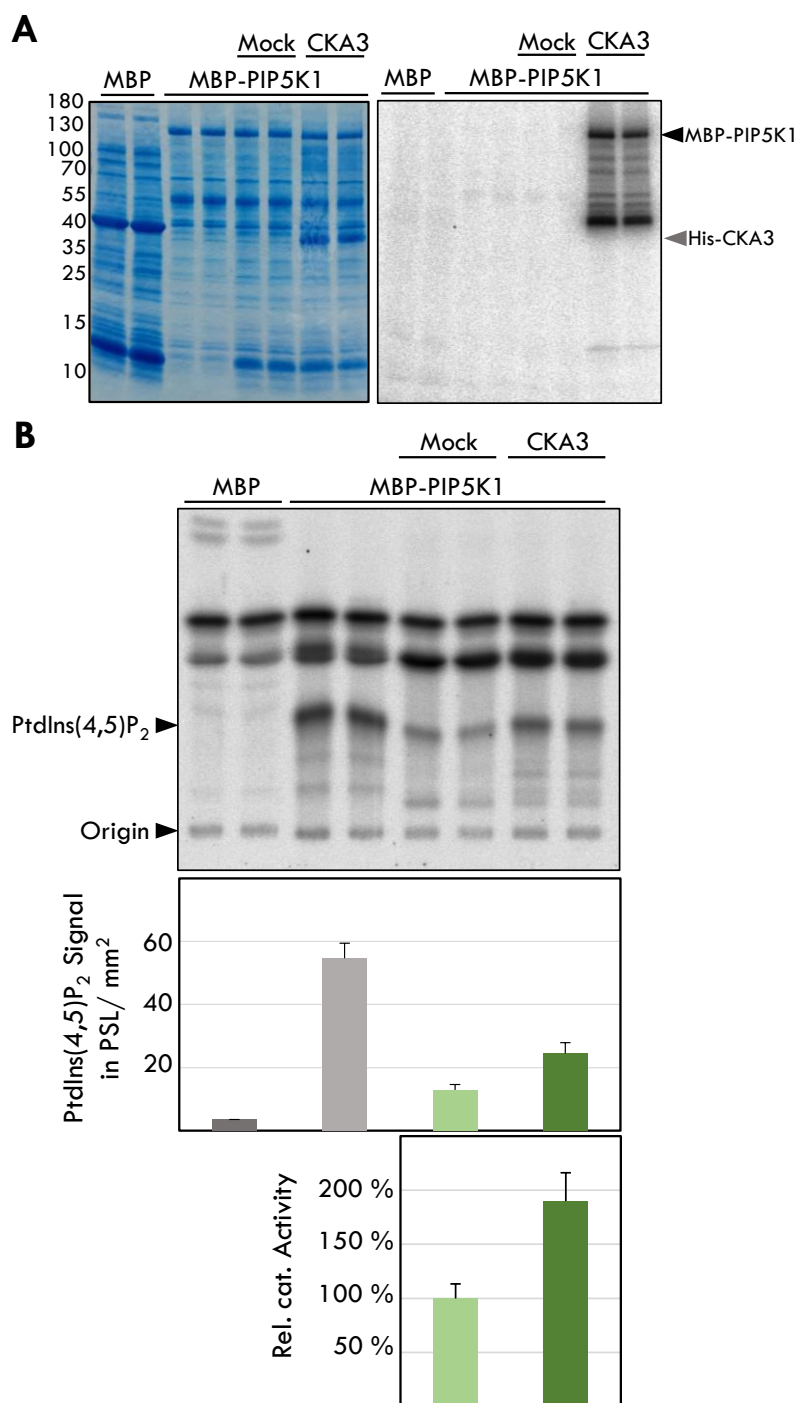


Figure 29 PIP5K1 shows enhanced catalytic activity after phosphorylation by CKA3. **A** PIP5K2 phosphorylation test coupled to **B** measurements of catalytic activity. Enriched recombinant MBP-PIP5K1 was incubated either with *E. coli* cell extract after expression of His-CKA3 or with control cell lysate (Mock) expressing an empty vector control. The samples were preincubated for 30 min at room temperature and split for phosphorylation test and catalytic activity assays. Phosphorylation test was separated by SDS-PAGE. Phosphorylated proteins were visualised by phosphorimager screens. Catalytic activity was measured by incubating samples with γ -[³²P]-ATP and PtdIns4P as substrate. By radioactive incorporation from γ -[³²P]-ATP into PtdIns(4,5)P₂ catalytic activity of MBP-PIP5K1 was measured. PIs were extracted and separated using TLC before radioactive signals were visualised using phosphorimager plates. Cor-

responding PtdIns(4,5)P₂ signal was analysed with TINA2.0 (Raytest, Straubenhardt, Germany) software and relative activity calculated. PSL-photo stimulates luminescence. The experiment was performed twice with similar results.

2.4 A new link between AGCVIII protein kinase PID and PI4P 5-kinase function

In addition to the possible regulation of PIP5K1 by the subunits of the protein kinase CK2, it could also be shown that there seems to be a connection between plant AGCVIII kinases such as PID and PIP5K1 and PIP5K2. The protein kinase PID is well

studied for its role in auxin signal transduction and maintaining the auxin polarity gradient by adjusting the localisation and catalytic activity of PIN proteins (Introduction Fig. 13, (Michniewicz et al., 2007; Huang et al., 2010; Adamowski and Friml, 2015; Dhonukshe et al., 2015; Weller et al., 2017; Glanc et al., 2021)). Interestingly, PID and PID-related protein kinase mutants showed the same Arabidopsis wavy root growth phenotype as PIP5K1 and PIP5K2 overexpression (Introduction Fig. 9 (Ischebeck et al., 2013; Dhonukshe et al., 2015)). Furthermore, comparisons of PID-overexpressing plants with *pip5k1-pip5k2* double mutant showed similar phenotypes such as the pronounced dwarfism (Introduction Fig. 9 (Benjamins et al., 2001b; Ischebeck et al., 2013)). Another link between the AGCVIII kinase PID and PIP5K1 and PIP5K2 is, that the PI4P 5-kinases are regulating the directed polar vesicle transport, resulting in a polar distribution of certain proteins. Thus, PIP5K1 and PIP5K2 contribute to the polar incorporation of PIN proteins into the endomembrane network (Ischebeck et al., 2013; Tejos et al., 2014). Thus, the regulation of polar auxin transport via PIN proteins is regulated by PID and PIP5K1 / PIP5K2, leading also to the hypothesis that also PID and PIP5K1 / PIP5K2 are interlinked on several regulation levels (Introduction Fig. 13). Based on these facts, it was investigated here in more detail, whether the AGCVIII kinase PID is a potential candidate of PI4P 5-kinase phosphorylation, thereby contributing to PI4P 5-kinase regulation.

2.4.1 AGCVIII protein kinase PID interacts with PIP5K1 and PIP5K2

On the basis that the signalling pathways of auxin transport and regulation of polar protein distribution may be co-regulated by PID and PIP5K1 / PIP5K2, protein-protein interactions between PID and PIP5K1 / PIP5K2 were suspected to occur in the cytosol or/ and at the plasma membrane-cytosol interface. To test or confirm protein-protein interaction split-ubiquitin-based YTH assays (see 4.19) were performed to test the physical interaction of PIP5K1 and/ or PIP5K2 with the AGCVIII kinase PID and close homologues WAG1 and WAG2 (Fig. 30A). The YTH assay indicated a protein-protein interaction between PIP5K1 and PIP5K2 with PID and WAG2 respectively (Fig. 30A). Neither PIP5K1 nor PIP5K2 interacted with WAG1 (Fig. 30A).

The positive results of the split ubiquitin based YTH assay were confirmed with *in vitro* pull-down assays (see 4.20). GST and GST-PID (appendix Fig. 41B and C) were immobilized to a glutathione agarose matrix and were then co-incubated with recombinant protein extracts of MBP-tagged PIP5K1 or -PIP5K2 (appendix Fig. 40A and B). After incubation and washing, proteins were coeluted with reduced L-glutathione and the elution fractions were analysed with western blot and

immunodetection with anti-GST and anti-MBP antibodies (Fig. 30B). The *in vitro* pull-down showed that both PI4P 5-kinases, PIP5K1 and PIP5K2, were coeluted with GST-PID confirming interaction with GST-PID (Fig. 30B).

To further verify protein-protein interaction under physiological conditions *in vivo*, a bimolecular fluorescence complementation test (BiFC) was performed (see 4.21). This test offers not only the possibility to document the protein-protein interaction in living plant cells, but also characterises the subcellular localisation of the interplay between PIP5K2 and PID. For this purpose, PID was fused to the N-terminal part of EYFP (n-EYFP) and PIP5K2 was fused to the C-terminal part of EYFP (c-EYFP) and transiently expressed in Arabidopsis leaf mesophyll protoplasts (see 4.12.4 for protoplast isolation and transformation, 4.22 for constructs and 4.21 for BiFC assay). As control, n-EYFP-PID interaction was tested with AGC kinase master regulator c-EYFP-PDK1 that has been reported to interact with PID (Introduction 1.3.2 (Mora et al., 2004; Zegzouti et al., 2006, 1; Xiao and Offringa, 2020)). Further c-EYFP-PIP5K2 interaction was tested with n-EYFP-PDK1 that was not interacting with PIP5K2 in unpublished experiments (Babette Pinkwart). The BiFC interaction partners and RFP for transformation control were expressed by a single vector (Walter et al., 2004) and fluorescence detected at the LSM880 (see 4.24.1)

Interaction studies of n-EYFP-PID and c-EYFP-PDK1 in our BiFC assay resulted in 97 % of transformed protoplasts displaying EYFP fluorescence (Fig. 30C and D). Expression of nEYFP-PDK1 and cEYFP-PIP5K2 provided an EYFP signal in 28,3 % of the transformed protoplasts (Fig. 30C and D) compared to 55 % for nEYFP-PID and cEYFP-PIP5K2, indicating an interaction between PIP5K2 and PID (Fig. 30C and D). The fluorescence observed for the co-expression of PIP5K2 and PID was more restricted to the plasma membrane while reconstitution of EYFP in the controls resulted in a more cytosolic signal (Fig. 30C). The BiFC experiments are consistent with the split-ubiquitin-based YTH and *in vitro* pull-down data and support interaction between PIP5K2 (and PIP5K1) and the AGCVIII protein kinase PID in plant cells.

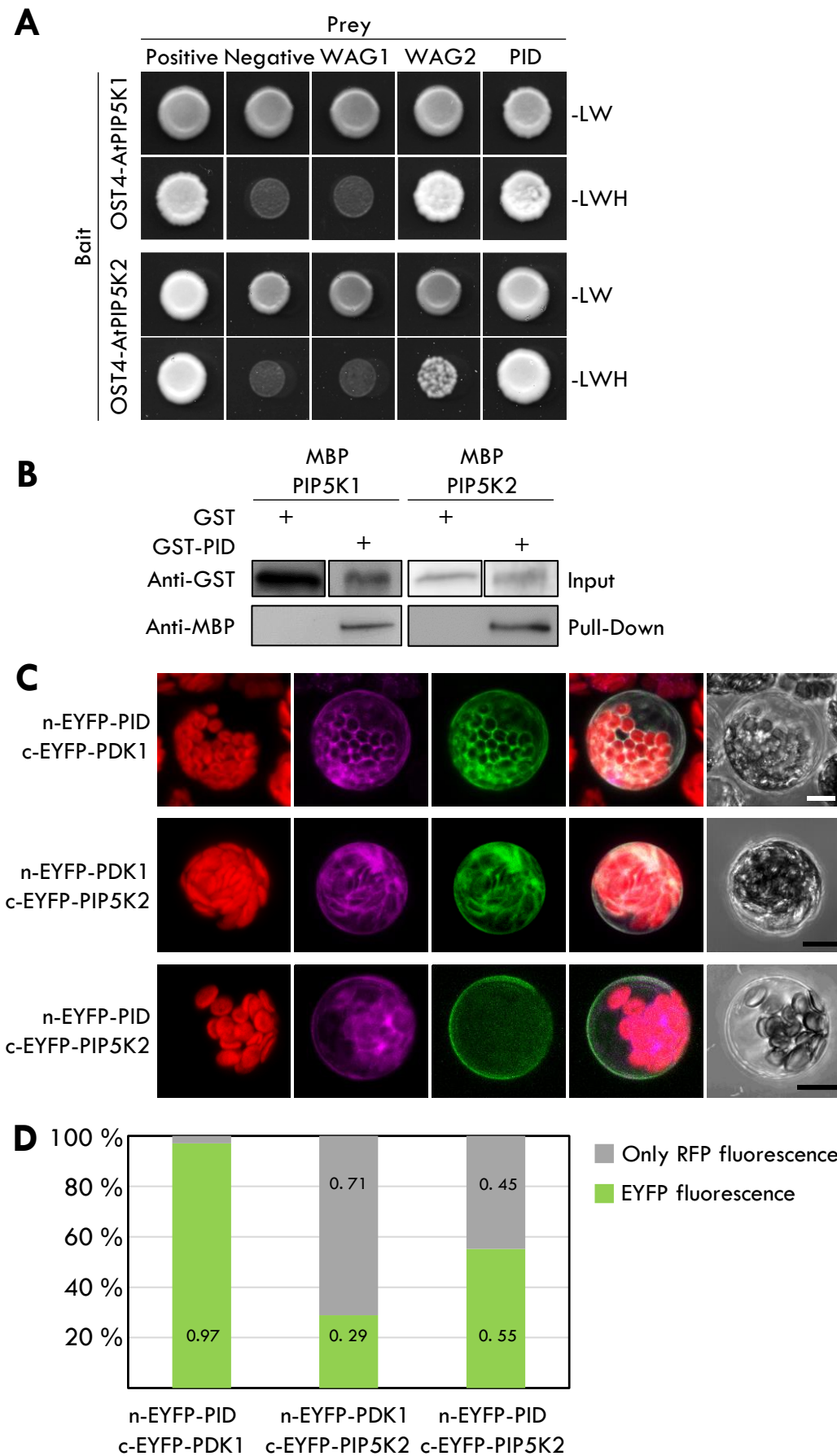


Figure 30 PID interacts with PIP5K1 and PIP5K2. The interaction of PIP5K1 and PIP5K2 with Arabidopsis AGCVIII protein kinases PID, WAG1 and WAG2 were tested in a split-

ubiquitin based Y2H, immune pull-down and bimolecular fluorescence complementation (BiFC) assays. **A** Yeast strain NMY51 was transformed with PIP5K1- and PIP5K2-OST4-fusion as baits. *pAI-Alg5* and *pDL2-Alg5* vectors were used as positive and negative control, respectively. Uniform yeast growth on selective media without leucine and tryptophane (SD-LW) indicated equal cell densities and the presence of both, bait and prey vectors. Protein-protein interaction is indicated by growth on SD medium without leucine, tryptophane and histidine (SD-LWH). Yeast colonies were grown at 30 °C for three days (PIP5K1) or six days (PIP5K2). A representative result of three replicates with five colonies of each tested combination is shown. **B** *In vitro* immuno pull-down of MBP-PIP5K1 (128 kDa), MBP-PIP5K2 (128.5 kDa) with GST-PID (75 kDa). GST (26 kDa) and GST-PID were immobilized on glutathione agarose and incubated either with MBP-PIP5K1 or MBP-PIP5K2. After washing, bound proteins were coeluted with L-glutathione. The pulled down MBP-tagged proteins were analysed with immunodetection using an anti-MBP antibody. The input GST and GST-PID proteins were detected using an anti-GST antibody. Chemiluminescence signals were detected with an ECL detection system. *In vitro* pull-down was performed three times, of which one was performed by master's student Babette Pinkwart. **C** BiFC test in *Arabidopsis mesophyll* protoplasts. The BiFC-2in1 vectors containing n-EYFP-PID and c-EYFP-PDK1, n-EYFP-PDK1 and cEYFP-PIP5K2, n-EYFP-PID and c-EYFP-PIP5K2, were transiently transformed into protoplasts. Shown are projections of z-stacks covering the entire protoplast with 1 µm intervals between sections. Autofluorescence of chlorophyll A is depicted in red, RFP transformation control in magenta, reconstituted EYFP in green. Scale bars, 10 µm **D** Evaluation of BiFC test displaying proportion of cells that displayed reconstituted EYFP fluorescence. Control of n-EYFP-PID and c-EYFP-PDK1 showed fluorescence of reconstituted EYFP in 33 out of 34 protoplasts (97%). N-EYFP-PDK1 and c-EYFP-PIP5K2 displayed 52 transformed protoplasts showing RFP fluorescence of which 15 (28.8%) showed reconstitutions of EYFP by green fluorescence. BiFC assay with n-EYFP-PID and c-EYFP-PIP5K2 showed RFP fluorescence in 203 transformed protoplasts of which 112 showed reconstitutions of EYFP by green fluorescence (55.2%). GST, glutathione S-transferase; MBP, maltose-binding protein; OST4, oligosaccharyltransferase 4.

2.4.2 PID phosphorylates (PIP5K1 and) PIP5K2 in the NLS region within the Lin-domain

From the experiments conducted so far on protein-protein interaction, it can be deduced that PID is a candidate for a protein kinase that may be responsible for the phosphorylation of PIP5K1 and PIP5K2. To investigate this *in vitro* kinase assays with MBP-PIP5K1 and MBP-PIP5K2 with MBP-PID were tested in a radioactive phosphorylation assay (see 4.15). The test is based on the incubation of the protein substrate with the protein kinase using radioactive γ -[³²P]-ATP. By using γ -[³²P]-ATP, the radioactively labelled γ -phosphate is used by the protein kinase for phosphorylation of the target protein and labels it. Via the subsequent separation of the proteins by SDS-PAGE (see 4.13.7) and the detection of radioactive phosphate incorporation with phosphorimager plates, it is possible to determine the phosphorylation of proteins (see 4.15). Figure 31 shows the Coomassie-stained gels as a loading control and the corresponding autoradiographs. The experiment in figure 31 revealed, that PID phosphorylates MBP-PIP5K1 and MBP-PIP5K2 *in vitro*, whereas MBP is no substrate for the PID AGCVIII kinase. In figure 31, the increase

of the phosphorylation signal of MBP-PIP5K2 with increasing amount of MBP-PID can be observed within the same incubation period.

To discover putative phosphorylation sites a MS-based approach was performed without radiolabelled ATP, as described in 2.3.2. The proteins were digested with trypsin and the phosphorylated peptides were identified by a targeted LC-MS-MS analysis (see 4.1.6), according to the masses of the predicted phosphorylated and non-phosphorylated peptides, in cooperation with the Mass Spec. facility (Dr. Dirk Dobritzsch and Dr. Matt Fuzard, Core Facility Proteomic Mass Spectrometry MLU). The analysed peptides covered up to 65 % of PIP5K2 (Appendix 6.2.2). Positions S274, S275, and S282 were all located on the same identified peptide (Fig. 31). However, the peptide with phosphorylated position S282 was identified more frequently than at positions S274 and S275. Using one of the MS experiments as an example, the identified peptide $_{272}\text{KKSSVDSGAGSLTGEK}_{287}$ (Fig. 31) was detected a total of eleven times, four of which were not phosphorylated, once at positions S274 and S275, and five times at position S282 (Appendix 6.2.2). Interestingly, S278 was not identified as phosphorylated in any of the MS-based experiments. This suggests specific phosphorylation of S274, S275, and S282 in the Lin-domain of PIP5K2 by PID.

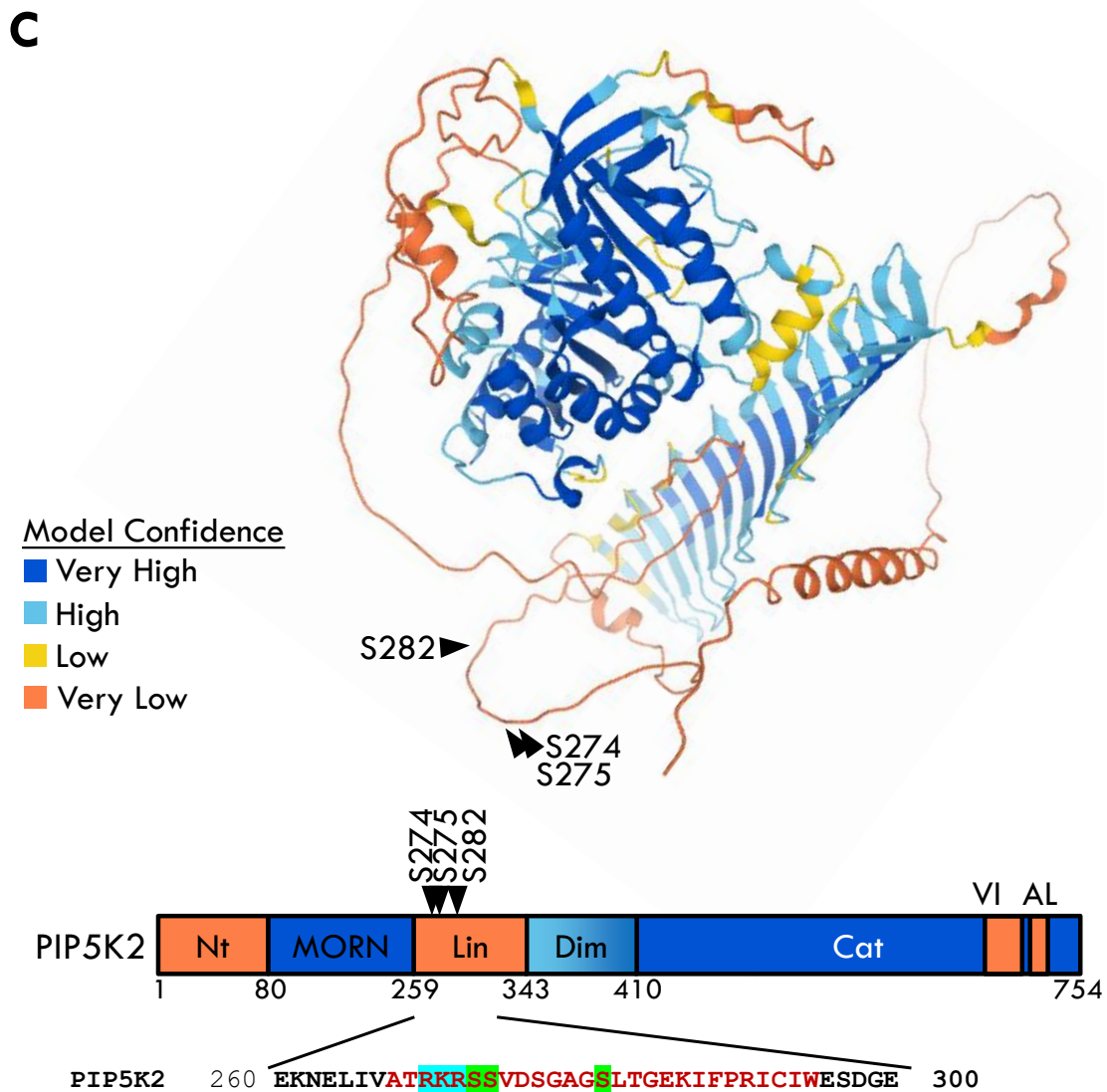
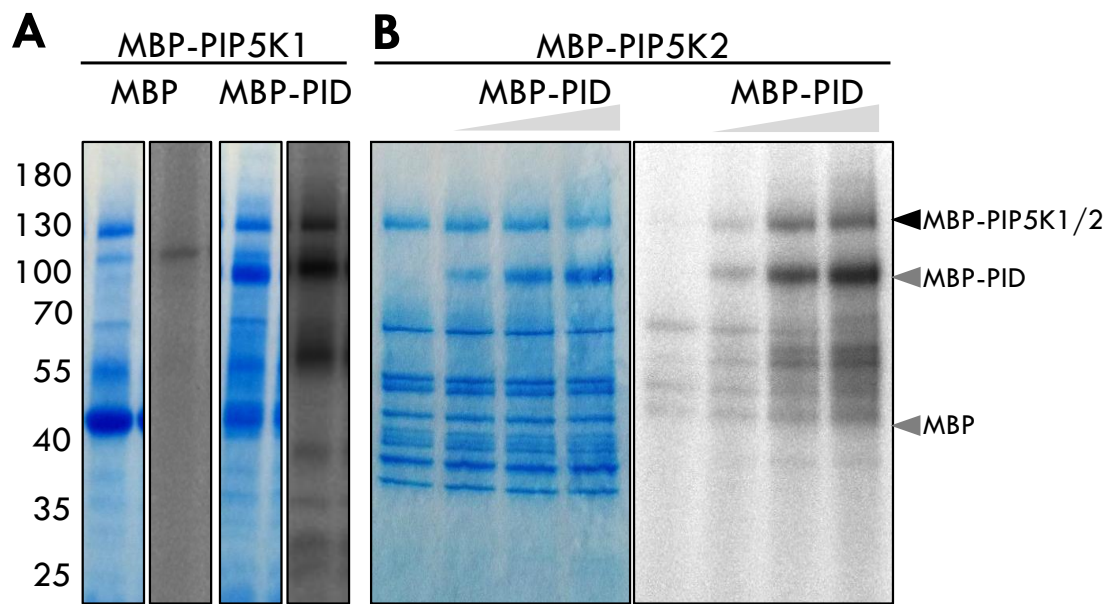


Figure 31 PID phosphorylates PIP5K2 in the NLS region of the Lin-domain. Enriched recombinant MBP-PIP5K1 and MBP-PIP5K2 were tested for MBP-PID mediated phosphorylation. **A** MBP-PIP5K1 and **B** MBP-PIP5K2 γ -[32 P]-ATP radioactive phosphorylation test

with MBP-PID. PI4P 5-kinase were incubated either with MBP-PID or elution buffer as control. The samples were incubated for 90 min at RT and separated by SDS-PAGE. Phosphorylated proteins were visualised by phosphorimager screens. Phosphorylation test of MBP-PIP5K1 and PID was performed once using technical triplicates. Phosphorylation test of MBP-PIP5K2 and MBP-PID was performed three times. **C** Shown is an alpha fold model (Jumper et al., 2021; Varadi et al., 2022) and a domain scheme of PIP5K2, in which the phosphorylation sites S274, S275 and S282 discovered by MS have been highlighted with black arrows. Amino acid sequence of phosphorylated PIP5K2 NLS regions is displayed in detail. Underlines sequence is the detected peptide in MS analysis. Green marked serine are the discovered phosphorylation sites. Red letters indicate characterised NLS, blue marked is the basic cluster RKR of the NLS. Nt, N-terminus; MORN, Membrane Occupation and Recognition Nexus; Lin, Linker; Dim, Dimerization; Cat, Catalytical domain; VI, Variable insert; AL, Activation loop. The MS measurement was supported by Dr. Dirk Dobritzsch and the ZMG Core Facility Proteomic Mass Spectrometry of the MLU. MS measurement was performed twice.

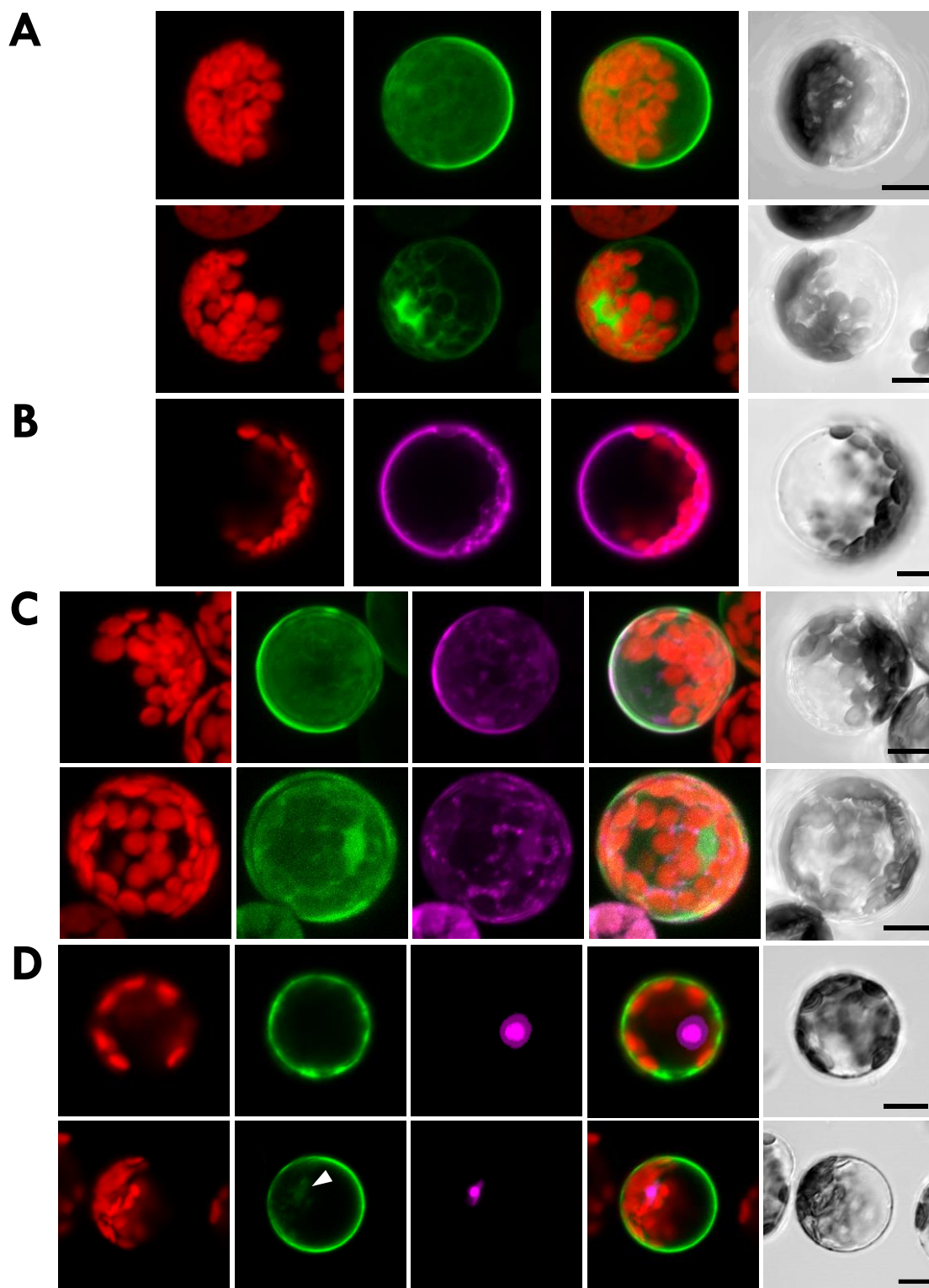
2.4.3 PIP5K2 does not show altered subcellular localisation upon phosphorylation by PID

PI4P 5-kinases are lipid-modifying enzymes that associate both at the plasma membrane and in the cell nucleus and most likely convert PtdIns4P into PtdIns(4,5)P₂. As already described (Introduction 1.2), phosphorylation can influence the functionality or accessibility of nuclear localisation signals and thus decisively influence the localisation of target proteins (Jans and Hubner, 1996; Schwab and Dreyer, 1997; Jensen et al., 1998; Harreman et al., 2004; Liku et al., 2005; Youn and Shin, 2006; Wang et al., 2021). Interestingly, the phosphorylation sites S274, S275 and S282 identified here are in the NLS of the Lin-domain of PIP5K2 (see 2.4.2 Fig. 31), suggesting that these phosphorylations may influence the subcellular localisation of PIP5K2. To determine the influence of phosphorylation on the subcellular localisation of PIP5K2, localisation studies were performed in which either the localisation of PIP5K2 cotransformed with PID (see 4.1.2.4) in wild type Arabidopsis protoplasts or the localisation of PIP5K2 in AGCVIII kinase overexpressor and mutant protoplasts has been studied. Therefore, localisation was monitored with PIP5K2-EYFP fusions under the control of the *pCaMV35S* promoter. For the cotransformation with PID, *pCaMV35S::PID-mCherry* constructs (see 4.22) were used. In addition, PIP5K2 A/ D substitution variants were created (see 4.1.1.2), in which the phosphorylation sites S274 and S275 were replaced by alanine or aspartic acid creating phospho-ablation or phospho-mimicry variants respectively. With these PIP5K2 variants localisation experiments were performed as described above.

Transient expression of wild type PIP5K2-EYFP in wild type Arabidopsis cells displayed a characteristic localisation at the plasma membrane (Fig. 32A upper panel) and in 53 % of the cells also in the nucleus (Fig. 32A lower panel) as it has already been described in the introduction and in chapter 2.1. Protoplasts

transformed with PID-mCherry displayed mCherry fluorescence mainly in the cytosol (Fig. 32B).

The localisation of PIP5K2-EYFP in co-expression with PID-mCherry did not show different PIP5K2 localisation (Fig 32C). Likewise, localisation studies with PIP5K2-EYFP and the use of PID overexpressing plants were changing the described subcellular localisation of PIP5K2-EYFP (Fig. 32D). Another approach using substitution of the phosphorylation sites S274 and S275 in the NLS range of PIP5K2 to alanine and aspartic acid, under the conditions here, had no influence on the subcellular localisation: Both variants, PIP5K2 S274A S275A-EYFP as well as PIP5K2 S274DS 275D-EYFP localised in the tested cells like the wildtype form PIP5K2-EYFP (Fig. 32E and F). Under these conditions, it could not be observed that the subcellular localisation of PIP5K2 is influenced by PID or the modification of PID phosphorylation sites.



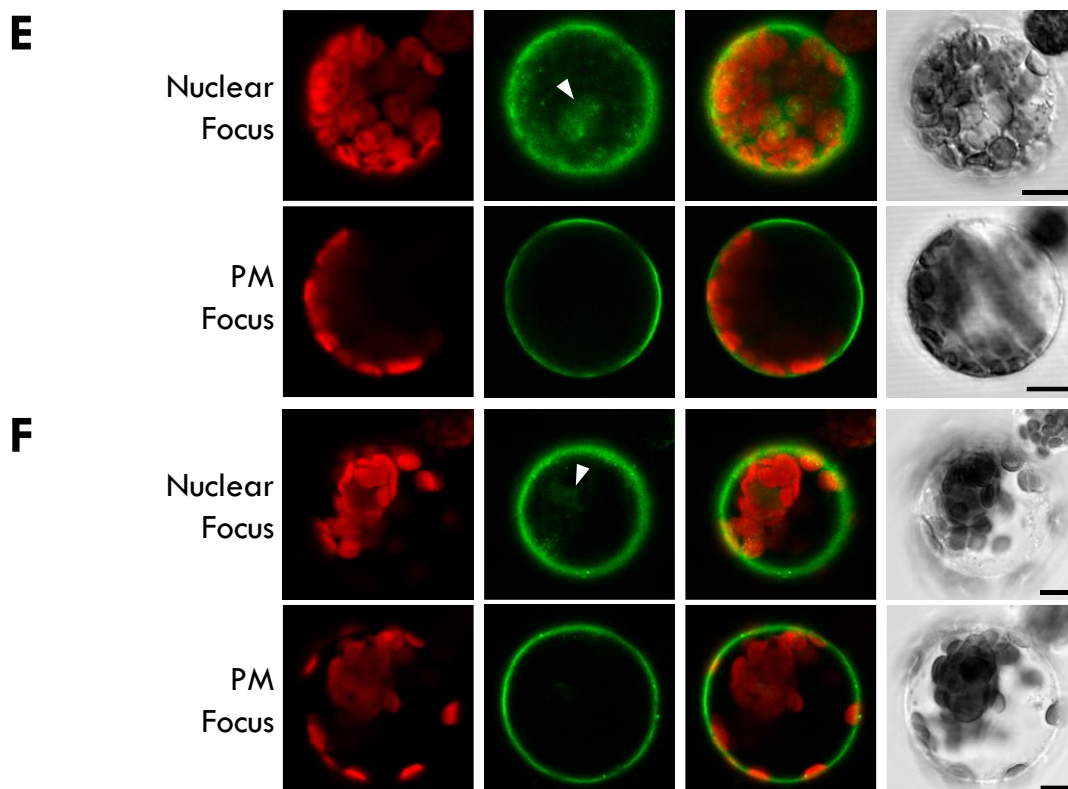


Figure 32 PIP5K2 apparently localises unaffected by PID. Arabidopsis mesophyll protoplasts were transiently transformed with *pEntryA-pCaMV35S::PIP5K2-EYFP*, *pEntryA-pCaMV35S::PIP5K2 S274A/D S275A/D-EYFP*, *pCaMV35S::PID-mCherry* and/ or *pEntryA-pCaMV35S::NLS-DsRed*. Subcellular localisation of fluorescent protein fusions was analysed with the LSM880. **A** Protoplasts expressing PIP5K2-EYFP. **B** Protoplast expressing PID-mCherry. **C** Protoplasts coexpressing PID-mCherry and PIP5K2-EYFP. **D** Protoplasts derived from PID-overexpressing Arabidopsis plants (Benjamins et al., 2001b) expressing PIP5K2-EYFP and NLS-DsRed. **E** Protoplasts expressing PIP5K2 S274A S275A-EYFP. **F** Protoplasts expressing PIP5K2 S274D S275D-EYFP. Shown are projections of z-stacks covering the entire protoplast with 1 μm intervals between sections (A, C) or confocal sections highlighting the nuclear or plasma membrane area (B, D, E; F). Autofluorescence of chlorophyll A is depicted in red, PID-mCherry and NLS-DsRed in magenta and PIP5K2-EYFP and substitution variants in green. Scale bars, 10 μm . Cells are representative for A (PIP5K2-EYFP), n= 24; B (PID-mCherry), n=14; C (PIP5K2-EYFP and PID-mCherry), n=12; D (PID OE plants, PIP5K2-EYFP), n=29; E (PIP5K2 S274AS275A-EYFP), n=40; F (PIP5K2 S274DS275D-EYFP), n=15.

2.4.4 Investigation of the nanodomain pattern of PIP5K2-EYFP and the A/ D variants at the plasma membrane

In previous experiments no influence on the subcellular localisation of PIP5K2 via phosphorylation by PID could be observed. It could well be that the phosphorylation has no influence on the localisation change of PIP5K2, or the influence is of a more subtle nature and cannot be easily investigated with the LSM technique. The plasma membrane association of PIP5K2 is relatively well studied. It could be shown with the appropriate microscopic methods that PIP5K2 is not uniformly distributed at the

plasma membrane, but in small foci (Introduction Fig. 2 (Fratini et al., 2021)). This distinct localisation at the plasma membrane can be influenced by changes in the Lin-domain (Stenzel et al., 2012; Fratini et al., 2021). To analyse the PIP5K2-EYFP membrane association a total-internal-reflective-fluorescence (TRIF) microscopy setup was chosen (see 4.24.3). *Arabidopsis mesophyll* protoplasts were transiently transformed with PIP5K2-EYFP or the substitution variants PIP5K2 S274A S275A-EYFP and PIP5K2 S274D S275D-EYFP (see 4.22) and the plasma membrane localisation was analysed using TIRF microscopy. Protoplast membranes were documented up to 2500 repeats with 300 ms intervals. Representative single frames, kymographs and lifetime of PIP5K2 foci at the plasma membrane are displayed in figure 33.

Using TIRF microscopy it was possible to detect PIP5K2-EYFP in defined regional spots at the plasma membrane, so called foci, visible as white dots in the single frame pictures (Fig 33A). The corresponding kymographs display a highly dynamic foci pattern by a noisy motif (Fig. 33A). More stable structures were indicated by single linear signals in the kymographs exemplary highlighted by blue markings in the PIP5K2 S274A S275A sample (Fig. 33A middle panel). The lifetime of the respective EYFP marked foci for the time of 0.3-4.2 s was shown in a diagram (Fig. 33B). During this observation period there were no statistically significant differences in the plasma membrane residence time of the foci after expression of the wild form PIP5K2-EYFP or the A/ D variants. The substitution of the phosphorylation sites PIP5K2 S274 S275 did not change the lifetime distribution of the detected EYFP foci. Interestingly, however, a difference in foci could be observed after a longer observation period (>30 s). It was shown that residence time of foci over 30 s at the plasma membrane after expression of PIP5K2 S274A S275A occurred about twice as often as that of PIP5K2-EYFP or the D-variant (Fig. 33B).

The TIRF microscopy experiments revealed that PIP5K2-EYFP and the A/ D variants form defined regional spots at the plasma membrane that are not overall altered when PID phosphorylation sites are substituted. Only at longer observation periods do the data suggest that PIP5K2 S274AS 2275A has a slightly longer lifetime at the plasma membrane than PIP5K2 wild type and the D variant (Fig. 33B). Overall, however, the effect is not particularly strong.

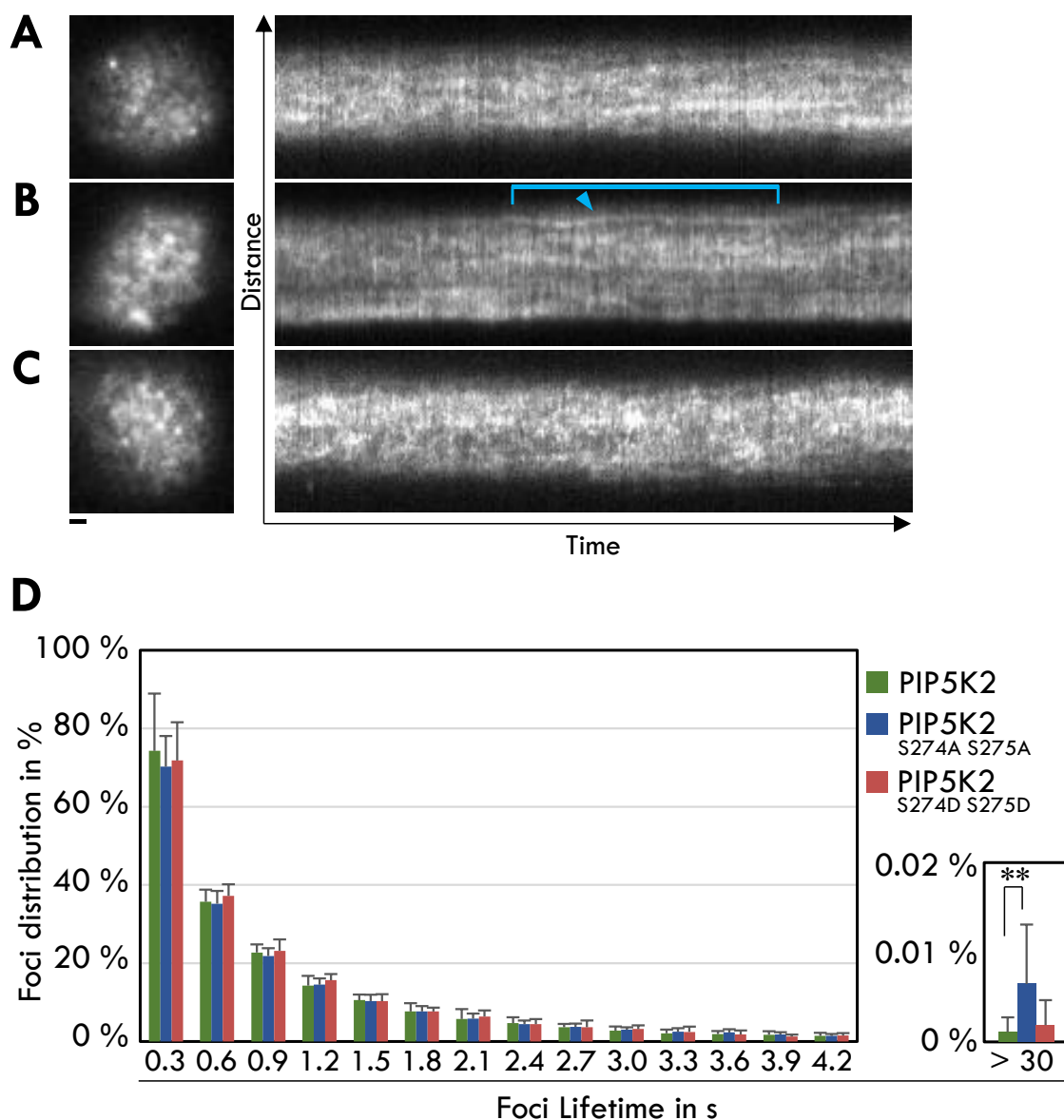


Figure 33 PIP5K2 forms defined foci at the plasma membrane. Protoplasts were transiently transformed with *pCaMV35S::PIP5K2-EYFP* or the *pCaMV35S::PIP5K2 S274 S275-EYFP A/ D* substitution variants. PI4P 5-kinase plasma membrane localisation was analysed using TIRF microscopy. **A** PIP5K2-EYFP, **B** PIP5K2 S274A S275A and **C** PIP5K2 S274D S275D membrane foci are displayed from one representative protoplast as single frame picture and corresponding 90 s kymographs. Scale bar measures 1 μm . The ImageJ TrackMate plugin was used to define and quantify PIP5K2-EYFP foci (Tinevez et al., 2017; Ershov et al., 2021). **D** Lifetime distribution of dynamic PIP5K2-EYFP (green), PIP5K2 S274A S275A-EYFP (blue) and PIP5K2 S274D S275D-EYFP (red) was plotted in percentage for 0.3 to 4.2 s and > 30 s. Asterisks indicates significant differences according to Student's T-test (** $P \leq 0.01$). Data represent 18 665 tracks from ten protoplasts for PIP5K2-EYFP, 41 920 tracks from 18 protoplasts for PIP5K2 S274A S275A-EYFP and 11 929 tracks from six protoplasts for PIP5K2 S274D S275D-EYFP.

2.4.5 Influence of Phosphorylation by PID on the catalytic activity of PIP5K2

Posttranslational modification of proteins, e.g., by phosphorylation, is considered a fast and effective regulatory mechanism to control protein activities (Stone and Walker, 1995; Pearce et al., 2010; Hempel et al., 2017; Menzel et al., 2019). The

data so far showed that PID phosphorylates PIP5K2, which leads to the question whether phosphorylation has a regulatory effect on PIP5K2. To investigate whether phosphorylation by PID has an influence on PIP5K2 activity, the recombinant enzymes were pre-incubated together, which should lead to phosphorylation of PIP5K2 by PID (see 4.15). Subsequently, the PI4P 5-kinase activity of the phosphorylated PIP5K2 enzyme was analysed. The formation of radioactive $\text{PtdIns}(4,5)\text{P}_2$ after addition of the lipid substrate $\text{PtdIns}4\text{P}$ in the presence of $\gamma\text{-}^{32}\text{P}\text{-ATP}$ was analysed (see 4.17). The results of the activity test were compared to equally treated samples containing identical amounts of the same MBP-PIP5K2 preparation without prior incubation with PID but with the buffer in which PID was present. In addition, PIP5K2 activity was measured without the addition of buffers or PID. This was tested to estimate the influence of the addition of further buffer additives on PI4P 5 kinase activity. Phosphoinositides were isolated and separated using thin-layer chromatography (TLC) plates (see 4.17.1.1). TLC plates were exposed to phosphorimager screen and analysed (Fig. 34).

The sample fraction that was used for phosphorylation control displayed phosphorylation signal of MBP-PIP5K2 by MBP-PID (Fig. 34A) as already described in section 2.3.4. Autophosphorylation of MBP-PID was also detectable (Fig. 34A). Catalytic activity assays showed that the used tag MBP and protein kinase MBP-PID do not produce $\text{PtdIns}(4,5)\text{P}_2$ compared to MBP-PIP5K2 controls (Fig. 34B right panels). Further, catalytic activity measurements revealed that MBP-PIP5K2 catalytic activity is altered upon using PID buffer control conditions or upon PIP5K2 phosphorylation by PID (Fig. 34B). Compared to the activity of the buffer control, the activity of MBP-PIP5K2 treated with MBP-PID was significantly increased 4.6-fold ($P \leq 0.001$). However, it must be noted here that the addition of the PID buffer to the MBP-PIP5K2 initially reduced the activity of PIP5K2 in comparison to the control without adding further additives (Fig. 34B). Nevertheless, PIP5K2 incubated with PID and phosphorylated still showed 1.53-fold ($P \leq 0.05$) and thus significantly more activity compared to completely untreated MBP-PIP5K2 (Fig. 34B).

In contrast to phosphorylation sites in the catalytic domain, which led to a decrease in PI4P 5-kinase enzymatic activity (Hempel et al 2017), phosphorylation in the N-terminal domains of PI4P 5-kinases apparently leads to an increase in activity, at least *in vitro*.

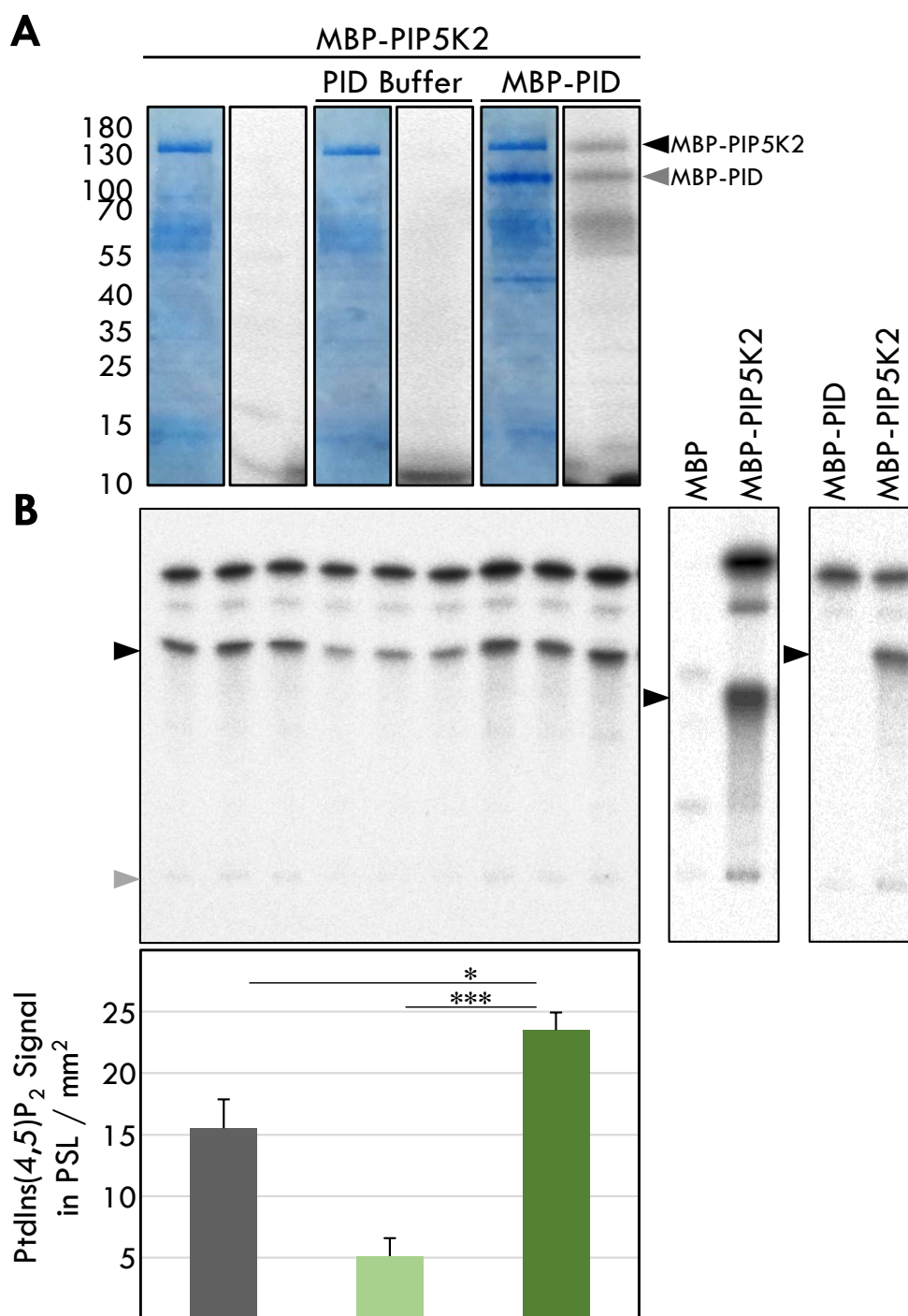


Figure 34 PIP5K2 displays increased catalytical activity upon phosphorylation by PID. Recombinant and enriched MBP-PIP5K2 and MBP-PID proteins were incubated together with **A** γ -[³²P]-ATP, and subsequently tested for **B** lipid kinase activity together with fresh γ -[³²P]-ATP and PtdIns4P as substrates. Protein phosphorylation and PtdIns(4,5)P₂ formation were determined from the same samples. For this purpose, the samples were split and one half separated in SDS-gels, while the other half was used in an activity assay. Lipids were extracted and separated by TLC. The SDS-gels and TLCs were analysed with a phosphorimager. Radioactive incorporation of γ -[³²P] into PtdIns(4,5)P₂ was used to measure the catalytic activity of PIP5K2. Corresponding PtdIns(4,5)P₂ signals was analysed with TINA2.0 software (Raytest, Straubenhardt, Germany) and relative activity was calculated. PSL, photo stimulated luminescence. The experiment was performed twice with similar results (*) Asterisk indicates significant differences according to Student's T-test (***) $P \leq 0.001$, * $P \leq 0.05$). Black triangle, PtdIns(4,5)P₂; grey triangle, origin.

2.4.6 Effects of AGCVIII protein kinases on the functionality of PIP5K2 *in vivo*

The data so far demonstrate a clear effect of PID on PIP5K2 function *in vitro*, raising the question whether these observations have relevance for *in vivo* functions of PIP5K2 in plants. To get an idea of whether PID phosphorylation of PIP5K2 might also be relevant in plants *in vivo*, PtdIns(4,5)P₂ lipid levels were measured in a *pid* mutant, the *PID pid wag1 wag2* triple mutant, and a PID overexpression line and compared with wild-type levels. Phosphoinositides were isolated from twelve-day old seedlings and separated using TLC. PtdIns(4,5)P₂ was reextracted and trans-methylated and analysed using gas chromatography (GC) (see 4.18.1.1). The analysis of the data is shown in figure 35.

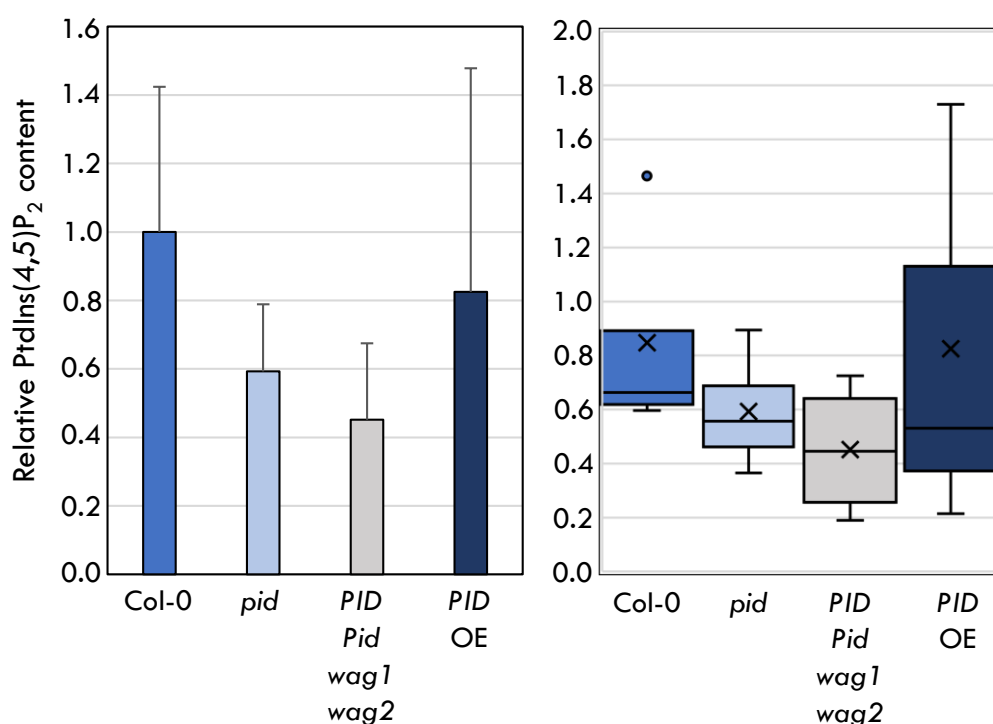


Figure 35 PtdIns(4,5)₂ levels are altered in *pid* mutants. Lipids were isolated from twelve-day old seedlings grown on 1/2 MS media under long day conditions. Lipid extracts were separated on TLCs, PtdIns(4,5)P₂ reextracted and fatty acids were transmethylated. Fatty acid methyl esters were analysed with GC-flame ionization detector and PtdIns(4,5)P₂ was quantified. For comparison purposes, the values were related to initial fresh weight and normalised to Col-0. Because of the high standard deviation of the PtdIns(4,5)P₂ data, different presentations of the results were chosen to try showing the differences comprehensively after all. The experiment was performed four times in duplicates or triplicates. *pid*, PINOID T-DNA insertion line SALK_049736; *PID pid wag1 wag2*, T-DNA insertion line derived by crossing of the *pid* mutant with *wag1* mutant SALK_002056 and *wag2* mutant SALK_070240, *PID OE*, *PID* overexpression line (Benjamins et al., 2001b) under the control of the *pCaMV35S* promoter.

Both the *pid* mutant line and the *pid PID wag1 wag2* triple mutant showed markedly, but not significantly, reduced PtdIns(4,5)P₂ levels compared with wild type (Fig. 35). The *PID* overexpression line showed comparable levels of PtdIns(4,5)P₂ to the wild

type (Fig. 35). Unfortunately, the data has high standard deviations, so the statistics (lowest value in one-way ANOVA: Col-0 to *Pid pid wag1 wag2* $p \leq 0.58$) could not confirm significant differences. Nevertheless, the data shows a tendency for the absence of PID phosphorylation to result in reduced PtdIns(4,5)P₂ formation in plants, consistent with the *in vitro* increase in PIP5K2 activity by PID phosphorylation shown in 2.4.5.

These results suggest that phosphorylation of PIP5K2 by PID affects PtdIns(4,5)P₂ levels in plants, thus completing the regulatory loop that controls polar growth.

3 Discussion

Posttranslational modifications, such as protein phosphorylation, are well described as a fast and reversible way to alter protein activity, localisation, and interaction of an enzyme with other proteins. In this work, the influence of cell types and phosphorylation on the dynamic nuclear compartmentation and enzymatic activity of plant PI4P 5-kinases, respectively, were among the factors investigated. Phosphorylation of PIP5K1 by the CK2 subunit CKA3 and of PIP5K1 and PIP5K2 by the AGCVIII kinase PID was observed. CKA3 interacted with PIP5K1 but not with PIP5K2, whereas PID interacted with both PI4P 5-kinases. Phosphorylation of PI4P 5-kinases PIP5K1 and PIP5K2 led to an increase in catalytic activity *in vitro*. This activating effect of PID on PI4P 5-kinases is apparently also present *in vivo*. In addition, one phosphorylation site recognised by CKA3 and three phosphorylation sites recognised by PID were identified by MS analysis.

3.1 The nuclear localisation of PIP5K2 is dynamic and regulated

PIP5K1, PIP5K2 or other PI4P 5-kinases analysed to date did not show exclusive localisation to the nucleus (Camacho et al., 2009; Ischebeck et al., 2013; Tejos et al., 2014; Gerth et al., 2017a). It is possible that nuclear localisation of PIP5K2 (and PIP5K1) is conditional and that nuclear localisation is restricted to specific cell types in specific tissues. Obviously, the frequency and intensity of nuclear localisation is dependent on the cellular situation, such as cell type, and on the developmental stage in combination to possibly external stimuli. The comparison of subcellular localisation patterns of identical PIP5K2-EYFP constructs in protoplasts from different tissues, root meristem stem cells (BY-2), and differentiated root cells or leaf protoplasts (Fig. 14 and 15) performed here supports the assumption that PIP5K2-EYFP localises only in specific cell types or at specific developmental stages in plant nuclei (Fig. 14 and 15).

It should be mentioned that the experiments were all carried out in protoplasts from a wide variety of tissues or cell cultures. In protoplasts, it is easier to express PI4P 5-kinases and to observe their subcellular localisation compared to other systems. Therefore, the protoplast system was chosen. Several other cell types and expression systems have already been tested in various preliminary work for this study, and it was found that the fluorescence intensities of the expressed PI4P 5-kinases in those systems were weak or undetectable and thus would not provide truly interpretable data. For example, two independent studies have shown

functional complementation of the *pip5k1-pip5k2* double mutant phenotype by fluorescently labelled variants of PIP5K2 (Ischebeck et al., 2013; Tejos et al., 2014). However, in both cases no or only very weak PIP5K2-EYFP fluorescence could be observed, which is why these Arabidopsis lines were unfortunately not usable for the studies here. Despite the weak fluorescence distribution, these lines showed polar localisation at the plasma membrane as well as nuclear fluorescence, especially in the meristematic tissue (Ischebeck et al., 2013; Tejos et al., 2014) and thus confirm the results obtained here.

The localisation studies performed in this work showed that PIP5K2 localises in small percentages to plant nuclei of all tissues tested, including Arabidopsis leaf, root, and tobacco BY-2 cell culture protoplasts (Fig. 14 and 15). As previously described, protoplasts from root-derived BY-2 cell cultures showed increased abundance and intensity of PIP5K2-EYFP in the nucleus (Fig 15A (Gerth et al. 2017a)). One hypothesis was that the BY-2 root proteome positively influences the nuclear localisation of PIP5K2 because these cells are more often in certain developmental stages of growth, are not differentiated, and are primarily in cell division. It remains an open question why PIP5K2-EYFP shows elevated nuclear signals in BY-2 protoplasts. An Arabidopsis root-based cell culture should additionally be established, and localisation studies repeated to determine if the nuclear signal of PIP5K2-EYFP is specific to BY-2 cells.

Auxin analogues were added to the growth media of cell cultures to ensure cell division and non-differentiation of cells. However, auxin also stimulates the expression of PIP5K1 and PIP5K2 (Mei et al., 2012). Surprisingly, Arabidopsis leaf cell culture did not show elevated levels of PIP5K2-EYFP in the nucleus (Fig. 15B). Similar results were documented with Arabidopsis protoplasts treated with auxin while expressing PIP5K2-EYFP (Fig. 14D). These findings support the tight regulation of the nuclear-cytoplasmic shuttling of PIP5K2. Neither the developmental stage of Arabidopsis leaf cell culture alone nor the root tissue alone were sufficient to increase nuclear localisation of PIP5K2-EYFP like it was observed in BY-2 protoplasts. The subcellular localisation of PIP5K2 appears to involve multiple levels of regulation, all of which need to be targeted.

The assumed dependence on a variety of regulatory influences nevertheless makes it necessary to repeat the investigations in intact plants in the future. Immunostains can also help, although they can provide artifact-related localisation signals.

The dynamic movement of PI4P 5-kinases between cytoplasm and nucleus depending on the changing cellular requirements is likely. A similar pattern has also been proposed for the PI4P 5-kinase *Mss4* in yeast (Audhya and Emr, 2003) and

PI4P 5-kinases in mammalian cells (Mellman et al., 2008) and is likely controlled by posttranslational modification (Audhya and Emr, 2003; Gerth et al., 2017b; Gerth et al., 2017a; Heilmann and Heilmann, 2022). However, information on posttranslational modification of plant PI4P 5-kinases has been scarcely researched so far (Hempel et al., 2017; Menzel et al., 2019).

3.2 Comparative biology: a PIP5K1 / 2 ortholog from poppy displays almost exclusive nuclear localisation.

It was hypothesised that the conditional nuclear localisation of PIP5K2 was due to the presence or absence of certain alpha-importin isoforms, masking of the relevant NLS in PIP5K2 due to certain protein conformation, possibly influenced by post-translational modifications, or all these together (Gerth et al., 2017b). The observation that PsPIP5K1 identified from poppy localises to the nucleus in almost all cell types studied, opened the possibility of using sequence comparisons and localisation studies to identify sequence determinants that regulate either plasma membrane or nuclear localisation or coordination between the two sites.

Experimental data showed that PsPIP5K1-EYFP indeed localises almost exclusively to the nucleus both heterologous in Arabidopsis and in the homologous system in poppy protoplasts (Fig. 17B and D). Protein-protein interaction studies also showed that PsPIP5K1 interacts with alpha-importins from Arabidopsis, like what was shown for PIP5K2 (Fig. 18). Sequence analyses also showed that the sequence in the Lin-domain encoding an NLS in PIP5K1 and PIP5K2 is also present in PsPIP5K1 and appears to be conserved (Fig 16C). However, there are additional amino acid residues in the PsPIP5K1 Lin-domain N-terminal to the conserved NLS sequence that are not present in PIP5K1 and PIP5K2 suggesting a possibly bipartite NLS in PsPIP5K1 (Fig 16C).

For control and comparison, the studies were also conducted with PIP5K2 and surprisingly it was discovered that PIP5K2 localised more frequently and more clearly in the nucleus of poppy protoplasts than in Arabidopsis protoplasts (Fig. 17E and F). Again, these results also suggest that the regulation of signalling PI4P 5-kinases must be multi-layered. On one hand, the almost exclusive nuclear localisation of PsPIP5K1 indicates that there are sequence determinants that differ from AtPIP5K2, but on the other hand, the increased nuclear localisation frequency of AtPIP5K2 in poppy protoplasts also indicates that there are different regulations within the different cell species, which can then act on the PI4P 5-kinases in a posttranslational manner and thus possibly explain the different expression of nuclear localisation.

However, the nature of these sequence determinants, posttranslational modifications and the enzymes playing a role in this are unclear.

3.2.1 The Lin-domain is key for PI4P 5-kinase function and subcellular localisation

The PI4P 5-kinases AtPIP5K2 and PsPIP5K1 show an amino acid identity of 69.4 %. This high similarity at the amino acid level usually indicates similar functions (Sangar et al., 2007). Nevertheless, both PI4P 5-kinases show different subcellular distribution (Fig. 17). Thus, the question arose by which amino acid region these differences may be determined. Within the PI4P 5-kinase isoforms, especially the N-terminus and the Lin-domain exhibit high variability and few conserved regions (Heilmann and Heilmann, 2015; Gerth et al., 2017a). It is hypothesised that the regulation of PI4P 5-kinases occurs via posttranslational modifications in these intrinsically disordered regions (Gerth et al., 2017b; Heilmann and Heilmann, 2022) and the importance of the Lin-domain specifically for PIP5K2 has been described previously (Stenzel et al., 2012; Fratini et al., 2021).

The exchange of the Lin-domains between AtPIP5K2 and PsPIP5K1 led to a reciprocal gain (AtPIP5K2-LinPs) and loss (PsPIP5K1-AtLin) of the nuclear localisation frequency (Fig. 19). Based on these results, it appears that the Lin-domains may determine, or at least have major impact on, the localisation of PI4P 5-kinases (Fig. 19 and 20). It is speculated that the Lin-domain acts as a scaffold and its structure changes accordingly after attachment/ binding to interaction partners or posttranslational modifications, so that either the localisation at the plasma membrane or the interaction with further protein partners or/ and the activity and/ or overall subcellular localisation can change (Fig. 36, (Stenzel et al., 2012; Gerth et al., 2017b; Fratini et al., 2021; Heilmann and Heilmann, 2022)).

Further sequence studies will reveal which amino acids are responsible for the differences in PsPIP5K1 and AtPIP5K2.

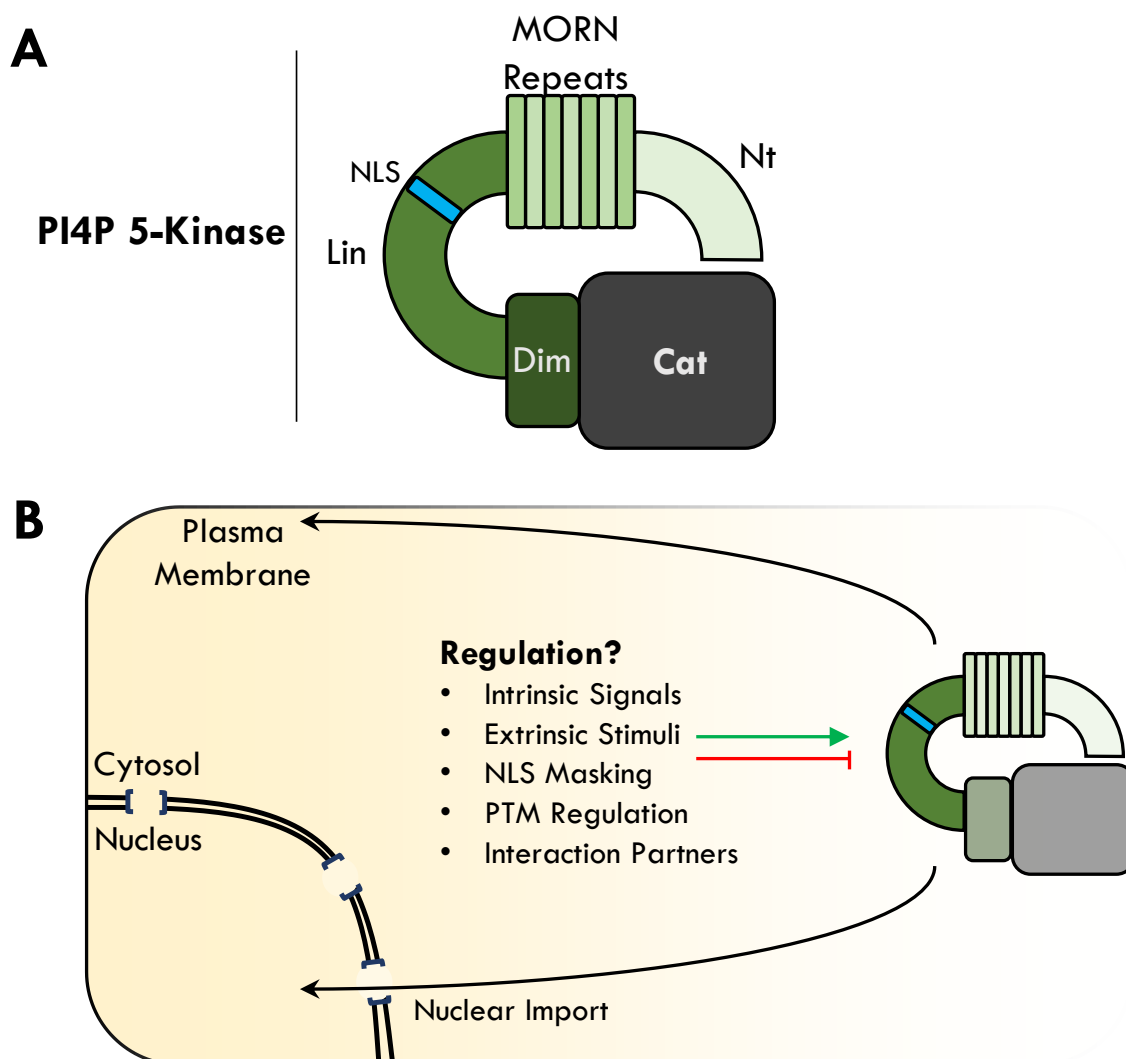


Figure 36 Model: The Lin-domain of PI4P 5-kinases mediates localisation and function. **A** Model of the domain structure of PI4P 5-kinases. The catalytical-, dimerization- and MORN domains are conserved regions. The Lin- and Nt-domain are intrinsically disordered and presumably responsible for the regulation of PI4P 5-kinases. Nt, N-terminus; MORN, Membrane Occupation and Recognition Nexus; Lin, Linker domain; Dim, Dimerization domain, Cat, Catalytic domain. **B** Data from this work and from publications (Stenzel et al., 2012; Fratini et al., 2021) highlight the linker domain as regulatory region for PI4P 5-kinase localisation and function. While the exact molecular mechanism is still unknown, the Lin-domain of PI4P 5-kinases may mediate both, nuclear and plasma membrane localisation.

3.2.2 Functional studies with PsPIP5K1 in tobacco pollen tubes and the *pip5k1 pip5k2* double mutant

Overexpression of PIP5K2 from Arabidopsis in tobacco pollen tubes resulted in a pollen tube tip swelling phenotype, probably caused by disruption of cytoskeleton dynamics (Ischebeck et al., 2010a; Ischebeck et al., 2010a; Stenzel et al., 2012; Gerth et al., 2017b; Fratini et al., 2021). The expression of PI4P 5-kinases homolog to PIP5K1/ PIP5K2 should induce a swell phenotype when overexpressed in tobacco pollen tubes. Therefore, the pollen tubes serve not only as a cell type for

localisation studies, but also to test the functionality of enzymes that influence the cytoskeleton. The localisation studies and phenotype analyses in tobacco pollen tubes showed that PsPIP5K1-EYFP and PIP5K2-LinPs-EYFP caused distinct pollen tube swelling, as described for AtPIP5K2-EYFP (Fig. 20 and 21). These included an immediate swelling pear-like phenotype, without establishment of a true pollen tube and abrogation of growth (Fig. 20 and 21). In addition, PsPIP5K1 was found to localise primarily to the nucleus of pollen tubes, often in nuclear speckles/ punctuated structures (Fig. 20B). This observation was particularly interesting because PsPIP5K1-EYFP expression resulted in very distinct swollen pollen tube phenotypes and it seems that PsPIP5K1 works in pollen tubes like PIP5K2 described at the plasma membrane (Fig. 20). This observation suggests that PsPIP5K1-EYFP does localise to the plasma membrane, albeit at levels that are difficult to detect, and that these levels are sufficient to affect cytoskeleton dynamics and thus pollen tube growth.

Expression of PsPIP5K1-EYFP in the *pip5k1 pip5k2* double mutant should provide insight into how homologous PsPIP5K1 is to AtPIP5K2 and how the distinct nuclear localisation of PsPIP5K1 affects the plant phenotype (double mutant phenotype see section 1.1.3). The plants examined here are in the T2 generation and must be characterised accordingly. However, it was important to get an impression of how PsPIP5K1 can replace Arabidopsis PI4P5 kinase enzymes. The *pip5k1 pip5k2* double mutant either transformed with *pPIP5K1::PsPIP5K1-EYFP* and the chimeric *pPIP5K1/2::PsPIP5K1_LinAt-EYFP* variant showed almost complete complementation. The overall phenotype of the *pip5k1 pip5k2* double mutant was rescued (Fig. 22 and 23). The plants showed almost normal growth, possibly slightly delayed compared to the untransformed Col-0 wild type but better growth than the double mutant transformed with wild type AtPIP5K2-EYFP (Fig 22 and 23). Both PsPIP5K1-EYFP and the chimeric construct PsPIP5K1_LinAt-EYFP complemented the double mutant, showing that they can fully take over the functions of either AtPIP5K2 or AtPIP5K1 under the conditions tested here. PsPIP5K1, although it also appears to localise to the nucleus in the double mutants, can apparently take over the functions of PIP5K1 / PIP5K2 at the plasma membrane. A direct read out for correct plasma membrane functions of PsPIP5K1 would be the verification of the correctly polar localised PIN proteins in the root cortex cells. This should be investigated in future studies, possibly with the help of immune stains.

Comment on the attempts to detect fluorescence in the transformed *pip5k1 pip5k2* double mutant plants:

Unfortunately, the localisation studies with the *pip5k1 pip5k2* double mutants transformed with the respective EYFP-PI4P 5-kinases were only possible in a few exceptions. For the control plants transformed with the wild form PIP5K1-EYFP no fluorescent seedling or single cell could be detected as described before (Ischebeck et al., 2013). Only a few seedlings transformed with PsPIP5K1-EYFP or PsPIP5K1-AtLin-EYFP showed fluorescence, which could then be clearly detected in the nucleus and at the plasma membrane of epidermal cells or in the cell nucleus of meristematic cells (Fig 22C). The difficulty of detecting fluorescently labelled PI4P 5-kinases in the homologous system has been described previously (Ischebeck et al., 2013; Tejos et al., 2014; Gerth et al., 2017b) and it was therefore not surprising that this was also problematic in the present cases. In the future, immunostaining could be considered a possibility for detection, even though this may result in non-specific signals due to fixation and the use of antibodies.

3.2.3 Observation of PsPIP5K1-EYFP in nuclear speckles

The localisation of PsPIP5K1 in nuclear speckles/ punctuated structures was interesting, partly because these punctate structures were also observed in localisation studies with PI-kinases and PtdIns(4,5)P₂ in mammalian cells (Rohrbach et al., 2015; Fiume et al., 2019). Nevertheless, the term speckles should be used with caution, “nuclear speckles” are defined as interchromatin granule clusters (ICG), which are enriched with splicing factors (Spector and Lamond, 2011). The observed punctuated structures might also be DNA damage foci or yet unidentified biomolecular condensates (Emenecker et al., 2020). Hence, no conclusion can be made about the nature of these punctuated structures observed in the nucleus with PsPIP5K1-EYFP expression.

For a mammalian PI4P 5-kinase enzyme, it was shown that the PI-kinase interacts with a non-canonical poly(A) polymerase and colocalises with nuclear speckles, thereby influencing the expression of specific mRNAs (Mellman et al., 2008). The same PI4P 5-kinase was described to interact in such speckles with p53, a transcription factor that regulates gene expression after DNA damage. The colocalisation of the enzymes was investigated using fluorescently labelled reporters known to interact in such punctate structures in the mammalian nucleus (Choi et al., 2019). Studies on the colocalisation of PsPIP5K1 and speckle-marker proteins, such as SAD1 or LSM5, splicing regulators of small nuclear ribonucleoproteins (snRNPs) from Arabidopsis or diverse others could provide insight into the nature of speckles and thus clues to possible functions of PI4P 5-kinases in the nucleus.

3.3 PIP5K1 and PIP5K2 are regulated by reversible protein phosphorylation

It is likely that PI4P 5-kinases are regulated by a variety of posttranslational control mechanisms. As discussed in the previous chapter, even hardly detectable concentrations of PI4P 5-kinase seem to be sufficient to either cause the correct functionality or lead to a glaring phenotype. At the same time, this also indicates that both localisation and activity must be regulated individually as well as in combination. The intrinsically disordered N-terminus, the Lin-domain and the variable insert within the catalytic domain are hypothesised to be the place of regulation for PI4P 5-kinase functions, primarily by reversible protein phosphorylation (Stenzel et al., 2012; Heilmann and Heilmann, 2015; Heilmann, 2016a; Gerth et al., 2017b; Gerth et al., 2017a; Hempel et al., 2017; Menzel et al., 2019; Fratini et al., 2021). In this study, we identified two putative protein kinases from different protein kinase families, The CK2 subunit CKA3 and The AGCVIII kinase PID that phosphorylate PIP5K1 and PIP5K2 *in vitro* (Fig. 25 and 31).

3.3.1 PIP5K1 interacts with the CK2 alpha-subunit CKA3

By *in silico* analysis of PIP5K1 and PIP5K2 amino acid sequence for classical CK2 phosphorylation motifs, multiple putative phosphorylation sites in the N-terminus and the Lin-domain were discovered (Fig. 8A). Also, the described subcellular localisation of both proteins, PI4P 5-kinases and CK2 subunits, showed overlap in the nucleus (Fig 2, 10). This led to the hypothesis that PIP5K2 is also phosphorylated by casein kinases and consequently regulated, as described for different yeast PI4P 5-kinases (Vancurova et al., 1999; Audhya and Emr, 2003). The interaction of PIP5K1 and PIP5K2 with CKA and CKB subunits was therefore tested in yeast two-hybrid studies, and the data showed that both PIP5K1 and PIP5K2 appear to interact with the CK2 beta-subunits CKB1 and CKB3, but only for PIP5K1 an interaction with the alpha-subunit CKA3 could be detected (Fig 24). Interestingly, PIP5K2 did not interact with any of the tested CK2 alpha subunits. PIP5K1 and PIP5K2 share 82.3 % amino acid identity, and in the N-termini of PIP5K1 and PIP5K2 typical amino acid motifs for CK2 protein kinases were identified (Fig 8A). This may indicate specificity of CKA3 for PIP5K1, because PIP5K1 and PIP5K2 are not completely identical, suggesting differential regulation of these sister enzymes. However, it also cannot be ruled out that the results of the yeast-two-hybrid tests are due to a different expression in the yeast cells. Western blots/ immuno detection of the protein candidates tested here in combination would provide information about protein expression in the best case. Since the promoters used in yeast-two-

hybrid tests are usually quite weak and protein isolation from yeast cells is not easy, such western blots do not always lead to protein detection. It is better to consider alternative methods for protein-protein interaction. One possibility would be to use BiFC like in chapter 2.4.1 to investigate protein-protein interaction. This method has the advantage that if the interaction between PIP5K1 and the CK2 subunits depends on localisation in the cell, this could also be detected immediately. In the future, the BiFC experiments will hopefully support the interaction results accordingly.

3.3.2 Phosphorylation of PIP5K1 by CKA3

The computer-aided software programs identified distinct CK2 phosphorylation sites in the N-terminus of PIP5K1 and the interaction of the CKA3 alpha-subunit of the protein kinase CK2 with PIP5K1 indicated that PIP5K1 could indeed be a substrate for CK2. Prior to the start of this project, no information about the phosphorylation of PIP5K1 specifically by a protein kinase was available.

Phosphorylation assays using recombinantly expressed MBP-PIP5K1, MBP-PIP5K2 and His-CKA3 showed a strong phosphorylation signal for MBP-PIP5K1 but not for MBP-PIP5K2 (Fig. 25). As already mentioned above, PIP5K1 and PIP5K2 are very similar, but there seems to be a specificity of CKA3 to PIP5K1, which is not explicable here, but was already shown in yeast-two-hybrid tests and confirmed by *in vitro* phosphorylations. It has always been emphasised that PIP5K1 and PIP5K2 have similar and overlapping functions in Arabidopsis, after all, the respective individual expression of PIP5K1 or PIP5K2 under their own homologous promoter could almost completely complement the phenotypes of the *pip5k1 pip5k2* double mutant (Ischebeck et al., 2013). However, it has also been shown that PIP5K1 and PIP5K2 have a slightly different expression pattern in the root (Tejos et al., 2014). The specificity of CKA3 for PIP5K1 may also be one of the differences between PIP5K1 and PIP5K2.

It was attempted to identify phosphorylation sites introduced by CKA3 in PIP5K1 by MS. Two phosphorylation sites of the amino acid residues S2 and S408 were identified (Fig. 26). The amino acid S2 is in the outermost N-terminus and is one of the phosphorylation sites predicted *in silico* in PIP5K1 (Fig. 8 and 26). The serine residue at position S408 lies in the dimerization domain of PIP5K1 and was phosphorylated in only one peptide. Parallel to the writing of this thesis, first experiments with PIP5K1 substitution variants were performed, in which positions S2 and S4 were exchanged for alanine and aspartate to create so-called phosphoablation and phosphomimikry variants (MSc. Marie Lebescond 2022). Initial results showed

that both the phosphoablation and phosphomimikry variants were still phosphorylated. This suggests that there must be additional phosphorylation sites in PIP5K1. On one hand this could be the serine at position S408, but on the other hand also other positions in other domains are possible.

For the experiments performed here, *E. coli* cell lysates were used after expression of CKA3, since CKA3 was always detectable in the sediment fraction after separation of the cell debris from the soluble supernatant (Appendix, Fig. 40). In addition, it could not be tested whether the other alpha subunits (CKA1 and CKA2) could phosphorylate PIP5K1 and PIP5K2 because CKA1 and CKA2 were not/ weakly expressed in *E. coli* (Appendix Fig. 40C); further approaches are needed to resolve this. For further studies it would be desirable to optimise the purification of CK2 subunits. This would also allow experiments in which the combination of CK2 alpha- and beta-subunits leads to the formation of the described tetrameric CK2 holoenzyme. It is possible that the holoenzyme shows different PI4P 5-kinase-substrate specificities than those that could be tested here so far with the subunits. In principle, of course, the data also indicate that mass spectrometric analysis needs to be further extended to ensure that all CKA phosphorylation sites in PIP5K1 are identified. With this information, the experiments discussed in the next sections can then be repeated.

3.3.3 Influence of CKA3 on the subcellular distribution of PIP5K1

So far phosphorylation at site (Serin S2) in PIP5K1 could be shown by CKA3, but no CKA3 phosphorylation site could be identified in the Lin-domain of PIP5K1 up to now. The hypothesis based on data from the yeast system (Audhya and Emr, 2003), that the NLS of PIP5K1 (and PIP5K2) is probably masked at some regulatory levels and only becomes accessible to the nuclear import machinery by post-translational modifications, led to the question whether phosphorylation by CKA3 leads to a localisation change of PIP5K1. Data from *in vivo* localisation experiments in Arabidopsis leaf protoplasts (Fig. 28) suggest that co-expression of PIP5K1 with CKA3 leads to a slight increase in nuclear localisation compared to that observed with PIP5K1 alone. Based on the results of this study, it remains unclear whether phosphorylation of PIP5K1 by CKA3 affects PIP5K1 localisation. However, these results must be seen in the context of the assumption that CKA3 probably phosphorylates further sites in PIP5K1, which cannot be considered here. Only the complete mass spectrometric analysis and corresponding tests with the respective substitution variants can really give an indication of an influence on the localisation of PIP5K1. In the future, other plant expression systems should also be considered, such as heterologous expression in *N. benthamiana* leaves. Also, the method of BiFC could be

a way to test for a possible change in subcellular localisation. Conversely, the expression of PIP5K1-EYFP in the previously described *cka1 cka2 cka3* triple mutant could be considered. This could reveal whether PIP5K1 has a different subcellular distribution in a *cka* mutant background than in wild-type plant cells, and potentially supporting the preliminary data described here.

3.3.4 Phosphorylation of PIP5K1 by CKA3 controls activity

In this work, it was shown that PIP5K1 is a substrate for the activity of the CKA3 protein kinase and is phosphorylated at serine residues at the outermost N-terminus (Serine S2). Based on data from yeast studies (Vancurova et al., 1999; Audhya and Emr, 2003), phosphorylation affects either the localisation or catalytic activity of PI4P 5-kinases. Since the effect of CKA3 phosphorylation on the localisation of PIP5K1 was not particularly clear, the hypothesis of activity change after phosphorylation should be tested here. For this purpose, recombinant MBP-PIP5K1 was incubated with CKA3 or, as a control, with the appropriate buffer, and *in vitro* PI4P 5-kinase activity assays were subsequently performed (Fig. 29). After incubation of MBP-PIP5K1 with CKA3, the catalytic activity of PIP5K1 was doubled (Fig. 29). The phosphorylation of PIP5K1 led to an enhanced catalytic activity of PIP5K1 *in vitro*.

So far, it has not been assumed that possible phosphorylation sites in the N-terminus and possibly in the dimerization domain of PIP5K1 could affect the catalytic activity of PIP5K1 after phosphorylation. By nature, phosphorylation in the catalytic domain, including variables insert and activation loop, was rather suspected to have an influence on catalytic activity. For example, AtPIP5K6 was shown to be phosphorylated by a MAPK, MPK6, at positions T590 and T597, leading to a significant reduction of PIP5K6 activity in *in vitro* and *in vivo* studies but no change in subcellular distribution or plasma membrane association were observed (Hempel et al., 2017; Menzel et al., 2019). Therefore, an activation of the enzymatic activity of PIP5K1 by phosphorylation in the N-terminal domains seems surprising. It cannot be ruled out here that additional phosphorylation sites of CKA3 may be located in the catalytic domains, and thereby enhancing PIP5K1 activity; however, it has also been shown that N-terminally truncated variants of PIP5K1 (Im et al., 2007) and of PIP5K2 (Stenzel et al. 2012) exhibit increased catalytic activity *in vitro*. It is discussed that the N-terminal domains of some PI4P 5-kinases may have autoinhibitory regulatory functions and only posttranslational modifications and resulting conformational change leads to full activation of the PI4P 5-kinase enzyme (Fig. 37, (Im et al., 2007, Stenzel et al. 2012)). This would also explain how phosphorylation at

the N-terminus led to the observed increase in PIP5K1 activity in the experiments performed here (Fig. 29).

After identification of all possible CKA3 phosphorylation sites in PIP5K1, this hypothesis can be further pursued. Circular dichroism or cross-linking experiments may then provide insight into a possible conformational change of phosphoablation versus phosphomimikry variants.

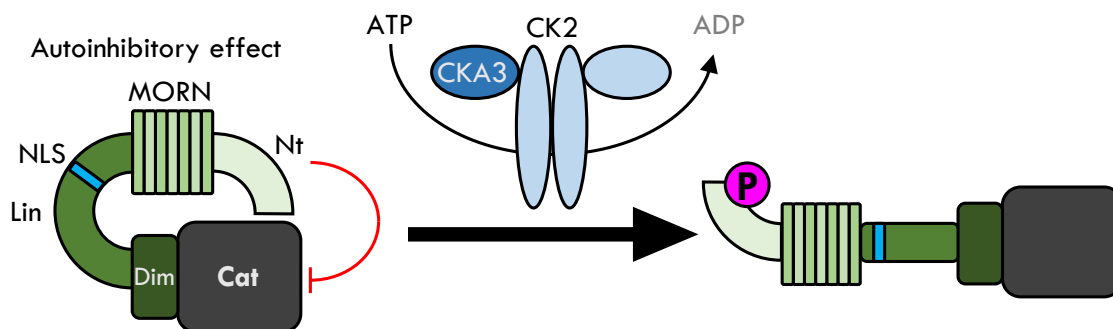


Figure 37 Model: Phosphorylation in the N-terminus of PIP5K1 by CKA3 competes with the autoinhibitory effect of the N-terminal domains. The N-terminal domains of type B PI4P 5-kinases have been reported to inhibit catalytical activity (Im et al. 2007; Stenzel et al. 2012). We propose here that CKA3 phosphorylation of the N-terminus re-arranges the conformation of the N-terminal domains to favour catalytic turnover of PIP5K1.

3.3.5 PIP5K1 and PIP5K2 interact with the AGCVIII protein kinase PID

The role of AGC3 kinases, which include PID, in the regulation of auxin transport and auxin signalling has already been intensively investigated (Christensen et al., 2000; Friml et al., 2004; Lee and Cho, 2006; Kleine-Vehn et al., 2009). It was shown that the subgroup AGC3 of the plant specific AGCVIII kinases, PID, WAG1 and WAG2 can phosphorylate the transmembrane auxin transporters PIN in a central cytosolic hydrophilic loop and therefore also influence the polar distribution of the PIN proteins in the corresponding membranes of the tissues (Dhonukshe et al., 2015). This polar distribution of PIN transporters is crucial for maintaining an auxin gradient and directed growth in the tissue. PI4P 5-kinases and PIs including PtdIns(4,5)P₂ are also themselves polar distributed in cells and are involved in the polar distribution of PIN proteins through the control of CME (Ischebeck et al., 2013; Tejos et al., 2014). Hence, there is a direct link of the PI pathway and the formation of the auxin gradient. Moreover, expression at transcriptional levels of PIP5K1 and PIP5K2 is enhanced by auxin itself, suggesting a regulatory loop here (Fig. 13, (Mei et al., 2012; Tejos et al., 2014)). A further link between PI regulation and AGCVIII kinase functions is formed by the reciprocal phenotypes of the respective mutants and overexpressors (Fig. 9, (Benjamins et al., 2001b; Ischebeck et al., 2013; Dhonukshe et al., 2015)). The preliminary results prior to this work, showing that PID

interacts with PIP5K2, were confirmed in this study. In split-ubiquitin-based yeast-two-hybrid studies, both PID and WAG2 were shown to interact with PIP5K2 (Fig. 30). In addition, the data suggest that PIP5K1 also appears to interact with the AGCVIII kinases PID and WAG2 (Fig. 30A and B). Here, in contrast to the interaction with CKA3, the sister isoforms PIP5K1 and PIP5K2 seem to function or be regulated in a similar way.

The interaction between PIP5K2 and PID was confirmed by *in vitro* pull-down assays and by *in vivo* BiFC-studies in Arabidopsis protoplasts (Fig. 30). This revealed that PIP5K2 and PID interaction takes place at the plasma membrane (Fig. 30C lower panel). Interestingly, the interaction between PDK1 and PID took place in the cytosol. The interaction of PIP5K2 with PID at the plasma membrane or plasma membrane-cytosol transition suggests that recruitment of PID also may play a role here, since PID otherwise tends to localise cytosolically (Fig 32B (Lee and Cho, 2006; Michniewicz et al., 2007; Kleine-Vehn et al., 2009)). This PID recruitment may result from direct interaction with PIP5K2, but it may also be due to PI binding of PID as described earlier (Introduction 1.3.2). The same line of arguments here may explain why a visible interaction of PIP5K2 and PDK1 in the cytosol of 28.3% of observed protoplasts may be artificial. Future studies would need to examine whether a substitution variant of PID that is impaired in lipid binding still exhibits this colocalisation in BiFC with PIP5K2 at the plasma membrane.

3.3.6 PID phosphorylates PIP5K2 in the NLS region of the Lin-domain

PID's ability to phosphorylate PIP5K2 *in vitro* was shown prior to this work (master's student Babette Pinkwart). But so far, the sites and function of PID-mediated PI4P 5-kinase phosphorylation were unclear. Because both PIP5K1 and PIP5K2 interacted with PID in the yeast two-hybrid protein interaction assay, both PI4P 5-kinases were tested for phosphorylation by PID *in vitro*, and the result showed that both PIP5K1 and PIP5K2 could be phosphorylated by PID (Fig. 31A). MS analysis of phosphopeptides revealed that PIP5K2 was phosphorylated at the serine residues at positions S274, S275 and S282 by PID (Fig. 31B). These three serine residues are in the Lin-domain of PIP5K2, directly adjacent to the basic RKR cluster of the characterized NLS (Fig. 31B). The identification of phosphorylation sites directly in or next to the NLS of PIP5K2 suggested direct regulation of the NLS in PIP5K2, as described for the strict regulation of dynamic localisation of yeast (*Mss4*) and human PI4P 5-kinases (*HsPIP5K1 α*) realised by posttranslational modifications (Audhya and Emr, 2003; Chakrabarti et al., 2015).

The mass spectrometric data which confirmed the third position, namely S282, in addition to the positions S274 and S275, were generated very late in this work, so that in this study only PIP5K2 substitution variants, in which positions S274 and S275 have been replaced by alanine or aspartate, were used. A PIP5K2 triple substitution variant in which all three putative phosphorylation sites were substituted is still missing. Likewise, no further studies with PIP5K1 have been conducted. In the future, it would certainly be a good support for the data if the phosphorylation sites for PIP5K1 were also identified.

3.3.7 PIP5K2-EYFP apparently localises unaffected by PID

One of the working hypotheses for this study was that the enzymes of the PI metabolism are regulated by posttranslational modifications, such as the well-described protein phosphorylation. With respect to dynamic plasma membrane nuclear localisation of proteins, phosphorylation is thought to affect the functionality or accessibility of nuclear localisation signals by masking or unmasking the signals and thus may critically influence the localisation of target proteins (Jans and Hubner, 1996; Schwab and Dreyer, 1997; Jensen et al., 1998; Harreman et al., 2004; Liku et al., 2005; Youn and Shin, 2006; Wang et al., 2021). Interestingly, the phosphorylation sites S274, S275 and S282 identified here are in the NLS of the Lin-domain of PIP5K2 (Fig. 31), suggesting that these phosphorylations may affect the subcellular localisation of PIP5K2.

However, subcellular localisation studies with PIP5K2-EYFP and the PIP5K2 S274S275 substitution variants in *Arabidopsis* protoplasts with and without altered PID expression did not detect any changes in subcellular localisation (Fig. 32). First preliminary results also show that PIP5K2-EYFP does not localise differently in *pid wag1 wag2* triple mutant protoplasts (appendix Fig. 42). The change in subcellular localisation may not be black or white, but more complex, and may require a larger number of cells to become meaningful. In addition, it should be considered, as previously mentioned, to carry out the localisation tests in intact tissues, as can be done, for example, after the infiltration of tobacco leaves. Also, detection of fluorescence by confocal laser scanning microscopy may not be sufficiently resolving. Phosphorylation of PIP5K2 by PID may result in a more subtle change in plasma membrane association than cannot be detected here by confocal LSM. Both PIP5K2 and PtdIns(4,5)P₂ are organised into nanodomains at the plasma membrane (Fratini et al., 2021). These nanodomains are most likely restricted in their lateral spread by regulators, either PI-phosphatases or enzymes that regulate PI4P 5-kinases directly (Fratini et al., 2021; Heilmann and Heilmann, 2022). To test, whether the nano-domain organisation of PIP5K2 and the respective substitution

variants differed, TIRF microscopy was used, but the fluorescence patterns of the substitution variants of PIP5K2 did not show detectable altered membrane association patterns or dynamics compared to PIP5K2-EYFP (Fig. 33).

Nevertheless, it should be considered that no substitution variants are yet available in which position S282 is mutated in addition to S274 and S275. Thus, a conclusive statement whether the phosphorylations lead to the regulation of the localisation - independent of their extent - is yet not possible.

3.3.8 The AGCVIII protein kinases affect PI4P 5-kinase activity *in vitro* and *in vivo*

There is much evidence for a mutual regulation of PIN, PID and PIP5K1 and PIP5K2. The protein kinase PDK1, which has an activating effect on many of the AGCVIII kinases (Anthony et al., 2004; Mora et al., 2004; Xiao and Offringa, 2020), has a PH domain that has been described to bind anionic lipids, including phosphoinositides (Tan et al., 2020). However, AGCVIII kinases themselves have also been shown to bind specifically to phosphoinositides via a conserved poly basic motif (Barbosa et al., 2016). It is hypothesised that both PDK1 and PID are recruited to the proper spatial-temporal context at the plasma membrane via this lipid binding, where they then act to regulate the polar distribution of PIN proteins according to their function (Fig. 38B (Barbosa et al., 2016)). Since phosphorylation can have an impact on the catalytic activities of their target proteins as mentioned earlier, the lipid kinase activity of PIP5K2 was tested after phosphorylation by PID (Fig. 34). The activity of PIP5K2 was increased 4.6-fold by incubation with PID compared with the buffer control and by approximately 1.5-fold compared with the completely untreated PIP5K2 sample (Fig. 34). It is possible that this is a positive feedback loop, where PID is recruited to the plasma membrane by interaction with PIP5K1 / PIP5K2 and binding to PIs, PIP5K1 / PIP5K2 are then activated by phosphorylation by PID, leading to further formation of PtdIns(4,5)P₂ and subsequently recruiting further PI-binding AGCVIII kinases, such as D6 PROTEIN KINASE (D6PK) and PROTEIN KINASE ASSOCIATED TO BRX (PAX) to the plasma membrane (Fig. 38B). D6PK and PAX are also known to be involved in the activation of PIN-mediated auxin transport (Zourelidou et al., 2014; Barbosa et al., 2016; Tan et al., 2020; Xiao and Offringa, 2020). Thus, this would trigger a self-reinforcing process and possibly contribute to the targeted polarisation of membranes as also already hypothesised in Heilmann and Heilmann 2022 (Fig. 38B). Of course, this is still very speculative and would need to be confirmed by further interaction studies and especially *in vivo* data.

The increase in activity due to the introduction of phosphorylation into the Lin-domain of PIP5K2 indirectly confirms the hypothesis that the N-terminal domains undergo a conformational change due to phosphorylation, thereby abolishing the autoinhibitory effect of the N-terminal domains on the catalytic domain of PIP5K1 and PIP5K2 (Fig. 38A). As mentioned before, CD spectra and cross-linking experiments will need to clarify the extent to which this interpretation of the data is correct.

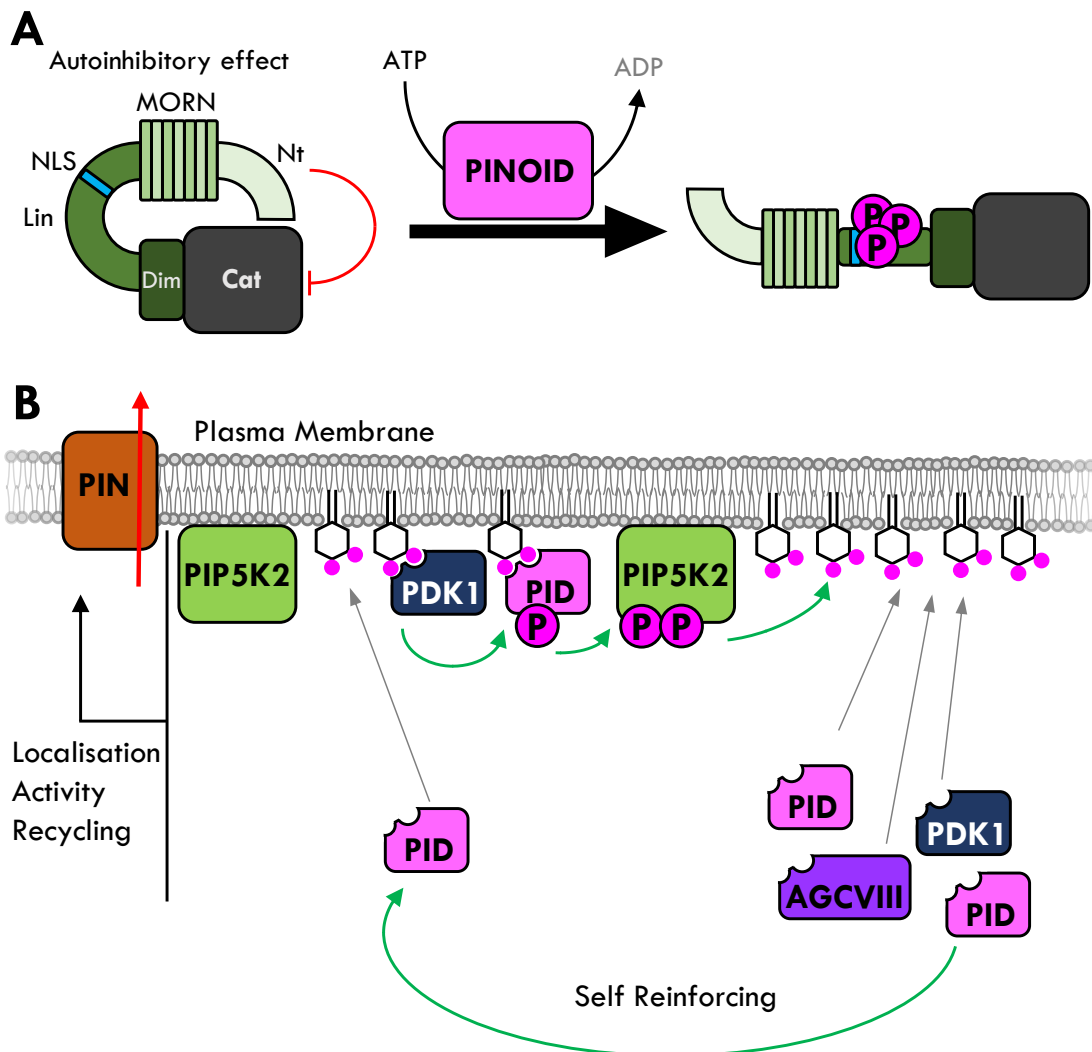


Figure 38: Model: Phosphorylation of PIP5K2 by PID increases catalytical activity promoting a self-reinforcing loop involved in the PIN mediated auxin gradient. A Comparable to the model of CK2 (see Fig. 37), N-terminal domains have an inhibitory effect on the catalytical activity (Im et al. 2007; Stenzel et al. 2012). It is possible that phosphorylation of the Lin-domain leads to a conformational change that subsequently results in full activation of PIP5K2. Nt, N-terminus; MORN, Membrane Occupation and Recognition Nexus; Lin, Linker domain; Dim, Dimerization domain, Cat, Catalytic domain. **B** AGC kinases such as PDK1 and PID have been reported to bind anionic lipids and/ or phosphoinositides directly (Barbosa et al 2016). PDK1 is recruited to the plasma membrane and activates PID by phosphorylation. Activated PID phosphorylates and activates PIP5K2 resulting in increased PtdIns(4,5)P₂ content that further recruits PID, PDK1 and other AGCVIII kinases such as D6PK and PAX that repeat and enhance this cycle. PID, PDK1, PIP5K2 and PtdIns(4,5)P₂ composition has been reported to regulate PIN transporter proteins by

influencing subcellular localisation, activity and clathrin mediated endocytosis. Red arrow indicates auxin flow.

The *in vitro* results showed that PID can activate PIP5K2 by phosphorylation are supported by measurements of intrinsic PtdIns(4,5)P₂ levels in plants with altered PID expression. The PtdIns(4,5)P₂ levels in the *pid* single mutant and the *pid PID wag1 wag2* triple mutants were significantly reduced, while *PID*-overexpressor plants showed comparable values to the wild type (Fig. 35). Due to the very low amounts of PIs, it is methodologically and technically always difficult to measure values with statistical significance, since measurements are always taken at the detection limit and lower PI contents make the evaluation technically even more difficult, which could explain the sometimes quite high standard deviations. But, together with the *in vitro* experiments showing increased catalytic activity of PIP5K2 upon PID phosphorylation, the decreased PtdIns(4,5)P₂ levels in the *PID* single and triple mutants, although not statistically significant, support the hypothesis that PID activates PI4P 5-kinases.

To better understand and investigate these complex interactions between PI metabolism, CME, protein phosphorylation, and possible activation of PIP5K1 or PIP5K2 by PID, this work created plant transformation constructs with the PIP5K2 substitution variants that could be used to stably transform the *pip5k1 pip5k2* double mutant. Expression of the phosphoablation variant PIP5K2 S274A S275A S282A or the corresponding phosphomimikry variant in the background of the *pip5k1 pip5k2* double mutant could then potentially shed light on the extent to which PID-mediated phosphorylation is physiologically relevant for the function of both PI4P 5-kinases and subsequently for the CME and thus for the polar distribution of PIN proteins. It would also be interesting to investigate which other AGCVIII kinases are involved in fine-tuning of PIP5K1 / PIP5K2 activities and localisations, or *vice versa*.

3.4 Regulators that need to be regulated

Reversible protein phosphorylation is the best studied posttranslational modification and can have a broad range of different effects. Functions include changes in catalytic activity, subcellular localisation, conformational changes and mediating binding to interaction partners. Theoretically, one phosphorylation could have multiple or all of the described functions.

Phosphoinositides are spatially and temporally restricted in micro- or nanodomains in membranes and synthesised or degraded according to cellular or local demand.

This biodynamic PI-network and the enzymes involved, including PI4P-5 kinases PIP5K1 and PIP5K2, are targets for regulation, presumably posttranslational modifications including phosphorylation.

In this study the two protein kinases CKA3 and PID have been described to phosphorylate either PIP5K1 or PIP5K2 in the N-terminus or Lin-domain to increase the *in vitro* catalytic activity. However, enhanced catalytic activity of PI-forming enzymes after phosphorylation are novel and striking results.

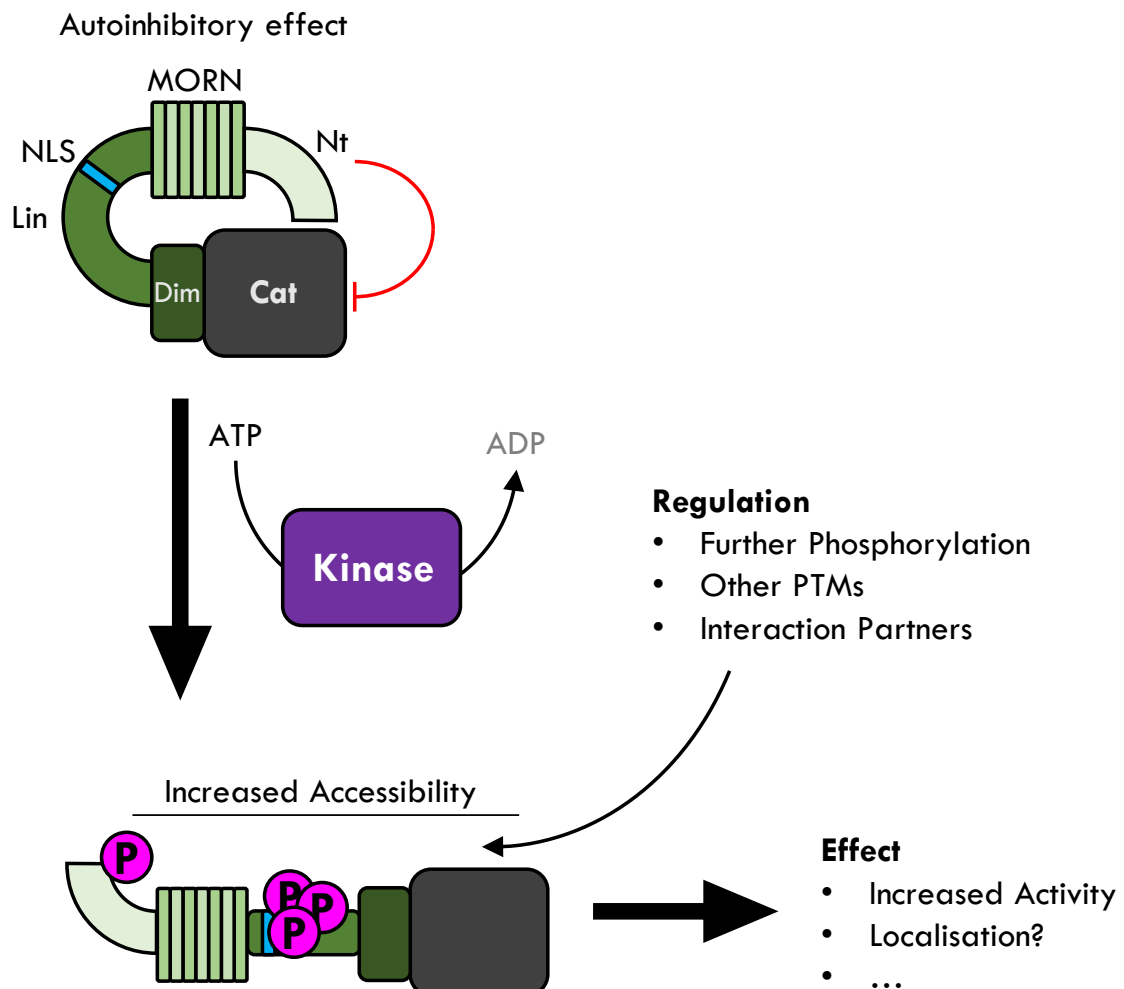


Figure 39 Model: PIP5K1 and PIP5K2 are regulated by protein phosphorylation. Protein kinases such as CKA3 and PID phosphorylate the N-terminal domains of PI4P 5-kinases PIP5K1 and PIP5K2, leading to a conformational change repealing the autoinhibitory effect of the N-terminal domains. Now accessible protein regions are targets for further posttranslational modifications or interaction partners that regulate PIP5K1 and PIP5K2 to modulate catalytic activity, subcellular localisation, or other parameters. Nt, N-terminus; MORN, Membrane Occupation and Recognition Nexus; Lin, Linker domain; Dim, Dimerization domain, Cat, Catalytic domain; PTM, posttranslational modification.

At first glance, it seems counterintuitive that phosphorylation of the N-terminal domains far upstream to the catalytic site increases the catalytic activity. But previously published studies showed that N-terminal truncated PIP5K1 variants exhibit

higher catalytic activity, suggesting that the N-terminal domains have an autoinhibitory effect on the catalytic domain (Im et al. 2007, Stenzel et al. 2012). Through the observations made here, it can be hypothesised that phosphorylation in the N-terminal domains, such as the N-terminus or the Lin-domain, results in a conformational change, abolishing the autoinhibitory effect of the N-terminal domains on the catalytic activity of PI4P 5-kinases like PIP5K1 and PIP5K2 (Fig. 37). Following this concept, the conformational change may also lead to further protein-protein interactions that were not possible before. Therefore, one can also imagine that the regulation of PI4P 5-kinases is multi-layered. The priming of a first modification possibly leads to a series of subsequent reactions, for example to further posttranslational modifications, which then spatiotemporally model the function of PI4P 5-kinases as it is also discussed in Heilmann and Heilmann 2022 (Fig. 39).

Consequently, the regulation of the putative nuclear-cytoplasm shuttling of plant PI4P-5 kinases could be influenced by many factors besides phosphorylation. As mentioned above, additional posttranslational modifications might require that a priming posttranslational modification is present first, thereby only being able to introduce additional posttranslational modifications, which then lead to a regulated NLS and subsequently a change in subcellular localisation. Shuttling or general localisation changes, even in the nano-domain range, may need more regulatory factors (Heilmann and Heilmann 2022).

4 Material and Methods

4.1 Chemicals and consumables

If not specifically mentioned chemicals were purchased from Sigma-Aldrich/ Merck (Munich/ Darmstadt, Germany), Carl Roth GmbH (Karlsruhe, Germany) or Appl-Chem (Darmstadt, Germany).

4.2 Enzymes and size indicators

Table 1 Enzymes and size indicators

Name/ Used for	Company/ Origin
PageRuler™ Prestained (SDS Page)	Thermo Fisher Scientific, Schwerte, Germany
PageRuler™ Unstained (SDS Page)	Thermo Fisher Scientific, Schwerte, Germany
GeneRuler 1 kb	Thermo Fisher Scientific, Schwerte, Germany
GeneRuler 100 bp	Thermo Fisher Scientific, Schwerte, Germany
All restriction enzymes e.g. Ascl, XhoI, NotI, EcoRI, EcoRV, Sall, SfiI	New England Biolabs Inc., Frankfurt, Germany
T4 DNA Ligase	New England Biolabs Inc., Frankfurt, Germany

4.3 Microorganisms

Table 2 Microorganisms

Organism and Application	Strain	Genotype	Distributing Company
<i>Escherichia coli</i> (Plasmid amplification and cloning)	NEB5α	fhuA2 Δ(argF-lacZ)U169 phoA glnV44 Φ80 Δ(lacZ)M15 gyrA96 recA1 relA1 endA1 thi-1 hsdR17	New England Biolabs, Frankfurt, Germany
<i>E. coli</i> (Amplifying ccdB-containing Gateway plasmids)	DE3.1	F- gyrA462 endA1 glnV44 Δ(sr1- recA) mcrB mrr hsdS20(rB-, mB-) ara14 galK2 lacY1 proA2rpsL20(Smr) xyl5 Δleu mtl1	Thermo Fisher Scientific, Dreieich, Germany
<i>E. coli</i> (Protein expression)	Rosetta 2 (DE3)	F- ompT hsdSB(rB- mB-) gal dcm (DE3) pRARE2 (CamR)	Novagene, Merck, Darmstadt, Germany
	BL21 (DE3)	fhuA2 [lon] ompTgal(λ DE3) [dcm] ΔhsdSλ DE3 = λ sBamHloΔEcoRI-B int:::(lacI::PlacUV5::T7gene1) i21 Δnin5	Thermo Fisher Scientific, Schwerte, Germany

<i>Agrobacterium Tumefaciens</i> (Plant transformation)	AGL-0	C58 pTiBo542; recA::bla, T-Regiondeletiert Mop(+) Cb(R)	(Lazo et al., 1991)
<i>Saccharomyces Cerevisiae</i> (Protein-protein interaction studies)	NMY51	MATa, his3Δ200, trp1-901, leu2-3,112, ade2, LYS2::(lexAop)4-HIS3, ura3::(lexAop)8-lacZ (lexAop)8-ADE2 GAL4)	Dualsystems Biotech, Zürich, Schweiz

4.4 Plants and plant cell cultures

Table 3 Plants and plant cell cultures

Appellation	Species	Transgene	Received by
Arabidopsis wildtype	<i>Arabidopsis thaliana</i> Columbia-0	none	Lehle seeds (http://www.arabidopsis.com)
<i>pip5k1</i>	<i>Arabidopsis</i> Col-0	T-DNA-insertion in <i>PIP5K1</i> (SALK_146728)	(Ischebeck et al., 2013)
<i>pip5k2</i>	<i>Arabidopsis</i> Col-0	T-DNA-insertion in <i>PIP5K2</i> (SALK_012487)	(Ischebeck et al., 2013)
<i>PIP5K1</i> <i>pip5k1 pip5k2</i>	<i>Arabidopsis</i> Col-0	Crossing of <i>pip5k1</i> (SALK_146728) and <i>pip5k2</i> (SALK_012487)	(Ischebeck et al., 2013)
<i>pip5k1 pip5k2</i> <i>pPIP5K2::PIP5K2-EYFP</i>	<i>Arabidopsis</i> Col-0	<i>pip5k1 pip5k2</i> complementation line, expresses <i>PIP5K2</i> tagged to <i>EYFP</i> under the control of its endogenous promotor (<i>pPIP5K2</i>)	(Ischebeck et al., 2013)
<i>pip5k1 pip5k2</i> <i>pPIP5K1::PsPIP5K1-EYFP</i>	<i>Arabidopsis</i> Col-0	<i>pip5k1 pip5k2</i> complementation line, expresses <i>PsPIP5K1</i> tagged to <i>EYFP</i> under the control of the intrinsic promotor of <i>PIP5K2</i> (<i>pPIP5K2</i>)	This study
<i>pip5k1 pip5k2</i> <i>pPIP5K1::PsPIP5K1 LinAt-EYFP</i>	<i>Arabidopsis</i> Col-0	<i>pip5k1 pip5k2</i> complementation line, expresses <i>PsPIP5K1_LinAt</i> tagged to <i>EYFP</i> under the control of the intrinsic promotor of <i>PIP5K1</i> (<i>pPIP5K1</i>)	This study
<i>pip5k1 pip5k2</i> <i>pPIP5K2::PsPIP5K1 LinAt-EYFP</i>	<i>Arabidopsis</i> Col-0	<i>pip5k1 pip5k2</i> complementation line, expresses <i>PsPIP5K1_LinAt</i> tagged to <i>EYFP</i> under the control of the intrinsic promotor of <i>PIP5K2</i> (<i>pPIP5K2</i>)	This study
<i>pCaMV35S::PID</i> OE	<i>Arabidopsis</i> Col-0	Overexpression line 10 that overexpresses <i>PINOID</i> strongly under the control of the <i>CaMV35S</i> promotor	(Benjamins et al., 2001a) Dr. Jiri Friml, Institute for Science and Technology, Klosterneuburg, Austria
<i>pid</i>	<i>Arabidopsis</i> Col-0	T-DNA-insertion in <i>PINOID</i> (SALK_049736)	(Dhonukshe et al., 2015) Dr. Jiri Friml, Institute for Science and Technology, Klosterneuburg, Austria

PID <i>pid- wag1 wag2</i>	<i>Arabidopsis</i> Col-0	Crossing of <i>pid</i> (SALK_049736) <i>wag1</i> (SALK_002056) and <i>wag2</i> (SALK_070240)	(Dhonukshe et al., 2015) Dr. Jiri Friml, Institute for Science and Technology, Klosterneuburg, Austria
Poppy Wildtype	<i>Papaver somniferum</i>	none	AG Marek, Faculty of Pharmacy Comenius University Bratislava
Tobacco wildtype	<i>Nicotiana tabacum</i> <i>Samsun</i>	none	Prof. Ingo Heilmann
Col-0 Cell Culture	<i>Arabidopsis</i> Col-0	Leaf Cell Culture derived from two-week-old seedlings	This study
BY-2 Cell Culture	<i>N. tabacum</i> <i>L. cv. Bright Yellow 2</i>	none	Dr. Katharine Bürstenbinder (Nagata et al., 1992)

4.5 Culture media

For solid medium preparations, 1.5% (w/v) micro agar was added to the media. All media were autoclaved at 121 °C for 15 min.

Table 4 Bacterial media

Media	Components for 1 l
LB	10 g tryptone 5 g yeast extract 10 g NaCl
2YT	16g tryptone 10 g yeast extract 10 g NaCl 2 g Glucose
YEB	1 g yeast extract 5 g beef powder 5 g peptone 5 g sucrose

4.5.1 Yeast media

Table 5 Yeast media

Media	Components for 1 l
YPAD	10 g Bacto yeast extract 20 g Bacto peptone 20 g Glucose monohydrate 40 mg adenine sulfate

SD	H ₂ O to 1 l
SD-LW	1.7 g yeast nitrogen base without amino acids
SD-LWH	5 g ammonium sulfate
	H ₂ O to 1 l
	10x -LW(H) drop out
	200 mg L-adenine hemisulfate
	200 mg L-arginine HCl
	(200 mg L-histidine HCl monohydrate)
	300 mg L-isoleucine
	300 mg L-lysine HCl
	200 mg L-methionine
	500 mg L-phenylalanine
	2000 mg L-threonine
	300 mg L-tyrosine
	200 mg L-uracil
	1500 mg L-valine
	200 mg L-serine.
	For 500 ml SD-LW(H) bottles:
	50 ml 20 % glucose
	50 ml drop out medium (LW(H))

4.5.2 Plant media

Table 6 Plant media

Media	Concentration/ Components for 1 l
½ MS	2.2 g MS salts including vitamins (Murashige and Skoog, 1962) 10 g sucrose pH 5.6 with KOH
BY-2 Cell Culture	30 g Sucrose 4.3 g MS salts (Duchefa, Haarlem, Netherlands) 0.2 g KH ₂ PO ₄ 1 mg Thiamine 200 µg 2,4-Dichlorophenoxyacetic acid pH 5,8 with KOH
Col-0 Cell Culture	30 g Sucrose 4.3 g MS salts (Duchefa, Haarlem, Netherlands) 10 ml Vitamin stock solution (see 4.8) 1 mg 2,4-Dichlorophenoxyacetic acid pH 5,8 with KOH
Col-0 Root Cell Media	60 g sucrose 4.4 g ½ MS salts (Duchefa, Haarlem, Netherlands)

Tobacco Pollen Medium	5 % sucrose 12.5 % PEG ₆₀₀₀ 0.03 % casein hydrolysate 15 mM MES-KOH pH 5.9 1 mM CaCl ₂ 1 mM KCl 0.8 mM MgSO ₄ 1.6 mM H ₃ BO ₄ 30 μM CuSO ₄
-----------------------	--

4.5.3 Media additives

Table 7 Media additives

Additive	Stock Solution	Final Concentration
Carbenicillin	100 mg/ ml	100 μg/ ml
Kanamycin	50 mg/ ml	50 μg/ ml
Rifampicin	50 mg/ ml in DMSO	50 μg/ ml
Glufosinate	10 mg/ ml	10 μg/ ml

4.5.4 Growth conditions

Tobacco plants were cultivated in the green house at minimum 16 h light per day. Arabidopsis and poppy were grown in A1000 plant chambers (Conviron, Cambridge, United Kingdom), PERCIVAL AR-66/L3 plant chambers (Percival Scientific, Perry, IA, USA) or custom made chambers/ rooms by NEMA (AES Systems Netschkau, Germany) either at long day conditions (16 h light at 21 °C, 8 h darkness at 18 °C; 55 % humidity) or short day conditions (10 h light at 21 °C, 14 h darkness at 18 °C; 55 % humidity) depending on the experimental setup.

Plants plated on 1/2 MS media (see 4.5.2) were stratified at 4 °C for three days before put into the growth chambers. For plants seeded on soil nine parts of Substrate 1 (Klasmann-Deilmann GmbH, Geeste, Germany) with one part of vermiculite were used as soil substrate. The soil substrate was steamed at 80 °C for 8-10 h before use. Plants used for protoplast isolation were grown under short-day conditions for six to eight weeks. Plants for stable transformation and seed propagation were grown for four to six weeks under short-day conditions, followed by long-day conditions to induce shoot growth.

Cell cultures were cultivated at room temperature in the dark at around 80 rpm and 23 °C. Cells were kept in the growth phase by refreshing small culture fractions

(5/ 10 ml BY-2, 10 ml of Col-0 cell culture) with fresh 30 ml media once per week. For the medias see 4.5.2.

Arabidopsis root cultures were grown at room temperature in root cell media (see 4.5.2) in the lab at 50 rpm for weeks until root protoplasts were isolated (see 4.22).

4.6 Growing arabidopsis cell cultures

During this study a new Arabidopsis leaf cell culture was established (Barkla et al., 2014). Cotyledons of two weeks old Arabidopsis seedlings were cut and placed on solid plant media (see 4.5.2). After four weeks grown calli were placed into liquid plant media and grown in the dark for four weeks at 25 °C and 90 rpm in 500 ml Erlenmeyer flasks. Since then, culture is renewed once per week by combining 30 ml of old cell culture with 100 ml of fresh media.

4.7 Vectors and plasmids

4.7.1 Vectors for protein expression in *E. coli*

Table 8 Vectors used for protein expression in *E. coli*

Vector	Selection marker	Description	Received by
<i>pMAL-c5G</i>	<i>Amp^R</i>	Contains a <i>mcs</i> and a N-terminal <i>malE</i> gene for maltose-binding-protein under the control of <i>ptac</i> promoter. MBP sequence was optimized for enrichment via amylose. MBP can be cleaved from protein of interest with the protease Genenase I.	New England Biolabs Inc., Frankfurt, Germany
<i>pGEX-4T-1</i>	<i>Amp^R</i>	Contains a <i>mcs</i> and a N-terminal GST tag the control of the <i>tac</i> promoter. Internal <i>lacIq</i> gene for expression. PreScission™ Protease, Thrombin, or Factor Xa recognition sites for cleaving the desired Protein from the fusion product are available.	Dr. Mareike Heilmann
<i>pET28b</i>	<i>Kan^R</i>	Contains a <i>mcs</i> and a 5'prime and 3'prime His ⁶ -tag under the control of T7 promoter and terminator	Dr. Mareike Heilmann

4.7.2 Vectors for protein-protein interaction studies

Table 9 Vectors used for yeast-two-hybrid studies

Vector	Selection marker	Description	Received by
<i>pBT3-C-OST4</i> (Y2H)	<i>Kan^R</i> for bacteria	Bait vector based on <i>pBT3-C</i> . Under control of <i>pCYC1</i> promotor a <i>mcs</i> and 3'the cDNAs coding for the C-terminal part of ubiquitin (<i>Cub</i> , aa 34–76), <i>LexA</i> DNA binding domain and <i>VP16</i>	Dualsystems Biotech, Zurich, Switzerland; and modified by Dr.

	<i>LEU2</i> for yeast	transactivation domain and <i>CYC1</i> terminator. Dr. Mareike Heilmann modified the vector by adding <i>OST4</i> (coding for oligosaccharyltransferase 4) via <i>XbaI</i> restriction sites.	Mareike Heilmann, MLU Halle Wittenberg
<i>pPR3-N</i> (Y2H)	<i>Amp^R</i> for bacteria <i>TRP1</i> for yeast	Prey vector that contains under control of <i>pCYC1</i> promoter the cDNA coding for the N-terminal part of ubiquitin (<i>NubG</i> , aa 1–38, 113 mutated to G) 5' of HA epitope tag and <i>mcs</i> , <i>CYC1</i> terminator.	Dualsystems Biotech, Zurich, Switzerland
<i>pPR3-C</i> (Y2H)	<i>Amp^R</i> for bacteria <i>TRP1</i> for yeast	Same as <i>pPR3-N</i> except that <i>NubG</i> is fused C-terminally to the prey	Dualsystems Biotech, Zurich, Switzerland
<i>pAl-Alg5</i> (Y2H)	<i>Amp^R</i> for bacteria <i>TRP1</i> for yeast	Prey vector that contains the cDNA of unmodified <i>Nub</i> fused to <i>Alg5</i> (dolichyl-phosphate beta-glucosyltransferase).	Dualsystems Biotech, Zurich, Switzerland
<i>pDL2-Alg5</i> (Y2H)	<i>Amp^R</i> for bacteria <i>TRP1</i> for yeast	Prey vector that contains the cDNA of <i>NubG</i> fused to <i>Alg5</i>	Dualsystems Biotech, Zurich, Switzerland
<i>pBiFCt-2in1-NC</i> (BiFC)	<i>Spec^R</i>	<i>attR3</i> and <i>attR2</i> recombination sites flank a <i>lacZ</i> expression cassette and allow to form N-terminal fusion proteins with the N-terminal half of EYFP. <i>attR1</i> and <i>attR4</i> recombination sites flank a <i>ccdB</i> gene and chloramphenicol resistance gene and allow to form C-terminal fusion proteins with the C-terminal half of EYFP. Contains the cDNA of RFP as transformation control. All expression cassettes are under the control of the <i>pCaMV35S</i> promoter and terminator.	(Grefen and Blatt, 2012)

4.7.3 Vectors for transient expression in plants and plant transformation

Table 10 Vectors used for transient expression and stable transformation of plants

Vector	Selection marker	Description	Received by
<i>pEntryA</i>	<i>Amp^R</i>	Based on <i>pUC18</i> , contains two different <i>SfiI</i> -restriction sites for the introduction of a promoter sequence and a multiple cloning site (<i>mcs</i>) followed by the polyA-terminator from the octopin synthase gene (<i>OCS</i>) from <i>Agrobacterium</i> . The promoter, <i>mcs</i> and <i>OCS</i> terminator are flanked by <i>att</i> -sites (<i>attL1</i> and <i>attL4</i>) for recombination with the dual Gateway™ system.	Dr. Mareike Heilmann, MLU Halle-Wittenberg
<i>pEntryD</i>	<i>Amp^R</i>	<i>pEntryD</i> corresponds to <i>pEntryA</i> , the difference are <i>att</i> -sites <i>L4</i> and <i>L2</i> flanking the cloning cartridge.	Dr. Mareike Heilmann, MLU Halle-Wittenberg
<i>pCAMBIA 3300.0GS</i>	<i>Kan^R</i> for bacteria <i>Basta^R</i> in plants	Contains a <i>ccdB</i> gene flanked by <i>attR1</i> and <i>attR2</i> recombination sites. Serves as a destination vector of the Gateway™ reaction. Contains left border and right border sequence for <i>Agrobacterium</i> mediated transformation in plants	Dr. Ellen Horning, Göttingen

4.8 Buffers and stock solutions

Table 11 Buffers and stock solutions

Buffer/ Stock Solution	Chemicals, if not mentioned, dissolved in water
10x TBS (Western Blot)	100 mM Tris-HCl pH 8 1.5 M NaCl
4x DNA-Loading Dye (Agarose Gel Electrophoresis)	60 % (v/v) glycerol 0.4 % (w/v) Orange G 0.03 % (w/v) bromophenol blue 0.03 % (w/v) xylene cyanole PP
5x Laemmli Loading Dye (SDS-PAGE)	4% (w/v) SDS 10% (v/v) Glycerine 10% (w/v) beta-Mercaptoethanol 0.04% (w/v) Bromphenole Blue 0.125 M Tris HCl pH 7
CTAB Extraction Buffer (DNA Extraction)	2 % (w/v) Cetrimonium bromide (CTAB) 100 mM Tris-HCl pH 8 1.4 M NaCl 2 % β -Mercaptoethanol (add shortly before use)
CTAB/ NaCl Buffer (DNA Extraction)	10 % CTAB 0.7 % NaCl
Enzyme Solution for Arabidopsis and poppy (Protoplasts)	0.4 M Mannitol 20 mM KCl 20 mM MES pH 5.7 1.5 % (w/v) Cellulase R10 (Serva) 0.4 % (w/v) Maceroenzyme R10 (Serva) 1 mg/ml BSA 10 mM CaCl ₂
Enzyme Solution for BY-2 Cells (Protoplasts)	0,25 M Mannitole 3,3 mM NaAcetate 50 mM CaCl ₂ 5 mg/ml BSA 0,1 % (w/v) Pektinase (Sigma) 0,5 % (w/v) Macerozyme R10 (Serva) 1 % (w/v) Cellulase R10 (Serva)
GST-Elution Buffer (<i>in vitro</i> Pull-Down)	25 mM Tris-HCl pH 7.2 75 mM NaCl 50 mM Glutathione

GST-Equilibration Buffer (<i>in vitro</i> Pull-Down)	25 mM Tris-HCl pH 7.2 75 mM NaCl
High Salt Buffer (RNA Isolation)	0.8 M Na-Citrate 1.2 M NaCl
His-Equilibration Buffer (Protein Enrichment)	25 mM Tris pH 8.0 75 mM NaCl (20mM Imidazole)
Lithium acetate Buffer (Y2H)	1 M lithium acetate 100 ml stock: 10.2 g lithium acetate dihydrate H ₂ O to 100 ml
Lithium acetate/ PEG master mix (Y2H)	50 %PEG ₄₀₀₀ 100 mM lithium acetate 1x TE buffer For 12 ml: 50 % PEG ₄₀₀₀ 9.6 ml 1.2 ml lithium acetate buffer 1.2 ml 10x TE buffer
Lithium acetate/ TE master mix (Y2H)	110 mM lithium acetate 1.1x TE buffer For 8 ml: 0.88 ml lithium acetate buffer 0.88 ml 10x TE buffer 6.24 ml H ₂ O
MMG (Protoplasts)	0.4 M Mannitole 15 mM MgCl ₂ 4 mM MES pH 5.7
PEG (Protoplasts)	0.2 M Mannitole 0.1 M CaCl ₂ 40% PEG
Protein Buffer CK2 (Protein Expression)	50 mM Tris-HCl pH 8 500 mM NaCl 20 mM Imidazole 0,5% TritonX-100 10% Glycerine 2 mM MgCl ₂
Protein Buffer PID (Protein Expression)	200 mM NaCl 25 mM Tris pH 7.5
Protein Buffer PIP5K1 (Protein Expression)	200 mM NaCl 20 mM Tris pH 7.5 1 mM EDTA

Protein Buffer PIP5K2 and PIP5K2 Substitution Variants (Protein Expression)	150 mM NaCl 50 mM Tris pH 7.5 1 mM EDTA
Protein Phosphorylation Buffer (PID Phosphorylation Assay)	50 mM Tris pH: 7.5 10 mM MgCl ₂ 0.1 mM EDTA 0.01 % Brji 35P 20 μM ATP (fresh)
SDS Running Buffer (SDS-PAGE)	25 mM Tris 192 mM Glycine 0.1 SDS
Sterilizing Solution (Arabidopsis seeds)	6% (v/v) Sodium hypochloride 1:1000 Triton X-100
TAE-Buffer (Agarose Gel Electrophoresis)	40 mM Tris 20 mM glacial acetic acid 1 mM EDTA
TBF Buffer (Chemically competent <i>E. coli</i>)	10 mM HEPES pH 6.7 15 mM CaCl ₂ 250 mM KCl pH to 6.7 with KOH after autoclaving: 55 mM MnCl ₂
TE Buffer (Y2H)	1 mM EDTA 10 mM Tris pH 7.5 10x Stock for 1 l: 100 ml 1M Tris-HCl pH 7.5 20 ml 0.5 M EDTA pH 8.0 H ₂ O to 1 l
TE-Buffer (Gateway® Cloning)	1 mM EDTA 10 mM Tris pH 8.0
Transfer Buffer (Western Blot)	25 mM Tris 192 mM Glycine 10% (v/v) Methanol 0.01% SDS
Trizol Buffer (RNA Isolation)	For 10 ml: 3.8 ml Phenol, saturated with 0.1 M Citrate Buffer pH 4.3 (Sigma) 2 ml 4 M Guanidiniumthiocyanate Solution 1 ml 4 M Ammoniumthiocyanate Solution 334 μl 3 M NaAcetate Solution pH 5.0 500 μl Glycerine 2.366 ml Water

Vitamin Stock Solution 100x	5000 mg Myo-inositol 25 mg Nicotinic acid 25 mg 2,4 pyridoxine HCl 5 mg Thiamine HCl H ₂ O ad 500 ml
W5 (Protoplasts)	154 mM NaCl 125 mM CaCl ₂ 5 mM KCl 2 mM MES pH 5.7
W1 (Protoplasts)	0.5 M Mannitole 20 mM KCl 4 mM MES pH 5.7

4.9 Preparation of RNA, DNA and cDNA from plants

4.9.1 Isolation of RNA from Arabidopsis

RNA was isolated from fresh plant tissue by precooling a mortar and pestle in liquid nitrogen and powdering the plant material. The plant powder was centred in the middle of the mortar using a nitrogen cooled spatula and 1 ml of TRIZOL solution (see 4.8) was added. After the mixture thawed completely it was transferred to a 2 ml reaction tube. A 15 min step of centrifugation at 20 000 g at 4°C followed. The supernatant was transferred into a fresh 1.5 ml reaction tube and 200 µl of chloroform was added and the tube and mixed for 20 s. The aqueous phase was put into a fresh 1.5 ml reaction tube and the RNA was precipitated by adding half a sample volume of isopropanol and high salt precipitation buffer (see 4.8) and inverted several times. The precipitation was incubated for 10 min at room temperature and the precipitated RNA centrifuged at 20 000g for 15 min at 4°C. The RNA pellet was washed two times with 900 µl of 85 % ethanol and dried for a few minutes. The RNA was dissolved in 30 µl of RNase/ DNase free water and freezed at -80 °C until used for further applications.

4.9.2 Isolation of genomic DNA from Arabidopsis

To extract gDNA from Arabidopsis, small 0.5 cm² leaf areas were cut of the plant and freezed in liquid nitrogen. The plant tissue was pulverised with 0.2 mm diameter and 0.3 mm diameter glass beads in a Retsch-TissueLyser for 60 s at max frequency (Disruption Preparation Unit2, Qiagen, Hilden, Germany). 250 µl of CTAB/β-mercaptoethanol DNA extraction buffer (see 4.8) was added to the pulverised tissue and placed to 65 °C for 30 min. An equal 250 µl volume of chloroform:

isoamyl alcohol (v/v 24:1) was added and mixed. The samples were centrifuged at 7500 g for 3 min at room temperature. Approx. 200 µl of the upper aqueous phase was transferred to a new 1.5 ml reaction tube. To precipitate the gDNA 20 µl of preheated (65°C) CTAB/ NaCl solution (see 4.8) was added and mixed. After 2 min incubation 220 µl of isopropanol was added and the tube inverted a few times. The precipitated DNA was centrifuged at 20 000 g at 4°C for 10 min. The DNA pellet was washed with 100 µl 85% ethanol, dried briefly and dissolved in 30 µl of RNase/ DNase free water.

4.9.3 Determining RNA and DNA Concentrations

DNA or RNA concentrations were measured at 260 nm using the NanoDrop2000 (VWR International, Darmstadt, Germany). The quality of nucleic acids was also analysed at the ratio of DNA/ RNA at 260/ 280 nm and present contaminations at 260/ 230 nm.

4.9.4 cDNA synthesis

Total RNA concentration was measured and normalised, and cDNA synthesized using the RevertAid H Minus First Strand cDNA Synthesis Kit (Thermo Fisher Scientific, Schwerte, Germany).

4.10 Separation of DNA and RNA in agarose gels

DNA and RNA was separated according to their size in 1 % to 2 % (w/v) agarose gels. The samples were mixed with 4x DNA-loading dye (see 4.8) and loaded into the gel. As size indicator a 1 kb or 100 bp DNA ladder (see 4.2) was loaded. The electrophoresis was performed in TAE running buffer (see 4.8) at 130 to 175 V until the yellow dye of the DNA loading buffer was running out of the gel. To visualise the DNA bands the gel was incubated in an ethidium bromide bath for 10 min and analysed using the gel detection system Quantum ST4 (Vilber Lourmat GmbH, Eberhardzell, Germany).

4.11 Molecular Biology Methods

4.11.1 Amplifying DNA fragments using polymerase-chain-reaction (PCR)

4.11.1.1 PCR for cloning

DNAs of interest needed to be amplified using PCR to clone them into a vector backbone. For this purpose, the Phusion® High Fidelity DNA-Polymerase with proof-reading ability was used (New England Biolabs Inc., Frankfurt, Germany) according to the manufacture's manual. As templates, already cloned plasmids with the DNA of interest, fresh cDNA preparations (see 4.9.4), or for amplification of promoters, genomic DNAs were used to amplify the DNA of interest. The primers used for each individual PCR reaction are listed in 6.3.1. The annealing temperature was adjusted for each primer pair. To reduce the annealing temperature of long primers and suppress secondary structure formation 1 % (v/v) DMSO was added to the PCR reaction. PCRs were analysed in agarose gels (see 4.10).

4.11.1.2 Modifying DNA sequences by fusion PCR

To introduce amino acid substitutions into proteins, corresponding cDNA was modified via the method of fusion PCR with appropriate primers (see 6.3) that introduced the change into the cDNA sequence at the site of mutagenesis. The forward and reverse mutagenesis primers overlapped and carried the corresponding changes in their sequence. In two separate PCR reactions, the 5' prime end primer of the corresponding cDNA was first used together with the reverse mutagenesis primer, and the forward mutagenesis primer was used together with the 3' prime end primer. The PCR fragments generated in both PCRs were analysed and extracted in an agarose gel (see 1.9) (see 1.10.3). In another PCR, the two fragments were merged by using the 5' - and 3' end primer pair, resulting in the substituted cDNA sequence. The final PCR product was analysed and extracted as described (see 4.11.3).

To introduce domain swaps a similar setup was assembled. In total four PCRs had to be performed. At first, cDNA of interest was amplified from its 5' prime start to the start of the domain swap. Second, the domain swap region was amplified using the other cDNA of interest. Third, the end of domain swap to the 3' prime end of the cDNA was amplified resulting in three overlapping fragments. In a fourth PCR all fragments were fused together using oligos for the 5' prime start and 3' prime end of the cDNA of interest. The final product was analysed and extracted as described (see 4.11.3). For specific primers see 6.3.1.

4.11.1.3 Taq-PCR

For genotyping and non-proofreading PCRs the ONETAQ[®] polymerase (VWR International, Darmstadt, Germany) without proofreading was used according to the manufacture's manual. Used primers for genotyping are displayed in 6.3.3.

4.11.2 Isolating plasmid DNA from *E. coli*

Plasmids were extracted and purified from *E. coli* using the GeneJET[™] Plasmid Miniprep Kit (Thermo Fisher Scientific, Schwerte, Germany). For larger plasmid quantity the CompactPrep Plasmid Midi Kit (Qiagen, Hilden, Germany) was used according to the manufacture's manual.

4.11.3 Isolating DNA from agarose gels

Restricted vectors, plasmids and PCR fragments were extracted from agarose gels using the GeneJET[™] Gel Extraction Kit according to the manufacture's manual.

4.11.4 Restriction of DNA

Vectors, plasmids and PCR products were digested using restriction enzymes (see 4.2) in CutSmart buffer (New England Biolabs, Frankfurt, Germany) and their optimal digestion temperature for at least one hour. To digest plasmids approx.-1-1.5 µg plasmid was used and analysed with an agarose gel (see 4.10.). For cloning vectors and PCR products the digestion was prolonged over night before they were extracted as described above.

4.11.5 DNA ligation

To ligate PCR products into vectors and plasmids the T4-DNA-Liagse (New England Biolabs Inc., Frankfurt, Germany) was used according to the manufacture's manual. Ligations were further transformed into *E. coli* NEB5α cells (see 4.11.8).

4.11.6 Gateway[®] cloning

Gateway[®] cloning was used to get constructs from the *pEntryA* or *pEntryD* vectors (see 4.7.3) into the *pCAMBIA3300.0GS* vector which was used for *A. tumefaciens* driven stable transformation of Arabidopsis. For this purpose, 1 µl of *pEntryA*, 1 µl of *pEntryD* and 1 µl of *pCAMBIA3300.0GS* were mixed with 6.5 µl of TE buffer (see 4.8) and 0.5 µl LR-Clonase[®] II Enzyme mix (Thermo Fisher Scientific, Schwerte, Germany). The reaction was incubated at room temperature overnight and

transformed completely into *E. coli* NEB5 α cells (see 4.11.8) and plated onto selective LB media.

4.11.7 Preparing chemo-competent *E. coli*

All work was done on ice. A 20 ml LB (see 4.5) preculture was inoculated with fresh *E. coli* cells and grown over night at 37 °C and 180 rpm. The 500 ml LB main culture was inoculated with five ml preculture and grown at 37 °C and 180 rpm until an optical density OD₆₀₀= 0.4-0.6 was reached. The cells were cooled down on ice for ten min and centrifuged at 3220 g at 4 °C for 15 min. The pellets were resuspended in 100 ml TBF buffer (see 4.8) and incubated for ten min on ice and sedimented again by centrifugation. The cells were resuspended in 40 ml TBF buffer and mixed with 0.7 % DMSO. The cells were incubated on ice for additional ten min and 300 μ l aliquots were prepared, frozen in liquid nitrogen and stored at -80°C until used for transformation.

4.11.8 Transforming chemo-competent *E. coli*

For transformation of ligation or Gateway reactions, 100 μ l of NEB5 α cells were mixed with the ligation mixture; for plasmid propagation (retransformations), 50 μ l of NEB5 α cells were mixed with 1 μ l of plasmid DNA; and for transformation of Rosetta2 or BL21(DE3), 1 μ l of the desired plasmid DNA was mixed with 50 μ l of the corresponding *E. coli* strain. The transformations were incubated on ice for at least 30 min followed by a heat shock at 42 °C for one min. The cells were placed back on ice and 900 μ l LB-media (see 4.5) was added. The transformation was incubated at 37 °C for at least one h. Transformation mixtures of ligations and Gateway reactions were completely plated on LB plates with appropriate antibiotics. Of the retransformations and transformations of Rosetta2 or BL21(DE3), only 100 μ l of the mixtures were plated on LB plates with the appropriate antibiotic.

4.11.9 Controlling DNA by sequencing

Plasmids were sequenced to validate the correct DNA sequence. The sequencing was performed by GATC Biotech AG (Eurofins Genomics Germany GmbH, Ebersberg, Germany). The sequences were analysed using Chromas (version 2.6.6, Technelysium Pty Ltd, South Brisbane, Australia), Multalin (Corpet, 1988) and BoxShade (version 3.21, K. Hofmann, M. Baron, ExPASy Bioinformatics Resource Portal, SIB Swiss Institute of Bioinformatics, Lausanne, Switzerland). Reference sequences were obtained from the NCBI gene database (National Center for Biotechnology Information, U.S. National Library of Medicine, Rockville Pike, Bethesda, MD, USA).

4.11.10 Preparing chemo-competent *A. tumefaciens*

With two ml of a preculture a 50 ml YEB (see 4.5.1) main culture was inoculated and grown to an optical density of $OD_{600} = 0.5$ at 25 °C and 95 rpm. The cells were centrifuged at 3220 g at 4 °C for 5 min and resuspended in 10 ml 0.15 M NaCl solution. The centrifugation was repeated, and the cells resuspended in one ml ice cold 75 mM CaCl solution. Aliquots of 200 µl were frozen in liquid nitrogen and stored at -80 °C.

4.11.11 Transforming chemo-competent *A. tumefaciens*

Cells were thawed by hand and 7.5 µl of Miniprep plasmid was added and the mixture incubated on ice for 30 min. The sample was frozen in liquid nitrogen and thawed at 37 °C. 800 µl YEB-media was added and the mixture incubated at 28 °C for one h. 200 µl of cells were plated onto solid YEB-media containing appropriate antibiotics and grown for two days at 28 °C.

4.11.12 Transforming Arabidopsis with *A. tumefaciens*

A modified floral dipping method after the principle of Clough and Bent was used for Arabidopsis transformation (Clough and Bent, 1998). A 30 ml YEB (see 4.5) preculture containing appropriate antibiotics was inoculated with a fresh *A. tumefaciens* colony and incubated overnight at 28 °C at 180 rpm. The main culture of 400 ml was set to an optical density of $OD_{600} = 0.1$ and was grown to an $OD_{600} = 0.8$ at 28 °C at 95 rpm. The cells were pelleted at 3220 g at 4 °C and washed with 200 ml fresh 5 % sucrose solution for 30 min. Right before transformation 100 µl of 0.05 % SilvetL77 were added and shooting Arabidopsis were dipped into the transformation solution for 5 s. The dipped plants were incubated in the dark overnight and kept humid for 24 h.

4.11.13 Selection of transformed Arabidopsis

Transformed Arabidopsis individuals were selected by using glufosinat solution directly (10 mg/l stock solution) on plants seeded on soil or by adding glufosinat (Thermo scientific, Schwerte, Germany) in 1/2 MS media (final concentration 10 µg/ml) and by checking the genotype using PCR techniques (see 4.11.1.3) with appropriate primers (see 6.3.3).

4.12 Cloning strategies

4.12.1 Constructs for the expression of recombinant proteins

For recombinant protein expression with 5' prime *MBP* fusions in *E. coli* Rosetta2 cells the respective cDNAs of PIP5K1, PIP5K2 and PID were amplified using PCR. Primers were designed to introduce restriction sites 5'- and 3' prime of the cDNA for ligation into *pMAL-c5G* (4.11.5) and in reading frame with the *MBP* tag (see table below for restriction sites and appendix 6.3.1 for primers).

In contrast to the use Rosetta2 cells for *MBP*-fusions, N-terminal *GST* fusions or poly histidine tags were expressed in *E. coli* BL21 using *pGEX-4T-1* and *pET28b* respectively (see 4.7.1) following similar cloning strategies (see table below for restriction sites and appendix 6.3.1 for specific primers).

Table 12 Plasmids for protein expression

Vector	Insert	Restriction Sites	Created by
<i>pMAL-c5G</i> (<i>MBP</i> fusion)	<i>PIP5K1</i>	NdeI-Sall	Dr. Mareike Heilmann
	<i>PIP5K2</i>	NotI-EcoRI	Dr. Jenny Lerche
	<i>PID</i>	NcoI-EcoRV	Dr. Jenny Lerche
<i>pGEX-4T-1</i> (<i>GST</i> -Fusion)	<i>PID</i>	Sall-NotI	Dr. Jenny Lerche
<i>pET28b</i> (His ₆ -Fusion N- and C-terminal)	<i>CKA1</i>	NdeI-Sall	This study
	<i>CKA2</i>	NdeI-Sall	This study
	<i>CKA3</i>	NdeI-Sall	This study
	<i>CKB1</i>	NdeI-Sall	This study
	<i>CKB2</i>	NdeI-Sall	This study
	<i>CKB3</i>	NdeI-Sall	This study

4.12.2 Constructs for split-ubiquitin based yeast-two-hybrid assays

For Y2H protein-protein interaction studies the *PBT3-C-OST4* vector (see 4.7.2) was used as bait while *pPR3-N/C* was used as prey. cDNA of interest was amplified using PCR introducing SfiIA and SfiIB restriction sites (see table below and appendix 6.3.1 for primers). In *pBT3-C-OST4*, cDNAs were introduced in reading frame with 5' *OST4* and 3' *Cub*, *LexA* and *VP16*. In *pPR3-N*, cDNAs were introduced in reading frame with 5' *NubG* (see table below and appendix 6.3.1 primers). Cloning methods were performed according to section 4.11.2 to 4.11.9.

Table 13 Plasmids for yeast-two-hybrid assays

Vector	Insert	Restriction Sites	Created by
<i>pBT3-C-OST4</i> (bait)	PIP5K1, PIP5K2	SfiIA-SfiIB	Dr. Mareike Heilmann
	PsPIP5K1		This study
<i>pPR3-N</i> (prey)	WAG1, WAG2	SfiIA-SfiIB	Dr. Jenny Lerche
	PID		Dr. Jenny Lerche
	IMPA3, IMPA6, IMPA9		Dr. Katharina Gerth
	CKA3		This study
<i>pPR3-C</i> (prey)	CKB1, CKB2		This study
	CKA1, CKA2	SfiIA-SfiIB	This study
	CKB3		This study

4.12.3 Constructs for bimolecular fluorescence complementation

For Bimolecular fluorescence complementation (BiFC) assays the *pBiFC2in1* vector was used (see 4.7.2). The first cDNA of interest was amplified using PCR introducing 5'prime attR3 and 3'prime attR2 sites for Gateway cloning to *pBiFC2in1* and 5'prime fusion to the N-terminal half of EYFP. Putative Interaction partner was amplified with PCR introducing 5'prime attR1 and 3'prime attR4 sites for fusion to C-terminal EYFP in the same *pBiFC2in1* vector. All specific oligos are listed in appendix 6.3.1 and constructs are listed below.

Cloning methods were used according to section 4.11.2 to 4.11.9

Table 14 Plasmids for BiFC assay

Vector	Insert	Created by
<i>pBiFC2in1</i>	PID	This Study
n-EYFP-PID	PDK1	
c-EYFP PDK1		
<i>pBiFC2in1</i>	PIP5K2	This study
n-EYFP-PDK1	PDK1	
c-EYFP PIP5K2		
<i>pBiFC2in1</i>	PIP5K2	This study
n-EYFP-PID	PID	
c-EYFP PIP5K2		

4.12.4 Constructs for transient expression in plant cells and stable transformation of Arabidopsis

For transient expression in protoplasts the *pEntryA* or *pEntryD* vector was used (see 4.7.3). In brief, desired promoters were amplified using PCR (see 4.11.1.1) introducing 5'prime SfilA and 3'prime SfilB restriction sites. Promoters were then ligated into *pEntryA* or *pEntryD*. When expressed in protoplasts, the *pCaMV35S* promoter was used. For pollen tube studies, the *pLAT52* promoter was used. For stable transformation in Arabidopsis, the intrinsic promoters of *PIP5K1* and *PIP5K2* were used.

AtPIP5K1, AtPIP5K2, AtPIP5K2 S274A S275A, AtPIP5K2 S274D S275D, PsPIP5K1, PsPIP5K1_LinAt, AtPIP5K2_LinPs cDNA and PID were amplified using PCR (see 4.11.1.1). Primers were designed to introduce 5'prime Ascl and 3'prime XhoI restriction sites for ligation into *pEntryA-EYFP* or *pEntryD-mCherry* (see table below and appendix 6.3.1 for primers). CKA3 was amplified and introduced into *pEntryD-mCherry* using 3'prime Ascl and 5'prime NheI restriction sites (see table below and appendix 6.3.1 for primers).

Nuclear markers *NLS-DsRed* and *NLS-CFP* were produced by PCR fusion of the NLS_{SV40} sequence (NLSSV40, strong NLS PKKKRKV of the large T-antigen of simian virus 40, (Kalderon et al., 1984)) 5'-prime to the *DsRed/CFP* sequence and introduced into *pEntryA* by 3'prime Ascl and 5'XhoI or 3'prime Ascl and 5'prime BamHI restriction sites respectively (see table below and appendix 6.3.1 for primers).

Whole constructs from *pEntryA* containing promoter, coding sequence of interest and *EYFP* fluorescence tag were cloned into the *pCAMBIA3300.0GS* vector (see 4.7.3) using Gateway® cloning (see 4.11.6).

Cloning methods were used according to section 4.11.2 to 4.11.9

Table 15 Plasmids used for expression in plants

Abbreviations: AT, Alicia Toto; BH, Barbora Hans; IS, Dr. Irene Stenzel; JL, Dr. Jenny Lerche; JZ, Juliane Zwoch; MH, Dr. Mareike Heilmann; PHD, This study.

Vector	Insert	Restriction Sites (Insert)	Restriction Sites (Tag)	Created by
<i>pEntryA-pCaMV35S::</i>	<i>PIP5K1-EYFP</i>	Ascl-XhoI	XhoI-NotI	MH
	<i>PIP5K2-EYFP</i>	Ascl-XhoI	XhoI-NotI	JL
	<i>PIP5K2 S274A S275A-EYFP</i>	Ascl-XhoI	XhoI-NotI	JL
	<i>PIP5K2 S274 DS275D-EYFP</i>	Ascl-XhoI	XhoI-NotI	JL
	<i>PsPIP5K1-EYFP</i>	Ascl-XhoI	XhoI-NotI	BH

<i>pEntryD- pCaMV35S::</i>	<i>PIP5K2_LinPs-EYFP</i>	Ascl-Xhol	Xhol-NotI	PHD
	<i>PsPIP5K1_LinAt-EYFP</i>	Ascl-Xhol	Xhol-NotI	PHD
	<i>NLS-DsRed</i>	Ascl-Xhol	-	MH
	<i>NLS-CFP</i>	Ascl-BamHI	-	AT
	<i>PID-mCherry</i>	Ascl-Xhol	NheI-BamHI	JL
	<i>CKA3-mCherry</i>	Ascl-NheI	NheI-BamHI	JZ
<i>pEntryA- pLAT52::</i>	<i>PIP5K2-EYFP</i>	Ascl-Xhol	Sall-Ascl	IS
	<i>PsPIP5K1-EYFP</i>	Ascl-Xhol	Sall-Ascl	PHD
	<i>PIP5K2_LinPs-EYFP</i>	Ascl-Xhol	Sall-Ascl	PHD
	<i>PsPIP5K1_LinAt-EYFP</i>	Ascl-Xhol	Sall-Ascl	PHD
<i>pCAM- BIA3300.0GS</i>	<i>pPIP5K1::PsPIP5K1-EYFP</i>	att- sites	-	PHD
	<i>pPIP5K1::PsPIP5K1_LinAt-EYFP</i>			PHD
	<i>pPIP5K2::PsPIP5K1_LinAt-EYFP</i>			PHD

4.13 Recombinant protein expression and enrichment

4.13.1 Expression of MBP- and GST-fusion proteins

A 50 ml preculture of 2YT media was inoculated with transformed Rosetta2 cells and incubated over night at 30 °C containing carbenicillin. The preculture was used to inoculate the 300 ml main culture to an optical density of approx. OD₆₀₀ 0.03 to 0.05. For MBP tagged proteins additional 0.2 % glucose was added to the media. The main culture was incubated in baffled flasks at 37 °C and 95 rpm until an OD₆₀₀ = 0.7 was reached. The cultures were cooled down on ice for 30 min and protein expression was induced by 1 mM IPTG. PI4P 5-kinase expressing cultures were then transferred to 28 °C for four hours and 95 rpm. The cultures were harvested to 250 ml falcons, centrifuged at 3220 g and 4 °C, freezed in liquid nitrogen and stored at -80 °C until they were further processed.

The expression of MBP and GST tagged PID was performed with slight changes: The expression time was increased to 18 h while the expression temperature was reduced to 20 °C.

As controls GST and MBP were expressed. Cells were grown at 37°C and expression was induced with 0.1 mM IPTG for 2 h. After expression, cells were harvested in aliquots of 50 ml at 3,220 x g and 4°C for 15 min, frozen in liquid nitrogen and stored at -80°C.

4.13.2 Expression of His-CK2 subunits

For recombinant expression a 30 ml LB media preculture with carbenicillin was started by adding one colony of freshly transformed BL21 (DE3) cells. Preculture was incubated over night at 30 °C and 180 rpm. Preculture was used to set $OD_{600} = 0.05-0.1$ of the 100 ml LB media main culture with carbenicillin. Main culture was grown at 37°C and 180 rpm until $OD_{600} = 0.6-0.8$. Main culture was cooled down on ice and expression induced by 0.6 M IPTG. Main culture was incubated 22 h at 18 °C and 180 rpm. Cells were harvested by centrifugation at 3220 g at 4°C, the supernatant discarded and the pellets freezed in liquid nitrogen and kept at -80 °C until further use.

4.13.3 Cell disruption with a high-pressure-homogeniser

MBP-PIP5K1, MBP-PIP5K2 and MBP-PID Protein pellets of 300 ml expression culture (see 4.13.1) were dissolved in 35 ml of the corresponding protein buffer (see 4.8) supplemented with 1 mM DTT, 1 mg/ml Lysozyme and Protein Inhibitor (cOmplete™, Mini, EDTA-free Protease Inhibitor Cocktail, Roche, Merck). The mixture was incubated on ice for about 30 min and inverted several times. For further disruption, a FRENCH™-PRESS (Gaulin, APV Homogeniser GmbH, Gatwick, UK) at 1200 bar was used for three times. The cell debris was removed by centrifuging at 20 000 g for 20 min at 4°C. The supernatant was stored on ice for further enrichment applications.

4.13.4 Cell disruption with ultrasonic

His-CK2 subunit pellets of 50 ml expression (see 4.13.2) culture were dissolved in 3 ml of CK2 protein buffer (see 4.8) with 1 mM DTT, 2 mg/ml lysozyme and 1x protease-Inhibitor Inhibitor (cOmplete™, Mini, EDTA-free Protease Inhibitor Cocktail, Roche, Merck). Samples were kept on ice for 30 min while inverted every ten min. Samples were sonicated with 6000 J using the Branson B12 Ultrasonics Sonifier (Branson, Emerson Electric, Dietzenbach-Steinberg, Germany). CKA3 was used as crude extract while CKB subunits were further purified (see below).

4.13.5 Enrichment of proteins by affinity chromatography

MBP-tagged proteins were enriched with an ÄKTA combined with a 5 ml MBP-Trap (GE Healthcare, Munich, Germany). For equilibration of the column, 100 ml of corresponding protein buffer (see 4.8) was used. Next, the supernatant was given completely onto the column under a constant flow of 0.5 ml/min. After washing with 100 ml of protein buffer the MBP tagged proteins were eluted using the same

protein buffer complemented with 10 mM maltose in two ml fractions. Each fraction was analysed by SDS-PAGE and coomassie staining. The elution fractions were aliquoted and frozen in liquid nitrogen and stored at -80 °C.

His-tagged CKB subunits were centrifuged after sonification at 12 000 g and 4°C for 15 min. The supernatant fraction was enriched by a two ml column with Ni-NTA (Nitrilotriacetic acid) (Qiagen, Hilden, Germany). Ni-NTA beads were washed three times using CK2 equilibration buffer without imidazole (see 4.8). Next, 1.5 ml supernatant protein fraction were loaded onto the column and incubated at room temperature for one h in an orbital shaker. Columns were washed four times using CK2 equilibration buffer with 20 mM imidazole (see 4.8). For elution 300 µl fractions using the same buffer with 200 mM imidazole was used. Imidazole was removed by size exclusion chromatography using PD-10 Desalting Columns (Avantor VWR, Darmstadt, Germany).

4.13.6 Determination of protein concentrations

Protein concentrations were analysed using a Bradford Assay (Bradford, 1976). 10 µl of protein sample were incubated with 1x 990 µl of Bradford reagent (5x Bradford reagent, SERVA Electrophoresis GmbH, Heidelberg, Germany) and incubated for 10 min at RT. The absorption at 600 nm was measured using an Ultrospec 3000 UV/Vis spectrometer (Pharmacia Biotech AG, Dübendorf, Germany). Relative protein concentrations were calculated using a standard curve from bovine serum albumin.

4.13.7 Separation of proteins with sodium dodecyl sulfate polyacrylamid gel electrophoresis (SDS-PAGE)

Protein samples were separated in an SDS-PAGE due to their molecular weight according to Laemmli (LAEMMLI, 1970). Samples were mixed with 5x Loading Dye (see 4.8) and loaded onto a self-made SDS Gel (5 % stacking and 10 % separation gel (w/v polyacrylamide) or onto a pre-casted 4–20 % SDS gradient gel (SERVAGel™ TG PRIMETM, SERVA Electrophoresis GmbH, Heidelberg, Germany). Gels were run at 25 mA (self-made) or 50 mA (precast) per gel in SDS running buffer (see 4.8) until the dye bromophenol blue of the Laemmli loading dye ran out of the gel. Prestained PageRuler™ was used as a protein size indicator. The gels were either used for immunodetection and Western Blot (see 4.14) or stained using Quick Coomassie® Stain (SERVA Electrophoresis GmbH, Heidelberg, Germany).

4.14 Immunodetection on nitrocellulose membranes (Westernblot)

After proteins were separated in an SDS-PAGE (see 4.13.7) proteins were transferred to a nitrocellulose membrane (Amersham Protran 0.45 NC, GE Healthcare GmbH, Solingen, Germany). This method follows the principle of Towbin et al. (Towbin et al., 1979). Proteins were transferred in transfer buffer (see 4.8) using a wet blotting system (Mini-PROTEAN® Tetra System Blotting Chamber (BioRad Laboratories GmbH, Munich, Germany)). The blotting procedure was stopped after 75 min at 60 V and max mA settings. The obtained membrane was incubated with a primary antibody diluted as suggested by the manufacturer in 5 % milk in TBS buffer (see 4.8, total: 10 ml, for antibodies see below) for one hour. The membrane was washed three times with 10 ml TBS buffer. Then the second antibody fused to horse radish peroxidase (HRP) diluted as suggested by the manufacturer in 3 % milk in TBS buffer (see 4.8, total: 10 ml, for antibodies see below) was incubated for one hour. The membrane was washed again three times with TBS. HRP detection was performed with SuperSignal™ West Femto Maximum Sensitivity Substrate (Thermo Fisher Scientific, Schwerte, Germany) in a Fusion Solo S (Vilber Lourmat GmbH, Eberhardzell, Germany) using the FusionCapt Advance Solo 7 (version 17.01) software.

4.14.1 Antibodies

Table 16 Primary- and secondary antibodies used in this study

Name	Dilution	Organism	Offering Company
α -Thiophosphate ester	1: 5 000 in 5 % milk in TBS buffer	rabbit	#SD2020, Thermo-Fisher Scientific Invitrogen, Schwerte, Germany
α -Penta-His	1: 3 000 in 5 % milk in PBS buffer	mouse	# 34660, Qiagen, Hilden, Germany
α -MBP	1: 10 000 in 5 % milk in TBS buffer	mouse	#E8032S, New England Biolabs Inc., Frankfurt, Germany
α -GST	1: 2 000 in 5 % milk in TBS buffer	goat	#27-4577-01, Merck, Darmstadt, Germany,
α -GFP	1: 7 500 in 5 % milk in TBS buffer	rabbit	#A-11122, Invitrogen, now Thermo Fisher Scientific, Schwerte, Germany
α -mouse HRP fusion	1: 7500 in 3 % milk in PBS buffer	goat	#AP130P, Merck, Darmstadt, Germany
α -goat HRP fusion	1: 7 500 in 3 % milk in PBS buffer	rabbit	#A5420, Merck, Darmstadt, Germany
α -rabbit HRP fusion	1:7000 in 3 % milk in PBS buffer	goat	#A6154, Merck, Darmstadt, Germany

4.15 *In vitro* protein phosphorylation assay

The reaction buffer depended on the use of the protein kinases. For PID phosphorylation assays phosphorylation buffer (see 4.8) was used while CK2 phosphorylation tests were conducted in NEB protein kinase buffer (New England Biolabs Inc., Frankfurt, Germany). Crude (His-CKA3) or purified (MBP-PID, MBP-PIP5K1, MBP-PIP5K2) protein extracts were added dependent to the experimental setup (If possible, target to kinase ratio was set 10:1). Non-radioactive phosphorylation tests were performed with 1 mM γ -S-ATP (Sigma Aldrich, Munich, Germany). Radioactive assays were conducted with 10 μ Ci γ -[³²P]-ATP per reaction. The reaction was incubated for one hour at room temperature. Non-radioactive phosphorylation tests were stopped by adding 1 μ l 0.5 M EDTA and alkylated using 2.5 mM p-nitrobenzyl mesylate (Abcam, Cambridge, United Kingdom). Radioactive assay was stopped by SDS-loading buffer (see 4.8). Samples were loaded on an SDS-PAGE and separated (see 4.13.7). Non-radioactive phosphorylation assays were transferred onto nitrocellulose membranes using Westernblot and immunodetected (see 4.14). For radioactive assays the gel was stained using Coomassie Quick Coomassie® Stain (SERVA Electrophoresis GmbH, Heidelberg, Germany). overnight. The gel was dried using a vacuum. The dried gel was analysed using radioactive sensitive imager plates (BAS-MP 2040s, Fujifilm, Düsseldorf, Germany) The image was developed and the radioactive signal visualised in the phosphorimager BAS-1500 (FUJIFILM Europe GmbH, Düsseldorf, Germany). Radioactive signal was analysed using TINA 2.0 software (Raytest, Straubenhardt, Germany).

4.16 Mass spectrometry and phosphopeptide analysis

The preparation and mass spec. experiments were performed in cooperation with the ZMG Core Facility Proteomic Mass Spectrometry from the Martin-Luther-University Halle-Wittenberg. To determine phosphorylation sites in target proteins a phosphorylation assay was performed using unlabelled ATP (see 4.15) in 100 μ l reaction volume. The samples were processed and digested with trypsin by Viktoria Burgdorf (ZMG, MLU). Either total peptides were purified with C-18 beads or phosphopeptides were concentrated using ProteoExtract® Phosphopeptide Enrichment TiO₂ Kit (Merck, Darmstadt, Germany) before measurements were taken at a LC-MS-MS setup with the Orbitrap Fusion Lumos Tribrid Mass Spectrometer (Fisher Scientific, Schwerte, Germany). The Proteome Discoverer software version 2.4 (PID) or the software PEAKS version X pro (CKA3) was used to analyse the data (both software from: Fisher Scientific, Schwerte, Germany).

4.17 Determination of PI4P 5-Kinase activity *in vitro*

To test the catalytical activity 6.2 μl of a 1 mg/ml stock solution PtdIns4P isolated from brain (Avanti Polar Lipids Inc., Merck, Darmstadt, Germany) was evaporated and resolved in 5 μl of a 2 % Triton X100 solution. The mixture was sonicated in an ice bath for 10 min and 10 μl of 75 mM MgCl_2 , 1 μl of 50 mM Na-molybdate, 2.5 μl of 30 mM Tris (pH 7.2), 1 μl of 50 mM ATP and 0.5 μl of 10 μCi γ - ^{32}P -ATP. 30 mM Tris pH 7.2 was added filled up to 20 μl of reaction volume. These 20 μl were mixed with 30 μl of protein mixture (If possible one μg , diluted with 30 mM Tris pH 7.2) and incubated for 15 min. The reaction was stopped by adding chloroform: methanol (v/v 1:2) to the reaction.

4.17.1.1 Lipid extraction and thin layer chromatography

1.5 ml of chloroform: methanol (v/v 1:2), 500 μl of 2.4 M hydrochloride acid solution and 250 μl of 0.5 M EDTA with pH: 8.0 were added to the reaction solution and mixed. After adding 500 μl of chloroform to the test tube, it was mixed again and left stationary until two separate phases were visible. The lower phase was transferred to a new test tube and the procedure was repeated by adding, mixing, and transferring 500 μl of chloroform from the reaction mixture to the new test tube. The newly obtained one ml chloroform phase was washed by adding 750 μl of 0,5 M hydrochloride acid solution in methanol: water (v/v 1:1). After mixing the lower phase was reextracted to a new test tube and the chloroform was evaporated using an airstream. The extracted lipids were resuspended in 20 μl chloroform and loaded one cm above the bottom end of a thin layer chromatography (TLC) plate (Si-60 Merck, Darmstadt, Germany). The mobile phase consisted of chloroform: methanol: water: ammoniumhydroxide (v/v/v/v 45: 45: 11: 4) and was preincubated with a Whatman® paper in the incubation chamber. The TLC plate was added to the chamber and developed for 40 to 45 min. The plate was dried and further analysed using a phosphorimager like described in 4.15.

4.18 Determination of PtdIns(4,5)P₂ content in Arabidopsis

The procedure is based on a protocol developed in our lab (Launhardt et al., 2021). PtdIns(4,5)P₂ levels were measured from twelve-day old seedlings grown on 1/2 MS media in long day conditions. Phosphoinositides were isolated from fresh plant tissue by precooling a mortar and pestle in liquid nitrogen and powdering the plant material. The powder was centred in the middle of the mortar using a nitrogen cooled spatula and thawed with one ml chloroform: methanol (v/v 1:2). The mixture was transferred into a glass reaction tube and the remaining plant tissue was

reextracted from the mortar by another 1 ml chloroform: methanol (v/v 1:2). The lipid extraction upon this point followed the same way as described in 4.17.1.1. To the thin layer chromatography (TLC) plate 5 µg of PtdIns4P, PtdIns(4,5)P₂ and Lyso-PC were added as references. The TLC with the standards was cut and dipped into a 10 % (w/w) CuSO₄, 8 % (w/w) H₃PO₄ solution. Heating up the TLC visualises the standards. The corresponding PtdIns(4,5)P₂ from the samples from the TLC were scratched out and transferred into a new glass tube.

4.18.1.1 Transmethylating fatty acids and gas chromatography analysis

The analysis of fatty acid methyl esters (FAMES) was performed as described (Launhardt et al., 2021). To each sample 5 µl (1 mg/ml) of tripentadecanoin were added as internal standard. Further 333 µl of toluene:methanol (1:2 v/v) and 167 µl of 0.5 M NaOCH₃ in methanol were added and the reaction was incubated at room temperature for 20 min while shaking. FAMES were extracted by adding 100 µl of 5 M NaCl and 2 ml of n-hexane and mixing. The samples were centrifuged at 600 g for 2 min at 4° and the upper phase was extracted into a new glass tube. The hexane was evaporated using an air stream and the FAMES were resuspended in 100 µl of acetonitrile and transferred into an inlay of a GC-vial. The solvent was evaporated and the FAMES resuspended in 10 µl of acetonitrile.

To analyse the FAME profile the GC-2010Plus (Shimadzu Deutschland GmbH, Duisburg, Germany) coupled to a flame ionisation detector and a DB-23 column (30 m x 0.25 mm; 0.25 µm coating thickness, Agilent Technologies, VWR International GmbH, Darmstadt, Germany) with helium as carrier gas was used. The samples were injected at 220 °C (AOC-20i Auto Injector, Shimadzu Deutschland GmbH, Duisburg, Germany) and the chromatography was performed with a temperature gradient. After one minute at 150 °C the temperature was increased to 200 °C at a 25 °C/ min rate followed by an increase to 250 °C at a rate of 4 °C/min and kept at 250 °C for 6 min. To identify the FAMES menhaden fish oil was always carried along as reference. For analysis and data extraction the GC Solution software was used (version 2.31.00, Shimadzu Deutschland GmbH, Duisburg, Germany)

4.19 Testing protein-protein interactions using the split-ubiquitin-yeast-two-hybrid-assay (Y2H)

To test potential protein-protein interactions the DUAL membrane Kit 3 (Dualsystems Biotech AG, Zurich, Switzerland) was used. The principle is based on a study by Johnsson and Varshavsky (Johnsson and Varshavsky, 1994). Highlighted in the study

of Möckli et al. (Möckli et al., 2007) a split-ubiquitin based Y2H localised to the cytosol was fused to the ER membrane by adding the bait proteins to the yeast protein oligosaccharyltransferase 4 (OST4). This advanced Y2H assay uses the general conserved eukaryotic mechanism that reconstituted ubiquitin fusion proteins are cleaved by ubiquitin-specific proteases at the last amino acid of ubiquitin. By using the N-terminal half of ubiquitin as prey (Nub, aa 1-38) and the C-terminal as bait (Cub, aa 37-76) that is fused to the transcription factor LexA-VP16, you get a reconstitution once bait and prey interact and only then the ubiquitin specific protease can cleave the transcription factor off which activates reporter genes in the nucleus. Genes activated are *HIS3* (histidine biosynthesis), *ADE2* (purine base biosynthesis) and *lacZ* (β -glucuronidase) allowing yeasts to survive on selective media (see 4.5.1). Each Y2H assay used *pAI-Alg5* as a positive control where spontaneous non-protein-protein interaction after reconstitution of the ubiquitin halves is displayed while a negative control using *pDL2-Alg5* uses a ubiquitin half not capable of reconstitution as negative control.

4.19.1 Preparing chemically competent *S. cerevisiae*

A fresh YPAD plate (see 4.5.1) of *NMY51* cells was reproduced every two weeks. 20 ml of YPAD media was inoculated with several *NMY51* colonies and grown overnight at 30 °C while shaking. YPAD main culture (50 ml/ seven transformations) was prepared, and the optical density set to $OD_{600} = 0.15$. Once an optical density of $OD_{600} = 0.6$ was reached the yeast cells were centrifuged at 2500 g for 5 min in 50 ml tubes. The pellet was resuspended in 10 ml TE buffer (see 4.8) and centrifuged again at 2500 g for 5 min. The pellet was resuspended in 1 ml lithium acetate/ TE master mix (see 4.8) and transferred into a 1.5 ml reaction tube. After centrifugation at 2500 g at 30 s the pellet was again resuspended in 700 μ l lithium acetate/ TE master mix. Cells were competent at this point and were stored for maximal two h at RT until used for transformation.

4.19.2 Transforming *S. cerevisiae*

For the transformation 1.5 ml reaction tubes with three μ l of bait and three μ l of prey Miniprep[®] construct plasmids were prepared. To transform chemically competent *NMY51* yeast cells 100 μ l cells were given to the prepared plasmids and 700 μ l of lithium acetate/ PEG master mix (see 4.8). The reaction tube was mixed and incubated at 30 °C for 30 min while shaking at 200 rpm. 80 μ l of DMSO were added and mixed. A heat shock at 42 °C followed for 18 min. The transformed cells were centrifugated at 700 g for 5 min and the pellet washed in 300 μ l 0.9 %

NaCl. The pellet was washed, resuspended in 100 μ l of 0.9 % NaCl and plated on SD-LW media (see 4.5.1.).

4.19.3 Analysing protein-protein interactions by Y2H

Five transformed yeast cell colonies of each construct pair were selected and re-plated onto SD-LW media and grown at 30°C for three days. Of these master plates yeast cells were extracted and put into 500 μ l TE-buffer (see 4.8). The optical density OD₆₀₀ was measured (Ultrospec 2100, Pro Pharmacia Biotech AG Düsseldorf, Germany) and for all samples an OD₆₀₀= 0.5 was set. Using these set dilutions three μ l of yeast cell suspension were dropped onto selective SD-LW- and SD-LWH media test. Yeast growth was documented using a scanner.

4.20 Testing protein-protein interactions with *in vitro* pull-down

To test *in vitro* interaction GST-PID had to be immobilised onto 100 μ l of Pierce™ glutathione agarose beads (Thermo Fisher Scientific, Schwerte, Germany). Glutathione agarose was washed three times in 600 μ l GST equilibration buffer (see 4.8) and centrifuged after each step for two minutes at 200 g. 300 μ l GST-PID crude extract (see 4.13) diluted in 300 μ l GST equilibration buffer or 50 μ l GST and 550 μ l GST-equilibration buffer were immobilised on the glutathione agarose beads in an incubation step at 4 °C for one hour in an orbital shaker. Beads were washed three times with GST equilibration buffer like described above. 100 μ l expressed and purified MBP-PIP5K1 or MBP-PIP5K2 (see 4.13.1) diluted in 500 μ l GST equilibration buffer was incubated with the GST-PID glutathione agarose beads over night at 4 °C in an orbital shaker. Samples were washed again three times and eluted using 50 μ l GST elution buffer (4.8) three times. Elution fraction proteins were detected using SDS-PAGE (see 4.13.7) and western blot (see 4.14) using anti-GST and anti-MBP antibodies (see 4.14.1).

4.21 Testing protein-protein interactions using bimolecular fluorescence complementation assay

Bimolecular fluorescence Complementation (BiFC) tests were used to validate Y2H and *in vitro* pull-down protein-protein interaction studies and to get insight into the subcellular location where interaction takes place. The proteins of interest to be tested for interaction were fused either to the N- or C-terminal half of EYFP. Only at close proximity e.g., interaction the EYFP reassembles and EYFP fluorescence can be detected. Constructs were transiently transformed into Arabidopsis leaf

mesophyll protoplasts and fluorescence detected with the LSM880 (see 4.22 and 4.24). BiFC vector also contains a pCaMV35S driven RFP as transformation control. Reconstitution of EYFP fluorescence indicated protein-protein interaction and provided information about the subcellular localisation of the interaction. For used constructs see 4.7.2 and 4.12.3.

4.22 Preparing and transforming Protoplasts

All protoplast isolation and protoplast transformation procedures are based on the method published by Yoo and co-workers from 2007 (Yoo et al., 2007).

Arabidopsis wildtype Col-0 plants were grown on soil for six to eight weeks in short day conditions. The leaves were either cut into 1 mm wide strips with a razor blade or taped on lab tape and the whole lower epidermis was ripped off with clear “Scotch” tape (3M, Saint Paul, United States). The leaf strips or epidermis free leaves were dipped into ten ml of enzyme solution (see 4.8) and vacuum infiltrated for 30 min. The samples were incubated in the dark for two hours to completely digest cell wall material. The epidermis free leaves were shaken gently to release the protoplasts into solution while leaves strips were stirred very gently. The protoplast containing solution was filtered through a 100 μm nylon mesh (Greiner Bio-One GmbH, Frickenhausen, Germany) and spun down at 200 g for two min at eleven $^{\circ}\text{C}$. The enzyme solution was removed, and the protoplast pellet resuspended in five ml of W5 washing buffer (see 4.8). From here the protoplasts were kept on ice until the transformation. The protoplasts were settled down by gravity by 40 min and washed with two ml of W5 buffer. The protoplasts were resuspended in two ml of MMG buffer (see 4.8) and the protoplast concentration was adjusted to get a light green solution. The quality of the protoplasts was validated at the microscope. At this point protoplasts ready for transformation.

For protoplast transformation one μg plasmid DNA was used per ten μl of protoplast solution. The plasmids were put into cell culture tubes in advance and protoplasts were added using cut pipette tips. The protoplasts were shaken gently and to each volume of protoplasts 1.1 volumes of PEG transformation buffer (see 4.8) were added. The transformation mixture was inverted several times. The transformation was incubated on the lab bench for ten min and stopped by adding 4.4 volumes of W5 buffer. The protoplasts were centrifuged at 200 g for two min at eleven $^{\circ}\text{C}$ and the supernatant was removed. The protoplast pellet was resuspended in one volume of W1 buffer (see 4.8) and incubated in the dark over night until used further at the microscope (see 4.24).

With slight changes protoplasts were isolated from opium poppy, *Arabidopsis* roots, Col-0 and BY-2 cell culture:

Poppy-, Col-0- and BY-2 protoplasts were digested overnight.

Col-0 cell culture-, root- and BY-2 cells were initially centrifuged at 400 g for 5 min and washed with 5 ml enzyme solution without enzymes.

Col-0 cell culture- and root protoplasts were always sedimented at 100 g for 5 min.

Col-0 cell culture- and root protoplasts were additionally filtered using a 20 μm mesh size nylon filter.

BY2- protoplasts were digested in a different enzyme solution (see 4.8).

4.22.1 NAA treatment of *Arabidopsis* leaf mesophyll protoplasts

Arabidopsis protoplasts were treated with auxin analogia NAA after a protocol published by Weiste and Dröge-Laser (Weiste and Dröge-Laser, 2014). 200 μl of protoplasts were treated with 0.25 μM NAA (Sigma-Aldrich, Munich, Germany) prior imaging or overnight. NAA was initially dissolved in one M NaOH and diluted with WI buffer.

4.23 Transforming tobacco pollen tubes

For transiently transforming pollen tubes and onion epidermis cells the PDS1000/He biolistic particle delivery system (Gene gun; Bio-Rad, Munich, Germany) was used. All chemicals and consumables were ordered at Bio-Rad. To prepare gold beads 50 μg of micro gold beads (diameter= 1 μm) were resuspended in one ml of ethanol and mixed well for two min. The gold beads were sedimented at 10 000 g for ten s and washed twice with one ml of ethanol and washed again twice with one ml of water. Finally, the gold beads were resuspended in one ml of water and aliquoted in 50 μl each and freezed in -20 $^{\circ}\text{C}$ until further use.

All steps were performed on ice. For each transformation 25 μg of gold beads were used. Six μg Midiprep[®] plasmid were added to the gold beads. The gold beads were mixed for 60 s. Following the same principle 50 μl of ice cold 2.5 M CaCl_2 and 20 μl of 0.1 M spermidine were added. The mixture was centrifuged at 10 000 g for ten s and the supernatant was removed completely. The gold pellet was washed two times in one ml of ice-cold ethanol and resuspended in 30 μl of ethanol. For each shot at the gene gun 15 μl of DNA coated gold beads were used.

To bombard pollen tubes, eight fully developed but young tobacco flowers were cut fresh from the plants and the anthers were harvested into a 50 ml reaction tube.

To release the pollen eight ml of tobacco pollen media (see 4.5.2) were added and the mixture was shaken. The pollen was centred onto a cellulose-acetate filter of two μm mesh size by a vacuum flow and kept humid by placing the filter onto a wet Whatman paper (Whatman, Maidstone, United Kingdom) in a petri dish.

The prepared DNA coated gold beads were loaded onto a washed macrocarrier and placed into the gene gun. A vacuum was grown in the chamber while helium was used to generate pressure in the helium afflux. At 1350 psi the fracture disc broke, and the DNA coated gold vesicles were fired onto the biological sample while a small steel mesh held back the macrocarrier.

Pollen was scratched from the cellulose-acetate filter and were resuspended in 250 μl of pollen media divided by 60 μl on three glass slides. These glass slides were incubated at room temperature in the dark and kept humid in a square petri dish for five h minimum to over night before used for analysis at the microscope (see 4.24.1).

4.24 Microscopy and Image Analysis

4.24.1 Lasers scanning microscope 880 (LSM880)

For localisation studies the inverted laser scanning microscope 880 was used (Carl Zeiss, Jena, Germany). Depending on the experimental setup 10x, 20x, 40x and/ or 63x objectives were used. CFP was excited at 458 and detected between 470–430 nm. EYFP was excited at 514 nm and detected between 520–555 nm, mCherry, RFP and DsRed at 561 nm and between 565–620 nm and chlorophyll A at 633 nm and between 680–720 nm. Different fluorophores were always detected in separate tracks for optimal filter settings and optimal signal intensity. Z-stacks were always prepared with 1 μm slices. Images were acquired with an 8-bit depth using ZEN Black image analysis software (version 14.0.18.201, Carl Zeiss, Jena, Germany). Image processing was performed using ImgJ (Version 1.53k, (Schindelin et al., 2012)).

4.24.2 Spinning disc microscope

Spinning disc microscopy was performed using Zeiss Cell observer SD with a Yokogawa CSU-X1 spinning disc unit and a 63x oil immersion objective (Carl Zeiss, Jena, Germany). EYFP was excited at 488 nm. A DAPI/FITC/TRITC ET Triple band emitter (AHF Analysetechnik, Tübingen, Germany, F67-000) was used. Images were acquired using ZEN Blue image analysis software (Carl Zeiss, Jena, Germany) and

Photometrics Evolve 512 Delta EM-CCD camera. Image processing was performed using ImageJ (Version 1.53k, (Schindelin et al., 2012)).

4.24.3 Elyra 7 with total internal reflection fluorescence (TIRF) module

For TIRF analysis of protoplasts the Elyra 7 (Carl Zeiss, Jena, Germany) was used. A 100x oil immersion objective with a numerical aperture of 1.46 was used. The TIRF angle was 66.92° while the collimator camera had to be adjusted for each protoplast. The laser power was set to maximum 10%. TIRF movies were recorded to a maximum of 2500 repeats of 300 ms each. ImageJ was utilised to analyse the foci pattern using the internal TrackMate plugin. The estimated blob diameter was set to 0.5 μm . Thresholds were set manually (mean intensity) and if needed fluorescence aggregates and/ or autofluorescence of chloroplasts was kept out by lowering the maximal intensity while very low intensity foci/ noise were removed by increasing minimal intensity thresholds. The maximum allowed linking distance and the gap-closing distance were set to 0.5 μm while the gap-closing max frame gap was set to zero. Foci data were extracted and further analysed with Microsoft Excel.

4.25 Computer-based analyses and online tools

4.25.1 PIP5K1 and PIP5K2 phosphorylation sites prediction

For *in silico* prediction of putative phosphorylation sites in PIP5K1 and PIP5K2 the database and prediction tool PhosPhAT 4.0 (Zulawski et al., 2013) GPS 5.0 (Wang et al., 2020a) and NetPhos 3.1 (Blom et al., 1999) were used to select putative phosphorylation sites. Prediction tools were used as described by the publishers. NetPhos is a tool for mammalian protein kinases, thus predictions for AGC kinases PKA, PKG and PKC were only considered. The selected putative phosphorylation sites are shown in figure 8.

4.25.2 Phylogenetic trees

Phylogenetic comparisons were made with MAFFT v.7.305 (Kato and Toh, 2010) and phylogeny calculated with maximum-likelihood-analysis (RAxML, (Stamatakis, 2014)). Tree is supported by bootstrap values at nodes (100-81: strongly supported; 80-70, well supported; 70-51 weakly supported; ≤ 50 , not supported). Phylogenetic trees were edited and transformed into .tiff format in software MEGA11 (Tamura et al., 2021).

4.25.3 Statistics and data management

Data were analysed for statistical relevance by two-sided Student's T-test or one-way ANOVA with subsequent Turkey's post-hoc test ($p \leq 0.05$). T-Test was performed in Microsoft Excel 365 (Microsoft Corporation, Redmond, WA, USA) and one-way ANOVA in the online tool "Statistic Kingdom" (2017).

Error bars in bar charts represent the sample standard deviation. The box plots depict the inner quartiles with the whiskers indicating the maximum and minimum. Values 1.5 times larger or smaller than the interquartile range (IQR) are regarded as outliers. Outliers are represented by circles. The cross marks the mean, the line in between the quartiles marks the median. Box plots were made with Microsoft Excel or "Shiny Boxplot - BoxPlotR", an R based box plot tool created by the research groups of Prof. Dr. Michael Tyres (Université de Montréal) and Rappsilber Laboratory (Berlin, Germany).

5 Literature

- Adamowski, M., and Friml, J.** (2015). PIN-Dependent Auxin Transport: Action, Regulation, and Evolution. *The Plant Cell* **27**:20–32.
- Allende, J. E., and Allende, C. C.** (1995). Protein kinase CK2: an enzyme with multiple substrates and a puzzling regulation. *The FASEB Journal* **9**:313–323.
- Alvarez-Venegas, R., Sadler, M., Hlavacka, A., Baluška, F., Xia, Y., Lu, G., Firsov, A., Sarath, G., Moriyama, H., Dubrovsky, J. G., et al.** (2006a). The Arabidopsis homolog of trithorax, ATX1, binds phosphatidylinositol 5-phosphate, and the two regulate a common set of target genes. *Proceedings of the National Academy of Sciences* **103**:6049–6054.
- Alvarez-Venegas, R., Xia, Y., Lu, G., and Avramova, Z.** (2006b). Phosphoinositide 5-Phosphate and Phosphoinositide 4-Phosphate Trigger Distinct Specific Responses of Arabidopsis Genes. *Plant Signaling & Behavior* **1**:140–151.
- Anthony, R. G., Henriques, R., Helfer, A., Mészáros, T., Rios, G., Testerink, C., Munnik, T., Deák, M., Koncz, C., and Bögre, L.** (2004). A protein kinase target of a PDK1 signalling pathway is involved in root hair growth in Arabidopsis. *EMBO J* **23**:572–581.
- Audhya, A., and Emr, S.** (2003). Regulation of PI4,5P2 synthesis by nuclear-cytoplasmic shuttling of the Mss4 lipid kinase. *The EMBO journal* **22**:4223–36.
- Bak, G., Lee, E.-J., Lee, Y., Kato, M., Segami, S., Sze, H., Maeshima, M., Hwang, J.-U., and Lee, Y.** (2013). Rapid Structural Changes and Acidification of Guard Cell Vacuoles during Stomatal Closure Require Phosphatidylinositol 3,5-Bisphosphate[C][W]. *Plant Cell* **25**:2202–2216.
- Barbosa, I. C. R., Shikata, H., Zourelidou, M., Heilmann, M., Heilmann, I., and Schwechheimer, C.** (2016). Phospholipid composition and a polybasic motif determine D6 PROTEIN KINASE polar association with the plasma membrane and tropic responses. *Development* **143**:4687–4700.
- Barkla, B. J., Vera-Estrella, R., and Pantoja, O.** (2014). Growing Arabidopsis in vitro: cell suspensions, in vitro culture, and regeneration. In *Arabidopsis protocols*, pp. 53–62. Springer.
- Benjamins, R., Quint, A. B., Weijers, D., Hooykaas, P., and Offringa, R.** (2001a). The PINOID protein kinase regulates organ development in Arabidopsis by enhancing polar auxin transport Advance Access published 2001.
- Benjamins, R., Quint, A., Weijers, D., Hooykaas, P., and Offringa, R.** (2001b). The PINOID protein kinase regulates organ development in Arabidopsis by enhancing polar auxin transport. *Development* **128**:4057–4067.
- Bibby, A. C., and Litchfield, D. W.** (2005). The multiple personalities of the regulatory subunit of protein kinase CK2: CK2 dependent and CK2 independent roles reveal a secret identity for CK2beta. *Int J Biol Sci* **1**:67–79.
- Blom, N., Gammeltoft, S., and Brunak, S.** (1999). Sequence and structure-based prediction of eukaryotic protein phosphorylation sites1 Edited by F. E. Cohen. *Journal of Molecular Biology* **294**:1351–1362.
- Bögre, L., Ökrész, L., Henriques, R., and Anthony, R. G.** (2003). Growth signalling pathways in Arabidopsis and the AGC protein kinases. *Trends in Plant Science* **8**:424–431.

- Boldyreff, B., and Issinger, O.-G.** (1997). A-Raf kinase is a new interacting partner of protein kinase CK2 β subunit. *FEBS Letters* **403**:197–199.
- Bradford, M. M.** (1976). A rapid and sensitive method for the quantitation of microgram quantities of protein utilizing the principle of protein-dye binding. *Analytical biochemistry* **72**:248–254.
- Bu, Q., Zhu, L., Dennis, M. D., Yu, L., Lu, S. X., Person, M. D., Tobin, E. M., Browning, K. S., and Huq, E.** (2011). Phosphorylation by CK2 Enhances the Rapid Light-induced Degradation of Phytochrome Interacting Factor 1 in Arabidopsis*. *Journal of Biological Chemistry* **286**:12066–12074.
- Burnett, G., and Kennedy, E. P.** (1954). THE ENZYMATIC PHOSPHORYLATION OF PROTEINS. *Journal of Biological Chemistry* **211**:969–980.
- Calderon, R. H., Dalton, J., Zhang, Y., and Quail, P. H.** (2022). Shade triggers posttranscriptional PHYTOCHROME- INTERACTING FACTOR-dependent increases in H3K4 trimethylation. *Plant Physiology Advance Access* published June 8, 2022, doi:10.1093/plphys/kiac282.
- Camacho, L., Smertenko, A. P., Pérez-Gómez, J., Hussey, P. J., and Moore, I.** (2009). Arabidopsis Rab-E GTPases exhibit a novel interaction with a plasma-membrane phosphatidylinositol-4-phosphate 5-kinase. *Journal of Cell Science* **122**:4383–4392.
- Carella, P.** (2020). Good Fats, Bad Fats: Phosphoinositide Species Differentially Localize to Plant-Pathogen Interfaces and Influence Disease Progression[OPEN]. *The Plant Cell* **32**:1355–1356.
- Chakrabarti, R., Sanyal, S., Ghosh, A., Bhar, K., Das, C., and Siddhanta, A.** (2015). Phosphatidylinositol-4-phosphate 5-Kinase 1 α Modulates Ribosomal RNA Gene Silencing through Its Interaction with Histone H3 Lysine 9 Trimethylation and Heterochromatin Protein HP1- α *. *Journal of Biological Chemistry* **290**:20893–20903.
- Chen, H.-H., Qu, L., Xu, Z.-H., Zhu, J.-K., and Xue, H.-W.** (2018). EL1-like Casein Kinases Suppress ABA Signaling and Responses by Phosphorylating and Destabilizing the ABA Receptors PYR/PYLs in Arabidopsis. *Molecular Plant* **11**:706–719.
- Choi, S., Chen, M., Cryns, V. L., and Anderson, R. A.** (2019). A nuclear phosphoinositide kinase complex regulates p53. *Nat Cell Biol* **21**:462–475.
- Christensen, S. K., Dagenais, N., Chory, J., and Weigel, D.** (2000). Regulation of Auxin Response by the Protein Kinase PINOID. *Cell* **100**:469–478.
- Ciruela, A., HINCHLIFFE, K. A., DIVECHA, N., and IRVINE, R. F.** (2000). Nuclear targeting of the β isoform of Type II phosphatidylinositol phosphate kinase (phosphatidylinositol 5-phosphate 4-kinase) by its α -helix 7. *Biochemical Journal* **346**:587–591.
- Clarke, J. H., LETCHER, A. J., D'SANTOS, C. S., HALSTEAD, J. R., IRVINE, R. F., and DIVECHA, N.** (2001). Inositol lipids are regulated during cell cycle progression in the nuclei of murine erythroleukaemia cells. *Biochemical Journal* **357**:905–910.
- Clough, S. J., and Bent, A. F.** (1998). Floral dip: a simplified method for Agrobacterium-mediated transformation of Arabidopsis thaliana. *The plant journal* **16**:735–743.
- Colin, L. A., and Jaillais, Y.** (2020). Phospholipids across scales: lipid patterns and plant development. *Current Opinion in Plant Biology* **53**:1–9.

- Corpet, F.** (1988). Multiple sequence alignment with hierarchical clustering. *Nucleic acids research* **16**:10881–10890.
- Daamen, F.** (2022). Dissertation: Phosphoinositides modulate auxin-dependent transcription by controlling the histone acetyltransferase GCN5 in Arabidopsis Advance Access published 2022.
- Dai, M., Zhang, C., Kania, U., Chen, F., Xue, Q., Mccray, T., Li, G., Qin, G., Wakeley, M., Terzaghi, W., et al.** (2012). A PP6-Type Phosphatase Holoenzyme Directly Regulates PIN Phosphorylation and Auxin Efflux in Arabidopsis. *The Plant Cell* **24**:2497–2514.
- D'Alessandro, S., Golin, S., Zanin, S., Cendron, L., Zottini, M., and Ruzzene, M.** (2019). Phosphorylation of p23-1 cochaperone by protein kinase CK2 affects root development in Arabidopsis. *Sci Rep* **9**:9846.
- Daniel, X., Sugano, S., and Tobin, E. M.** (2004). CK2 phosphorylation of CCA1 is necessary for its circadian oscillator function in Arabidopsis. *Proceedings of the National Academy of Sciences* **101**:3292–3297.
- Desrivères, S., Cooke, F. T., Parker, P. J., and Hall, M. N.** (1998). MSS4, a Phosphatidylinositol-4-phosphate 5-Kinase Required for Organization of the Actin Cytoskeleton in *Saccharomyces cerevisiae* *. *Journal of Biological Chemistry* **273**:15787–15793.
- DeWald, D. B., Torabinejad, J., Jones, C. A., Shope, J. C., Cangelosi, A. R., Thompson, J. E., Prestwich, G. D., and Hama, H.** (2001). Rapid Accumulation of Phosphatidylinositol 4,5-Bisphosphate and Inositol 1,4,5-Trisphosphate Correlates with Calcium Mobilization in Salt-Stressed Arabidopsis. *Plant Physiol* **126**:759–769.
- Dhonukshe, P., Aniento, F., Hwang, I., Robinson, D. G., Mravec, J., Stierhof, Y.-D., and Friml, J.** (2007). Clathrin-Mediated Constitutive Endocytosis of PIN Auxin Efflux Carriers in Arabidopsis. *Current Biology* **17**:520–527.
- Dhonukshe, P., Huang, F., Galvan-Ampudia, C. S., Mähönen, A. P., Kleine-Vehn, J., Xu, J., Quint, A., Prasad, K., Friml, J., Scheres, B., et al.** (2015). Plasma membrane-bound AGC3 kinases phosphorylate PIN auxin carriers at TPRXS(N/S) motifs to direct apical PIN recycling. *Development* **142**:2386–2387.
- Dieck, C., Boss, W., and Perera, I.** (2012a). A Role for Phosphoinositides in Regulating Plant Nuclear Functions. *Frontiers in plant science* **3**:50.
- Dieck, C. B., Wood, A., Brglez, I., Rojas-Pierce, M., and Boss, W. F.** (2012b). Increasing phosphatidylinositol (4,5) bisphosphate biosynthesis affects plant nuclear lipids and nuclear functions. *Plant Physiology and Biochemistry* **57**:32–44.
- Divecha, N., Roefs, M., Los, A., Halstead, J., Bannister, A., and D'Santos, C.** (2002). Type I PIPkinases Interact with and Are Regulated by the Retinoblastoma Susceptibility Gene Product—pRB. *Current Biology* **12**:582–587.
- Doughman, R. L., Firestone, A. J., and Anderson, R. A.** (2003). Phosphatidylinositol phosphate kinases put PI4,5P(2) in its place. *J Membr Biol* **194**:77–89.
- Dowler, S., CURRIE, R. A., CAMPBELL, D. G., DEAK, M., KULAR, G., DOWNES, C. P., and ALESSI, D. R.** (2000). Identification of pleckstrin-homology-domain-containing proteins with novel phosphoinositide-binding specificities. *Biochemical Journal* **351**:19–31.
- Elge, S., Brearley, C., Xia, H.-J., Kehr, J., Xue, H.-W., and Mueller-Roeber, B.** (2001). An Arabidopsis inositol phospholipid kinase strongly expressed in procambial cells: Synthesis of PtdIns(4,5)P2 and PtdIns(3,4,5)P3 in insect cells by 5-phosphorylation of precursors. *The Plant Journal* **26**:561–571.

- Emenecker, R. J., Holehouse, A. S., and Strader, L. C.** (2020). Emerging Roles for Phase Separation in Plants. *Developmental Cell* **55**:69–83.
- Ershov, D., Phan, M.-S., Pylvänäinen, J. W., Rigaud, S. U., Blanc, L. L., Charles-Orszag, A., Conway, J. R. W., Laine, R. F., Roy, N. H., Bonazzi, D., et al.** (2021). Bringing Track-Mate into the era of machine-learning and deep-learning Advance Access published September 20, 2021, doi:10.1101/2021.09.03.458852.
- Eyster, K. M.** (2007). The membrane and lipids as integral participants in signal transduction: lipid signal transduction for the non-lipid biochemist. *Advances in Physiology Education* **31**:5–16.
- Fang, F., Ye, S., Tang, J., Bennett, M. J., and Liang, W.** (2020). DWT1/DWL2 act together with OsPIP5K1 to regulate plant uniform growth in rice. *New Phytologist* **225**:1234–1246.
- Fernandis, A. Z., and Subrahmanyam, G.** (1998). Protein tyrosine phosphorylation activates rat splenic type II phosphatidylinositol 4-kinase in vitro. *FEBS Letters* **441**:432–436.
- Fernandis, A. Z., and Subrahmanyam, G.** (2000). Tyrosyl phosphorylation and activation of a type II phosphatidylinositol 4-kinase by p56lck in concanavalin A stimulated rat splenic lymphocytes. *Molecular Immunology* **37**:273–280.
- Ferrarese, A., Marin, O., Bustos, V. H., Venerando, A., Antonelli, M., Allende, J. E., and Pinna, L. A.** (2007). Chemical Dissection of the APC Repeat 3 Multistep Phosphorylation by the Concerted Action of Protein Kinases CK1 and GSK3. *Biochemistry* **46**:11902–11910.
- Filhol, O., Martiel, J.-L., and Claude, C.** (2004). Protein kinase CK2: a new view of an old molecular complex. *EMBO reports* **5**:351–355.
- Fiume, R., Faenza, I., Sheth, B., Poli, A., Vidalle, M. C., Mazzetti, C., Abdul, S. H., Campagnoli, F., Fabbrini, M., Kimber, S. T., et al.** (2019). Nuclear Phosphoinositides: Their Regulation and Roles in Nuclear Functions. *Int J Mol Sci* **20**:2991.
- Flotow, H., and Roach, P. J.** (1991). Role of acidic residues as substrate determinants for casein kinase I. *Journal of Biological Chemistry* **266**:3724–3727.
- Fratini, M., Krishnamoorthy, P., Stenzel, I., Riechmann, M., Matzner, M., Bacia, K., Heilmann, M., and Heilmann, I.** (2021). Plasma membrane nano-organization specifies phosphoinositide effects on Rho-GTPases and actin dynamics in tobacco pollen tubes. *The Plant Cell* **33**:642–670.
- Friml, J., Yang, X., Michniewicz, M., Weijers, D., Quint, A., Tietz, O., Benjamins, R., Ouwkerk, P. B. F., Ljung, K., Sandberg, G., et al.** (2004). A PINOID-Dependent Binary Switch in Apical-Basal PIN Polar Targeting Directs Auxin Efflux. *Science* **306**:862–865.
- Furt, F., König, S., Bessoule, J.-J., Sargueil, F., Zallot, R., Stanislas, T., Noirot, E., Lherminier, J., Simon-Plas, F., Heilmann, I., et al.** (2010). Polyphosphoinositides Are Enriched in Plant Membrane Rafts and Form Microdomains in the Plasma Membrane. *Plant Physiology* **152**:2173–2187.
- Galván-Ampudia, C. S., and Offringa, R.** (2007). Plant evolution: AGC kinases tell the auxin tale. *Trends in Plant Science* **12**:541–547.
- Garcia, P., Gupta, R., Shah, S., Morris, A. J., Rudge, S. A., Scarlata, S., Petrova, V., McLaughlin, S., and Rebecchi, M. J.** (1995). The pleckstrin homology domain of phospholipase C-delta 1 binds with high affinity to phosphatidylinositol 4,5-bisphosphate in bilayer membranes. *Biochemistry* **34**:16228–16234.

- Gaullier, J.-M., Simonsen, A., D'Arrigo, A., Bremnes, B., Stenmark, H., and Aasland, R.** (1998). FYVE fingers bind PtdIns(3)P. *Nature* **394**:432–433.
- Gerth, K., Lin, F., Menzel, W., Krishnamoorthy, P., Stenzel, I., Heilmann, M., and Heilmann, I.** (2017a). Guilt by Association: A Phenotype-Based View of the Plant Phosphoinositide Network. *Annual Review of Plant Biology* **68**:349–374.
- Gerth, K., Lin, F., Daamen, F., Menzel, W., Heinrich, F., and Heilmann, M.** (2017b). Arabidopsis phosphatidylinositol 4-phosphate 5-kinase 2 contains a functional nuclear localization sequence and interacts with alpha-importins. *The Plant Journal* **92**:862–878.
- Gerth, K.** (2018). Dissertation: Phosphoinositide im Kern pflanzlicher Zellen - Kernlokalisierung der ubiquitären PI4P 5-Kinase PIP5K2 und ihr Einfluss auf die Entwicklung von Arabidopsis thaliana Advance Access published 2018.
- Glanc, M., Van Gelderen, K., Hoermayer, L., Tan, S., Naramoto, S., Zhang, X., Domjan, D., Včelařová, L., Hauschild, R., Johnson, A., et al.** (2021). AGC kinases and MAB4/MEL proteins maintain PIN polarity by limiting lateral diffusion in plant cells. *Current Biology* **31**:1918–1930.e5.
- Goldstein, L.** (1958). Localization of nucleus-specific protein as shown by transplantation experiments in Amoeba proteus. *Experimental Cell Research* **15**:635–637.
- Grefen, C., and Blatt, M. R.** (2012). A 2in1 cloning system enables ratiometric bimolecular fluorescence complementation (rBiFC). *BioTechniques* **53**:311–314.
- Guo, L., Winzer, T., Yang, X., Li, Y., Ning, Z., He, Z., Teodor, R., Lu, Y., Bowser, T. A., Graham, I. A., et al.** (2018). The opium poppy genome and morphinan production. *Science* **362**:343–347.
- Hanks, S. K., and Hunter, T.** (1995). The eukaryotic protein kinase superfamily: kinase (catalytic) domain structure and classification1. *The FASEB Journal* **9**:576–596.
- Hardtke, Ghoda, and Deng, X. W.** (2000). HY5 stability and activity in Arabidopsis is regulated by phosphorylation in its COP1 binding domain. *The EMBO Journal* **19**:4997–5006.
- Harreman, M. T., Kline, T. M., Milford, H. G., Harben, M. B., Hodel, A. E., and Corbett, A. H.** (2004). Regulation of Nuclear Import by Phosphorylation Adjacent to Nuclear Localization Signals *. *Journal of Biological Chemistry* **279**:20613–20621.
- Hathaway, G. M., and Traugh, J. A.** (1979). Cyclic nucleotide-independent protein kinases from rabbit reticulocytes. Purification of casein kinases. *Journal of Biological Chemistry* **254**:762–768.
- Heilmann, I.** (2016a). Phosphoinositide signaling in plant development. *Development* **143**:2044–2055.
- Heilmann, I.** (2016b). Plant phosphoinositide signaling - dynamics on demand. *Biochimica et Biophysica Acta (BBA) - Molecular and Cell Biology of Lipids* **1861**:1345–1351.
- Heilmann, M., and Heilmann, I.** (2015). Plant phosphoinositides—complex networks controlling growth and adaptation. *Biochimica et Biophysica Acta (BBA) - Molecular and Cell Biology of Lipids* **1851**:759–769.
- Heilmann, M., and Heilmann, I.** (2022). Regulators regulated: Different layers of control for plasma membrane phosphoinositides in plants. *Current Opinion in Plant Biology* **67**:102218.

- Heilmann, I., Perera, I. Y., Gross, W., and Boss, W. F.** (1999). Changes in Phosphoinositide Metabolism with Days in Culture Affect Signal Transduction Pathways in *Galdieria sulphuraria*. *Plant Physiology* **119**:1331–1340.
- Heilmann, I., Perera, I. Y., Gross, W., and Boss, W. F.** (2001). Plasma Membrane Phosphatidylinositol 4,5-Bisphosphate Levels Decrease with Time in Culture. *Plant Physiology* **126**:1507–1518.
- Hempel, F., Stenzel, I., Heilmann, M., Krishnamoorthy, P., Menzel, W., Golbik, R., Helm, S., Dobritsch, D., Baginsky, S., Lee, J., et al.** (2017). MAPKs Influence Pollen Tube Growth by Controlling the Formation of Phosphatidylinositol 4,5-Bisphosphate in an Apical Plasma Membrane Domain. *The Plant Cell* **29**:3030–3050.
- Huang, F., Kemel Zago, M., Abas, L., van Marion, A., Galván-Ampudia, C. S., and Offringa, R.** (2010). Phosphorylation of Conserved PIN Motifs Directs Arabidopsis PIN1 Polarity and Auxin Transport. *The Plant Cell* **22**:1129–1142.
- Humphrey, S. J., James, D. E., and Mann, M.** (2015). Protein Phosphorylation: A Major Switch Mechanism for Metabolic Regulation. *Trends in Endocrinology & Metabolism* **26**:676–687.
- Im, Y. J., Davis, A. J., Perera, I. Y., Johannes, E., Allen, N. S., and Boss, W. F.** (2007). The N-terminal Membrane Occupation and Recognition Nexus Domain of Arabidopsis Phosphatidylinositol Phosphate Kinase 1 Regulates Enzyme Activity *. *Journal of Biological Chemistry* **282**:5443–5452.
- Ischebeck, T., Stenzel, I., and Heilmann, I.** (2008). Type B Phosphatidylinositol-4-Phosphate 5-Kinases Mediate Arabidopsis and *Nicotiana tabacum* Pollen Tube Growth by Regulating Apical Pectin Secretion. *Plant Cell* **20**:3312–3330.
- Ischebeck, T., Seiler, S., and Heilmann, I.** (2010a). At the poles across kingdoms: phosphoinositides and polar tip growth. *Protoplasma* **240**:13–31.
- Ischebeck, T., Vu, L. H., Jin, X., Stenzel, I., Löffke, C., and Heilmann, I.** (2010b). Functional Cooperativity of Enzymes of Phosphoinositide Conversion According to Synergistic Effects on Pectin Secretion in Tobacco Pollen Tubes. *Molecular Plant* **3**:870–881.
- Ischebeck, T., Stenzel, I., Hempel, F., Jin, X., Mosblech, A., and Heilmann, I.** (2011). Phosphatidylinositol-4,5-bisphosphate influences Nt-Rac5-mediated cell expansion in pollen tubes of *Nicotiana tabacum*. *The Plant Journal* **65**:453–468.
- Ischebeck, T., Werner, S., Krishnamoorthy, P., Lerche, J., Meijón, M., Stenzel, I., Löffke, C., Wiessner, T., Im, Y. J., Perera, I. Y., et al.** (2013). Phosphatidylinositol 4,5-Bisphosphate Influences PIN Polarization by Controlling Clathrin-Mediated Membrane Trafficking in Arabidopsis. *The Plant Cell* **25**:4894–4911.
- Jackson, M., Crick, D. C., and Brennan, P. J.** (2000). Phosphatidylinositol Is an Essential Phospholipid of *Mycobacteria* *. *Journal of Biological Chemistry* **275**:30092–30099.
- Jaillais, Y., and Ott, T.** (2020). The Nanoscale Organization of the Plasma Membrane and Its Importance in Signaling: A Proteolipid Perspective [OPEN]. *Plant Physiology* **182**:1682–1696.
- Jans, D. A., and Hubner, S.** (1996). Regulation of protein transport to the nucleus: central role of phosphorylation. *Physiological Reviews* **76**:651–685.
- Jensen, A. B., Goday, A., Figueras, M., Jessop, A. C., and Pagès, M.** (1998). Phosphorylation mediates the nuclear targeting of the maize Rab17 protein. *The Plant Journal* **13**:691–697.

- Jensen, R. B., LACOUR, T., ALBRETHSEN, J., NIELSEN, M., and SKRIVER, K.** (2001). FYVE zinc-finger proteins in the plant model *Arabidopsis thaliana*: identification of PtdIns3P-binding residues by comparison of classic and variant FYVE domains. *Biochemical Journal* **359**:165–173.
- Johnsson, N., and Varshavsky, A.** (1994). Split ubiquitin as a sensor of protein interactions in vivo. *Proceedings of the National Academy of Sciences* **91**:10340–10344.
- Jumper, J., Evans, R., Pritzel, A., Green, T., Figurnov, M., Ronneberger, O., Tunyasuvunakool, K., Bates, R., Žídek, A., Potapenko, A., et al.** (2021). Highly accurate protein structure prediction with AlphaFold. *Nature* **596**:583–589.
- Justin, A.-M., Hmyene, A., Kader, J.-C., and Mazliak, P.** (1995). Compared selectivities of the phosphatidylinositol-synthase from maize coleoptiles either in microsomal membranes or after solubilization. *Biochimica et Biophysica Acta (BBA) - Lipids and Lipid Metabolism* **1255**:161–166.
- Kalderon, D., Roberts, B. L., Richardson, W. D., and Smith, A. E.** (1984). A short amino acid sequence able to specify nuclear location. *Cell* **39**:499–509.
- Kang, H.-G., and Klessig, D. F.** (2005). Salicylic acid-inducible *Arabidopsis* CK2-like activity phosphorylates TGA2. *Plant Mol Biol* **57**:541–557.
- Katoh, K., and Toh, H.** (2010). Parallelization of the MAFFT multiple sequence alignment program. *Bioinformatics* **26**:1899–1900.
- Kleine-Vehn, J., Huang, F., Naramoto, S., Zhang, J., Michniewicz, M., Offringa, R., and Friml, J.** (2009). PIN Auxin Efflux Carrier Polarity Is Regulated by PINOID Kinase-Mediated Recruitment into GNOM-Independent Trafficking in *Arabidopsis*. *The Plant Cell* **21**:3839–3849.
- König, S., Ischebeck, T., Lerche, J., Stenzel, I., and Heilmann, I.** (2008). Salt-stress-induced association of phosphatidylinositol 4,5-bisphosphate with clathrin-coated vesicles in plants. *Biochemical Journal* **415**:387–399.
- Kosugi, S., Hasebe, M., Matsumura, N., Takashima, H., Miyamoto-Sato, E., Tomita, M., and Yanagawa, H.** (2009). Six Classes of Nuclear Localization Signals Specific to Different Binding Grooves of Importin α^* . *Journal of Biological Chemistry* **284**:478–485.
- Krohn, N. M., Stemmer, C., Fojan, P., Grimm, R., and Grasser, K. D.** (2003). Protein Kinase CK2 Phosphorylates the High Mobility Group Domain Protein SSRP1, Inducing the Recognition of UV-damaged DNA*. *Journal of Biological Chemistry* **278**:12710–12715.
- Kuroda, R., Kato, M., Tsuge, T., and Aoyama, T.** (2021). *Arabidopsis* phosphatidylinositol 4-phosphate 5-kinase genes PIP5K7, PIP5K8, and PIP5K9 are redundantly involved in root growth adaptation to osmotic stress. *The Plant Journal* **106**:913–927.
- Kusano, H., Testerink, C., Vermeer, J. E. M., Tsuge, T., Shimada, H., Oka, A., Munnik, T., and Aoyama, T.** (2008). The *Arabidopsis* Phosphatidylinositol Phosphate 5-Kinase PIP5K3 Is a Key Regulator of Root Hair Tip Growth. *Plant Cell* **20**:367–380.
- LAEMMLI, U. K.** (1970). Cleavage of structural proteins during the assembly of the head of bacteriophage T4. *nature* **227**:680–685.
- Lau, O. S., and Deng, X. W.** (2012). The photomorphogenic repressors COP1 and DET1: 20 years later. *Trends in Plant Science* **17**:584–593.
- Launhardt, L., Matzner, M., Heilmann, M., and Heilmann, I.** (2021). Analysis of Phosphoinositides from Complex Plant Samples by Solid-Phase Adsorption Chromatography and

- Subsequent Quantification via Thin-Layer and Gas Chromatography. *Methods Mol Biol* **2295**:379–389.
- Lazo, G. R., Stein, P. A., and Ludwig, R. A.** (1991). A DNA transformation-competent *Arabidopsis* genomic library in *Agrobacterium*. *Bio/technology* **9**:963–967.
- Lee, S. H., and Cho, H.-T.** (2006). PINOID Positively Regulates Auxin Efflux in *Arabidopsis* Root Hair Cells and Tobacco Cells. *The Plant Cell* **18**:1604–1616.
- Lee, Y., Lloyd, A. M., and Roux, S. J.** (1999). Antisense Expression of the CK2 α -Subunit Gene in *Arabidopsis*. Effects on Light-Regulated Gene Expression and Plant Growth1. *Plant Physiology* **119**:989–1000.
- Lee, Y., Kim, Y.-W., Jeon, B. W., Park, K.-Y., Suh, S. J., Seo, J., Kwak, J. M., Martinoia, E., Hwang, I., and Lee, Y.** (2007). Phosphatidylinositol 4,5-bisphosphate is important for stomatal opening. *The Plant Journal* **52**:803–816.
- Liku, M. E., Nguyen, V. Q., Rosales, A. W., Irie, K., and Li, J. J.** (2005). CDK Phosphorylation of a Novel NLS-NES Module Distributed between Two Subunits of the Mcm2-7 Complex Prevents Chromosomal Rereplication. *MBoC* **16**:5026–5039.
- Litchfield, D. W.** (2003). Protein kinase CK2: structure, regulation and role in cellular decisions of life and death. *Biochemical Journal* **369**:1–15.
- Lolli, G., Pinna, L. A., and Battistutta, R.** (2012). Structural Determinants of Protein Kinase CK2 Regulation by Autoinhibitory Polymerization. *ACS Chem. Biol.* **7**:1158–1163.
- Lolli, G., Ranchio, A., and Battistutta, R.** (2014). Active Form of the Protein Kinase CK2 $\alpha_2\beta_2$ Holoenzyme Is a Strong Complex with Symmetric Architecture. *ACS Chem. Biol.* **9**:366–371.
- Lou, Y., Gou, J.-Y., and Xue, H.-W.** (2007). PIP5K9, an *Arabidopsis* Phosphatidylinositol Monophosphate Kinase, Interacts with a Cytosolic Invertase to Negatively Regulate Sugar-Mediated Root Growth. *The Plant Cell* **19**:163–181.
- Lu, S. X., Liu, H., Knowles, S. M., Li, J., Ma, L., Tobin, E. M., and Lin, C.** (2011). A Role for Protein Kinase Casein Kinase2 α -Subunits in the *Arabidopsis* Circadian Clock. *Plant Physiology* **157**:1537–1545.
- Lundbæk, J. A., Collingwood, S. A., Ingólfsson, H. I., Kapoor, R., and Andersen, O. S.** (2010). Lipid bilayer regulation of membrane protein function: gramicidin channels as molecular force probes. *J R Soc Interface* **7**:373–395.
- Marhava, P., Aliaga Fandino, A. C., Koh, S. W. H., Jelínková, A., Kolb, M., Janacek, D. P., Breda, A. S., Cattaneo, P., Hammes, U. Z., Petrášek, J., et al.** (2020). Plasma Membrane Domain Patterning and Self-Reinforcing Polarity in *Arabidopsis*. *Developmental Cell* **52**:223-235.e5.
- Meggio, F., and Pinna, L. A.** (2003). One-thousand-and-one substrates of protein kinase CK2? *FASEB J* **17**:349–368.
- Mei, Y.** (2014). *Arabidopsis* PIP5K2 Is Involved in Salt Tolerance. In *Functional Characterization of Arabidopsis Phosphatidylinositol Monophosphate 5-kinase 2 in Lateral Root Development, Gravitropism and Salt Tolerance* (ed. Mei, Y.), pp. 63–77. Dordrecht: Springer Netherlands.

- Mei, Y., Jia, W.-J., Chu, Y.-J., and Xue, H.-W.** (2012). Arabidopsis phosphatidylinositol mono-phosphate 5-kinase 2 is involved in root gravitropism through regulation of polar auxin transport by affecting the cycling of PIN proteins. *Cell Res* **22**:581–597.
- Meijer, H. J. G., BERRIE, C. P., IURISCI, C., DIVECHA, N., MUSGRAVE, A., and MUNNIK, T.** (2001). Identification of a new polyphosphoinositide in plants, phosphatidylinositol 5-monophosphate (PtdIns5P), and its accumulation upon osmotic stress. *Biochemical Journal* **360**:491–498.
- Mellman, D. L., Gonzales, M. L., Song, C., Barlow, C. A., Wang, P., Kendziorski, C., and Anderson, R. A.** (2008). A PtdIns4,5P2-regulated nuclear poly(A) polymerase controls expression of select mRNAs. *Nature* **451**:1013–1017.
- Menzel, W., Stenzel, I., Helbig, L.-M., Krishnamoorthy, P., Neumann, S., Eschen-Lippold, L., Heilmann, M., Lee, J., and Heilmann, I.** (2019). A PAMP-triggered MAPK cascade inhibits phosphatidylinositol 4,5-bisphosphate production by PIP5K6 in Arabidopsis thaliana. *New Phytologist* **224**:833–847.
- Mergner, J., Frejno, M., List, M., Papacek, M., Chen, X., Chaudhary, A., Samaras, P., Richter, S., Shikata, H., Messerer, M., et al.** (2020). Mass-spectrometry-based draft of the Arabidopsis proteome. *Nature* **579**:409–414.
- Michniewicz, M., Zago, M. K., Abas, L., Weijers, D., Schweighofer, A., Meskiene, I., Heisler, M. G., Ohno, C., Zhang, J., Huang, F., et al.** (2007). Antagonistic Regulation of PIN Phosphorylation by PP2A and PINOID Directs Auxin Flux. *Cell* **130**:1044–1056.
- Mockaitis, K., and Estelle, M.** (2008). Auxin Receptors and Plant Development: A New Signaling Paradigm. *Annu. Rev. Cell Dev. Biol.* **24**:55–80.
- Möckli, N., Deplazes, A., Hassa, P. O., Zhang, Z., Peter, M., Hottiger, M. O., Stagljär, I., and Auerbach, D.** (2007). Yeast split-ubiquitin-based cytosolic screening system to detect interactions between transcriptionally active proteins. *Biotechniques* **42**:725–730.
- Mora, A., Komander, D., van Aalten, D. M. F., and Alessi, D. R.** (2004). PDK1, the master regulator of AGC kinase signal transduction. *Seminars in Cell & Developmental Biology* **15**:161–170.
- Moreno-Romero, J., and Martínez, M. C.** (2008). Is there a link between protein kinase CK2 and auxin signaling? *Plant Signaling & Behavior* **3**:695–697.
- Moreno-Romero, J., Armengot, L., Marquès-Bueno, M. M., Cadavid-Ordóñez, M., and Martínez, M. C.** (2011). About the role of CK2 in plant signal transduction. *Mol Cell Biochem* **356**:233–240.
- Mueller-Roeber, B., and Pical, C.** (2002). Inositol Phospholipid Metabolism in Arabidopsis. Characterized and Putative Isoforms of Inositol Phospholipid Kinase and Phosphoinositide-Specific Phospholipase C. *Plant Physiology* **130**:22–46.
- Mulekar, J. J., and Huq, E.** (2014). Expanding roles of protein kinase CK2 in regulating plant growth and development. *Journal of Experimental Botany* **65**:2883–2893.
- Mulekar, J. J., and Huq, E.** (2015). Arabidopsis casein kinase 2 α 4 subunit regulates various developmental pathways in a functionally overlapping manner. *Plant Science* **236**:295–303.
- Mulekar, J. J., Bu, Q., Chen, F., and Huq, E.** (2012). Casein kinase II α subunits affect multiple developmental and stress-responsive pathways in Arabidopsis. *The Plant Journal* **69**:343–354.

- Murashige, T., and Skoog, F.** (1962). A revised medium for rapid growth and bio assays with tobacco tissue cultures. *Physiologia plantarum* **15**:473–497.
- Muschiatti, J., Dircks, L., Vancanneyt, G., and McCormick, S.** (1994). LAT52 protein is essential for tomato pollen development: pollen expressing antisense LAT52 RNA hydrates and germinates abnormally and cannot achieve fertilization. *Plant J* **6**:321–338.
- Nagata, T., Nemoto, Y., and Hasezawa, S.** (1992). Tobacco BY-2 Cell Line as the “HeLa” Cell in the Cell Biology of Higher Plants. In *International Review of Cytology* (ed. Jeon, K. W.) and Friedlander, M.), pp. 1–30. Academic Press.
- Ndamukong, I., Jones, D. R., Lapko, H., Divecha, N., and Avramova, Z.** (2010). Phosphatidylinositol 5-Phosphate Links Dehydration Stress to the Activity of ARABIDOPSIS TRITHORAX-LIKE Factor ATX1. *PLOS ONE* **5**:e13396.
- Niefind, K., Guerra, B., Ermakowa, I., and Issinger, O.-G.** (2001). Crystal structure of human protein kinase CK2: insights into basic properties of the CK2 holoenzyme. *EMBO J* **20**:5320–5331.
- Nieva, C., Busk, P. K., Domínguez-Puigjaner, E., Lumberras, V., Testillano, P. S., Risueño, M.-C., and Pagès, M.** (2005). Isolation and Functional Characterisation of Two New bZIP Maize Regulators of the ABA Responsive Gene rab28. *Plant Mol Biol* **58**:899–914.
- Nováková, P., Hirsch, S., Feraru, E., Tejos, R., van Wijk, R., Viaene, T., Heilmann, M., Lerche, J., De Rycke, R., Feraru, M. I., et al.** (2014). SAC phosphoinositide phosphatases at the tonoplast mediate vacuolar function in Arabidopsis. *Proceedings of the National Academy of Sciences* **111**:2818–2823.
- Ohlrogge, J., and Browse, J.** (1995). Lipid biosynthesis. *Plant Cell* **7**:957–970.
- Park, S. J., Itoh, T., and Takenawa, T.** (2001). Phosphatidylinositol 4-Phosphate 5-Kinase Type I Is Regulated through Phosphorylation Response by Extracellular Stimuli*. *Journal of Biological Chemistry* **276**:4781–4787.
- Park, H.-J., Ding, L., Dai, M., Lin, R., and Wang, H.** (2008). Multisite Phosphorylation of Arabidopsis HFR1 by Casein Kinase II and a Plausible Role in Regulating Its Degradation Rate *. *Journal of Biological Chemistry* **283**:23264–23273.
- Pearce, L. R., Komander, D., and Alessi, D. R.** (2010). The nuts and bolts of AGC protein kinases. *Nat Rev Mol Cell Biol* **11**:9–22.
- Pinna, L. A.** (1990). Casein kinase 2: An ‘eminence grise’ in cellular regulation? *Biochimica et Biophysica Acta (BBA) - Molecular Cell Research* **1054**:267–284.
- Pribat, A., Sormani, R., Rousseau-Guettin, M., Julkowska, M. M., Testerink, C., Joubès, J., Castroviejo, M., Laguerre, M., Meyer, C., Germain, V., et al.** (2011). A novel class of PTEN protein in Arabidopsis displays unusual phosphoinositide phosphatase activity and efficiently binds phosphatidic acid. *Biochemical Journal* **441**:161–171.
- Qin, L., Zhou, Z., Li, Q., Zhai, C., Liu, L., Quilichini, T. D., Gao, P., Kessler, S. A., Jaillais, Y., Datla, R., et al.** (2020). Specific Recruitment of Phosphoinositide Species to the Plant-Pathogen Interfacial Membrane Underlies Arabidopsis Susceptibility to Fungal Infection[OPEN]. *The Plant Cell* **32**:1665–1688.
- Rademacher, E. H., and Offringa, R.** (2012). Evolutionary Adaptations of Plant AGC Kinases: From Light Signaling to Cell Polarity Regulation. *Front Plant Sci* **3**:250.

- Rao, V. D., Misra, S., Boronenkov, I. V., Anderson, R. A., and Hurley, J. H.** (1998). Structure of Type II β Phosphatidylinositol Phosphate Kinase: A Protein Kinase Fold Flattened for Interfacial Phosphorylation. *Cell* **94**:829–839.
- Riera, M., Figueras, M., López, C., Goday, A., and Pagès, M.** (2004). Protein kinase CK2 modulates developmental functions of the abscisic acid responsive protein Rab17 from maize. *Proceedings of the National Academy of Sciences* **101**:9879–9884.
- Rödiger, A., Galonska, J., Bergner, E., Agne, B., Helm, S., Alseekh, S., Fernie, A. R., Thieme, D., Hoehenwarter, W., Hause, G., et al.** (2020). Working day and night: plastid casein kinase 2 catalyses phosphorylation of proteins with diverse functions in light- and dark-adapted plastids. *The Plant Journal* **104**:546–558.
- Rohrbach, T. D., Shah, N., Jackson, W. P., Feeney, E. V., Scanlon, S., Gish, R., Khodadadi, R., Hyde, S. O., Hicks, P. H., Anderson, J. C., et al.** (2015). The Effector Domain of MARCKS Is a Nuclear Localization Signal that Regulates Cellular PIP2 Levels and Nuclear PIP2 Localization. *PLOS ONE* **10**:e0140870.
- Ryu, H., Kim, K., Cho, H., Park, J., Choe, S., and Hwang, I.** (2007). Nucleocytoplasmic Shuttling of BZR1 Mediated by Phosphorylation Is Essential in Arabidopsis Brassinosteroid Signaling. *The Plant Cell* **19**:2749–2762.
- Salinas, P., Fuentes, D., Vidal, E., Jordana, X., Echeverria, M., and Holuigue, L.** (2006). An Extensive Survey of CK2 α and β Subunits in Arabidopsis: Multiple Isoforms Exhibit Differential Subcellular Localization. *Plant and Cell Physiology* **47**:1295–1308.
- Salvi, M., Sarno, S., Cesaro, L., Nakamura, H., and Pinna, L. A.** (2009). Extraordinary pleiotropy of protein kinase CK2 revealed by weblogo phosphoproteome analysis. *Biochimica et Biophysica Acta (BBA) - Molecular Cell Research* **1793**:847–859.
- Sangar, V., Blankenberg, D. J., Altman, N., and Lesk, A. M.** (2007). Quantitative sequence-function relationships in proteins based on gene ontology. *BMC Bioinformatics* **8**:294.
- Santarius, M., Lee, C. H., and Anderson, R. A.** (2006). Supervised membrane swimming: small G-protein lifeguards regulate PIPK signalling and monitor intracellular PtdIns(4,5)P2 pools. *Biochemical Journal* **398**:1–13.
- Schindelin, J., Arganda-Carreras, I., Frise, E., Kaynig, V., Longair, M., Pietzsch, T., Preibisch, S., Rueden, C., Saalfeld, S., Schmid, B., et al.** (2012). Fiji: an open-source platform for biological-image analysis. *Nat Methods* **9**:676–682.
- Schönberg, A., Bergner, E., Helm, S., Agne, B., Dünschede, B., Schünemann, D., Schutkowski, M., and Baginsky, S.** (2014). The Peptide Microarray “ChloroPhos1.0” Identifies New Phosphorylation Targets of Plastid Casein Kinase II (pCKII) in Arabidopsis thaliana. *PLOS ONE* **9**:e108344.
- Schwab, M. S., and Dreyer, C.** (1997). Protein phosphorylation sites regulate the function of the bipartite NLS of nucleolin. *Eur J Cell Biol* **73**:287–297.
- Smith, C. D., and Wells, W. W.** (1983). Phosphorylation of rat liver nuclear envelopes. II. Characterization of in vitro lipid phosphorylation. *Journal of Biological Chemistry* **258**:9368–9373.
- Sousa, E., Kost, B., and Malhó, R.** (2008). Arabidopsis Phosphatidylinositol-4-Monophosphate 5-Kinase 4 Regulates Pollen Tube Growth and Polarity by Modulating Membrane Recycling. *The Plant Cell* **20**:3050–3064.
- Spector, D. L., and Lamond, A. I.** (2011). Nuclear Speckles. *Cold Spring Harb Perspect Biol* **3**:a000646.

- Stamatakis, A.** (2014). RAxML version 8: a tool for phylogenetic analysis and post-analysis of large phylogenies. *Bioinformatics* **30**:1312–1313.
- Stenzel, I., Ischebeck, T., König, S., Hołubowska, A., Sporysz, M., Hause, B., and Heilmann, I.** (2008). The Type B Phosphatidylinositol-4-Phosphate 5-Kinase 3 Is Essential for Root Hair Formation in *Arabidopsis thaliana*. *Plant Cell* **20**:124–141.
- Stenzel, I., Ischebeck, T., Quint, M., and Heilmann, I.** (2012). Variable Regions of PI4P 5-Kinases Direct PtdIns(4,5)P₂ Toward Alternative Regulatory Functions in Tobacco Pollen Tubes. *Frontiers in Plant Science* **2**.
- Stevenson, J. M., Perera, I. Y., and Boss, W. F.** (1998). A Phosphatidylinositol 4-Kinase Pleckstrin Homology Domain That Binds Phosphatidylinositol 4-Monophosphate*. *Journal of Biological Chemistry* **273**:22761–22767.
- Stone, J. M., and Walker, J. C.** (1995). Plant Protein Kinase Families and Signal Transduction. *Plant Physiology* **108**:451–457.
- Strahl, T., and Thorner, J.** (2007). Synthesis and Function of Membrane Phosphoinositides in Budding Yeast, *Saccharomyces cerevisiae*. *Biochim Biophys Acta* **1771**:353–404.
- Sugano, S., Andronis, C., Green, R. M., Wang, Z.-Y., and Tobin, E. M.** (1998). Protein kinase CK2 interacts with and phosphorylates the *Arabidopsis* circadian clock-associated 1 protein. *Proceedings of the National Academy of Sciences* **95**:11020–11025.
- Sugano, S., Andronis, C., Ong, M. S., Green, R. M., and Tobin, E. M.** (1999). The protein kinase CK2 is involved in regulation of circadian rhythms in *Arabidopsis*. *Proceedings of the National Academy of Sciences* **96**:12362–12366.
- Tamaru, T., Hirayama, J., Isojima, Y., Nagai, K., Norioka, S., Takamatsu, K., and Sassone-Corsi, P.** (2009). CK2 α phosphorylates BMAL1 to regulate the mammalian clock. *Nat Struct Mol Biol* **16**:446–448.
- Tamura, K., Stecher, G., and Kumar, S.** (2021). MEGA11: Molecular Evolutionary Genetics Analysis Version 11. *Molecular Biology and Evolution* **38**:3022–3027.
- Tan, S., Zhang, X., Kong, W., Yang, X.-L., Molnár, G., Vondráková, Z., Filepová, R., Petrášek, J., Friml, J., and Xue, H.-W.** (2020). The lipid code-dependent phosphoswitch PDK1–D6PK activates PIN-mediated auxin efflux in *Arabidopsis*. *Nat. Plants* **6**:556–569.
- Tejos, R., Sauer, M., Vanneste, S., Palacios-Gomez, M., Li, H., Heilmann, M., van Wijk, R., Vermeer, J. E. M., Heilmann, I., Munnik, T., et al.** (2014). Bipolar Plasma Membrane Distribution of Phosphoinositides and Their Requirement for Auxin-Mediated Cell Polarity and Patterning in *Arabidopsis*. *The Plant Cell* **26**:2114–2128.
- Tinevez, J.-Y., Perry, N., Schindelin, J., Hoopes, G. M., Reynolds, G. D., Laplantine, E., Bednarek, S. Y., Shorte, S. L., and Eliceiri, K. W.** (2017). TrackMate: An open and extensible platform for single-particle tracking. *Methods* **115**:80–90.
- Towbin, H., Staehelin, T., and Gordon, J.** (1979). Electrophoretic transfer of proteins from polyacrylamide gels to nitrocellulose sheets: procedure and some applications. *Proceedings of the National Academy of Sciences* **76**:4350–4354.
- Ugalde, J.-M., Rodriguez-Furlán, C., Rycke, R. D., Norambuena, L., Friml, J., León, G., and Tejos, R.** (2016). Phosphatidylinositol 4-phosphate 5-kinases 1 and 2 are involved in the regulation of vacuole morphology during *Arabidopsis thaliana* pollen development. *Plant Science* **250**:10–19.

- van Wijk, K. J., Friso, G., Walther, D., and Schulze, W. X.** (2014). Meta-Analysis of Arabidopsis thaliana Phospho-Proteomics Data Reveals Compartmentalization of Phosphorylation Motifs. *The Plant Cell* **26**:2367–2389.
- Vancurova, I., Choi, J. H., Lin, H., Kuret, J., and Vancura, A.** (1999). Regulation of Phosphatidylinositol 4-Phosphate 5-Kinase from *Schizosaccharomyces pombe* by Casein Kinase I*. *Journal of Biological Chemistry* **274**:1147–1155.
- Varadi, M., Anyango, S., Deshpande, M., Nair, S., Natassia, C., Yordanova, G., Yuan, D., Stroe, O., Wood, G., Laydon, A., et al.** (2022). AlphaFold Protein Structure Database: massively expanding the structural coverage of protein-sequence space with high-accuracy models. *Nucleic Acids Research* **50**:D439–D444.
- Venerando, A., Ruzzene, M., and Pinna, L. A.** (2014). Casein kinase: the triple meaning of a misnomer. *Biochemical Journal* **460**:141–156.
- Vilela, B., Nájjar, E., Lumberras, V., Leung, J., and Pagès, M.** (2015). Casein Kinase 2 Negatively Regulates Abscisic Acid-Activated SnRK2s in the Core Abscisic Acid-Signaling Module. *Molecular Plant* **8**:709–721.
- Walter, M., Chaban, C., Schütze, K., Batistic, O., Weckermann, K., Näke, C., Blazevic, D., Grefen, C., Schumacher, K., Oecking, C., et al.** (2004). Visualization of protein interactions in living plant cells using bimolecular fluorescence complementation. *The Plant Journal* **40**:428–438.
- Wang, P., Shen, L., Guo, J., Jing, W., Qu, Y., Li, W., Bi, R., Xuan, W., Zhang, Q., and Zhang, W.** (2019). Phosphatidic Acid Directly Regulates PINOID-Dependent Phosphorylation and Activation of the PIN-FORMED2 Auxin Efflux Transporter in Response to Salt Stress. *Plant Cell* **31**:250–271.
- Wang, C., Xu, H., Lin, S., Deng, W., Zhou, J., Zhang, Y., Shi, Y., Peng, D., and Xue, Y.** (2020a). GPS 5.0: An Update on the Prediction of Kinase-specific Phosphorylation Sites in Proteins. *Genomics, Proteomics & Bioinformatics* **18**:72–80.
- Wang, P., Hsu, C.-C., Du, Y., Zhu, P., Zhao, C., Fu, X., Zhang, C., Paez, J. S., Macho, A. P., Tao, W. A., et al.** (2020b). Mapping proteome-wide targets of protein kinases in plant stress responses. *Proceedings of the National Academy of Sciences* **117**:3270–3280.
- Wang, R., Wang, R., Liu, M., Yuan, W., Zhao, Z., Liu, X., Peng, Y., Yang, X., Sun, Y., and Tang, W.** (2021). Nucleocytoplasmic trafficking and turnover mechanisms of BRASSI-NAZOLE RESISTANT1 in *Arabidopsis thaliana*. *Proceedings of the National Academy of Sciences* **118**:e2101838118.
- Wang, G., Gao, G., Yang, X., Yang, X., and Ma, P.** (2022). Casein kinase CK2 structure and activities in plants. *Journal of Plant Physiology* **276**:153767.
- Watari, M., Kato, M., Blanc-Mathieu, R., Tsuge, T., Ogata, H., and Aoyama, T.** (2022). Functional Differentiation among the Arabidopsis Phosphatidylinositol 4-Phosphate 5-Kinase Genes PIP5K1, PIP5K2 and PIP5K3. *Plant and Cell Physiology* **63**:635–648.
- Weiste, C., and Dröge-Laser, W.** (2014). The Arabidopsis transcription factor bZIP11 activates auxin-mediated transcription by recruiting the histone acetylation machinery. *Nat Commun* **5**:3883.
- Weller, B., Zourelidou, M., Frank, L., Barbosa, I. C. R., Fastner, A., Richter, S., Jürgens, G., Hammes, U. Z., and Schwechheimer, C.** (2017). Dynamic PIN-FORMED auxin efflux carrier phosphorylation at the plasma membrane controls auxin efflux-dependent growth. *Proceedings of the National Academy of Sciences* **114**:E887–E896.

- Welters, P., Takegawa, K., Emr, S. D., and Chrispeels, M. J.** (1994). AtVPS34, a phosphatidylinositol 3-kinase of *Arabidopsis thaliana*, is an essential protein with homology to a calcium-dependent lipid binding domain. *Proc Natl Acad Sci U S A* **91**:11398–11402.
- Williams, M. E., Torabinejad, J., Cohick, E., Parker, K., Drake, E. J., Thompson, J. E., Hortter, M., and DeWald, D. B.** (2005). Mutations in the *Arabidopsis* Phosphoinositide Phosphatase Gene SAC9 Lead to Overaccumulation of PtdIns(4,5)P₂ and Constitutive Expression of the Stress-Response Pathway. *Plant Physiol* **138**:686–700.
- Xiao, Y., and Offringa, R.** (2020). PDK1 regulates auxin transport and *Arabidopsis* vascular development through AGC1 kinase PAX. *Nat. Plants* **6**:544–555.
- Xue, H.-W., Pical, C., Brearley, C., Elge, S., and Müller-Röber, B.** (1999). A Plant 126-kDa Phosphatidylinositol 4-Kinase with a Novel Repeat Structure: CLONING AND FUNCTIONAL EXPRESSION IN BACULOVIRUS-INFECTED INSECT CELLS*. *Journal of Biological Chemistry* **274**:5738–5745.
- Yan, T. F., and Tao, M.** (1982). Purification and characterization of a wheat germ protein kinase. *Journal of Biological Chemistry* **257**:7037–7043.
- Yanisch-Perron, C., Vieira, J., and Messing, J.** (1985). Improved M13 phage cloning vectors and host strains: nucleotide sequences of the M13mpl8 and pUC19 vectors. *Gene* **33**:103–119.
- Yoo, S.-D., Cho, Y.-H., and Sheen, J.** (2007). *Arabidopsis* mesophyll protoplasts: A versatile cell system for transient gene expression analysis. *Nature protocols* **2**:1565–72.
- Youn, J. H., and Shin, J.-S.** (2006). Nucleocytoplasmic Shuttling of HMGB1 Is Regulated by Phosphorylation That Redirects It toward Secretion. *The Journal of Immunology* **177**:7889–7897.
- Zegzouti, H., Anthony, R. G., Jahchan, N., Bögre, L., and Christensen, S. K.** (2006). Phosphorylation and activation of PINOID by the phospholipid signaling kinase 3-phosphoinositide-dependent protein kinase 1 (PDK1) in *Arabidopsis*. *Proceedings of the National Academy of Sciences* **103**:6404–6409.
- Zhang, L., Li, Z., Garraway, J., Cai, Q., Zhou, Y., Li, X., Hu, Z., Zhang, M., and Yang, J.** (2020a). The casein kinase 2 β subunit CK2B1 is required for swollen stem formation via cell cycle control in vegetable *Brassica juncea*. *The Plant Journal* **104**:706–717.
- Zhang, Z., Li, Y., Huang, K., Xu, W., Zhang, C., and Yuan, H.** (2020b). Genome-wide systematic characterization and expression analysis of the phosphatidylinositol 4-phosphate 5-kinases in plants. *Gene* **756**:144915.
- Zhao, Y., Yan, A., Feijó, J. A., Furutani, M., Takenawa, T., Hwang, I., Fu, Y., and Yang, Z.** (2010). Phosphoinositides Regulate Clathrin-Dependent Endocytosis at the Tip of Pollen Tubes in *Arabidopsis* and Tobacco[W]. *Plant Cell* **22**:4031–4044.
- Zhong, R., Burk, D. H., Nairn, C. J., Wood-Jones, A., Morrison, W. H., III, and Ye, Z.-H.** (2005). Mutation of SAC1, an *Arabidopsis* SAC Domain Phosphoinositide Phosphatase, Causes Alterations in Cell Morphogenesis, Cell Wall Synthesis, and Actin Organization. *The Plant Cell* **17**:1449–1466.
- Zhou, J., Doorbar, J., Xiao Yi Sun, Crawford, L. V., McLean, C. S., and Frazer, I. H.** (1991). Identification of the nuclear localization signal of human papillomavirus type 16 L1 protein. *Virology* **185**:625–632.
- Zourelidou, M., Absmanner, B., Weller, B., Barbosa, I. C., Willige, B. C., Fastner, A., Streit, V., Port, S. A., Colcombet, J., de la Fuente van Bentem, S., et al.** (2014). Auxin efflux by

PIN-FORMED proteins is activated by two different protein kinases, D6 PROTEIN KINASE and PINOID. *eLife* **3**:e02860.

Zulawski, M., Braginets, R., and Schulze, W. X. (2013). PhosPhAt goes kinases—searchable protein kinase target information in the plant phosphorylation site database PhosPhAt. *Nucleic Acids Res* **41**:D1176–D1184.

6 Appendix

6.1 Additional Figures

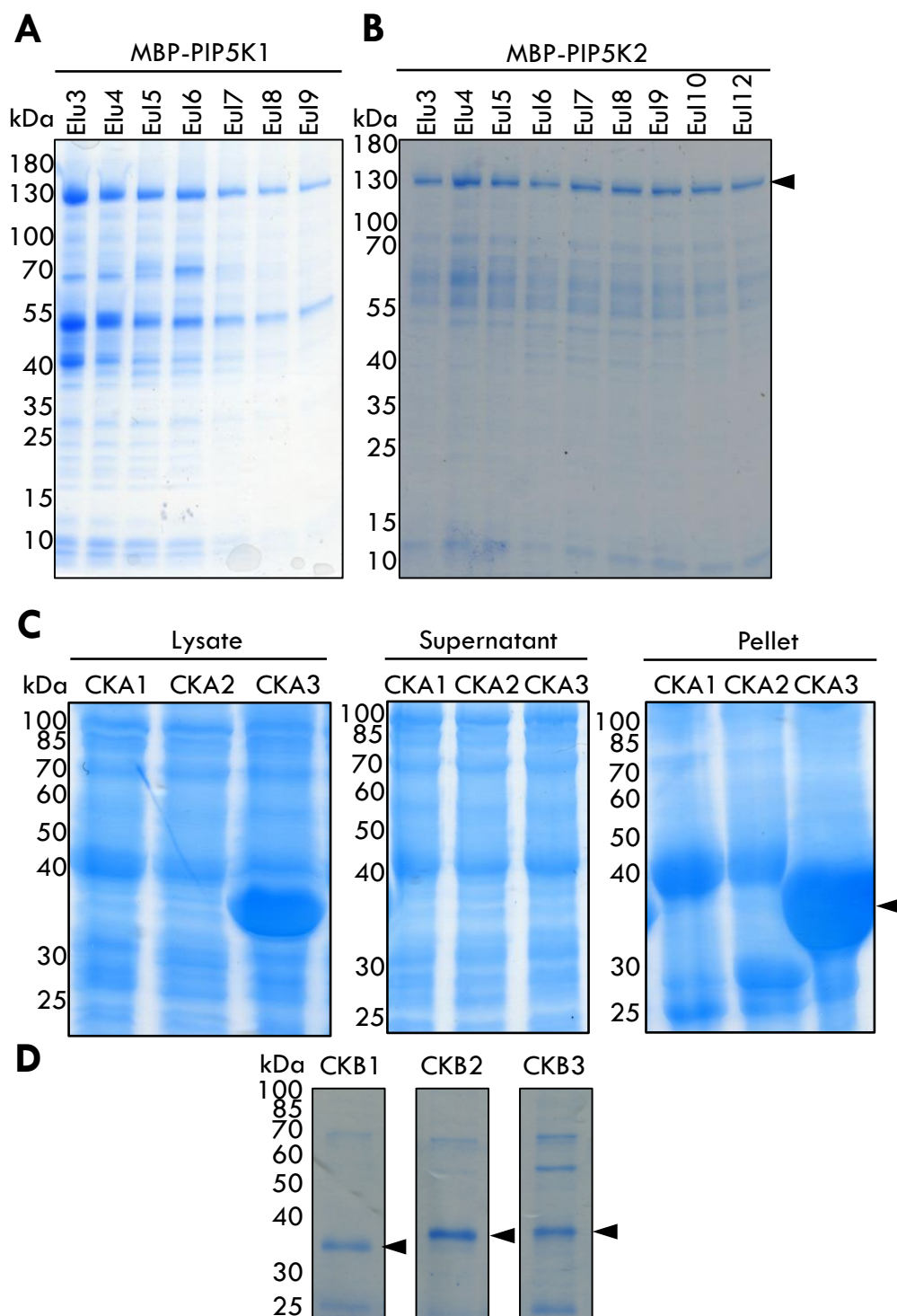


Figure 40 Proteins used for phosphorylation and activity tests. Coomassie stained SDS-PAGE of: **A** enriched MBP-PIP5K1, **B** enriched MBP-PIP5K2, **C** His-CKA lysates and **D** enriched and desalted CKB subunits. MBP-PIP5K1 and MBP-PIP5K2 elution fractions were used in sections 2.3.2, 2.3.4, 2.4.1, 2.4.2 and 2.4.5. We had difficulties to express His-CKA1 and His-CKA2 and get His-CKA3 in the supernatant, thus in this study His-CKA3 lysate was used in sections 2.3.2 and 2.3.4. His-CKB subunits were used in 2.3.2. CK2

subunits were expressed and purified by master's student Juliane Zwoch. Black arrows indicate full length protein. Expected molecular size of full-length proteins: MBP-PIP5K1, 128 kDa; MBP-PIP5K2, 128 kDa; His-CKA1, 49 kDa; His-CKA2, 48 kDa; His-CKA3, 41 kDa; His-CKB1, 34 kDa; His-CKB2, 34 kDa; His-CKB3, 33 kDa.

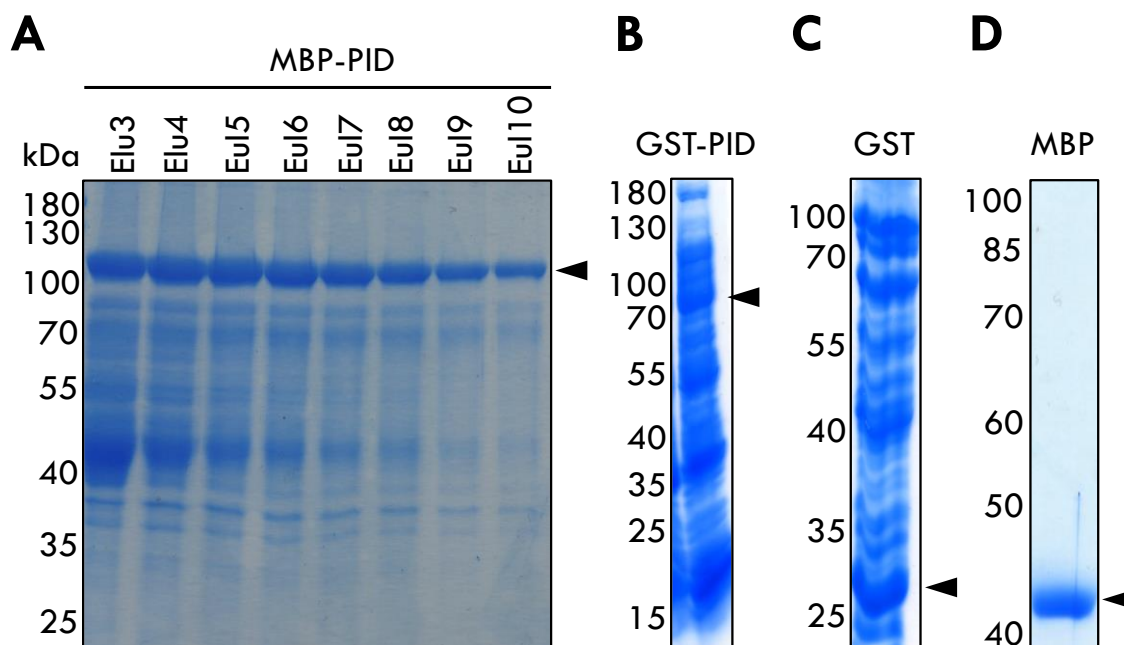


Figure 41 MBP-PID, GST-PID, MBP and GST used in this study. Coomassie stained SDS-PAGE of **A** enriched MBP-PID, **B** supernatant fraction of GST-PID expression, **C** supernatant fraction of GST expression and **D** enriched MBP. MBP and MBP-PID were used in sections 2.4.2 and 2.4.5. GST and GST-PID were used for *in vitro* pull-down in section 2.4.1. GST was expressed by Benita Schmitz.

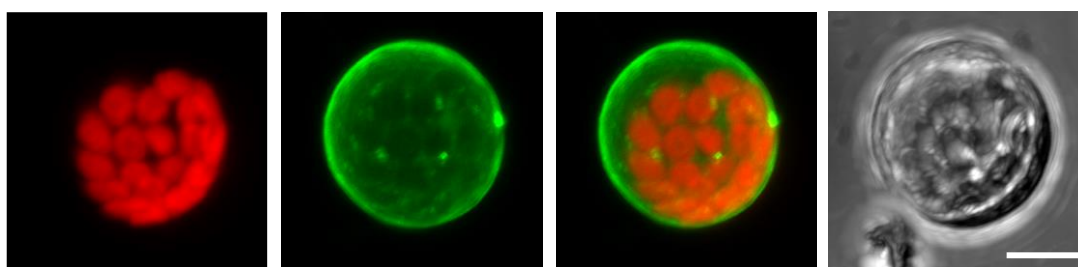


Figure 42 PIP5K2 seemingly localises unaffected in *PID pid wag1 wag2* mutants. Arabidopsis *PID pid wag1 wag2* triple mutant mesophyll protoplasts were transiently transformed with *pEntryA-pCaMV35S::PIP5K2-EYFP*. Subcellular localisation of fluorescent protein fusions was analysed with the LSM880. Displayed is one protoplast expressing PIP5K2-EYFP. Shown is a projection of a z-stacks covering the entire protoplast with 1 μ m intervals between sections. Autofluorescence of chlorophyll A is depicted in red and PIP5K2-EYFP in green. Scale bar, 10 μ m. Image is representative for five cells in total.

6.2 Additional MS Data

6.2.1 His-CKA3/ MBP-PIP5K1 phosphorylation test

Peptide TiO₂ enrichment:

68 % Coverage; 164 peptides, 83 Unique.

Maltose Binding Protein-

```

1 MS DSEEEEEEEASEVILSSVVQKKKK NLRFGEEVERRDGLVLLAQSTPMVRSRSQGT
61 RRVTPPLVDVEKPLPNGDLYIGSFSGGFPHGSGKYLWKDGCMYEGDWKR GKASGKGF
121 WPSGATYEGEFKSGRMEGFGTFTGADGDTYRGTWVADRKHGHGQKRYANGDFYEGTWRRN
181 LQDGRGRYVWRNGNQYTGWRSGVISGKGLLVWPNGNRYEGLWENGIPKGNVFTWSDGS
241 SCVGAWNESNIMRSFFNGVEKNDLIVGNRKRSSVDSGAGSLGGEKVFPRICIWESDGEAG
301 DITCDIIDNVEASMIYRDRISVDRDGFQFKKNPCWFNGEAKKPGOTISKGHKKYDMLN
361 LQLGIRYSVGKHASIVRDLKQTDGDFPKEKFWTRFPPEGKTTTPPHQSVDFRWKDYCPLVF
421 RRLRELQVDPKAYMLAICGNDAALRELSSPGKSGSFFYLTDQDDRFMIKTVKKSEVKVLLR
481 MLPSYKHKVCQYENSLVTRFYGVHCIPVGGQKTRFIVMGNLFCSEYRIQRRFDLKGSSH
541 GRSTAKPEGEIDETTTLKDLDLNFSRLQRNWXQELMQIKRDCEFLAERIMDYSLLVG
600 VHFRRDNTGKMGSLPFVLRSGRIDSYQNEKFMRGCRFLEAELQMDRILAGRKPSIRLG
661 ANMPAKAERMARRSDFDQYSSGGASYPSHGEMYEVVLYFGVIDILQDYDITKKIEHAYKS
721 LQADPASISAVDPKLYSKRFRDFISRIFIEEG

```

Phosphorylated peptides:

S2:

```

MS (+79.97) DSEEEEEEEASEVILSSVVQK
YVHMS (+79.97) DSEEEEEEEASEVILSSVVQK
YVHMS (+79.97) DSEEEEEEEASEVILSSVVQK
DAQTNSSNNNNNNNNNNLGPAAHYVHMS (+79.97) DSEEEEEEE
AHYVHMS (+79.97) DSEEEEEEEASEVILSSVVQK
DAQTNSSNNNNNNNNNNLGPAAHYVHMS (+79.97) DSEEEEEEE
DAQTNSSNNNNNNNNNNLGPAAHYVHMS (+79.97) DSEEEEEEE
DAQTNSSNNNNNNNNNNLGPAAHYVHMS (+79.97) DSEEEEEEEA
HYVHMS (+79.97) DSEEEEEEEASEVILSSVVQK
MS (+79.97) DSEEEEEEEASEVILSSVVQK

```

Phosphorylated peptide:

S408:

TTPPHQS (+79.97) VDFR

6.2.2 MBP-PID/ MBP-PIP5K2 phosphorylation test

Total peptide:

65 % coverage; 376 peptides, 48 Unique

Maltose Binding Protein-

```

1 MMREPLVSEEEEEATEVLLVEKTKLCKRRGDEEKTEERRDDLLLLALTPMVRSKSQGTT
61 RRVTPPPPVDVEKPLPNGDLYMGTFSGGFPNGSGKYLWKDGCMYEGEWKR GKASGKGF
121 SWPSGATYEGEFKSGRMEGSGTFVGVGDYRGSWVADRKQGHGQKRYANGDYEGTWRRN
181 NLQDGRGRYVWRNGNQYTGWRNGVICGKGVLAWPNGNRYEGQWENGVPKGSVFTWADG
241 SSWIGSWNESSNLMRNFFDIEKNELVATRKRSSVDSGAGSLTGEKIFPRICIWESDGEAG
301 AGDITCDIVDNVEASVIYRDRISIDKDGFRQFRKNPCCFSGEAKKPGETISKGHKKYDLM
361 LNLQHGIRYSVGKHASVVRDLKQSDDFPSEKFWTRFPPEGSKTTPPHLSVDFRWKDYCPL
421 VFRRLRELFTVDPADYMLAICGNDAALRELSSPGKSGSFFYLTDQDDRFMIKTVKKSEVKVL
481 LRMLPSYKHKVCQYENTLVTRFYGVHCIPVGGQKTRFIVMGNLFCSEYRIQRRFDLKGSS
541 SHGRYTSKPEGEIDETTTLKDLDLNFAFRLQRNWXQELMTQIKRDCEFLAERIMDYSLLVG
600 VGVHFRDNTGDKMGSLPFVLRSGKIESYQSEKFMRGCRFLEAELQMDRILAGRKPLIR
661 LGANMPARAERMARRSDYDQYSSGGTNYQSHGEVYEVVLYFGIIDILQDYDISKKIEHAY
721 KSLQADPASISAVDPKLYSRRFRDFISRIFIEDG

```

Phosphorylated peptide:**S282:**

RSSVDSGAGS(+79.97) LTGEKI

Peptide TiO₂ enrichment:**56 % Coverage; 82 peptides, 46 Unique.**

Maltose Binding Protein-

1 MMREPLVSEEEEEATEVLLVEKTKLCKRRGDEEKTEERRDLLLLALTPMVRKSQGT
61 RRVTPTPPPVDVEKPLPNGDLYMGTFSGGFPNGSGKYLWKDGCMYEGEWKRGKASGKGKF
121 SWPSGATYEGEFKSGRMEGSGTFVGVGDGTYRGSWVADRKQGHGQKRYANGDYEGTWRR
181 NLQDGRGRYVVMNGNQYTGEWRNGVICGKGVLAWPNGNRYEGQWENGVPKSGVFTWADG
241 SSWIGSWNESSNLMRNFFDGIKNEELIVATRKRSSVDSGAGSLTGEKIFPRICIWESDGE
301 AGDITCDIVDNVEASVIYRDRISIDKDGFRQFRKNPCCFSGEAKKPGETISKGHKKYDLM
361 LNLQHGI RYSVGKHASVVRDLKQSDFD PSEKFWTRFPPEGSKTTTPHLSVDFRWKDYCPL
421 VFRRLRELFTVDPADYMLAICGN DALRELSSPGKSGSFFYLTQDDRFMIKT VVKKSEVKVL
481 LRMLPSYYKHVCQYENTLVTRFYGVHC IKPVGGQKTRFIVMGNLFCSEYRIQRFDLKS
541 SHGRYTSKPEGEIDETTTLKDLDLNFAFRLQRN WYQELMTQIKRDCEFLAERIMDYSLI
600 VGVHFRDDNTGDKMGLSPFVLRSGKIESYQSEKFMRGCRFLEAELQMDRILAGRKPLIR
661 LGANMPARAERMARRSDYDQYSSGGTNYQSHGEVYEVVLYFGIIDILQDYDISKKIEHAY
721 KSLQADPASISAVDPKLYSRRFRDFISRI FIEDG

Phosphorylated peptides:**S274:**

KRS(+79.97) SVDSGAGSLTGEKI

S275:

KRS(+79.97) VDSGAGSLTGEKI

S282:

KRSSVDSGAGS(+79.97) LTGEKI

KRSSVDSGAGS(+79.97) LTGEKI

RSSVDSGAGS(+79.97) LTGEKI

RSSVDSGAGS(+79.97) LTGEKI

RSSVDSGAGS(+79.97) LTGEKI

6.3 Oligonucleotides**6.3.1 Primers used for cloning****Table 17** Primers for cloning

Used for	Name	Sequence	Originated by
<i>pEntry</i> cloning	PsPIP5K1 Ascl for	ATGCGGCGGCCATGCGAGAATCTATAGGTTGT	Barbora Hans
	PsPIP5K1 XhoI rev	ATGCCTCGAGTGATTATCTTCTAAAAAGAT	Barbora Hans
	PIP5K2 XhoI rev	ATGCCTCGAGGCCGTCTTCGATGAAGATTCTG	Dr. Mareike Heilmann
	PIP5K2 Ascl for	ATGCGGCGGCCATGATGCGTAACCGCTTGT	Dr. Mareike Heilmann
	PIPK1 S2S4A Asclfor	ATGCGGCGGCCATGGCAGATGCAGAAGAAGAC- GAAGAAGAAGAAGAAGC	Juliane Zwoch

	PIPK1 S2S4D Asclfor	ATGCGGCGCGCCATGGATGATGATGAAGAAGAC- GAAGAAGAAGAAGAAGC	Juliane Zwoch
	PID Xhol rev	ATGCCTCGAGATGTTACGAGAATCAGACGGTG	Babette Pinkwart
	PID Ascl for	ATGCGGCGCGCCCTCAAAGTAATCGAACGCC	Babette Pinkwart
	CKA1 -Ascl-for	ATGCGGCGCGCCATGATAGATACGCTTTTCTT	This study
	CKA1-Xhol-rev	ATGCCTCGAGTTGACTTCTCATTCTGCT	This study
	CKA3-Ascl-for	ATGCGGCGCGCCATGTCGAAAGCTAGGGTTTA	This study
	CKA3-NheI-rev	ATGCGCTAGCCTGAGTTCGTAGTCTGCTGC	This study
	CKB1 -Ascl-for	ATGCGGCGCGCCATGTATAGAGACAGAGGAAC	This study
	CKB1-Xhol-rev	ATGCCTCGAGCGGTTTGTGTAATTTGAACC	This study
	CKB3-Ascl-for	ATGCGGCGCGCCATGTACAAGGAACGTAGTGG	This study
	CKB3-Xhol-rev	ATGCCTCGAGTGGTTTGTGTACCTGAAGC	This study
	PID-Xhol-for	ATGCCTCGAGATGTTACGAGAATCAGACGGT	Dr. Mareike Heilmann
	PID-BamHI-rev	ATGCGGATCCTCAAAGTAATCGAACGC	Dr. Mareike Heilmann
PsPIP5K1 substitu- tion vari- ants	Ps-AtLinfor	TTGGTTGCTGGAATAATATTGAGAAGATGAGTT	This study
	Ps-AtLinrev	AACTATTCTTCTCAATATTATCCAGCAACCAA	This study
	Ps_AtLinb_for	TCAGCGGTGAGGCTAAGAAACCTGGTCAAACCGT	This study
	Ps_ATLinb_rev	ACGGTTTGACCAGGTTTCTTAGCCTCACCGCTGA	This study
	At_PSLinf_for	GGAATTTCTTTGATGGGAATTTGAAGAATCAGTT	This study
	At_PsLinf_rev	AACTGATTCTTCAAATCCCATCAAAGAAATCC	This study
	At_PsLinb_for	TTACAGGCGAGGCTAAGAAACCTGGAGAGACGAT	This study
	At_PsLinb_rev	ATCGTCTCTCCAGGTTTCTTAGCCTCGCCTGTAA	This study
PIP5K2 substitu- tion vari- ants	PIP5K2 S274A for	GCGACTAGGAAGAGAGCTTCGGTTGATAGTGGC	Babette Pinkwart
	PIP5K2 S274A rev	GCCACTATCAACCGAAGCTCTTCTTAGTTCGC	Babette Pinkwart
	PIP5K2 S274D for	GCGACTAGGAAGAGAGATTCGGTTGATAGTGGC	Babette Pinkwart
	PIP5K2 S274D rev	GCCACTATCAACCGAATCTCTTCTTAGTTCGC	Babette Pinkwart
	PIP5K2 S275A for	ACTAGGAAGAGATCTGCGGTTGATAGTGGCGCT	Babette Pinkwart
	PIP5K2 S275A rev	AGCGCCACTATCAACCGCAGATCTTCTTAGT	Babette Pinkwart
	PIP5K2 S275D for	ACTAGGAAGAGATCTGACGTTGATAGTGGCGCT	Babette Pinkwart
	PIP5K2 S275D rev	AGCGCCACTATCAACGTCAGATCTTCTTAGT	Babette Pinkwart
pEntry promotor cloning	pPIP5K1 -Sfil-for	ATGCGGCCATTACGGCCTGACAATATAAAAATCATAT	This study
	pPIP5K1 -Sfil-rev	ATGCGGCCGAGGCGGCCAGAGAATCTTCAC- TCCAGT	This study
	pPIP5K2-Sfilfor	ATGCGGCCATTACGGCCTTTTGTATAATCATTACCT	This study

<i>pMAL-c5G</i> cloning	pPIP5K2-Sfilrev	ATGCGGCCGAGGCGGCCCTACTCATCAGA-GAAACCCT	This study
	PsPIP5K1 - NotI-for	ATGCGCGGCCGCATGCGAGAATCTATAGGTTGT	This study
	PsPIP5K1 - Sall-rev	ATGCGTCGACTGATTATCTTCTAAAAAGAT	This study
	PIPK1 -NdeI-for	ATGCCATATGAGTGATTGAGAAAGACGAA	Dr. Mareike Heilmann
	PIPK1 -Sall-rev	ATGCGTCGACTTAGCCCTCTCAATGAAGAT	Dr. Mareike Heilmann
	PIPK2-NotI_for	ATGCGCGGCCGCATGATGCGTGAACCGCTTGT	Dr. Mareike Heilmann
	PIPK2-EcoRI_rev	ATGCGAATTCTTAGCCGTCTCGATGAAGA	Dr. Mareike Heilmann
	PID NcoI for	ATGCCCATGGGCATGTTACGAGAATCAGACGG	Babette Pinkwart
	PID EcoRV rev	ATGCGATATCTCAAAGTAATCGAACGCCG	Babette Pinkwart
<i>pGEX-4T-1</i>	PID Sall for	ATGCGTCGACTCATGTTACGAGAATCAGACGGT	Babette Pinkwart
	PID NotI rev	ATGCGCGGCCGCAAAGTAATCGAACGCCG	Babette Pinkwart
<i>pET28b</i> cloning	CKA1-Ascl-for	ATGCGGCGCGCCATGATAGATACGCTTTTCTT	Juliane Zwoch
	CKA1-XhoI-rev	ATGCCTCGAGTTGACTTCTCATTCTGCT	Juliane Zwoch
	CKA3-Ascl-for	ATGCGGCGCGCCATGTCGAAAGCTAGGGTTTA	Juliane Zwoch
	CKA3-NheI-rev	ATGCGCTAGCCTGAGTTCGTAGTCTGCTGC	Juliane Zwoch
	CKB1-Ascl-for	ATGCGGCGCGCCATGTATAGAGACAGAGGAAC	Juliane Zwoch
	CKB1-XhoI-rev	ATGCCTCGAGCGGTTTGTGTAATTTGAACC	Juliane Zwoch
	CKB3-Ascl-for	ATGCGGCGCGCCATGTACAAGAACGTAGTGG	Juliane Zwoch
	CKB3-XhoI-rev	ATGCCTCGAGTGGTTTGTGTACCTTGAAGC	Juliane Zwoch
<i>pPR3N</i> cloning	PID-SfiIA	ATGCGGCCATTACGGCCATGTTACGAGAATCAGAC-GGT	Dr. Mareike Heilmann
	PID-SfiIB-rev	ATGCGGCCGAGGCGGCCCTCAAAGTAATCGAAC-GCCGCT	Dr. Mareike Heilmann
	WAG1-SfiIA-for	ATGCGGCCATTACGGCCATGGAAGACGAC-GGTATTACCT	Dr. Mareike Heilmann
	WAG1-SfiIB	ATGCGGCCGAGGCGGCCCTTATAGCTTTTACCCACATAA	Dr. Mareike Heilmann
	WAG2-SfiIA	ATGCGGCCATTACGGCCATGGAACAAGAAGATTC-TATT	Dr. Mareike Heilmann
	WAG2-SfiIB-rev	ATGCGGCCGAGGCGGCCCTTAAACGCGTTT-GCGACTCGCGTA	Dr. Mareike Heilmann
	IMPA3.SfiIA.for	ATGCGGCCATTACGGCCATGTCTCTCAGAC-CTAGCGCGAA	Dr. Katharina Gerth

pPR3C cloning	IMPA3.+2.SfilB.rev	ATGCGGCCGAGGCGGCCTTAATAAAGTTGAATT- GACCAGGA	Dr. Katharina Gerth	
	IMPA6.SfilA.for	ATGCGGCCATTACGGCCATGTCTTACAAACCAA- GCGCGAA	Dr. Katharina Gerth	
	IMPA6.SfilB.rev	ATGCGGCCGAGGCGGCCTTACCAAAGTT- GAATCCACCCGTA	Dr. Katharina Gerth	
	IMPA9 Sfil for	ATGCGGCCATTACGGCCATGGCG- GATGATGGCTCCGCCT	Dr. Katharina Gerth	
	IMPA9 Sfil rev	ATGCGGCCATTACGGCCATGGCG- GATGATGGCTCCGCCT	Dr. Katharina Gerth	
	CKA3-Sfil-for	ATGCGGCCATTACGGCCATGTCGAAA- GCTAGGGTTTAT	This study	
	CKA3-Sfil-rev	ATGCGGCCGAGGCGGCCTTACTGAGTTCGTAG- TCTGCT	This study	
	CKB1-Sfil-for	ATGCGGCCATTACGGCCATGTATAGACAGAG- GAA	This study	
	CKB1-Sfil-rev	ATGCGGCCGAGGCGGCCTCACGGTTTGTGAATTT- GAA	This study	
	CKB2-Sfil-for	ATGCGGCCATTACGGCCATGTATAGGGAGA- GAGGTAT	This study	
	CKB2-Sfil-rev	ATGCGGCCGAGGCGGCCTCACGGCTTGTG- TAGCTTGAA	This study	
	CKA1-Sfil-for	ATGCGGCCATTACGGCCATGATAGATACGCTTTTCTT	This study	
	CKA1-Sfil-rev	ATGCGGCCGAGGCGGCCTCATT- GACTTCTCATTCTGCT	This study	
	CKA2-Sfilfor	ATGCGGCCATTACGGCCATGCACCTAATCTTCTTCTT	This study	
	CKA2-Sfilrev	ATGCGGCCGAGGCGGCCTATTGAG- TCCTCATCTGCT	This study	
	CKB3-Sfilfor	ATGCGGCCATTACGGCCATGTACAAGGAACGTAG- TGG	This study	
	CKB3-Sfilrev	ATGCGGCCGAGGCGGCCTCATGGTTTGTGTAC- CTTG	This study	
	PIP5K2.OST4.SfilA.for	ATGCGGCCATTACGGCCAATGATGCGTGAACCGCTT	Dr. Katharina Gerth	
	pBiFct- 2in1 cloning	PIP5K2.OST4.SfilB.rev	TGCGGCCGAGGCGGCCAAGCCGCTTTCGATGAA- GATT	Dr. Katharina Gerth
		PsPIPK1-Sfilost4f	ATGCGGCCATTACGGCCAATGCGA- GAATCTATAGGTTGT	This study
PsPIPK1-Sfilost4r		ATGCGGCCGAGGCGGCCAATGAT- TTATCTTCAAAAAGAT	This study	
PID-P3-for		GGGGACAACITTTGTATAATAAAGTTGGAATGTTAC- GAGAATCAGACGG	This study	
PID-P2-revSTOP		GGGGACCACITTTGTACAAGAAA- GCTGGGTTCAAAAGTAATCGAACGCCG	This study	
PDK1-P3-for		GGGGACAACITTTGTATAATAAAGTTGGAATGTTGG- CAATGGAGAAAGAATT	This study	
PDK1-P2-revSTOP		GGGGACCACITTTGTACAAGAAA- GCTGGGTTCAAGCGTTCTGAAGAGTCTCGA	This study	
PDK1-P1-for		GGGGACAAGTTTGTACAAAAA- GCAGGCTTAATGTTGGCAATGGAGAAAGAATT	This study	
PDK1-P4-revSTOP		GGGGACAACITTTGTATAGAAAAGTT- GGGTTCAAGCGTTCTGAAGAGTCTCGA	This study	
PIP5K2-P1 for		GGGGACAAGTTTGTACAAAAA- GCAGGCTTAATGATGCGTGAACCGCTTGT	This study	
PIP5K2-P4revSTOP		GGGGACAACITTTGTATAGAAAAGTT- GGGTTAGCCGCTTTCGATGAAGA	This study	

6.3.2 Primers used for sequencing

Table 18 Primers for sequencing

Used for	Name	Sequence	Originated by
pCaMV35S ocs terminator	p35S_for	TATATAAGGAAGTTCATT	Dr. Mareike Heilmann
	ocs-rev	TTTACAACGTGCACAACAGAA	Dr. Mareike Heilmann
pUC vectors	M13-for	CCCAGTCACGACGTTGTAAAACG	(Yanisch-Perron et al., 1985)
	M13-rev	AGCGGATAACAATTCACACAGG	(Yanisch-Perron et al., 1985)
pMAL-c5G	pMAL-for	ATGCCGAACATCCCGCAGAT	New England Biolabs
	pMAL-rev	TTGTCTACTCAGGAGAGCGTT	New England Biolabs
pGEX-4T-1	pGEX-for	GGGCTGGCAAGCCACGTTTGGTG	Dr. Mareike Heilmann
	pGEX-rev	CCGGGAGCTGCATGTGCAGAGG	Dr. Mareike Heilmann
pBT3-C-OST4	pBT3-for	CATGATCATATGGCATGCATG	Dr. Mareike Heilmann
	pBT3-LexA-rev	ACACCTCTTGTGCTGGCCA	Dr. Mareike Heilmann
pPR3-N	pPR3N-for	TGCAGATTTTCGTAAGACTTT	Dr. Mareike Heilmann
	pPR3N-rev	ATAACTAATTACATGACT	Dr. Mareike Heilmann
PIP5K1 Promotor	pPIP5K1_for1	GTGGTGAATCGCCGGA-GAAATGTG	This study
	pPIP5K1_for2	TCTGAGATTGAGGAACATTGTG	This study
PIP5K2 Promotor	pPIP5K2_for1	TCTAGGAATCTCTCCCAACG	This study
	pPIP5K2_for2	TTCTTCACCCTAATCCGTAATCG	This study
PIP5K1	PIP5K1-m1-for	AAATGGGAATCAGTATACT	Dr. Mareike Heilmann
	PIP5K1-m2-for	AAAGGAGAAAATTTGGACAA	Dr. Mareike Heilmann
	PIP5K1-m3-for	AGCTTATGAAGCAAATAAAA	Dr. Mareike Heilmann
	PIP5K1-m2-rev	TTGTCCAAAATTTCTCCTTT	Dr. Mareike Heilmann
	PIP5K1-m3-rev	TTTTATTTGCTTCATAAGCT	Dr. Mareike Heilmann
	PIP5K2	PIP5K2_m1_for	AAACGGAAGAGAGAAGAGACG
PIP5K2_m1_rev		CGTCTCTTCTCTCCGTTT	This study
PIP5K2_m2_for		CTGGGAGAATGGAAGGATCTG	This study
PIP5K2_m2_rev		CAGATCCTCCATTCTCCAG	This study
PIP5K2_m3_for		GGTGTGCTTGCTTGGCCTAATG	This study
PIP5K2_m3_rev		ATTAGGCCAAGCAAGCACACC	This study
PIP5K2_m4_for		GTTGGCGTCACTCCGTGATG	This study
PIP5K2_m4_rev		CATCACGGAAGTGAACGCCAAC	This study
PsPIP5K1	PsPIP5K1m1for	ATTGGAAAAATGGGGTTATTA	This study
	PsPIP5K1m1rev	TAATAACCCCATTTTTCCAAT	This study
	PsPIP5K1m2for	AACTCAGGCCTCAGACTT	This study
	PsPIP5K1m2rev	AAGTCTGAAGGCCTGAGTT	This study
	PsPIP5K1m3for	AAAACAGATTCAGCTGCTGT	This study
	PsPIP5K1m3rev	ACAGCAGCTGAATCTGTTTT	This study

CK2 subunits	PsLinfor	GAAGAGGAAGTTAGCTGA- GAAGA	This study
	PsLinrev	TCCTCTCAGCTAAACTTCCTCTC	This study
	CKA1-m-for	ACTTCTGCCATTACACAAGGA	This study
	CKA1-m-rev	TCCTTGTGAATGGCAGAAGT	This study
	CKA2-m-for	GAATAATGCACAGAGATGTC	This study
	CKA2-m-rev	GACATCTCTGTGCATTATTC	This study
	CKA3-m-for	TAGATCATCAGCTGCGTAAA	This study
	CKA3-m-rev	TTTACGCAGCTGATGATCTA	This study
	CKB1-m-for	AGTCAGCAGCTGAGATGTTG	This study
	CKB1-m-rev	CAACATCTCAGCTGCTGACT	This study
	CKB2-m-for	AGTTCCTTACTACGACTATG	This study
	CKB2-m-rev	CATAGTCGTAGTAAGGAAGT	This study

6.3.3 Primers used for genotyping plants

Table 19 Primers for genotyping

Name	Sequence	Originated by
LBb1.3	ATTTGCCGATTCGGAAC	Salk Institute
PID-LP	CAGTCGGGAAACTCAACTGTC	Salk Institute
PID-RP	ATTTGCGATGAAAGTTGTGG	Salk Institute
WAG1-LP	TATATTGCGCAGGGTTTGTC	Salk Institute
WAG1-RP	TCTCGATCTCAGCTTCACCTC	Salk Institute
WAG2-LP	TAAAGGAATATCCGAACGCC	Salk Institute
Wag2-RP	CCAAAACCCCAAACATAAAC	Salk Institute
PIP5K1-LP	ACTAAAGGGCAATAATCCTTCACC	Salk Institute
PIP5K1-RP	GCAAATTCTCATGGCCAAGTGGA	Salk Institute
PIP5K2-LP	CAGGTTTGATACAATGCACACCAT	Salk Institute
PIP5K2-RP	TGGGAGTCTGATGGAGAAGCTG	Salk Institute
EYFP rev	CTTGCCGGTGGTGCAGATGAACCTCAG	Dr. Katharina Gerth
PsPIP5K1 m3 for	AAAACAGATTCAGCTGCTGT	This study
PIP5K2 m3 for	GGTGTGCTTGCTTGGCCTAATG	This study

Figures

Figure 1 PI network and domain structure of PI4P 5-kinases	3
Figure 2 PIP5K2 localises in microdomains at the plasma membrane and to the nucleus in developmental young root cells	6
Figure 3 PIP5K2 contains a functional NLS	7
Figure 4 PIs are involved in several plasma membrane associated processes	8
Figure 5 Overexpression of PI4P 5-kinases from different clades in pollen tubes cause different phenotypes.....	9
Figure 6 The <i>pip5k1 pip5k2</i> double mutant shows a severe phenotype.....	11
Figure 7 PIP5K2_NLS _{AAA} can partially rescue the <i>pip5k1 pip5k2</i> double mutant phenotype	13
Figure 8 PIP5K1 and PIP5K2 have multiple putative phosphorylation sites.....	16
Figure 9 Arabidopsis with altered PI4P 5-kinase and AGC3 protein kinase expression share reciprocal phenotypes	17
Figure 10 CK2 subunits localise mainly to the nucleus	19
Figure 11 Plant CK2 regulates circadian clock and photomorphogenesis.....	20
Figure 12 Origin of AGC3 protein kinases PID, WAG1 and WAG2	23
Figure 13 The direction of auxin flow is determined by the polar PIN localisation.....	24
Figure 14 PIP5K2 localises dynamically to plant nuclei in Arabidopsis mesophyll protoplasts	27
Figure 15 PIP5K2-EYFP displays enhanced nuclear localisation in BY-2 protoplasts	29
Figure 16 AtPIP5K1 and AtPIP5K2 have a close homologue in opium poppy	31
Figure 17 AtPIP5K2 displays enhanced nuclear localisation in poppy protoplasts.....	34
Figure 18 PsPIP5K1 interacts with Arabidopsis alpha-importins	36
Figure 19 The Lin-domain of PI4P 5-kinases greatly modulates the subcellular localisation	38
Figure 20 Effects of PsPIP5K1 overexpression on tobacco pollen tube phenotype.....	41
Figure 21 Effects of chimeric AtPIP5K2_LinPs overexpression on tobacco pollen tube phenotype	42
Figure 22 PsPIP5K1 and PsPIP5K1_LinAt complement the <i>pip5k1 pip5k2</i> double mutant shortened root phenotype.....	46
Figure 23 PsPIP5K1 and PsPIP5K1_LinPs complement the <i>pip5k1 pip5k2</i> double mutant	47
Figure 24 PIP5K1 and PIP5K2 interact with CK2 isoforms	49
Figure 25 CKA3 phosphorylates PIP5K1 <i>in vitro</i>	51
Figure 26 CKA3 phosphorylates PIP5K1 in position S2 and S408	52
Figure 27 CKA3 localises to plant nuclei in Arabidopsis mesophyll and tobacco BY-2 protoplasts	54

Figure 28 CKA3 coexpression increases PIP5K1 localisation to the nucleus in protoplasts	56
Figure 29 PIP5K1 shows enhanced catalytical activity after phosphorylation by CKA3.	58
Figure 30 PID interacts with PIP5K1 and PIP5K2	61
Figure 31 PID phosphorylates PIP5K2 in the NLS region of the Lin-domain	64
Figure 32 PIP5K2 apparently localises unaffected by PID	68
Figure 33 PIP5K2 forms defined foci at the plasma membrane	70
Figure 34 PIP5K2 displays increased catalytical activity upon phosphorylation by PID.	72
Figure 35 PtdIns(4,5) ₂ levels are altered in <i>pid</i> mutants	73
Figure 36 Model: The Lin-domain of PI4P 5-kinases mediates localisation and function.	79
Figure 37 Model: Phosphorylation in the N-terminus of PIP5K1 by CKA3 competes with the autoinhibitory effect of the N-terminal domains	86
Figure 38: Model: Phosphorylation of PIP5K2 by PID increases catalytical activity promoting a self-reinforcing loop involved in the PIN mediated auxin gradient.	90
Figure 39 Model: PIP5K1 and PIP5K2 are regulated by protein phosphorylation.....	92
Figure 40 Proteins used for phosphorylation and activity tests	142
Figure 41 MBP-PID, GST-PID, MBP and GST used in this study	143
Figure 42 PIP5K2 seemingly localises unaffected in <i>PID pid wag1 wag2</i> mutants	143

Tables

Table 1 Enzymes and size indicators.....	94
Table 2 Microorganisms.....	94
Table 3 Plants and plant cell cultures.....	95
Table 4 Bacterial media.....	96
Table 5 Yeast media.....	96
Table 6 Plant media.....	97
Table 7 Media additives.....	98
Table 8 Vectors used for protein expression in <i>E. coli</i>	99
Table 9 Vectors used for yeast-two-hybrid studies.....	99
Table 10 Vectors used for transient expression and stable transformation of plants...	100
Table 11 Buffers and stock solutions.....	101
Table 12 Plasmids for protein expression.....	110
Table 13 Plasmids for yeast-two-hybrid assays.....	111
Table 14 Plasmids for BiFC assay.....	111
Table 15 Plasmids used for expression in plants.....	112
Table 16 Primary- and secondary antibodies used in this study.....	116
Table 17 Primers for cloning.....	145
Table 18 Primers for sequencing.....	149
Table 19 Primers for genotyping.....	150

Danksagung

Ich möchte mich bestimmt und herzlich bei so vielen Menschen bedanken! Ohne die Hilfe so vieler, wäre diese Arbeit nie zustande gekommen.

So gilt mein erster und größter Dank meiner Betreuerin Dr. Mareike Heilmann. Danke Mareike für dieses großartige Projekt! Danke für all deine Betreuung, das Teilen und Vermitteln so vieler wissenschaftlicher Praktiken und Methoden, sowie das Helfen in allen Lebenssituationen. Danke für dein stets offenes Ohr und deine Unterstützung über die volle Zeit der Doktorarbeit. Vielen Dank für den sehr familiären Umgang, den du mit mir und deinen anderen Angestellten pflegst. Und Danke für all die Anekdoten und witzigen Momente, die mir in Erinnerung bleiben werden!

Prof. Dr. Ingo Heilmann möchte ich auch ein riesiges Dankeschön aussprechen. Vielen Dank Ingo für die offene und willkommene Aufnahme in deine Arbeitsgruppe, noch in Zeiten meines Masterstudiums als Forschungsgruppenpraktikant, aus dem nun final eine ganze Doktorarbeit entstand. Danke für all deine Vorschläge, Anregungen und Kritik bezüglich des Projektes. Danke auch dir für dein stets offenes Ohr bzw. deine offene Bürotür und deine Hilfe in den letzten Jahren, sowie deine stets optimistische Denkweise. Als Vorsitzender und Mit-Initiator des RTG2498 möchte ich dir auch noch mal gesondert für deine Arbeit danken, die meine Doktorandenstelle erst ermöglichte.

Meinen (voraussichtlichen) Gutachtern Prof. Dr. Marcel Wiermer und Prof. Dr. Klaus Humbeck möchte ich ebenfalls für die Zeit danken, die sie meiner Arbeit widmen.

Der „Research Training Group 2498: Communication and Dynamics of Plant Cell Compartments“ und der damit verbundenen Deutschen Forschungsgemeinschaft möchte Ich für die Finanzierung danken. Besonderen Dank an meine RTG-Thesis Committee Mitglieder Prof. Dr. Steffen Abel und Prof. Dr. Klaus Humbeck für euren Input in unseren regelmäßigen Meetings. Danke an unsere RTG-Koordinatorin Julia Grimmer für das Erklären und Überwinden bürokratischer Hürden. Danke an alle RTG PIs und RTG-Kommilitonen für euer Feedback und alle Trainings und Kurse, die mir das RTG ermöglicht hat. Besonders möchte Ich mich außerdem für die Möglichkeit bedanken, den FEBS-Workshop in Primosten zu besuchen und mein Projekt dort zu präsentieren.

Dem Servicebereich Isotopenlabor unter der Führung von PD Dr. Margret Köck (bis 2021) und Dr. Dirk Dobritzsch möchte ich für die Möglichkeit danken, radioaktive Arbeiten durchzuführen. Dirk gilt weiterhin mein Dank für Unterstützung in allen IT-basierten Problemen, sowie ein riesiges Dankeschön für die Unterstützung mit MS basierten Experimenten in der Core Facility Proteomic Mass Spectrometry.

Ich möchte mich bei Dr. Jenny Lerche und Dr. Katharina Gerth für Ihre Vorarbeiten bedanken, auf denen meine Arbeit basiert. Weiterhin gilt mein Dank der Kooperation mit der AG Marek aus Bratislava und Barbora Hans für das Einführen der Mohn PI4P 5-Kinase in unserer Arbeitsgruppe.

Meiner Kollegin Dr. Franziska Daamen möchte Ich ebenfalls ein riesiges Dankeschön aussprechen. Danke Franzi für all deine Hilfe in der Wissenschaft und viele schöne Stunden geteilt im Labor und Büro gleichermaßen. Danke auch für deine Vorbildfunktion und das Paradebeispiel wie man es richtig macht. Große Dankbarkeit gilt weiterhin meinen Doktorandenkollegen Larissa Launhardt, Monique Matzner und Christoph Kastner, sowie den neu dazugekommen Promotionsstudenten Johanna Uhlenberg, Johanna Nordmeier, Benita Schmitz und Angela Lopez. Vielen Dank euch allen für Unterstützung im Labor, das Vermitteln von Methoden und Tricks, lehrreiche Diskussionen, das Bereitstellen von Plasmiden und Proteinen, sowie erholsame Freizeitgestaltung. Besonders Ulli gilt hier mein Dank für etliche kulinarische Ausflüge.

Unseren Postdocs Praveen Krishnamoorthy und Marta Fratini möchte ich außerdem für Ihre Geduld bedanken, die sie mir beim Beibringen der TIRF-Mikroskopie entgegenbrachten. Unserer Postdoc Irene danke Ich für das Bereitstellen des pLAT52 Promotors und für die Pflege der Tabakpflanzen im Gewächshaus.

Der AG Nucleus von Mareike mit Benita und Franzi möchte ich hier noch einmal gesondert für eine äußerst einprägsame, lehrreiche und spaßige Zeit danken. Der gesamten AG Heilmann möchte ich ein ehrliches Lob und Dankbarkeit für die angenehme Arbeitsatmosphäre aussprechen! Für technische Arbeiten, durchgeführt von Marion Sonntag und Kristin Peters möchte ich ebenfalls danken, die mir etliche Experimente vereinfacht haben.

Meinen Bachelorstudentinnen Marie Lebescond, Thea Stephan und Julia Urbainski, sowie Masterstudentin Juliane Zwoch möchte ich für eine lehrreiche und amüsante Zeit als Betreuer und eine fortlaufend fruchtbare Zusammenarbeit danken, die mir besonders viel Freude bereitet hat. Besonders freut mich weiterhin, dass Marie meine Nachfolge im Zuge des RTGs nach Ihrem Masterabschluss in der AG Heilmann angetreten hat.

Ein riesiges Dankeschön an alle Korrekturleser. Ihr habt was Gut bei mir.

Danke Sunny!

Be like a proton and stay positive.

Curriculum Vitae

Lennart Schwalgun

Date of Birth: 14.11.1994
Place of Birth: Berlin
Nationality: German

Work

Since 02.2023 Quality Specialist at CHEPLAPHARM GmbH

Education

- 06.2019-12.2022 **PhD as Member of the RTG 2498**
Communication and Dynamics of Plant Cell Compartments
Martin Luther University Halle-Wittenberg
Research Group Nuclear Phosphoinositides (Dr. Mareike Heilmann)
Department of Plant Biochemistry (Prof. Dr. Ingo Heilmann)
Defence 26.03.2023
- 02.2019-06.2019 **Research Associate**
Martin Luther University Halle-Wittenberg
Research Group Nuclear Phosphoinositides (Dr. Mareike Heilmann)
Department of Plant Biochemistry (Prof. Dr. Ingo Heilmann)
- 09.2016-11.2019 **Master of Science – Biochemistry**
Martin Luther University Halle-Wittenberg
- 09.2013-09.2016 **Bachelor of Science – Biochemistry**
Martin Luther University Halle-Wittenberg

Publications and Conferences

Jana Ordon, Johannes Gantner, Jan Kemna, Lennart Schwalgun, Maik Reschke, Jana Streubel, Jens Boch, Johannes Stuttmann, (2017) Generation of chromosomal deletions in dicotyledonous plants employing a user-friendly genome editing toolkit. *Plant J.* 89, 155–168.

Lennart Schwalgun, Mareike Heilmann (September 2021) The nuclear cytoplasmic shuttling of plant PI4P 5-kinases. FEBS Workshop 2021 Plant Organellar Signalling Primosten, Croatia (Talk)

Lennart Schwalgun, Mareike Heilmann (June 2019) The nuclear cytoplasmic shuttling of plant PI4P 5-kinases. Plant Science Student Conference PSSC IPB Halle, Germany. (Talk)

Erklärung

Hiermit erkläre ich, dass ich die vorliegende Dissertation selbständig und ohne fremde Hilfe verfasst habe, keine anderen als die angegebenen Quellen und Hilfsmittel benutzt habe und die den benutzten Werken wörtlich oder inhaltlich entnommenen Stellen als solche kenntlich gemacht habe.

Des Weiteren erkläre ich, bisher keine vergeblichen Promotionsversuche unternommen zu haben und die Dissertation in der gegenwärtigen bzw. in einer anderen Fassung nicht bereits an einer anderen Fakultät vorgelegt zu haben.

Halle (Saale), _____

Lennart Schwalgun